INVESTIGATING THE ROLE OF TOLL-LIKE RECEPTOR 9 IN CHRONIC LYMPHOCYTIC LEUKAEMIA

EMMA MARION KENNEDY

Submitted in partial fulfilment of the requirements for the degree of Doctor of Philosophy from the University of Sussex and the University of Brighton for a programme of study undertaken at the Brighton and Sussex Medical School

July 2021

Abstract

B-cell Receptor (BCR) signalling plays a critical role in the progression of Chronic Lymphocytic Leukaemia (CLL) and BCR-targeted kinase inhibitors, such as ibrutinib and idelalisib, have recently revolutionised its treatment. Despite these advances, CLL remains an incurable malignancy and the identification of novel molecular targets is paramount. This thesis investigates Toll-Like Receptor 9 (TLR9), a pattern recognition receptor of the innate immune system, which becomes activated in response to unmethylated CpG DNA. Importantly, our team have shown significantly increased levels of unmethylated CpG DNA motifs within the plasma of CLL patients relative to healthy individuals. We hypothesise that this arises from CLL cell apoptosis and the subsequent exposure of unmethylated mitochondrial self-DNA could be fuelling CLL progression through an auto-stimulatory feedback loop.

CLL cells traffic from the peripheral blood to the secondary lymphoid tissues where they become activated and proliferate, and CLL cell migration is therefore vital for survival and progression. Data presented in this thesis demonstrates that activation of primary CLL cells through TLR9 (using the agonist ODN 2006) induces a more activated and migratory phenotype including the upregulation of cell surface CD69, CD49d and CD38. Furthermore, the expression of intracellular TLR9 is higher in migrated vs non-migrated CLL cells. Interestingly, despite these uniform phenotypic changes, ODN 2006 stimulated an ***increase*** in CLL cell migration in only a subset of '**Responder**' patient samples. These migratory responses to ODN 2006 were inhibited by the use of a TLR9 antagonist (ODN INH-18), showing these responses to be TLR9-dependent.

CLL patients can be divided into two main prognostic subgroups according to the mutational status of the BCR immunoglobulin gene (IGHV) and previous studies have reported patients with unmutated IGHV genes (U-CLL) to have a poorer clinical outcome due to a heightened propensity for BCR signalling relative to patients with mutated IGHV genes (M-CLL). ODN 2006 stimulated a significant ***increase*** in CLL cell migration in the M-CLL but not U-CLL subgroup. Many U-CLL patient samples were ***non-responsive,*** and a subset even showed a ***decrease*** in CLL cell migration following TLR9 agonism. Preliminary data suggests TLR9 'Responder' and 'Non/Reverse Responder' samples to have different NF-κB activation signatures in response to ODN 2006.

In view of these results, the potential rationale for the therapeutic inhibition of both the BCR and TLR9 was investigated. In Responder samples, the simultaneous inhibition of BCR and TLR9 signalling (with ODN INH-18 and ibrutinib) showed a synergistic effect on the reduction of ODN 2006-induced CLL cell migration and NF-κB activation. Additionally, ibrutinib exposure appeared to increase the sensitivity of U-CLL Non/Reverse Responder samples to stimulation with ODN 2006. This indicates that TLR9 signalling could mediate ibrutinib resistance in both M-CLL and U-CLL patients. Taken together, these data highlight a role for TLR9 in CLL cell activation and migration and suggest that dual targeting of the BCR and TLR9 may be a promising therapeutic strategy for CLL patients.

Table of Contents

Table of Tables:

Table of Figures:

Acronyms:

(AID)	Activation-induced cytidine deaminase
(AP-1)	Activator protein 1
(ATM)	Ataxia-telangiectasia mutated
(BCA)	Bicinchoninic acid assay
(BCL-2)	B-cell lymphoma 2
(BCR)	B-cell receptor
(BIRC3)	Baculoviral IAP repeat containing 3
(BM)	Bone marrow
(BMSCs)	Bone marrow derived stromal cells
(BR)	Bendamustine and rituximab
(BSMS)	Brighton and Sussex Medical School
(BTK)	Bruton's tyrosine kinase
(CHD2)	Chromodomain helicase DNA binding protein 2
(CI)	Combination index
(CLL)	Chronic lymphocytic leukaemia
(CpG-ODN)	CpG-rich oligonucleotide
(DAMPs)	Danger associated molecular patterns

(DD) Death domain

(dH_20) Distilled H_20

(DMSO) Dimethyl sulfoxide

(ECM) Extracellular matrix

(ED50) Effective dose 50

(ELISA) Enzyme-linked immunosorbent assay

(ER) Endoplasmic reticulum

(FACS) Fluorescence-activated cell sorting

(FC)(R) Fludarabine + cyclophosphamide ± rituximab

(FCS) Foetal calf serum

(FMO) Fluorescence minus one

(FSC-A) Forward scatter-area

(FSC-H) Forward scatter-height

(FVD) Fixable viability dye

(HCl) Hydrochloric acid

(HEVs) High endothelial venules

IGHV Immunoglobulin heavy chain variable region

(IL-4) Interleukin-4

(IMGT) ImMunoGeneTics

(IRAK-4) Interleukin-1 receptor-associated kinase 4

(ITAMs) Immunoreceptor tyrosine-based activation motifs

(IκB) I-kappa-B

(IκBα) I-kappa-Bα

(LDT) Lymphocyte doubling time

(LN) Lymph nodes

(LN-CLL) Lymph node-derived CLL cells

(MAPK) Mitogen-activated protein kinase

(M-CLL) IGHV-mutated

(MFI) Mean fluorescence intensity

(mtDNA) Mitochondrial DNA

(MyD88) Myeloid differentiation response 88

(NaCl) Sodium chloride

(NF-kB) Nuclear factor kappa B

(NIK) NF-κB-inducing kinase

(ODN) Oligonucleotide

(OS) Overall survival

(PAMPs) Pattern associated molecular patterns

(PB) Peripheral blood

(PB-CLL) PB-derived CLL cells

(PBMCs) Peripheral blood mononuclear cells

(PBS) Phosphate buffered saline

(PBS-T) PBS-Tween 20

(PFA) Paraformaldehyde

(PFS) Progression free survival

(PI3K) Phosphatidylinositol 3-kinase

(PLCγ2) Phosphatidylinositol-4,5-biphosphate phosphodiesterase gamma-2

(PRRs) Pattern recognition receptors

(QOL) Quality of life

(RIPA) Radioimmunoprecipitation

(RSCH) The Royal Sussex County Hospital

(SD) Standard deviation

(SDS) Sodium dodecyl sulfate

(SEM) Standard error of the mean

(SF3B1) Spliceosome factor 3b 1

(SSC-A)	Side scatter-area
(Sseq)	Sanger sequencing
(STAT3)	Signal transducer and activator of transcription 3
(sTLR9)	Surface TLR9
(SYK)	Spleen associated tyrosine kinase
(TCR)	T-cell receptor
(TIR)	Toll/interleukin 1 receptor domain
(TLR)	Toll-like receptor
(TLR9)	Toll-like receptor 9
(TP53)	Tumor protein P53
(TRAF6)	Tumour necrosis factor 6
(TTFT)	Time to first treatment
(U-CLL)	IGHV-unmutated
(u-CpG)	Unmethylated CpG
(V(D)J)	V (variable), D (diversity) and J (joining)
(VCAM-1)	Vascular cell adhesion protein 1
(VLA-4)	Very late antigen-4

Acknowledgements

Firstly, I would like to say a massive thank you to my incredible supervisors Andrea Pepper and Chris Pepper who have given me an overwhelming amount of time and support over the past three years. I am extremely lucky to have had you both to guide me through this experience, particularly during these last few months when Andrea, you have lived and breathed this thesis with me. I am so very grateful for your efforts and recognise that you truly go above and beyond for your students! I would also like to thank the other members of Team Pepper: Gemma Hamilton, Tom Burley, Simon Mitchell, Eleni Ladikou and Kim Sharp. Thank you, Gemma, for being the queen of reagent ordering and always making sure our team has everything we need to keep our experiments running smoothly and thank you, Tom, for helping me out with my recent western blotting optimisations. Thank you also to Helen Stewart and Sarah Unterberger for their knowledge of western blotting!

This research would not have been possible without the help of the haematology department at The Royal Sussex County Hospital. I would like to thank Rosalynd Johnston in particular for her involvement in the patient recruitment and sample collection aspect of this project. I am also extremely grateful to all the CLL patients who consented for their blood samples to be used by our team and wish them the best in their treatment journey.

I would like to take a moment to acknowledge (but not thank!) the COVID-19 pandemic! When I moved to Brighton to begin my PhD project, I could never have imagined that three years later I would be writing my thesis, whilst living alone in complete lockdown. It has been a strange and unique experience (and a struggle at times) but I would like to say a massive thank you to all of the people who have supported me, including:

MY PARENTS: Thank you for providing me with a lovely flat in Brighton Marina to live in (rent-free) and for sending regular survival packages filled with doughnuts, chocolate and fleecy loungewear! I couldn't have achieved this without your help.

MY FRIENDS (Cathryn [Moose], Andy, Layla, Catherine, Jo, Annelie [Sonoma] and Gemma): Thank you for checking in on me via text messages/Snapchat/Zoom while I have been in lockdown alone for months on end. I am very lucky to have such great friends!

MY LOCKDOWN BUDDIES: When I say I have lived alone, I have not been completely alone, and I cannot finish this acknowledgements page without thanking my beautiful lockdown buddies: Fiona Ratty, Nancy Notts, Sidney Sausage and Ernie Burns (The Rattinis). Their ratty-antics have kept me entertained through lockdown and made this experience so much more bearable!

Author's Declaration:

I declare that the research contained in this thesis, unless otherwise formally indicated within the text, is the original work of myself. The thesis has not been previously submitted to this or any other university for a degree and does not incorporate any material already submitted for a degree.

Emma Kennedy

23.07.21

1.0: Introduction

1.1: What is Chronic Lymphocytic Leukaemia (CLL)?

Chronic Lymphocytic Leukaemia (CLL) is an incurable haematological malignancy characterised by the clonal accumulation of CD5/CD19-positive mature-looking B-lymphocytes within the peripheral blood (PB) and secondary lymphoid tissues[1]. Whilst CLL is a typically slow growing and indolent malignancy (with 5- and 10-year survival rates of ~91% and 81% respectively, in patients diagnosed between the ages of 60-69[2]), a subset of patients experience an aggressive disease course with rapid disease progression[3]. CLL is a malignancy of immense biological and clinical heterogeneity[3] and there consequently remains a lot to be discovered regarding the complex pathology of this disease.

1.2: Epidemiology and Disease Presentation

CLL is most prevalent in western populations where it comprises 22-30% of all leukaemia diagnoses and 90% of all chronic lymphoid cancers[1,4-6]. An estimated 3,800 people are diagnosed with CLL each year in the UK, accounting for 1% of all new cancer diagnoses[4]. The UK incidence rate of CLL equates to ~3 in 100,000 males and ~2 in 100,000 females[6]; approximately 60% of all CLL cases are male[5].

A typical CLL patient is diagnosed in late adulthood between the ages of 64-70; approximately 80% of patients are >60 years old at the time of diagnosis and the risk of CLL development increases steadily with age[5,6]. Interestingly, up to 25% of CLL diagnoses occur in asymptomatic patients following routine blood tests, and these patients may continue to live symptom-free for many years[6]. Patients who are

diagnosed with symptomatic and/or advanced stage CLL most typically present with lymphadenopathy (80%) and/or splenomegaly (50%) with accompanying symptoms such as: fatigue, fevers, night sweats and weight loss[6,7]. These symptoms are a result of the clonal accumulation of malignant B-cells within the peripheral blood and secondary lymphoid tissues and the consequential malfunction of the immune system and normal haematopoiesis; patients often develop both anaemia and thrombocytopenia in addition to experiencing recurrent infections[6,7].

1.3: Diagnosis, Clinical Staging and Prognosis of CLL

A diagnosis of CLL requires a multidisciplinary investigation. Patients undergo a series of routine and specialised laboratory tests accompanied by a physical staging examination. A final diagnosis is reached by amalgamating data from: peripheral blood differential cell counts; morphological assessment and immunophenotyping.

White Blood Cell Differentials: A persistent lymphocytosis, for a minimum of three months, is indicative of leukaemia and can be identified from a routine full blood count analysis[7].

Morphology: A blood film is created to assess the morphology of the persistent B-lymphocytosis. CLL cells are identified as small, mononuclear B-cells with limited cytoplasm and are characteristically interspersed with large 'smudges' of apoptotic material[7]. 'Smudge cells' are technical artefacts which are fairly specific to CLL; they are caused by the rupture of their characteristically fragile cell membranes during the preparation of a blood film.

Clonality: B-cell Receptor (BCR) clonality can be inferred by flow cytometry. In a healthy individual, B-lymphocytes are polyclonal and express BCR-light chain polypeptides at a ratio of 2:1. In patients with a malignant B-lymphocytosis, the clonal BCR will express either kappa (κ) or lambda (λ) light chains and these cells will dominate the B-cell population. A skewed light chain ratio is indicative of B-cell clonality[7].

Phenotype: Flow cytometry is used to identify a CLL-like phenotype. A CLL diagnosis is dependent on the expression of a specific panel of cell surface markers i.e., expression of CD5 (normally expressed on T-cells and not B-cells), CD19, CD23 and low expression of CD20 and surface IgM[7]. In addition to the 'required' CLL panel Rawstron et al.,[8] suggested that a firm diagnosis of CLL should also depend upon the expression of 4-5 of the following 'recommended' antigens: CD43, CD79b, CD81, CD200, CD10 and ROR1.

Following a diagnosis of CLL, clinical staging examinations are performed to assess the severity of disease at initial presentation. This enables clinical decisions to be made regarding potential treatment initiation and also gives an indication of prognosis. Patients undergo both a physical examination and a full blood count analysis and are staged according to either the Rai (1975) or Binet (1981) staging guidelines for CLL. Both methods were devised in the mid-late 1970's (with Binet being revised in 1981) and are still widely used in modern clinical analyses[9-11]; the staging criteria for each method are outlined below in Table 1 (Rai) and Table 2 (Binet). As CLL progresses, patients typically experience lymphocytosis →

lymphadenopathy → splenomegaly/organomegaly → haematological disturbance (i.e., anaemia and thrombocytopenia).

Table 1.1: The Rai (1975) Clinical Staging System for the Clinical Staging of CLL

Rai Stage	Clinical Symptoms
0	PB + BM lymphocytosis
1	PB + BM lymphocytosis Enlarged nodes
2	PB + BM lymphocytosis Enlarged nodes Enlarged spleen and/or liver
3	PB + BM lymphocytosis Enlarged nodes Enlarged spleen and/or liver Anaemia (<11g/dL)
4	PB + BM lymphocytosis Enlarged nodes Enlarged spleen and/or liver Anaemia (<11g/dL) Thrombocytopenia (<100,000/μL)

PB= peripheral blood, BM= bone marrow

Table 1.2: The Binet (1981) Clinical Staging System for the Clinical Staging of CLL

Binet Stage	Clinical Symptoms
A	PB + BM lymphocytosis
B	PB + BM lymphocytosis ≤2 involved areas
C	PB + BM lymphocytosis ≥ 2 involved areas ± Anaemia (<10g/dL) ± Thrombocytopenia (<100,000/μL)

PB= peripheral blood, BM= bone marrow

Patients progress through the above outlined stages of CLL with remarkable heterogeneity and a significant limitation of both the Rai and Binet staging systems is their inability to predict the rate of disease progression in individual cases. As many as 80% of CLL cases are diagnosed in the early stages of disease and patients will either experience an indolent disease course, with stable/slow progression or an aggressive disease course with rapid progression[12]. A number of prognostic biomarkers now complement the Rai and Binet staging system and are outlined in Table 1.3 overleaf:

Table 1.3: Prognostic Markers to Complement the Clinical Staging of CLL

Prognostic Marker	Good/Poor Prognosis
Patient Age >65yrs	***Poor Prognosis:*** Increased number of driver mutations, reduced tolerance for chemo(immuno)therapeutic intervention and reduced overall survival[13,14]
Lymphocyte Doubling Time (LDT)	A LDT of 12 or less months identifies a population of patients with ***poor prognosis***, a LDT higher than 12 months is indicative of ***good prognosis.*** [15,16]
Markers of BCR Signalling	***(See: BCR Activation in CLL: 1.7.3)***
IGHV-Mutated (M-CLL)	***Good Prognosis:*** Indolent disease, slow disease progression, longer TTFT (9.2 years). [17,18,19,3]
IGHV-Unmutated (U-CLL)	***Poor Prognosis:*** Aggressive disease, rapid progression, high number of driver mutations, shorter TTFT (3.5 years) and inferior response to chemo(immuno)therapeutic agents. [17,18,19,3,20]

Prognostic Marker	Good/Poor Prognosis
Markers of BCR Signalling	(***See: BCR Activation in CLL: 1.7.3)***
Zap-70 Expression (>20% +ve: intracellular)	***Poor Prognosis:*** Aggressive disease, associated with U-CLL, shorter TTFT (2.9 years vs. 9.2 years)[19].
Genetic Aberrations	***(See Chromosomal Aberrations: 1.6.2.1 and Genetic Mutations 1.6.2.2)***
Deletion: Chr. 13q *(Chr.13q (del))*	***Good Prognosis***: Stable disease with increased TTFT (92 months vs. 42 months)[21].
Deletion: Chr. 11q *(Chr.11q (del))*	***Poor Prognosis*** Advanced, aggressive and symptomatic disease, younger age of onset, extensive nodal involvement, shorter TTFT (13 months vs. 42 months)[21].
Deletion: Chr. 17p *(Chr. 17p (del))*	***Poor Prognosis****:* Advanced, aggressive and symptomatic disease, short TTFT (9 months vs. 42 months), poor response to chemotherapy and extremely low 5-year survival rate (10.1%).[21,22]

Prognostic Marker	Good/Poor Prognosis
Genetic Aberrations	***(See Chromosomal Aberrations: 1.6.2.1 and Genetic Mutations 1.6.2.2)***
TP53 Mutation	***Poor Prognosis:*** Biologically equivalent to Chr.17p (del) as TP53 is located on Chr.17p[3].
Driver Mutations (NOTCH1, ATM, SF3B1, BIRC3, CHD2, TP53, MyD88)	***Poor Prognosis:*** The number of low frequency driver mutations correlates with TTFT and OS. TP53 and SFB1 are independent markers of PFS, TTFT, OS. TP53 mutations are biologically equivalent to Chr.17p (del) as TP53 is located on Chr.17p.[3,23]
Biochemical Parameters	
β_2-Microglobulin (MHC class I associated protein)	***Poor Prognosis:*** High concentrations are associated with shorter PFS, TTFT, lower rates of complete remission and OS[24].
Markers of Tissue Homing	***(See: Transendothelial Cell Migration: 1.7.1)***
CD38 Expression (>20-40% +ve: cell surface) *The precise threshold for CD38 positivity has been debated and groups have used cut off values of 20-40%.*	***Poor Prognosis:*** Progressive disease, lymphocyte doubling time <12 months, shorter TTFT (73% vs. 25% require treatment <5years), inferior response to chemotherapy[16,25,26]

Prognostic Marker	Good/Poor Prognosis
Markers of Tissue Homing	***(See: Transendothelial Cell Migration: 1.7.1)***
CD49d Eexpression (>30% +ve: cell surface)	***Poor Prognosis:*** Progressive disease, shorter TTFT (58% vs. 32% require treatment <5years), strong predictor of OS.[27,28]**.**

OS = overall survival, PFS = progression free survival and TTFT = time to first treatment. The biological relevance of each prognostic marker is detailed in the given referenced sections.

An international prognostic index has been devised by a group of international CLL investigators incorporating 5 independent prognostic markers of overall survival i.e., age, clinical staging, IGHV-mutational status, β_2-microglobulin concentration and TP53 status[13]. By assigning each marker with a weighted numerical risk value, individual patients are assessed and given a calculated risk score of between 0-10 and are categorised accordingly into: low (0-1), intermediate (2-3), high (4-6) and very high-risk (7-10) groups. The 5-year overall survival rates of each group are 93.2%, 79.3%, 63.3% and 23.3%, respectively[13].

1.4: Clinical Approach

The clinical approach to the management of CLL is remarkably unusual in comparison to other cancers. Following a diagnosis of CLL, the majority of patients will **not** require immediate treatment[5]. Instead, a unique monitoring procedure coined 'watch and wait' is implemented to track the rate of disease progression and identify the optimal time for treatment initiation. For the most-part, CLL is a chronic illness with slow

progression and up to a third of CLL patients may never require therapeutic intervention. In a recent paper, Herling et al.,[29] concluded that there was no overall survival benefit to early intervention, even in the most clinically high-risk patients. In fact, earlier studies have reported chemotherapeutic exposure, or treatment with the targeted agent ibrutinib, can promote clonal evolution, resulting in the emergence of aggressive and resistant subclones[23,30,31]. Premature treatment of indolent cases of CLL may therefore be detrimental to patient prognosis and longevity and treatment initiation should be reserved for late-stage disease.

An unconventional approach like this carries an enormous emotional burden. In 2007, Levin et al.,[32] conducted a quality of life (QOL) study with a focus on the comparative mental wellbeing of CLL patients categorised into 'watch and wait' and 'active-treatment' subgroups. Despite having indolent and early-stage disease, the depression and anxiety scores of the 'watch and wait' patient group were the same as those of the 'active-treatment' patient group. These scores were also found not to improve with time suggesting that 'watch and wait' patients experience a prolonged emotional burden whilst living with this chronic illness. It is also worthy of note that the 'watch and wait' patients reported similar bodily pain scores to the 'active-treatment' patients, suggesting that this malignancy has a negative physical and psychological effect on the daily lives of treatment-naïve patients.

Current treatment options for CLL comprise of harsh chemo(immuno)therapy regimens or lifelong prescriptions of orally administered, targeted therapies including: ibrutinib, idelalisib and venetoclax, (targeting Bruton's Tyrosine Kinase (BTK), Phosphatidylinositol 3-kinase (PI3K) and B-cell Lymphoma 2 (BCL-2),

respectively). Although the development of targeted therapies has revolutionised the treatment of CLL, these agents control rather than cure the disease. (*Treatment options for CLL are discussed in further detail in a later section*).

1.5: Healthy B-Cells and the Adaptive Immune Response

CLL is characterised by the accumulation of mature-looking malignant B-cells. The physiological form and function of a mature B-cells is outlined below:

1.5.1: What is a B-Cell?

B-cells are small, mononuclear white blood cells comprising 5-10% of the lymphocyte population[33]. Lymphocytes constitute 25-33% of the total white blood cell count[33] and are critical components of adaptive immunity; despite existing in relatively low numbers, B-lymphocytes play a pivotal role in mediating an immune response. B-cells survey the peripheral blood and secondary lymphoid tissues and become activated following BCR engagement by antigen. As a result of BCR-stimulated activation, antigen-experienced B-cells are stimulated to proliferate and to differentiate into antibody-secreting cells. The resulting antibodies are tailored to the targeted antigen, enabling a highly specific immune attack. Mature B-cells can be divided into three differentially distinct subgroups:

1) Naïve B-cell (i.e., antigen inexperienced): a resting and inactive B-cell which is yet to recognise a complementary antigen
2) Plasma cell (i.e., an antigen experienced and differentiated B-cell): an activated antibody secreting B-cell, no longer expressing surface BCR

3) Memory B-cell: (i.e., an antigen experienced and long-lived B-cell): a quiescent and antigen-specific contributor to immune memory; memory B-cells are rapidly activated following a secondary invasion of the corresponding pathogen (Figure 1.1)

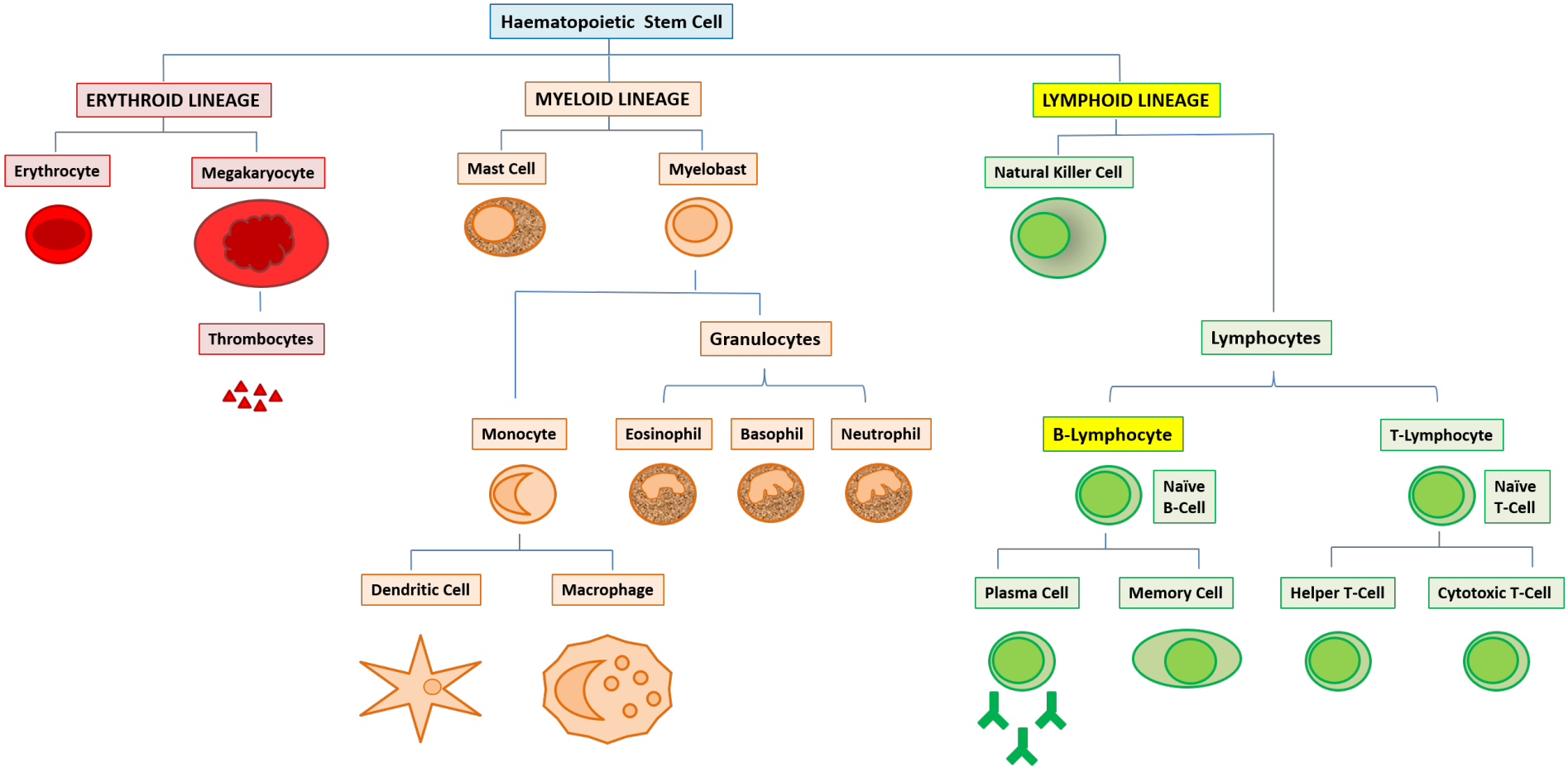

Figure 1.1: Blood Cell Lineages. B-cells (B-lymphocytes) derive from the lymphoid lineage of haematopoiesis and together with T-cells (T-lymphocytes) comprise the 'lymphocyte' population of white blood cells. B-cells are small, mononuclear cells and upon antigen-activation, can differentiate into antibody secreting plasma (effector) cells or larger, quiescent memory cells (which rapidly re-activate in the event of a secondary infection).

1.5.2: B-Cell Receptor (BCR) Diversity

Antigenic structures are highly variable from pathogen to pathogen and B-cells are therefore required to recognise an enormous array of 'non-self' molecular patterns. BCR diversity is therefore fundamental to antigen recognition. In a healthy individual, the B-cell population is polyclonal, meaning that each naïve B-cell expresses a BCR of unique antigen specificity; this incredible repertoire enables responses to an immensely diverse range of invading pathogens from a relatively small pool of naïve cells. Once activated, the now antigen-experienced B-cell undergoes clonal expansion to drastically increase the abundance of the relevant BCR.

The BCR complex is composed of a membrane bound immunoglobulin (antibody) and a signal transducing heterodimer (Igα/Igβ); the co-receptor CD19 is also in close proximity to the complex and acts to enhance the intensity of BCR signalling (Figure 1.2a). The antigen-binding domain resides within the immunoglobulin component of the receptor and is assembled during B-cell development following a unique somatic recombination event called V(D)J recombination[34-36].

Immunoglobulins (antibodies) are Y-shaped glycoproteins consisting of 4 polypeptide chains (i.e., 2x heavy chains and 2x light chains)[37]. The heavy chain of an immunoglobulin determines the antibody effector function and in naïve B-cells can be transcribed as mu (μ) or delta (δ) isotypes. The light chain of an immunoglobulin contributes only to antigen specificity and can be transcribed as one of two isoforms: kappa (κ) or lambda (λ). In the BCR complex, the receptor-immunoglobulin is composed of the μ-heavy chain (i.e., IgM) and either the κ or λ light chains. Figure

1.2b depicts the structure of an IgM antibody and shows the antigen binding domain, formed from the variable regions of both the heavy and light Ig chains[37].

B-cell receptor diversity is initially generated by genetic rearrangement. The variable region of the heavy chain is composed of V (variable), D (diversity) and J (joining) sections, each of which can be transcribed from a multitude of available somatic gene fragments[37]. During BCR development, chromosomal breakages are established at each locus and a unique combination of V, D and J segments are ligated together in a process called V(D)J recombination; the process is then repeated at the variable region of the light chain (which contains V and J sections only)[36]. Each BCR expresses a unique amalgamation of heavy and light chain variable fragments and is consequently of unique antigen specificity; V(D)J recombination gives rise to an extraordinary 10^{15} possible combinations [34].

Remarkably, following antigen-exposure, the affinity of the BCR-IgM for the recognised antigen can be further improved. During a process named somatic hypermutation, a succession of point mutations is introduced into the variable regions of both the heavy and light chains, resulting in conformational changes in the antigen-binding domain[37]. The mutational status of the BCR-IgM can be used to distinguish an antigen-naïve B-cell from an antigen-experienced B-cell. Somatic hypermutation is mediated by the enzyme Activation-Induced Cytidine Deaminase (AID), which stimulates the deamination of cytosine to uracil and consequentially induces mismatch lesions within the DNA template; these lesions are then preferentially repaired by error-prone polymerases encouraging the onset of genetic mutations[35,37]. The mutation rate of the Ig loci is ~6 orders of magnitude higher than

elsewhere in the genome, enabling a huge capacity for diversification and hence the generation of a highly targeted immune response[35].

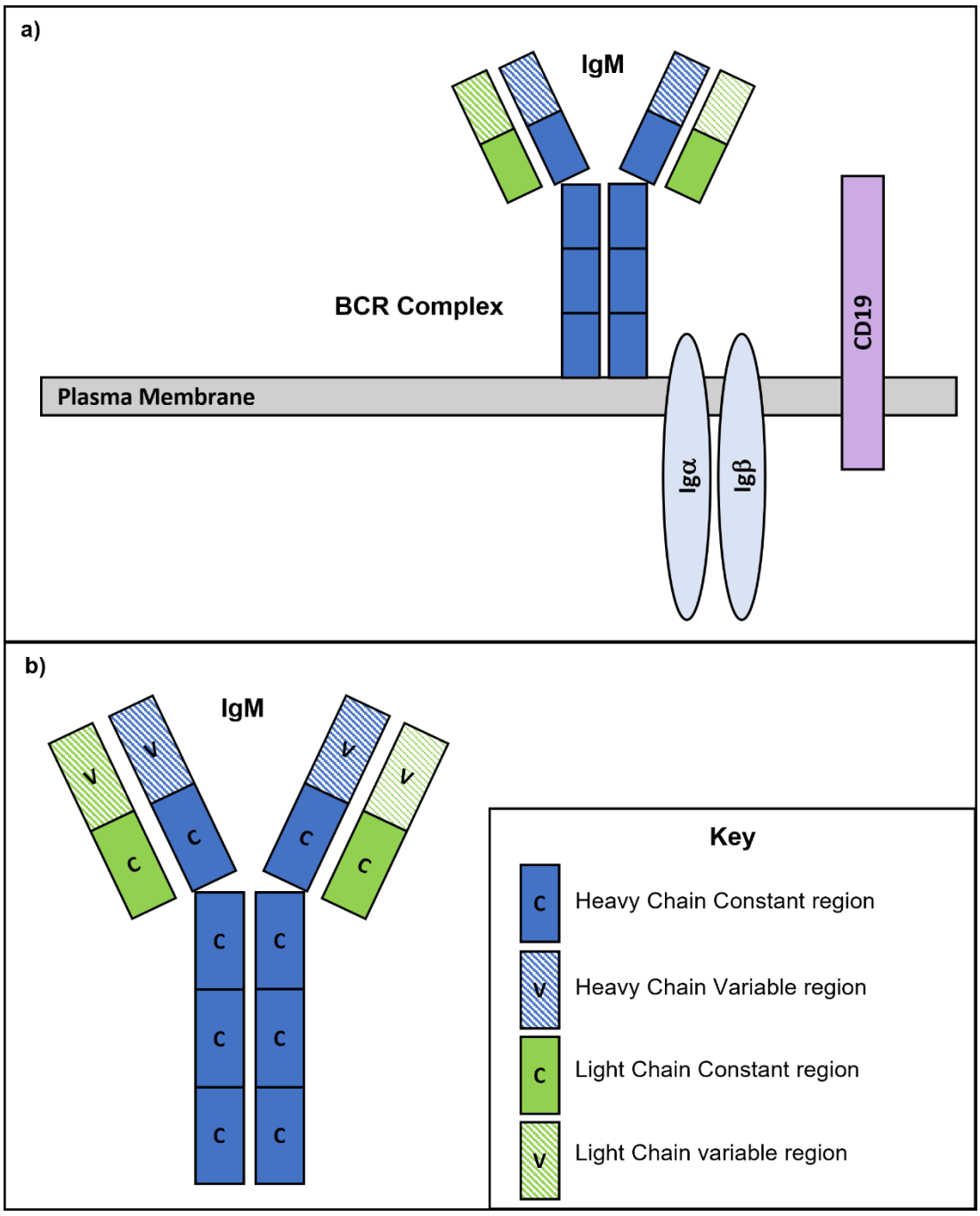

Figure 1.2: The B-Cell Receptor Complex. a) the B-cell receptor complex (BCR) comprises a surface-bound IgM molecule, a signal transducing heterodimer (Igα/Igβ) and the signal enhancing co-receptor CD19. b) The IgM component of the BCR complex consists of 2x (μ) heavy chain and 2x (κ or λ) light chain polypeptides. Each heavy chain is made up of 4x constant domains and 1x variable domain and each light chain is made up of 1x constant and 1x variable domain.

1.5.3: BCR Signalling

Following BCR-antigen binding, the tyrosine kinase, Lyn, phosphorylates tyrosine residues within the immunoreceptor tyrosine-based activation motifs (ITAMs) of the signal transducing heterodimer, Igα/Igβ, and also tyrosine residues within the cytoplasmic tail of the BCR co-receptor, CD19[38]. Following phosphorylation of the Igα/Igβ ITAMs, the tyrosine kinase, SYK, is recruited enabling the recruitment and activation of Bruton's Tyrosine Kinase (BTK). In turn, BTK recruits and activates PLCγ2 enabling the initiation of a number of signalling cascades including MAPK and NF-κB activation[38]. In parallel, PI3K is recruited to phosphorylated CD19, which can also induce NF-κB activation via AKT[38] (Figure 1.3). Activation of NF-κB is critical for the development, activation, proliferation and survival of B lymphocytes.

1.5.4: B-Cell Trafficking

Lymphocyte trafficking is an integral component of the adaptive immune response. Given the polyclonality of the B-cell population, it is vital that the correct B-cells encounter the correct antigens. In order to enhance the likelihood of complementary pairings, B-cells and antigen regularly exit the circulation and migrate into specialised secondary lymphoid tissues (i.e., the lymph nodes, the bone marrow and the spleen)[39]. The secondary lymphoid tissues are the social hub of the immune system where naïve B-cells and T-cells, congregate together with antigen and antigen presenting cells (the lymph nodes (LN) are the main site of B-cell activation and proliferation)[40]. Lymphocytes exit the circulation following transendothelial migration and enter the secondary lymphoid tissues through specialised high

endothelial venules (HEVs); this process is mediated via the expression of cell surface adhesion molecules i.e., selectins (e.g., CD62L) and integrins (e.g., $\alpha4\beta1$)[41,42].

Upon entry into the LNs, naïve B- and T-cells are shuttled into discrete designated areas to explore multiple interactions with resident antigen presenting cells[39]. Naïve B-cells are contained within specialised 'follicles' and in the event of antibody recognition, BCR-signalling is initiated and activated B-cells migrate towards LN areas containing antigen-activated T-cells[39]. Activated B- and T-cells then interact via CD40:CD40L, stimulating a second activation signal resulting in the initiation of an antigen-specific immune response. Conversely, if a B-cell does not recognise any of the LN-resident antigens, it exits the LN unchanged and re-enters the circulation[39].

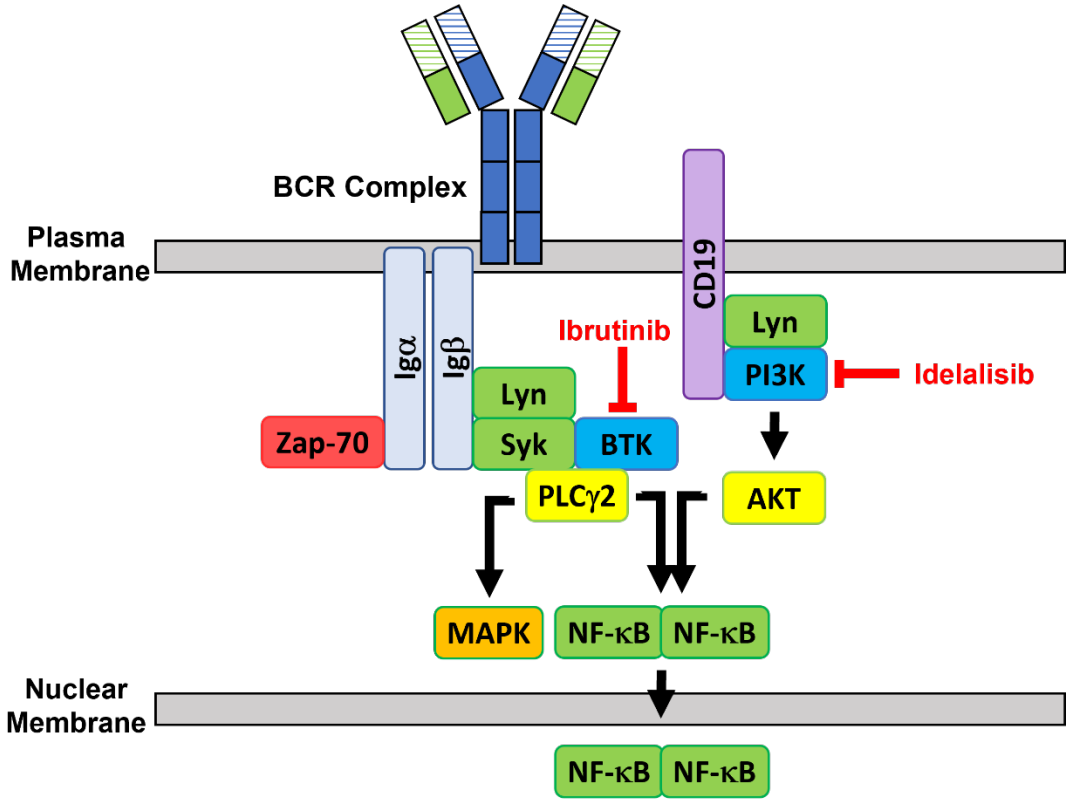

Figure 1.3: The B-cell Receptor Signalling Pathway. Following BCR-antigen binding, the Igα/Igβ is phosphorylated by Lyn. This leads to the recruitment and activation of SYK and in turn, the recruitment and activation of BTK. BTK recruits and activates PLCγ2 resulting in the initiation of MAPK signalling and NF-κB activation. In parallel, Lyn phosphorylates CD19, enabling the recruitment and activation of PI3K, which induces the activation of NF-κB via AKT. In CLL, aberrant expression of the T-cell associated ZAP-70 kinase, amplifies BCR signalling. Targeted agents ibrutinib and idelalisib inhibit BTK and PI3K activation respectively, leading to the inhibition of BCR signalling.

1.6: CLL Pathology

A CLL cell is a malignant derivative of a mature B-cell. As mentioned earlier, CLL cells are small, mononuclear B-cells with limited cytoplasm and a distinctive diagnostic phenotype. CLL cells express a number of B-cell differentiation markers, including: CD5; CD19; CD23 and low level CD20 and also have reduced expression of membrane-bound IgM, relative to healthy B-cells[7]. As the malignant clone proliferates, it monopolises the peripheral blood and secondary lymphoid tissues and B-cell polyclonality is lost. Each CLL cell expresses a common (clonal) BCR which dominates over physiological diversity. The clonal expansion of CLL cells occurs irrespective of affinity maturation and patients can be divided into two clinically distinct subgroups dependent on the mutational status of the BCR. IGHV-mutated CLL cells (M-CLL) have undergone somatic hypermutation and show <98% homology with germline Ig sequences, whilst IGHV-unmutated cells (U-CLL) have not undergone somatic hypermutation and show ≥98% homology with germline Ig sequences[7,17,18].

1.6.1: CLL Cell of Origin

In 1999, Hamblin et al.,[18] suggested U-CLL and M-CLL to comprise two separate diseases deriving from distinct stages of differentiation (i.e., U-CLL from antigen-naïve and M-CLL from antigen-experienced B-cells). These suggestions sparked a two-decade long search for the healthy B-cell counterpart. In 2012, a comparative transcriptome analysis of B-cell subsets with CLL, revealed both M-CLL and U-CLL to cluster with naïve and CD5+ B-cells whilst memory B-cell subsets were located on a distinct and separate branch of the dendrogram; this appeared to refute the idea of

M-CLL cells being closer to antigen-experienced B-cell subsets than antigen-naïve B-cells and placed M-CLL and U-CLL closer together[43]. Both M-CLL and U-CLL were transcriptionally closest to CD5+ B-cells and it was concluded that U-CLL may derive from IGHV-unmutated CD5+ B-cells and M-CLL from a distinct IGHV-mutated CD5+ subset, which co-expresses the memory cell marker CD27[43]. Epigenetic studies have identified a discordance between gene expression and DNA methylation patterns in CLL and have suggested U-CLL cells to derive from naïve CD5+ B-cells and M-CLL to derive from memory B-cells[44]. A more recent publication however has suggested a less rigid classification, hypothesising that CLL may originate from a continuum of B-cell maturation states[45]; this group identified increased epigenetic maturity, as defined by increased gene methylation, to be a marker of disease indolence.

1.6.2: Aetiology of CLL

There is no single hallmark mutation underpinning the development of CLL. CLL is a malignancy of vast biological heterogeneity and individual patients express a combination of low frequency genomic changes[3,21,30]; CLL-associated oncogenic protein expression profiles result from an amalgamation of cytogenetic aberrations and genetic mutations encompassing: BCR-signalling; inflammatory-signalling; cell cycle regulation; apoptotic control; DNA damage repair; chromatin remodelling; NF-κB signalling; NOTCH1-signalling and RNA metabolism[3,23].

1.6.2.1: Chromosomal Aberrations

In 2000, an extensive study by Döhner et al.,[21] revealed that 82% of CLL cases demonstrated at least one cytogenetic abnormality. The biological implications of

the four most frequently found chromosomal aberrations i.e., (del) 13q14; (del) 11q; trisomy 12 and (del) 17p are outlined below:

Deletion of Chromosome 13q (Chr.13q (del)) is the most commonly occurring cytogenetic aberration in CLL and is present in approximately 55% of cases[21]. The Chr.13q locus codes for the tumour suppressing miRNA complex: miRNA-15a and miRNA-16-1 associated with the suppression of both apoptosis and B-cell proliferation[46,47]. In the absence of miRNA-15a/miRNA-16-1, CLL cells have shown increased levels of BCL-2 and a greater propensity for cell cycle entry and G0/G1-S phase progression[46,47]. In an *in vitro* experiment using a miRNA-15a/miRNA-16-1 knockout mouse model, Klein et al.,[47] showed the spontaneous development of CLL in 21% of transgenic mice.

Despite the apparent oncogenic potential of chr.13q14(del), this frequently occurring aberration appears to significantly contribute to the chronic pathology of CLL. Patients harbouring chr.13q14 deletions as a lone chromosomal abnormality often experience an extremely ***stable*** disease course with a ***good*** clinical prognosis; strikingly, the clinical outcomes of Chr.13q-deleted patients are ***improved*** relative to patients with normal karyotype[21]. Loss of miRNA-15a/miRNA16-1 also gives rise to an upregulation of the tumour suppressor, P53[48]. P53 is a ubiquitous translational activator and has been coined 'the guardian of the genome' due to its complex anti-proliferative and pro-apoptotic functions; P53 can recognise and assess the severity of cellular stresses (e.g., DNA damage or oncogenic protein expression) and respond by initiating either a temporary or indefinite repression of the cell cycle followed by the induction of apoptosis of aberrant cells[49]. Deletion of Chr.13q14 therefore results

in a conflict of genotypic changes rendering affected cells simultaneously cell cycle-restricted and survival-induced. A further complexity of this aberration is its altered prognostic effect depending on its frequency within the tumour population and the size of the deletion. Patients with ≥65.5% CLL cells harbouring a Chr.13q deletion have a shorter time to first treatment (TTFT) than those with <65.5% CLL cells harbouring a Chr.13q deletion[50] and larger deletions are associated with an increased risk of disease progression[51].

Deletion of Chromosome 11q (Chr. 11q (del)): is present in ~18% of CLL cases[21]**.** Unlike Chr.13q (del), this aberration is associated with advanced, aggressive and symptomatic disease; patients with a Chr.11q deletion are often diagnosed at a younger age and suffer extensive nodal involvement[21,52]. The molecular consequences of a loss of Chr.11q include the loss of Ataxia-Telangiectasia Mutated (ATM) and Baculoviral IAP repeat containing 3 (BIRC3). ATM is a tumour suppressor gene and important mediator of the DNA damage response and loss of ATM functionality results in genome instability[53]. In 36% of patients with Chr.11q(del), additional mutations within the remaining ATM allele are present, and these patients have shown to have a poorer clinical outcome, relative to those harbouring Chr.11q(del)-alone[54]. BIRC3 is a negative regulator of NF-κB signalling and has been associated with a defective response to chemotherapy[55].

Trisomy 12: can be identified in 16% of CLL cases and is perhaps the least well-defined aberration[21]. It has however been associated with an increased cell surface expression of CD49d and a propensity for lymph node residency[26,56,57]. CD49d is coded for by the ITGA4 gene and functions as the alpha subunit of the integrin $\alpha 4\beta 1$;

it plays an integral role in the transendothelial trafficking of CLL cells from the peripheral blood to the secondary lymphoid tissues and is associated with progressive disease[42,58-60]. Zucchetto et al., [56] reported 89% of trisomy 12 patients to be CD49d positive as a result of a significant hypomethylation at the ITGA4 locus. Trisomy 12 patients have an intermediate prognosis[21], however the proportion of CLL cells expressing this aberration appears to affect disease progression. Patients with ≥60% trisomy 12 positive CLL cells have been found to have a worse prognosis relative to patients with <60% trisomy 12 positive CLL cells[61].

Deletion of Chromosome 17p (Chr.17p (del)): is present in 7% of CLL cases[21]. As described for Chr.11q (del), Chr.17p has been identified as a late onset aberration, associated with advanced, symptomatic and aggressive disease[21,22,30]; Chr.17p is also characteristically associated with a poor response to chemo(immuno)therapy[22] and has been found to exist at higher frequencies in relapsed patients following therapeutic intervention[30]. Contrary to Chr.13q (del), Chr.17p (del) results in the loss of function of the tumour suppressor P53, since the TP53 gene encoding the P53 protein is located at the Chr.17p locus[53]. *The prognostic implications of each chromosomal aberration are outlined above in Table 1.3*.

1.6.2.2: Genetic Mutations

In addition to chromosomal aberrations, a vast array of CLL-associated genetic mutations have been identified by Whole Exome Sequencing. In 2015, Puente et al.,[3] uncovered 36 recurrently mutated genes in a cohort of 452 CLL patients. Of these: NOTCH1 (NOTCH-signalling); ATM (cell cycle); SF3B1 (RNA metabolism); BIRC3 (NF-κB-signalling); CHD2 (chromatin structure); TP53 (apoptosis) and MyD88

(inflammatory signalling) were identified as being driver mutations in CLL. Despite being the seven most frequently mutated genes in CLL, each mutation was only identified in a minor subset of CLL patients ranging from 12.6% (NOTCH1) to 4% (MyD88). This again highlights the extensive biological heterogeneity of this malignancy.

1.7: The CLL Microenvironment

In addition to the above-described genetic aberrations, CLL progression is highly dependent upon microenvironmental interactions. The CLL microenvironment facilitates a complex network of immunogenic stimulation via BCR and innate immune receptors, cytokine signalling and physical contact with non-malignant accessory cells; these external stimuli promote CLL cell activation, proliferation and survival[40,62]. The reliance of CLL upon such interactions is highlighted by the fact that isolated CLL cells cannot maintain their viability in the absence of supporting cytokines and/or accessory cells. Co-culture experiments using: T-cells, endothelial cells, stromal cells and/or nurse like cells have been shown to greatly improve the *in vitro* viability of CLL cells[63-66].

Clinical progression is, at least in part, dependent upon the kinetics of CLL proliferation versus CLL apoptosis; in progressive disease, the rate of CLL cell birth is greater than the rate of cell death whilst in stable disease, the rates are in equilibrium[67]. Interestingly, irrespective of disease status, 99.5% of circulating CLL cells are arrested in the G0/G1 phase of the cell cycle, yet the CLL clone can expand by 0.1 to 1.75% per day (i.e., 10^9 to 10^{12} cells)[68]. Proliferation is environment-dependent and occurs almost exclusively within the lymph node niche[40]; CLL cell

migration from the peripheral blood to the secondary lymphoid tissues has therefore been identified as a fundamental contributor to the pathology of CLL. The secondary lymphoid tissues are protective havens for CLL proliferation and survival; tissue-resident CLL cells are exposed to antigen, pathogen associated molecular patterns (PAMPs), danger associated molecular patterns (DAMPs), cytokines and chemokines and cell: cell contact with: T-cells, stromal cells, nurse-like cells and macrophages[69].

Activated CLL cells further manipulate the microenvironmental niche by secreting a selection of disease promoting chemokines, consequently creating a positive feedback loop to promote their own survival and proliferation. Secretion of CCL3, CCL4, CCL12, IL-6 and IL-8 induces the recruitment of tumour-promoting accessory cells including macrophages and regulatory T-cells and the suppression of normal T-cell function[70,71]. Accessory cells can then contribute to CLL progression in either a paracrine manner (via the secretion of cytokines and chemokines) or via direct cell: cell contact (e.g., the binding of stromal cell expressed CD31 to CLL expressed CD38). Additionally, LN-derived CLL cells (LN-CLL) exhibit an immunosuppressive phenotype, thus evading immune-cytotoxicity and gaining immune-tolerance[62].

CLL has been described as a disease of two compartments since peripheral blood (PB) and tissue resident CLL cells exhibit distinctly different phenotypic signatures, reflective of their microenvironmental encounters[40,60]. Comparative gene expression profiling of *ex vivo* PB and lymph node (LN)-derived CLL cells placed BCR-signalling at the epicentre of the activated and proliferative LN-phenotype, suggesting BCR-activation to only occur within the LN niche; BCR and NF-κB-target genes were also reported to be significantly upregulated in LN-CLL relative to PB-CLL[40]. The bone

marrow niche is another important contributor to CLL cell survival and direct cell:cell contact with bone marrow derived stromal cells (BMSCs) has shown to induce an upregulation of the anti-apoptotic protein BCL-X_L and consequently confer resistance to a number of chemo(immuno)therapeutic and targeted agents[66,72]. Additionally, it has been shown to induce transcriptional changes in CLL cell adhesion to facilitate BM retention[72].

In contrast, PB-derived CLL cells (PB-CLL) are devoid of activation signals and therefore exhibit a non-activated and non-proliferative phenotype[40,62]. High basal levels of anti-apoptotic proteins e.g., BCL-2 however render PB-CLL cells capable of prolonged survival relative to healthy B-cell counterparts[73]. Additionally, PB-CLL show an overexpression of chemokine receptors specific for niche-resident chemokines, signifying a phenotype primed for tissue homing[62]. Directional CLL cell migration from the peripheral blood to the secondary lymphoid tissues (i.e., tissue homing) is a complex process that plays an important role in the pathology of CLL; tissue-homing is orchestrated by a plethora of adhesion molecules and chemokine/chemokine receptor interactions.

1.7.1: Transendothelial Cell Migration

CLL-cell-specific invadosome-like structures have been identified at the surface membrane of migratory CLL cells comprising markers of CLL cell adhesion (CD49d and CD44v), extracellular matrix degradation (MMP-9) and tissue-homing and proliferation (CD38). Together, these molecules are thought to co-ordinate CLL cell motility and extravasation; the surface expression of both CD49d and CD38 have been reported to be higher in migrated CLL cells relative to non-migrated CLL

cells[42,59,60] and both proteins show strong correlation with the chemokine receptor CXCR4 and chemotaxis towards its ligand CXCL12[74,75]. CXCR4 is the highly specific receptor for the LN and BM-secreted chemokine CXCL12 and plays a fundamental role in CLL cell tissue homing and clinical lymphadenopathy[39,42,76]. CD49d comprises the α-subunit of the integrin $\alpha4\beta1$/very late antigen-4 (VLA-4). Integrins are essential adhesion receptors implicated in the transendothelial migration of leukocytes across the endothelium; CD49d recognises both vascular cell adhesion protein 1 (VCAM-1) and fibronectin[74]. VCAM-1 is an endothelial and BM stromal cell-expressed adhesion molecule and fibronectin is an extracellular matrix (ECM)-expressed glycoprotein[74]. Together these interactions facilitate adhesion and rolling of CLL cells homing to the LN and BM compartments[42,74]. Furthermore, CD49d expression correlates to clinical lymphadenopathy, high BM infiltration and disease progression and has been identified as an independent prognostic marker of both TTFT and OS[27,42,58,74,75]. Interestingly, whilst CD49d was found to be required for the transendothelial migration of CLL cells, healthy B-cells did not show the same dependency and instead utilised an alternate alpha subunit (i.e., α_L)[42].

CD38 is a transmembrane glycoprotein comprising both enzymatic and receptor functionality and has been described to exert a diverse range of roles relating to cell metabolism, cell adhesion, survival and proliferation[74]. Although the wide range of CD38-stimulated effects are not fully understood, CD38 can be used as a marker of activation and recent cell division in CLL[67,74]. CD38 positivity has been correlated with an extremely short lymphocyte doubling time of <12 months, which is reflected in the more aggressive disease course in CD38 positive CLL patients[25]. There has been much debate over the years as to the 'cut off' percentage for CD38 positivity

however, using a cut off of >30% CD38 positive CD5+/CD19+ CLL cells, a study by Del Poeta et al.,[25] showed 73% of CD38 positive patients required treatment within 5 years of diagnosis, in contrast to just 25% of CD38 negative patients. This subgroup also displays an inferior response to chemotherapy[25].

1.7.2: Chemotaxis

CLL cells migrate towards the LN/BM niche against a chemotactic gradient. Gene expression profiling revealed PB-CLL to overexpress the chemokine receptors: CCR7, CXCR4, and CXCR5 signifying that PB-derived CLL cells are primed for tissue homing[62]. Each of the overexpressed receptors recognise specific chemokines, enabling directional trafficking. CCR7 is perhaps the earliest utilised receptor, recognising CCL19 and CCL21 upon the surface of high endothelial vesicles (specialised vessels promoting lymphocyte extravasation); CCR7 binding of CCL21 increases the expression of MMP-9, further promoting the extravasation and invasion of CLL cells[77].

CXCR4 and CXCR5 can then direct CLL cells towards their tissue resident ligands: CXCL12 and CXCL13 respectively[39,42,76]; both CXCL12 and CXCL13 are highly expressed within the BM and LN[62]. CXCR4 is particularly highly expressed in CLL and its expression can be correlated with disease progression as a result of increased tissue-homing[76]. In addition to the chemotactic role of CXCL12, activation of CXCR4 results in the increased adhesion of CD49d to endothelial and BM stromal expressed VCAM-1 and also the increased survival of CXCL12-stimulated CLL cells[74,76].

1.7.3: BCR Activation in CLL

BCR-signalling is stimulated in the LN-niche in response to a variety of antigens (and auto-antigens)[40,62]. CLL cells have been shown to react to a diverse range of pathogenic and self-antigens including: Cytomegalovirus; lipopolysaccharides; DNA; histones; insulin and cytoskeletal components of apoptotic cells, thus inferring the specificity of the CLL clone[78,79]. The responsiveness of CLL cells to antigen is implied in their downregulated expression of surface IgM; IgM is internalised post-antigen ligation therefore reducing its surface-expression[80]. BCR-signalling induces an activated and proliferative CLL phenotype and heavily contributes to the pathogenesis of CLL.

As previously described, CLL patients can be divided into two distinct subgroups according to the mutational status of the BCR-receptor immunoglobulin: i.e., IGHV-unmutated (U-CLL) and IGHV-mutated (M-CLL). The BCRs of U-CLL patients have not undergone somatic hypermutation and are consequently polyreactive. Conversely, the BCRs of M-CLL patients ***have*** undergone somatic mutation and consequently their BCRs have a higher antigen specificity when compared to their unmutated counterparts[78]; M-CLL cells are also less likely to recognise autoreactive antigens[79]. The biological differences in the BCR-signalling of the two subtypes is thought to contribute to the distinct clinical behaviour of the two subgroups. The IGHV-mutational status of a patient is a reliable prognostic marker, which remains consistent throughout the course of a patient's disease[17,18]. The U-CLL subgroup defines a cohort of patients with aggressive and poor prognosis disease with rapid progression and an inferior response to chemotherapeutic agents; the average TTFT

of U-CLL vs M-CLL patients is 3.5 years vs 9.2 years[19]. The differences between the BCR-signalling of U-CLL and M-CLL are outlined below:

1.7.3.1: IGHV-Unmutated CLL (U-CLL)

The U-CLL subgroup is associated with the aberrant expression of the tyrosine kinase ZAP-70[81]. In healthy B-cells, the BCR-signal is transduced via the BCR tyrosine kinase 'SYK' following antigen-receptor binding; antigen recognition stimulates the phosphorylation of SYK, which in turn initiates a B-cell activating signalling cascade (Figure 1.3). In U-CLL patients however the T-cell receptor-associated equivalent of SYK (i.e., ZAP-70) is often co-expressed alongside SYK, resulting in an intensified transmission of the BCR activation signal[81]. BCR-stimulated ZAP-70 positive CLL cells have shown significantly increased global tyrosine phosphorylation relative to ZAP-70 negative CLL cells[81]. ZAP-70 shows a strong association with U-CLL and therefore contributes to the highly activated phenotype characteristic of this aggressive subgroup[19,81]. In addition to ZAP-70, a number of genes have been revealed to be differentially expressed between the U-CLL and M-CLL subgroups. Strikingly, 47% of these identified genes are associated with BCR-activation[82].

U-CLL cells appear to be more highly dependent upon the CLL microenvironment and exhibit a greater sensitivity to BCR-activation than the more indolent M-CLL subgroup[83]. A study by Lanham et al.,[84] reported that 80% of U-CLL cases vs 20% of M-CLL cases positively responded to anti-IgM stimulation; the majority of M-CLL cases were shown not to activate SYK. In support of these findings Herishanu et al.,[40] described BCR target genes to be upregulated to a greater extent in the LN compartment of U-CLL relative to M-CLL. In U-CLL, BCR-stimulation induces the

upregulation of genes involved in BCR-signal transduction, transcription, cell cycle regulation and cytoskeletal organisation, leading to cell cycle progression and proliferation[85]. In addition to enhanced BCR signalling, U-CLL patients have been reported to harbour a greater number of driver mutations relative to M-CLL[3] and to have an overall association with the expression of other poor prognostic markers i.e., chr.17p(del)/TP53 mutations; NOTCH1 mutations and the expression of CD38 and ZAP-70[17-19,30,86].

1.7.3.2: IGHV-Mutated CLL (M-CLL)

BCR-signalling is not usually induced following BCR-activation in the M-CLL subgroup[80,84,85]. Instead, stimulation of M-CLL with anti-IgM usually promotes CLL cell anergy - a non-responsive and non-proliferative state of cell lethargy[80]. In healthy B-cells, anergy occurs as a result of sustained antigen ligation in the absence of a secondary activation signal and is associated with the onset of negative regulatory pathways[80]. Interestingly, whilst anergic healthy B-cells undergo apoptosis in response to an upregulation of the pro-apoptotic protein BIM, M-CLL cells evade BIM-mediated apoptosis through the overexpression of anti-apoptotic protein, BCL-2[80]. This means that despite being anergic, M-CLL cells can persist for significant durations thus fuelling the indolent and persistent nature of CLL. It is however important to note that M-CLL is not entirely indolent and that subsets of poorer prognosis M-CLL co-express unfavourable prognostic markers and are more responsive to BCR activation:

- A subset of CD38-expressing M-CLL patients for example have been identified showing positive/proliferative responses to stimulation with anti-IgM[80] and

these patients consequentially experience an uncharacteristically progressive disease.

- A subset of M-CLL patients with high surface expression of both CXCR4 and CD49d ($CXCR4^{hi}/CD49d^{hi}$) display a comparatively heightened dependence upon the BCR signalling pathway and a clinical outcome analogous to that of U-CLL[28].
- A subset of M-CLL patients with mutations in the Toll-like Receptor signalling adapter molecule MyD88, exhibit a shorter time to first treatment[87] and an overall prognosis comparable to U-CLL[88]. Toll-like receptor signalling is outlined below.

1.7.4: Toll-Like Receptor Signalling in CLL

B-cells respond to a broad range of pathogen-associated molecular patterns (PAMPs), which stimulate the Toll-like Receptor (TLR) family of innate pattern recognition receptors (PRRs). The TLR family comprises 10 type 1 integral membrane glycoproteins, each with individual ligand specificities for distinct PAMPs. TLRs are expressed upon the plasma membrane (i.e., TLR1, TLR2, TLR4, TLR5, TLR6 and TLR10) and endosomal membranes (i.e., TLR3, TLR7, TLR8 and TLR9) and most family members are expressed in B and CLL cells. Plasma membrane-expressed TLRs recognise and respond to structural components of extracellular pathogens e.g., lipopolysaccharide (TLR4) or flagellin (TLR5), whilst endosome-expressed TLRs respond to endocytosed nucleic acids e.g., double stranded RNA (TLR3) or unmethylated CpG-DNA (TLR9)[89].

In B-cells, all TLRs stimulate a highly conserved Myeloid differentiation response 88 (MyD88)-dependent signalling pathway; MyD88 is an adaptor protein comprising a c-terminus Toll/interleukin 1 receptor (TIR) domain and an N-terminus Death domain (DD)[90]. Upon ligand binding, the TIR domains of both the receptor and MyD88 interact to activate MyD88 and to recruit Interleukin-1 receptor-associated kinase 4 (IRAK-4) followed by IRAK-1 and IRAK-2; together, these proteins form the 'Myddosome' complex. A second adaptor protein: Tumour necrosis factor 6 (TRAF6) is then recruited to the Myddosome resulting in the activation of signalling cascades to activate the transcription factors: NF-κB, Activator protein 1 (AP-1) and signal transducer and activator of transcription 3 (STAT3)[90]. Figure 1.4 shows the TLR signalling pathway following activation of endosomal TLR9. TLR-signalling has been referred to as the third essential signal for B-cell activation; in 2006, Ruprecht and Lanzavecchia[91], reported B-cells stimulated with both signal 1 (BCR-activation) and signal 2 (T-cell engagement) showed incomplete activation. In the presence of TLR-activation (signal 3), the B-cells showed expansive proliferation, isotype switching and plasma cell differentiation. *In vitro* TLR stimulation revealed TLR1, TLR2, TLR6 and TLR9 to have the highest propensity for NF-κB and STAT3 activation in CLL cells[92]. Furthermore, gene expression profiling has identified an upregulation of TLR and TLR-signalling associated genes in LN-CLL, relative to PB-CLL in both U-CLL and M-CLL patients. Strikingly, the extent of amplification matched that observed for both the BCR and NF-κB signatures described above[93]. Interestingly co-stimulation of CLL cells using a mixture of TLR1, 2, 6 and 9 agonists was shown to increase the chemotactic response of CLL towards a CXCL12-gradient[92]. CXCL12 is a BM/LN-derived chemokine and chemotactic responses to this chemokine are indicative of CLL cell tissue homing

capacity. In support of these findings, the rate of CLL cell accumulation within the secondary lymphoid tissues was described to increase *in vivo* in a study utilising TIR8-knockout mice; TIR8 is a TLR decoy receptor/negative regulator of TLR signalling[94].

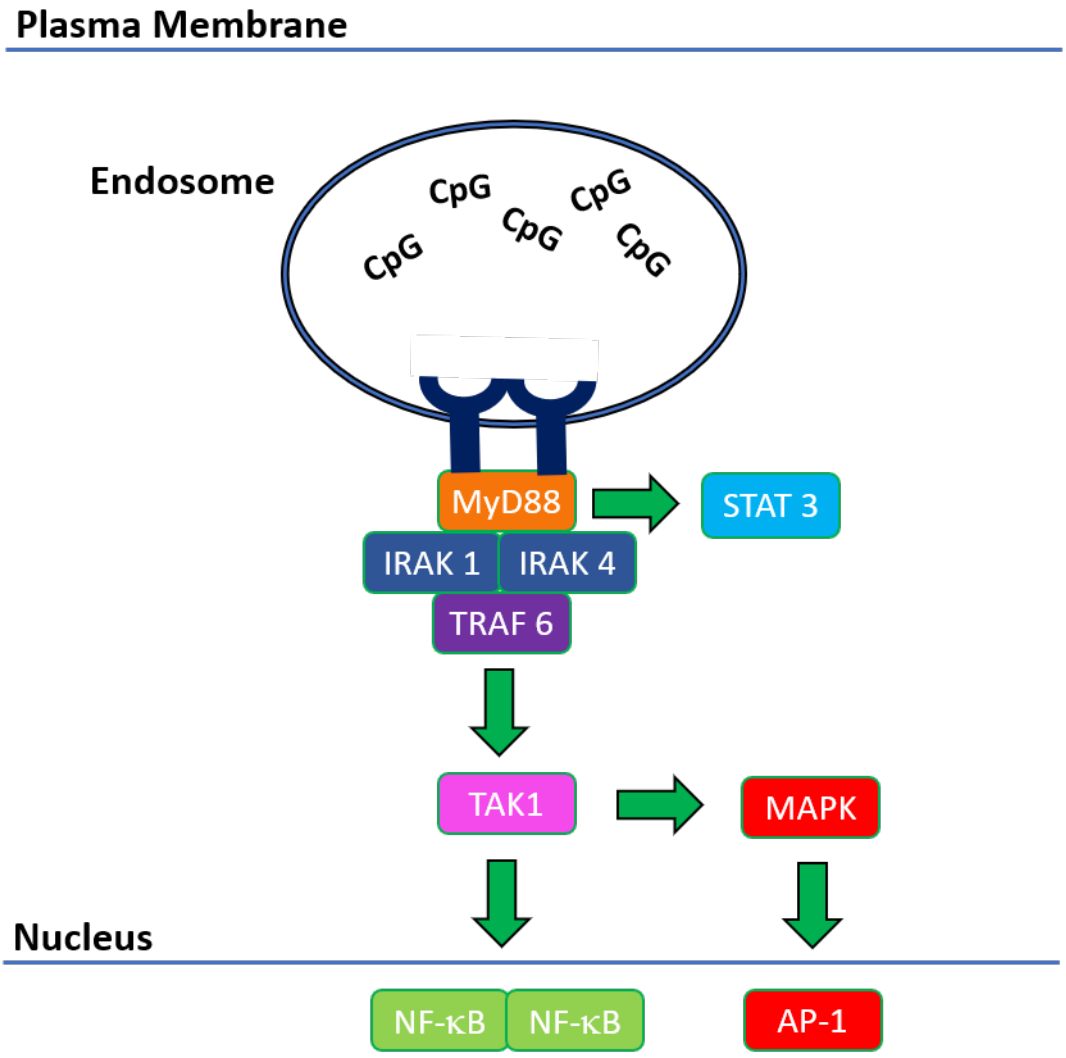

Figure 1.4: Toll-Like Receptor Signalling Pathway. TLR9 is located within the endosomal membrane and is activated in the presence of CpG DNA. Upon ligand binding, the adaptor protein MyD88 is recruited to the cytoplasmic N-terminus of TLR9, and recruits IRAK-4 followed by IRAK-1 and IRAK-2. A second adapter protein: TRAF6 is recruited, which stimulates the recruitment of TAK1. TAK1 then initiates both NF-κB activation and MAPK signalling, which culminates in the activation of AP-1. MyD88 can also stimulate the activation of STAT3.

1.7.4.1: MyD88 Mutation

MyD88 has been identified as the seventh most frequently mutated gene in CLL. An activating mutation within the TIR domain (L265P) of MyD88 can be found in ~4% of the CLL population and is associated with increased NF-κB and STAT activation, enhanced NF-κB-DNA binding potential and heightened cytokine secretion[86,92]. Interestingly, MyD88 was found to be the most mutated gene (with a frequency of 11.5%) in a cohort of 212 Chinese patients from Hong Kong and Singapore[95].

MyD88-L265P has not only been described as oncogenic, but also as a driver mutation of CLL[3,30,86]. Within an individual patient, MyD88-L265P mutations are often clonal rather than sub-clonal, indicating an early occurrence in CLL development[30]. Curiously, despite TLR-signalling being upregulated to a greater extent in the lymph nodes of U-CLL patients relative to M-CLL patients, the occurrence of MyD88-L265P is almost exclusively confined to M-CLL[3,86,88,93,87]. This suggests an as yet unexplained selective pressure upon MyD88 activation in M-CLL. Within the M-CLL subgroup, MyD88-mutated patients exhibit a shorter time to first treatment[87] and an overall prognosis comparable to the more aggressive U-CLL subgroup[88]. Although only present in ~4% of the CLL population, the evident recurrence and early onset of activating MyD88 mutations, implicate the TLR family in the development of CLL. This thesis specifically focuses on the potentially oncogenic role of Toll-Like Receptor 9 (TLR9).

1.7.5: NF-κB Activation in CLL

NF-κB comprises a family of five transcription factors (i.e., RelA (p65), p52, p50, RelB and c-Rel) and is at the epicentre of the CLL microenvironment[96]. NF-κB-signalling is

an integral component for the activation and survival of both M-CLL and U-CLL[83] and constitutive NF-κB activation is evident in both the PB and LN compartments[62]. Of the two compartments, the NF-κB gene signature is most prominently found in LN-CLL relative to PB-CLL[93], which is logical since both BCR and TLR-signalling culminate in the activation of NF-κB signalling. Additionally, many other microenvironmental stimuli also operate via NF-κB-signalling including CD40L, chemokine signalling and stromal cell interactions[96]. In 2017, Jayappa et al.,[97] found a mixture of environmental stimuli conferred resistance to a combination of ibrutinib and venetoclax *in vitro* by activating NF-κB independently of the BCR.

Prior to stimulation, NF-κB subunits are sequestered as homo/heterodimers in the cytoplasm. Upon stimulation, the complexes translocate into the nucleus and bind to target DNA sequences to initiate transcription. NF-κB activation can result from stimulation of either the canonical or non-canonical NF-κB signalling pathways and target genes are homo/heterodimer specific[98]. This level of complexity in regulation enables a greater sensitivity and specificity to individual stimuli. Each pathway has been described in a review by Mansouri et al[96]. In the canonical NF-κB signalling pathway, the cytosolic NF-κB subunits RelA (p65) and p50 are bound to the inhibitory protein IκB. Activation of an upstream IκB-kinase complex (comprising: IKKα; IKKβ and IKKγ) leads to the phosphorylation of IκB, targeting it for ubiquitination and proteolytic degradation. RelA and p50 are then free to translocate into the nucleus. The non-canonical pathway utilises p52 and RelB only. In unstimulated cells, p52 is sequestered in the cytosol as a larger (P100) pre-cursor protein. Upon stimulation, NF-κB-inducing kinase (NIK) activates IKKα which in turn phosphorylates p100,

marking it for proteolytic cleavage. p52/Rel B dimers are then free to translocate into the nucleus. NF-κB promotes the transcription of a plethora of disease-related genes encompassing CLL cell proliferation, survival, migration and pro-inflammatory signalling[96] (Figure 1.5).

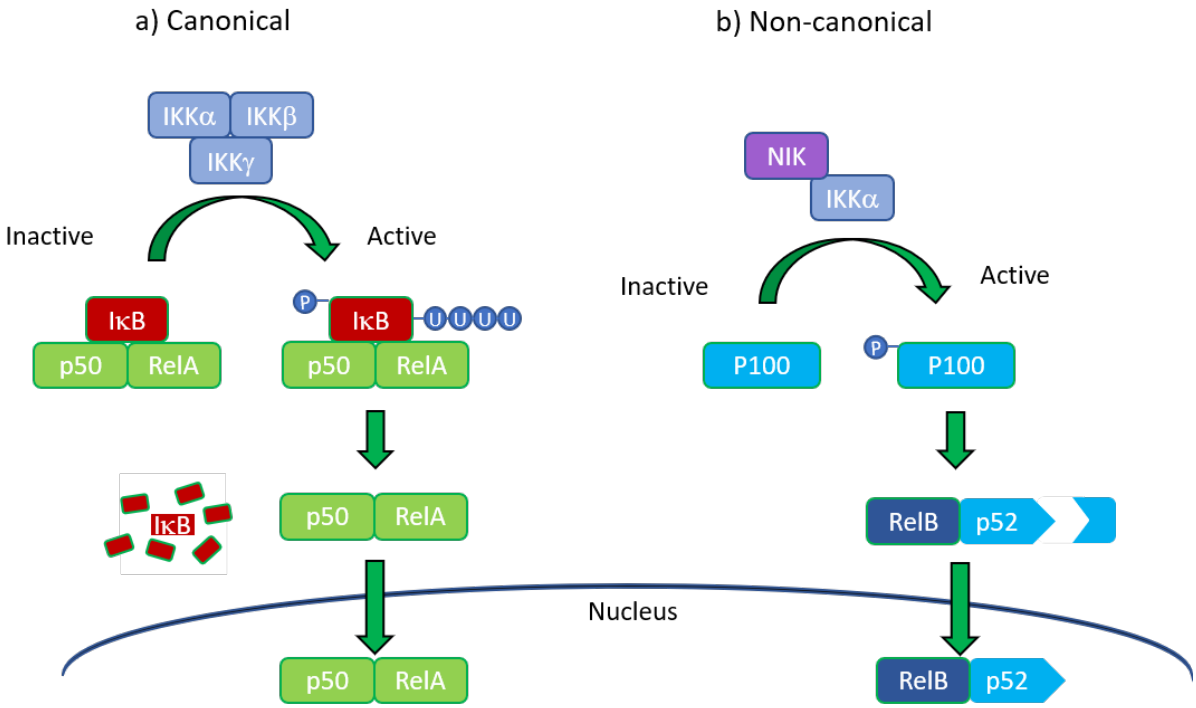

Figure 1.5: Canonical and Non-Canonical NF-κB Activation. a) The canonical NF-κB activation pathway. In unstimulated cells, p50 and RELA (p65) are sequestered in the cytoplasm bound to the inhibitory protein IκB. Following upstream activation, the IκB-kinase complex (comprising: IKKα; IKKβ and IKKγ) phosphorylates IκB, targeting it for ubiquitination and proteolytic degradation. p50 and RelA are then free to translocate into the nucleus and initiate the transcription of NF-κB target genes. b) The non-canonical pathway utilises the p52 and RelB NF-κB subunits-only. In unstimulated cells, p52 is sequestered in the cytosol as a larger (P100) pre-cursor protein. Upon stimulation, NF-κB-inducing kinase (NIK) activates IKKα which in turn phosphorylates p100, marking it for proteolytic cleavage. p52/RelB are then free to translocate into the nucleus and initiate the transcription of NF-κB target genes.

1.8: Current Therapeutic Options for the Treatment of CLL

1.8.1: Chemo(immuno)therapy

Until recently, therapeutic options for the treatment of CLL have been extremely limited. Historically, CLL patients were treated with chlorambucil or fludarabine monotherapies, or steroids such as prednisone and these approaches achieved very limited success[99]. This was then followed by the development of more toxic regimens of chemo(immuno)therapies e.g., fludarabine and cyclophosphamide (FC) ± rituximab (a B-cell-specific monoclonal antibody) (FC(R)). FCR was the first treatment to show improved survival but unfortunately, patients often endure multiple significant toxicities including severe neutropenia (84%) and consequential bacterial/viral infections (39%). This regimen is therefore unsuitable for many CLL patients and is particularly poorly tolerated in patients over 65 years of age[14]. In addition to the short-term toxicity of chemo(immuno)therapy, the CLL8 trial reported that 15.3% of FCR-treated patients developed secondary malignancies within 6 years of treatment[20]. Whilst older patients have been shown to better tolerate an alternative chemoimmunotherapy regimen: Bendamustine and Rituximab (BR), the progression-free survival (PFS) of BR-treated patients is lower than that of FCR-treated patients[14]. Consequently, chemo(immuno)therapeutic options are generally reserved for the younger, fitter demographic.

For those who are able to withstand FCR, the response rates are heterogeneous. M-CLL patients with favourable cytogenetics achieve the most complete and durable responses to FCR[20,22,100]; a long-term follow-up of FCR-treated M-CLL patients reported an 83% survival rate at 6 years post-treatment[20]. Patients expressing

markers of poor prognosis CLL have an inferior response to FCR. In a retrospective multi-centre analysis of first line FCR-treated patients the 5-year PFS for U-CLL patients was just 36.3%[22]. This PFS dropped to just 8.7% by 12.8 years in a longer-term retrospective analysis of a phase II clinical trial[100]. Comparatively, the 5- and 12.8-year PFS figures for M-CLL patients were 58.6% and 53.9%, respectively[22,100]. Irrespective of IGHV mutational status, poor prognostic chromosomal aberrations have been shown to drastically affect the efficacy of FCR; patients with del(11q) and del(17q) showed 5-year PFS rates of 18.4% and 10.9%, respectively, relative to ~50% in the remaining cohort[22].

1.8.2: Targeted Therapies

In recent years, a number of targeted agents have proven extremely beneficial for the treatment of CLL patients, even in those who have relapsed following chemo(immuno)therapy[101-104]. Both ibrutinib and idelalisib are designed to target kinases operating downstream of the BCR, inhibiting Bruton's Tyrosine Kinase (BTK) and Phosphatidylinositol-3 kinase delta (PI3Kδ), respectively (Figure 1.3). Venetoclax is a BCL-2 inhibitor, designed to eliminate the anti-apoptotic effects of BCL-2 and promote CLL cell apoptosis. The successes and downfalls of each are discussed below.

B-Cell Receptor Targeted Kinases

Ibrutinib: binds to the active site of BTK to inhibit its enzymatic activity and consequently halts BCR-signalling upstream[105]. As previously described, BCR-signalling is the primary mechanism of B-cell activation and the loss of such an integral signalling pathway exerts a dramatic effect upon CLL cell proliferation,

survival, migration and adhesion[105]. Following the initiation of ibrutinib therapy, patients experience a large-scale redistribution of tissue-resident CLL cells into the peripheral blood as CLL cells lose the ability to signal via integrin and chemokine receptors[105]. Whilst 'trapped' within the circulation, the CLL cells are no longer protected by the lymphoid microenvironmental niche and are starved of essential activation signals[40,62]. Over time, the CLL cells are unable to persist and the initial increase in lymphocytosis is followed by a gradual decrease caused by tumour cell apoptosis. Ibrutinib was initially granted FDA approval to be used as a first-line therapeutic for patients deemed unsuitable for treatment with chemotherapy i.e., patients with unfavourable genetic aberrations (IGHV-unmutated, Chr.17p (del)/TP53-del/mutated) and patients who are older or medically unfit[102]. Subsequently, it was approved as a second-line treatment for relapsed/refractory patients following an initial first-line chemotherapeutic intervention[102]. Clinical data has shown ibrutinib to achieve a 5-year progression-free survival rate of 92% (in previously untreated patients) and 44% (in previously relapsed/refractory patients)[101]. Recently, the FDA approval for ibrutinib has been extended to all CLL patients when used in combination with Rituximab; this change was implemented in 2020 following the analysis of clinical data comparing ibrutinib + rituximab to standard FCR chemo(immuno)therapy[106]. In this trial, both the PFS and OS of ibrutinib + rituximab-treated patients were reported to exceed those of FCR-treated patients.

Although initially promising, it soon became evident that ibrutinib was not a curative agent as the majority of patients fail to achieve complete systemic disease clearance. In a 5-year follow up study investigating the safety and efficacy of ibrutinib

treatment, complete responses were found in just 29% of previously untreated patients and 10% of previously relapsed/refractory patients[101]. This indicates that ibrutinib can achieve disease control but not a complete disease eradication. A small number of disease-promoting CLL cells are thought to persist during treatment with ibrutinib, perhaps 'hiding' in the secondary lymphoid tissues where they evade therapy. If treatment is ended, these residual CLL cells can repopulate the tumour resulting in the reappearance of lymphadenopathy and other disease-related symptoms[107]. Ibrutinib therefore requires a life-long commitment to therapy.

Patients currently remain on ibrutinib therapy until the point of disease progression or the development of intolerable adverse events. Although ibrutinib is generally better tolerated than the chemo(immuno)therapeutic options listed above, it is not without side effects; common side effects include: diarrhoea, fatigue, nausea, cytopenia, rashes, fever, hypertension, pneumonia and atrial fibrillation[101,105]. Concerningly, ibrutinib has also been associated with cardiac arrhythmias and even sudden death in patients with no prior medical history of cardiac issues[108]; this drug therefore cannot be tolerated by all CLL patients.

With any long-term therapy comes the risk of acquired resistance. In the case of ibrutinib, a point mutation (C418S) at the ibrutinib binding site reduces the affinity of ibrutinib for BTK[109]. Patients can also acquire gain-of-function mutations within the downstream PLCγ2 protein, enabling BTK to be bypassed[109,110]. In a recent real-word study investigating the genetic landscape of a cohort of 30 ibrutinib-treated patients, 57% and 13% of patients had developed BTK and PLCγ2-mutations respectively following 3 years on therapy; these mutations were found to be

indicative of a future relapse[111]. When detected however, these mutations are only found in a small subset of the malignant clone[112], suggesting that there are other mechanisms of resistance contributing to the refractory and progressive responses of many patients to ibrutinib. Furthermore, 15-30% of ibrutinib-resistant cases are not associated with known mutations, suggesting there to be other unidentified mechanisms at play[110,111].

Idelalisib: is targeted against PI3Kδ (an alternative downstream kinase of the BCR) and induces rather similar effects to ibrutinib. Following treatment with Idelalisib, patients experience a rapid redistribution of CLL cells from the secondary lymphoid tissues into the peripheral blood[104]. Despite these similarities however, Idelalisib is far more toxic than ibrutinib with a wide range of toxicities including cytopenia, colitis and diarrhoea, liver damage and serious infections such as sepsis, pneumonia and reactivation of cytomegalovirus[102,104]. Idelalisib is consequently reserved as a later stage treatment option rather than a first-line therapeutic[102,104] and is FDA approved for use in in refractory/relapsed patients in combination with the CD20 monoclonal antibody, Rituximab.

Next Generation BTK-Inhibitors: A number of second and third generation BTK-inhibitors have been designed to improve upon the identified downfalls of ibrutinib. One of the problems encountered by patients undergoing treatment with ibrutinib is the wide-ranging list of side-effects[101,105,108]. These side effects are likely due to off-target effects as in addition to inhibiting the kinase activity of BTK, ibrutinib has also been found to inhibit a number of C481-containing kinases including other members of the TEC family of kinases and EGFR[113].

Second generation molecules such as acalabrutinib and zanabrutinib bind BTK with greater selectivity and are generally better tolerated when compared with ibrutinib[114,115]. In a cohort of patients who were unable to tolerate ibrutinib, a remarkable 72% of ibrutinib-induced adverse events did not occur following treatment with acalabrutinib and a further 13% occurred at a lower grade[114]. Acalabrutinib has recently been FDA approved for the treatment of CLL and zanabrutinib is in phase III clinical trials[115]. Although the improved tolerability of these agents is promising, a major limitation of both acalabrutinib and zanabrutinib is their dependence on the C481 residue of BTK[115]; second generation BTK inhibitors are still susceptible to C481S mutation-mediated resistance[116].

LOX-305 is a third generation BTK inhibitor and has been designed to bind BTK independently of the C481 loci and has been shown to be effective against ibrutinib-resistant cell lines *in vitro*[117]. It has also been shown to induce a 94% decrease in phospho-BTK in C481-mutated patient samples, compared with a just a 50% reduction induced by ibrutinib[117]. Early clinical data for LOX-305 suggested this molecule to be highly tolerable in a small cohort of patients[118].

Venetoclax:

Alternatively, relapsed patients may be treated with venetoclax, a potent inhibitor of the anti-apoptotic protein BCL-2. As previously discussed, CLL cells can persist in an anergic yet pro-survival state and this is largely due to the aberrant overexpression of BCL-2[80]. Removing or inhibiting this important pro-survival signal is a logical therapeutic strategy in CLL. Venetoclax operates independently of BCR-signalling and has proven highly efficient at inducing rapid onset apoptosis[103]. With such an efficient

induction of CLL cell apoptosis, comes the risk of tumour lysis syndrome, a dangerous adverse event in which the large-scale release of intracellular components results in an overwhelming chemical imbalance and organ toxicity[119]. For this reason, careful management is required concerning the administration of venetoclax and treatment is initiated slowly; patients receive low starting doses, which are incrementally increased over time[102].

Venetoclax is currently approved for relapsed/refractory CLL patients and its efficacy is not limited by high-risk aberrations such as Chr.17p (del) or P53 (del/mut)[102-104]. In a phase I clinical trial of relapsed/refractory patients, venetoclax achieved an overall response rate of 79% and a complete response rate of 20% after their first year of therapy[120]. As with all therapeutic agents however, mechanisms of acquired resistance to Venetoclax have emerged including a disruptive Gly101Val mutation within the BCL-2 protein and compensatory upregulation of alternative anti-apoptotic proteins[104].

Ibrutinib + Venetoclax

Given the limitations of each single agent, a dual targeted approach may improve the likelihood of a complete response to treatment. Numerous clinical trials are in progress to test different combinations of currently available oral therapeutics and a particularly promising example is ibrutinib with venetoclax. Clinical data from a recently published phase II trial reports the effects of 3 cycles of ibrutinib-alone followed by 6-12 cycles of ibrutinib + venetoclax in high risk, treatment naïve patients[121]. After just 6 cycles of combinational therapy, an incredible 73% of patients had achieved a complete remission signifying the strong synergistic interaction of

ibrutinib with venetoclax. This combination also provided additional safety benefits compared with the use of venetoclax alone, since the delayed initiation of venetoclax (following the three cycles of ibrutinib-alone) reduced the risk of venetoclax-associated tumour lysis syndrome. Dual targeting of BTK and BCL-2 therefore appears to substantially improve the clinical responses of high-risk patients to therapy. An *in vitro* study by Jayappa et al.,[97] however, has suggested a potential mechanism of resistance to the proposed combination of ibrutinib and venetoclax. The group stimulated *ex vivo* CLL cells with a cocktail of microenvironmental stimuli, stimulating BCR-independent activation pathways and found their 'microenvironmental agonist mix' (comprising CpG ODN, CD40L and IL-10) antagonised the apoptotic effects of ibrutinib + venetoclax in a TLR9-dependent manner.

1.9: Toll-Like Receptor 9 as a Novel Therapeutic Target

TLR9 is a member of the TLR family of pattern recognition receptors (outlined above) and recognises unmethylated CpG (u-CpG) motifs in the DNA of invading pathogens[122]. Stimulation of TLR9 initiates the highly conserved TLR-signalling pathway (TLR - MyD88 - IRAK1/IRAK4), which culminates in the activation of the transcription factors NF-κB and STAT3. TLR9 therefore poses an alternate mechanism of NF-κB activation to the conventionally targeted BCR-pathway. Interestingly, the phenotype of CpG-stimulated healthy B-cells has been likened to that of CLL; Bekeredjian-Ding et al.,[123] reported an upregulation of the cell surface markers CD5, CD23 and CD25, in addition to the expression of a T-cell receptor signalling associated kinase, ZAP-70. ZAP-70 is associated with aggressive disease progression and a clinically poor prognosis[19].

1.9.1: Expression and Sub-Cellular Llocalisation of TLR9

In physiological conditions, antigen-naïve B-cells express very low levels of TLR9 and consequently, CpG-ODN has minimal stimulatory effect[124]. Following BCR-engagement however, TLR9 is significantly upregulated and CpG-ODN enhances the antigenic-response[91,124,125]. The absence of functional TLR9 in antigen-naïve B-cells is thought to maintain the specificity of the humoral response by inhibiting the clonal expansion of non-specific B-cells[124]. However, in memory B-cells TLR9 is maintained at a high basal level and this B-cell subset is responsive to stimulation with CpG-alone[124].In CLL, TLR9 is expressed in both U-CLL and M-CLL cells and has proven to be functional in the absence of other stimuli[92,93]. Dadashian et al.,[93] demonstrated this functionality using a proximity ligand assay and *ex vivo* LN-CLL samples; TLR9 co-localised with MyD88, IRAK1 and phosphorylated IκBα. Furthermore, TLR9 is expressed at higher levels in LN-CLL relative to PB-CLL and has been implicated in CLL cell proliferation, survival and resistance to therapy[126].

In addition to temporal expression, the cellular location of functional TLR9 is highly regulated; functional TLR9 is sequestered at the endosomal membrane in order to evade potential interaction with self-DNA[127]. In resting conditions, TLR9 resides in the endoplasmic reticulum (ER) as an inactive pre-protein and is recruited to the endosomal membrane following CpG endocytosis[128-130]. The trafficking of pre-TLR9 to CpG-containing endosomes is complex and involves golgi-dependent secretion, temporary cell surface expression and re-internalisation[131]. TLR9 function is only enabled once integrated into the endosomal membrane and post pH-dependent proteolytic cleavage[130]. Functional TLR9 therefore only encounters endocytosed and processed pathogenic DNA[128-130].

Our team at Brighton and Sussex Medical School, have identified aberrant expression of functional TLR9 at the cell surface of small sub-clonal populations of primary CLL cells. In this study, intra-patient expression of surface TLR9 (sTLR9) was correlated with elevated endosomal TLR9 and an activated and migratory phenotype[132]. sTLR9 expression was hypothesised to reflect extensive TLR9 signalling in this sub-population of CLL cells, and this apparent loss of regulatory control further implicates TLR9 in CLL pathology.

1.9.2: TLR9-Stimulatory Circulating Cell-Free DNA in CLL

In addition to the recognition of pathogen associated molecular patterns (PAMPS), TLR9 is known to recognise endogenous CpG-containing damage associated molecular patterns (i.e., DAMPs)[133]. DAMPs are released in the event of cellular stress/damage and during apoptosis. As previously discussed, even clinically stable cases of CLL exhibit a high turnover of CLL cells each day, with up to 2% of the CLL clone undergoing apoptosis within a 24-hour period[67]. Apoptotic bursts are also evident during treatment with cytotoxic/cytostatic agents. This high turnover inevitably results in the circulation of cellular debris within the peripheral blood, which potentially contains TLR9-stimulatory material.

The presence of circulating tumour DNA was confirmed in a cohort of relapsed/refractory CLL patients and has been found to correlate with disease burden[134]. Although the bulk of tumour-derived DNA would not be expected to be recognised by the innate immune system, mitochondrial DNA (mtDNA) is almost entirely unmethylated and consequently contains u-CpG motifs[135,136]; mtDNA has been shown to stimulate TLR9 in a number of inflammatory conditions and

cancers[133]. Interestingly, in addition to apoptosis, Ingelsson et al.,[137] uncovered a potentially self-propagating release mechanism in which B-cells and CLL cells expel fibrous mtDNA-containing structures in response to stimulation with CpG-ODN; these structures are thought to function as inflammatory second messengers.

The aforementioned study by our group, correlated plasma levels of cell-free DNA with clinical markers of progressive disease. High concentrations of cell-free DNA were identified in the U-CLL subset and were strongly correlated with CD38 expression, shorter lymphocyte doubling times and shorter TTFT. Furthermore, plasma from CLL patients was found to contain much higher levels of the TLR9 agonist, unmethylated mtDNA, compared to that from healthy controls[132].

1.9.3: The Role of TLR9 in CLL Cell Proliferation and Survival

Synthetic CpG-rich oligonucleotides (CpG-ODN) can be used to mimic the presence of TLR9-stimulatory PAMP/DAMP sequences *in vitro*; CpG-ODN is readily endocytosed and activates TLR9 from within the endosomal compartments. Multiple studies have investigated the effects of CpG-ODN upon CLL cell proliferation and survival and have highlighted a disease promoting role for TLR9 in the progression of aggressive subtypes of CLL[138-140]. In patients with U-CLL or unfavourable cytogenetic lesions, CpG-ODN has shown to promote intense activation of ERK, AKT and JNK and to consequently initiate cell cycle entry and CLL cell proliferation[138]. It has also shown to decrease the sensitivity of poor prognosis patients to therapeutic agents such as fludarabine and a combination of ibrutinib + venetoclax[97,140]. In these patients, CpG ODN promotes CLL cell survival by inhibiting PARP and caspase cleavage and upregulating anti-apoptotic proteins such as MCL-1, BCL-X_L, and survivin[97,140].

Interestingly, the more indolent M-CLL subgroup is associated with a *non-proliferative* response to CpG-stimulation, in which ERK, AKT and JNK are only weakly activated, and cells remain arrested in the G1 phase of the cell cycle[138,139]. A more aggressive CpG-*proliferative* M-CLL subset however has been identified and associated with a poorer clinical outcome relative to CpG-*non-proliferative* M-CLL[139]. These data implicate TLR9 in both disease progression and therapy evasion.

1.9.4: The Potential Role of TLR9 in CLL Cell Migration

Although a role for TLR9 in the migration of CLL cells is yet to be defined, TLR9 has been repeatedly associated with the metastatic potential of a number of solid tumour types. TLR9 has been found to be aberrantly expressed in human lung, breast, brain, prostate and gastric cancer cell lines[141-145] and to be responsive to stimulation with synthetic oligonucleotides (ODN). CpG ODN was shown to increase both the invasion and migration of each of the above-mentioned cell types in a TLR9-dependent manner. In further support of these findings, results could be replicated when stimulating with bacterial DNA (i.e., *E. coli* and *H. pylori* in prostate and gastric cancer, respectively)[143,145]. The expression of TLR9 has been verified in primary lung, breast and prostate cancer[142-144] and has been associated with both an increased propensity for lymph node metastasis and a shorter PFS in prostate cancer patients[144].

The molecular mechanisms behind TLR9-induced invasion and migration are yet to be deciphered however Xu et al.,[141] described the CXCL12-CXCR4-AKT axis as being a 'crucial' component in the lung cancer cell line, 95D. CXCR4 was reported to be upregulated in this cell line post stimulation with CpG ODN and inhibition of this

chemokine receptor was subsequently shown to inhibit TLR9-mediated migration[141]. A microarray performed in a prostate cancer cell line has also implicated CXCR4 in TLR9-driven metastasis along with a number of other genes including the matrix metalloproteinases: MMP-13 and MMP-2[144]. According to this study, functional gene oncology analysis identified 'regulation of programmed cell death'; 'regulation of locomotion' and 'response to calcium ion' to be the three highest scoring molecular and cellular functions of TLR9. The 'regulation of leucocyte migration' was also identified during the microarray analysis suggesting that TLR9 has the potential to promote the migration of CLL cells. In a recent publication by Giménez Carabaza et al.,[92] CLL migration was shown to increase post-stimulation with a cocktail of TLR-agonists targeting TLR1, TLR2, TLR6 and TLR9. The group however did not distinguish receptor-specific contributions to the observed increase in migratory function.

1.10: Project Rationale

Chronic Lymphocytic Leukaemia is a largely indolent disease associated with an older patient demographic with 5- and 10-year survival rates of 91% and 81%, respectively[2]. Despite these promising sounding statistics however, CLL is both biologically and clinically heterogeneous and a subgroup of patients experience an aggressive disease course with rapid progression. Unfortunately, progressive disease is particularly associated with younger onset CLL, and these patients experience a shorter TTFT and often belong to the poor prognosis U-CLL subgroup[146]. The life expectancy of younger CLL patients is therefore greatly reduced relative to age-matched healthy individuals[2]. Additionally, as earlier described, the unconventional 'watch and wait' approach to the treatment of CLL brings a considerable

psychological burden to untreated patients as they anxiously persist without medical intervention. For those patients who do receive treatment, currently available therapeutics are either extremely harsh, with significant side-effects or they require a life-long commitment to therapy. Given the long-term nature of targeted treatments, the NHS is faced with a considerable financial burden; in 2016, the annual purchasing cost of ibrutinib to treat a single CLL patient was approximately ~£56,000[147]. The development of novel and potentially curative therapies for CLL would therefore be of great benefit to both the patient and healthcare providers.

Currently available BCR-targeted therapies induce a marked redistribution of tissue-resident CLL cells into the peripheral blood[105]. Whilst 'trapped' within the circulation, CLL cells are devoid of microenvironmental activation signals and ultimately undergo apoptosis. Unfortunately, some CLL cells are able to persist for the duration of therapy and can remain protected within the lymphoid niche. These agents therefore fail to achieve a complete systemic disease clearance and consequently cannot be deemed curative as cell counts will rise if treatment is terminated[101,107]. CLL cell migration/tissue-homing has therefore become a fundamentally important investigative target as a 'curative' treatment plan would need to promote the release of **all** tissue-resident CLL cells, including those that are refractory to current therapeutic regimens. It is highly likely that such a regime would require the simultaneous inhibition of multiple signalling pathways and the identification of novel therapeutic targets is both timely and paramount.

Our group has generated considerable evidence to support the concept that Toll-like Receptor 9 (TLR9) is a potential candidate. We have found unmethylated CpG DNA

to be 12.9-fold higher in the plasma of CLL patients relative to healthy controls[132] and we believe that these motifs could act as a potent stimulus for TLR9. TLR signalling is upregulated in LN vs PB CLL cells to the same extent as BCR and NF-κB signalling[93] and the TLR-associated adapter protein, MyD88, has been identified as an early driver mutation in a subset of CLL patients[3,30,86]. Furthermore, M-CLL patients harbouring MyD88 mutations experience a clinical outcome closer to that of the poor prognostic U-CLL subgroup[87,88]. TLR9 stimulatory CpG-oligonucleotides are known to promote CLL cell proliferation and survival *in vitro*[97,138-140] although the effect of CpG-stimulation upon CLL cell migration remains to be determined. Numerous groups have associated TLR9 activation with the metastasis of solid tumours[141-145] yet this work remains to be done in the context of CLL. In 2018, Giménez Carabaza et al.,[92] reported an agonist mix (containing ligands for TLR1, 2, 6 and 9 together) stimulated an increase in the chemotactic response of CLL cells to the chemokine CXCL12 but did not distinguish the individual effect of each ligand; this study therefore implicates a potential role for TLR9 in CLL cell migration however it remains unclear which of the ligands may have induced the migratory effect.

TLR9 can activate NF-κB independently of the BCR through a MyD88-dependent signalling pathway (Figure 1.4) and may therefore act as a compensatory mechanism in the absence of BCR-signalling. The central hypothesis of this thesis is that TLR9 may promote CLL cell migration independently of BCR-signalling and that this may be a mechanism of resistance to therapies such as ibrutinib. If this is the case, then dual targeting of the BCR and TLR9 pathways may induce a synergistic inhibition of CLL cell migration. Such a finding would be of clinical importance and may hold the potential to enhance the lymphocyte redistribution abilities of currently available

BCR-targeted agents. This project will investigate TLR9 as a potential novel therapeutic target for the treatment of CLL. The effect TLR9 activation/inhibition upon CLL cell migration will be investigated using primary patient material and potential synergies with existing BCR-targeted therapies will be explored.

1.11: Project Hypothesis and Aims

Hypothesis:

Toll-like receptor 9 (TLR9) promotes B-cell activation and migration in Chronic Lymphocytic Leukaemia (CLL).

Project Aims:

- To optimise a protocol for the activation and inhibition of TLR9 in primary CLL cells
- To investigate the effects of TLR9 activation upon CLL cell migration
- To investigate potential differences in the migratory responses of U-CLL and M-CLL patients to TLR9 activation
- To investigate the potential synergistic effect of a dual targeted inhibition of BCR and TLR9 upon CLL cell migration

2.0: Materials and Methods

2.1: Reagents

Reagent	Source
BD™ CompBeads	BD
BDFACSDiva™ CS&T Research Beads	BD
Bovine Serum Albumin (BSA)	Sigma
Dimethyl Sulphoxide (DMSO)	Sigma
Dulbecco's Phosphate Buffered Saline (PBS) (Modified without calcium chloride and magnesium chloride)	Sigma
Fixable Viability Dye eFlour™ 780	eBioscience/Invitrogen
Foetal Calf Serum (F9665) (FCS)	Sigma
Histopaque	Sigma
Hydrochloric Acid (HCl)	Sigma
Immuno-Blot Low Fluorescence PVDF Membrane/Filter Paper Set	Bio-Rad
Recombinant Human IL-4	RayBiotech
Ibrutinib	Selleckchem
Isopropyl Alcohol	Sigma
L-Glutamine	Sigma
Methanol	Sigma-Aldrich
NP-40	Sigma

Reagent	Source
ODN 2006 (TLR9 Agonist – CpG ODN, Class B)	Invivogen
ODN INH-18 (TLR9 Antagonist, Class B)	Invivogen
Paraformaldehyde (PFA)	Sigma
Penicillin-Streptomycin (10 000 units Penicillin, 10mg Streptomycin/mL)	Sigma
PBS (tablets)	Sigma
Powdered Milk	Marvel
Precision Plus Protein™ Kaleidoscope™ Prestained Proteins Standards (ladder)	Bio-Rad
Recombinant Human CXCL12	BioLegend
Roswell Park Memorial Institute-1640 Medium (RPMI-1640) (with sodium bicarbonate, without L-glutamine)	Sigma
SIGMAFAST™ Protease Inhibitor Tablets	Sigma
Sodium Chloride (NaCl)	Sigma
Sodium Deoxycholate	Sigma
Sodium Deoxycholate	Sigma
Sodium Dodecyl Sulphate (SDS)	Sigma
Trizma Base Solution	Sigma
TruPAGE DTT Sample Reducer	Sigma
TruPAGE LDS Sample Buffer (4x)	Sigma
TruPAGE Precast Gels (4-12%) (12 well)	Sigma

Reagent	Source
TruPAGE TEA-Tricine SDS Running Buffer (20x)	Sigma
TruPAGE Transfer Buffer (20x)	Sigma
Trypan Blue solution (0.4%)	Sigma-Aldrich
Tween-20	Sigma-Aldrich
True-Phos™ Perm Buffer	BioLegend
Fixation Buffer	BioLegend
Stain Buffer	BioLegend

2.2: Project Specific Plasticware

Plasticware	Source
Transwell Polycarbonate Membrane Cell Culture Inserts – 5.0μm Pore (6.5mm)	Sigma

2.3: Kits

Kit	Source
Fixation/Permeabilization Solution Kit	BD Sciences
EasySep Human B Cell Enrichment Kit (w/o CD43)	Stemcell Technologies
Pierce™ BCA Protein Assay Kit	ThermoFisher Scientific
DNeasy Blood and Tissue Kit	Qiagen

2.4: Antibodies

2.4.1: Flow Cytometry Antibodies

Antibody	Fluorophore	Clone	Source
CD3	APC	HIT3a	BioLegend
CD3	Alexa Fluor 488	HIT3a	BioLegend
CD5	PE/Cy7	UCHT2	BioLegend
CD19	Pacific Blue	HIB19	BioLegend
CD19	Alexa Fluor 488	HIB19	BioLegend
CD19	APC	HIB19	BioLegend
CD38	APC	HB-7	BioLegend
CD38	PE	HIT-2	BioLegend
CD49d	PerCP/Cy5.5	9F10	BioLegend
CD49d	PE	9F10	BioLegend
CD62L	Brilliant Violet 650	DREG-56	BioLegend
CD69	Brilliant Violet 510	FN50	BioLegend
CD69	Brilliant Violet 785	FN50	BioLegend
CD69	PE	FN50	BioLegend
CD289 (TLR9)	PE	eB72-1665	eBioscience
CXCR4	PerCP/Cy5.5	12G5	BioLegend
Phospho NF-κB-p65 (ser529)	PE	13A3-1	BioLegend

2.4.2: Western Blot Antibodies

Primary Antibodies

Antibody	Host	Clone	Dilution	Source
Purified anti-β-actin (Poly IgG)	Rabbit	Poly6221	1: 500	BioLegend
Purified anti IkB-α (IgG2b)	Mouse	3D6C02	1: 2500	BioLegend

Secondary Antibodies

Antibody	Host	Reactivity	Dilution	Source
IRDye® 680RD Goat anti-Rabbit IgG	Goat	Rabbit IgG	1: 15000	LI-COR
IRDye® 800CW Goat anti-Mouse IgG_{2b}-Specific	Goat	Mouse IgG_{2b}	1: 15000	LI-COR

2.5: Media

2.5.1: Complete Media

- 500ml RPMI-1640 medium
- 5ml Penicillin-Streptomycin (10 000 units Penicillin, 10mg Streptomycin/mL)
- 5ml L-Glutamine
- 50ml Foetal calf serum [FCS] (10%)

2.5.2: Freezing Media

- 80% FCS (80%) + 20% DMSO

2.6: Buffers

2.6.1: CLL Cell Isolation Buffer

- Dulbecco's PBS + 2% FCS + 1mM EDTA

2.6.2: RIPA Buffer

- 25mM Tris HCl (pH 7.6)
- 150mM NaCl
- 1% NP-40
- 1% Sodium deoxycholate
- 0.1% SDS
- 1x SIGMA*FAST*™ Protease Inhibitor

2.6.3: Blocking Buffer

- PBS + 5% powdered milk

2.6.4: Blocking Buffer-Tween

- PBS + 5% powdered milk + 0.1% Tween 20

2.7: Primary Patient Material

2.7.1: Ethics

Ethical approval (REC 17/SW/0263) was obtained for the collection of primary patient material.

Treatment-naïve patients with a diagnosis of Chronic Lymphocytic Leukaemia were recruited during routine outpatient appointments at The Royal Sussex County Hospital (RSCH). Peripheral blood samples were collected into EDTA/Lithium Heparin/Sodium Heparin vacuettes after informed consent had been taken in accordance with the Declaration of Helsinki. Samples were anonymised prior to receipt and transported to the Brighton and Sussex Medical School (BSMS) under a material transfer agreement between RSCH and BSMS. Isolated PBMC CLL samples were also gifted from collaborators at Kings College London and Aviano, Italy.

2.7.2: Density Gradient Preparation of Leukocytes from Whole Blood Samples

6-7ml of whole blood was layered onto 5ml of Histopaque in a 15ml falcon tube and centrifuged at 900g for 30 minutes (with zero deceleration). The leukocyte-containing buffy coat layer was collected using a plastic Pasteur pipette and transferred to a clean 15ml falcon tube. The cells were washed twice in 10mls of

Phosphate Buffered Saline (PBS) by centrifuging at 300g for 10 minutes (with full deceleration).

2.7.3: Storage and Recovery of Peripheral Blood Mononuclear Cells (PBMCs)

Storage: PBMCs were frozen in 1ml aliquots of 0.5ml complete media + 0.5ml freezing media (materials section 2.5) at a density of ~$5x10^7$ cells/ml. Aliquots were initially frozen at -80°C in isopropyl-filled Mr Frosty freezing containers (Nalgene) and transferred into liquid nitrogen within 2 weeks.

All tissue banking was executed in compliance with the guidelines of REC 17/SW/0263, with each sample being recorded using FreezerPro software.

Recovery: Frozen aliquots were retrieved from liquid nitrogen and promptly defrosted in a water bath at 37°C. Cells were transferred into 10ml of sterile PBS in a 15ml falcon tube and washed twice (i.e., centrifuged at 300g for 10 minutes) to remove all traces of Dimethyl Sulfoxide (DMSO).

Cell Resting: Following recovery, cells were incubated in complete media + IL-4 (5μg/ml) overnight at 37°C/5% CO_2.

2.8: Cell Culture/Cell Counts

Cells were cultured in complete media (materials section 2.5.1) at 37°C/5% CO_2 + IL-4 (5μg/ml). Cell counts were performed either manually or using the Countess II cell counter as described below:

Manual Cell Counts: A 10μl aliquot of cell suspension was added to 10μl 0.4% trypan blue and mixed well. 10μl was added to the well of a haemocytometer and live/dead cells were manually counted under a microscope at 20x magnification.

Automated Cell Counts: A 10μl aliquot of cell suspension was added to 10μl 0.4% trypan blue and mixed well. 10μl was added to the well of a Countess Cell Counting Chamber Slide and the slide was inserted into the Countess II cell counter to obtain both the absolute cell count and viability.

2.9: CLL Cell Purification

Cells were resuspended in 250μl isolation buffer (materials section 2.6.1) at a density of $1.25x10^7$. The EasySep Human B Cell Enrichment Kit w/o CD43 was used to isolate CLL cells as per the manufacturer's guidelines. CLL cell purification was confirmed by flow cytometry as detailed below.

2.10: Flow Cytometry

The phenotyping data presented in this thesis was collected from three different flow cytometer instruments due to the project starting during an equipment cross-over period. An 8-colour BD LSR II was initially used to optimise the conditions for TLR9 activation/inhibition but was later replaced by a 21-colour Beckman Coulter CytoFLEX LX. In the interim, transwell migration experiments had been designed to use a smaller 4-colour BD Accuri flow cytometer and all transwell migration experiments were quantified using this instrument for continuity. The CytoFLEX LX was used for all subsequent phenotyping experiments.

2.10.1: Flow Cytometry using a BD LSR II

Live CLL cells were identified as CD5+/CD19+/Fixable Viability Dye (FVD)-.

Table 2.1: Antibody Panel A: LSR II

Antibody	Clone	Fluorophore	Volume (For $\leq 1x10^6$ cells)
CD5	UCHT2	PE-Cy7	2 μl
CD19	HIB19	Pacific Blue	2 μl
CD38	HB-7	APC	2 μl
CD49d	9F10	PerCP-Cy5.5	2 μl
CD69	FN50	Brilliant Violet 510	2 μl
FVD	N/A	eFluor™ 780	1 μl

2.10.1.1: Extracellular Staining for the LSR II

PBMCs were collected into FACS tubes at densities of $3x10^5$-$1x10^6$ in 1ml PBS + 1μl FVD. The tubes were incubated for 30 minutes at 4°C and washed twice in PBS (centrifuging the cells at 350g for 7 minutes). The selected antibodies were added to a 100μl cell suspension in PBS and tubes were incubated at 4°C for 20 minutes. The cells were washed twice and either: a) resuspended in 200μl PBS (for immediate FACS analysis) or b) fixed in 200μl 1% Paraformaldehyde (PFA) (for storage at 4°C and FACs analysis within 3 days).

2.10.1.2: Antibody Compensations for the LSR II

Fluorophore compensations were required for each antibody panel run on the LSR II flow cytometer; each antibody was run through the LSR II in isolation bound to commercially available positive and negative compensation beads.

A series of FACS tubes were set up: one for each of the antibodies on the panel. The compensation beads were vortexed prior to use and one drop of both +ve BM™ CompBeads and -ve BM™ CompBeads was added to each tube in 100µl PBS. 2.5µl of each antibody was added to the corresponding FACS tube and vortexed; the antibody-bead complexes were protected from light and incubated at room temperature for 15 minutes. The beads were then washed in 2ml PBS (centrifuging at 200g for 10 minutes), resuspended in 500µl PBS and stored at 4°C before running through the LSR II flow cytometer. Compensations were calculated using FACsDIVA software.

2.10.1.3: Viability Compensation for the LSR II

Viability dye compensations were performed using live/dead cells in place of the compensation beads described above. FVD staining was used to label non-viable cells and to exclude them from phenotypic analysis.

$5x10^5$ cells were resuspended in 1ml PBS or complete media (materials section 2.5.1) and equally split into two 1.5ml Eppendorf tubes. Eppendorf tube 1 was rested at room temperature for 20 minutes (live cells) whilst Eppendorf tube 2 was placed on a heat block set at 60°C for 20 minutes (dead cells). Live and dead cells were mixed together, transferred into a FACs tube and centrifuged for 350g for 5 minutes. The cells were resuspended in 1ml PBS + 1µl FVD and incubated at 4°C for 30 minutes

before being washed twice in 2ml PBS and resuspended in 500µl PBS or 500µl PFA. The cells were stored at 4°C before being run through the LSR II flow cytometer. Compensations were calculated using FACsDIVA software.

2.10.1.4: Analysis using the LSR II

Cells were analysed by multicolour flow cytometry and results were analysed using FACsDIVA software. The following gating strategy identified live CLL cells from a pool of stained live/dead PBMCs: Lymphocytes were firstly identified from a forward scatter-area (FSC-A)/side scatter-area (SSC-A) scatter plot (Figure 2.1a) and forward gated into a FSC-A/forward scatter-height (FSC-H) scatter plot. The FSC-A/FSC-H scatter plot identified singlet lymphocytes (Figure 2.1b) which were forward gated into a SSC-A/FVD (eFluor™ 780) scatter plot. Live singlet lymphocytes were identified as eFluor™ 780 negative (Figure 2.1c) and forward gated into a CD5 (PE-Cy7)/CD19 (Pacific Blue) scatter plot. CLL cells were identified as CD5+/CD19+ and forward gated for phenotypic analysis (Figure 2.1d). Percentage positivity was determined using a fluorescence minus one (FMO) tube and Mean Fluorescence Intensity (MFI) was based on the CD5+/CD19+ gated population.

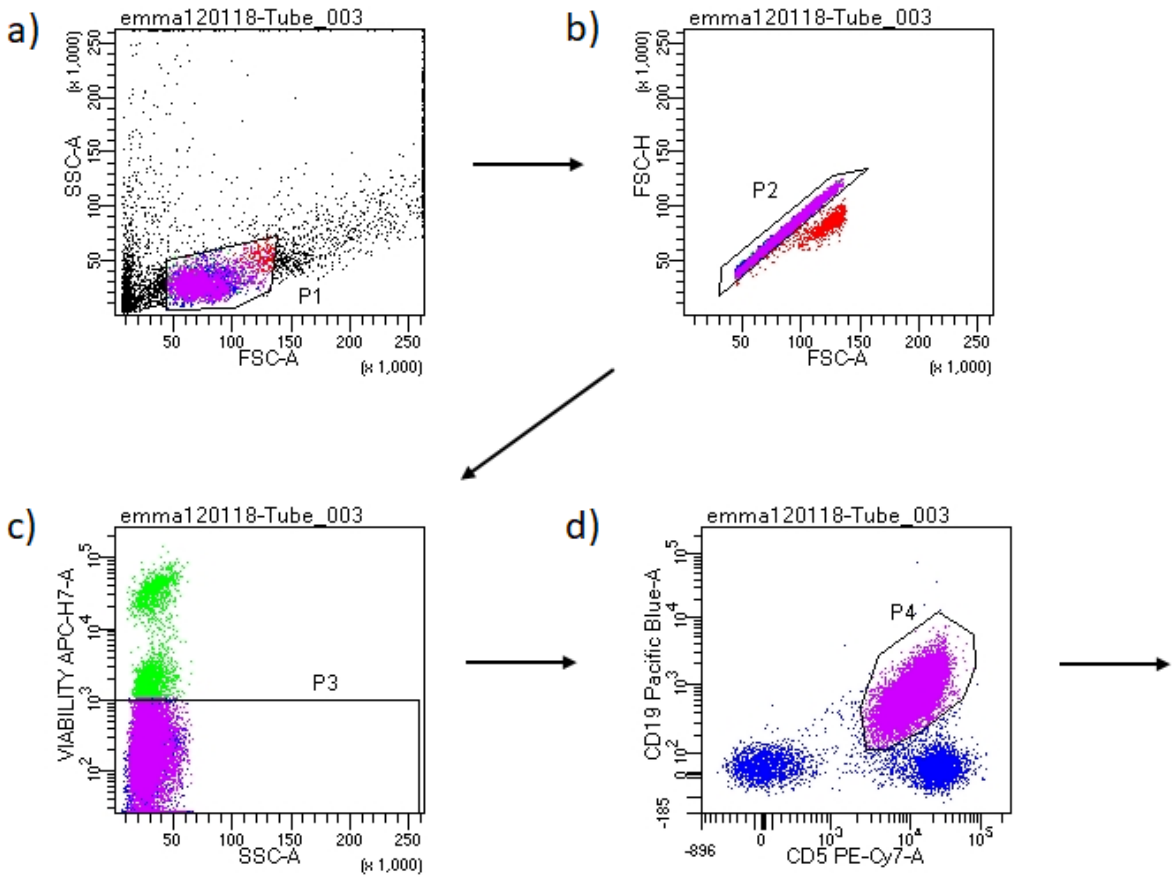

Figure 2.1: Gating Strategy for Multi-Colour Analysis on the LSR II Flow Cytometer.
a) Lymphocytes (P1) were identified from FSC-A/SSC-A scatter plots. b) Singlet lymphocytes (P2) were identified from FSC-A/FSC-H scatter plots. c) Live singlet lymphocytes (P3) were identified from SSC-A/FVD (eFluor™ 780) scatter plots. d) CLL cells (P4) were identified from CD5 (PE-Cy7)/CD19 (Pacific Blue) scatter plots. Phenotypic analysis was performed on CD5+/CD19+/FVD- CLL cells (P4).

2.10.2: Flow Cytometry using a BD Accuri

The BD Accuri is a 4-colour flow cytometer and phenotyping panels were consequently minimised for this machine. In the following panels, CLL cell identification was achieved using CD19 and CD3 in place of CD5. This was due to technical problems earlier identified on the LSR II flow cytometer with the accurate identification of post-culture CLL cells with CD19 and CD5-alone. Post culture CLL cells showed a markedly reduced expression of CD19, relative to baseline/post-thaw levels, and in some samples, the CLL (CD5+/CD19+) population became indistinguishable from the T-cell (CD5+/CD19-) population (Appendix 7.3.2, Figure 7.4). CD3 is a T-cell surface marker and was used to remove the T-cell population from the lymphocyte gate and CLL cells were identified as CD19+/CD3- (Figure 2.2).

Table 2.2: Antibody Panel B: Accuri

Antibody	Clone	Fluorophore	Volume (For $\leq 1x10^6$ cells)
CD3	HIT3a	APC	2 μl
CD19	HIB19	Alexa Fluor 488	2 μl
CD49d	9F10	PerCP-Cy5.5	2 μl
CD69	FN50	PE	2 μl

2.10.2.1: Extracellular Staining for the Accuri

PBMCs were collected into 1.5ml Eppendorf tubes at densities of $3x10^5$-$1x10^6$, centrifuged at 7000rpm/300g for 8 minutes and resuspended in 100µl PBS. The selected antibody panel was added as shown above and the tubes were vortexed and incubated at 4^oC for 20 minutes. The Accuri flow cytometer was used to analyse the results of transwell migration experiments and so the cells were not washed post-staining. This was to ensure that the migration cell counts were accurate and that CLL cells had not been damaged/lost in the washing process.

2.10.2.2: Analysis using the Accuri

Cells were analysed by multicolour flow cytometry and results were analysed using CFlow software. The Accuri Flow Cytometer does not require pre-acquisition fluorophore compensations and antibody panel compensations were adjusted manually post-acquisition. Accuri antibody panels did not include FVD and live lymphocytes were therefore identified by FSC-A and SSC-A-alone (Figure 2.2a). Live lymphocytes were forward gated into FSC-A/FSH-A plots for singlet lymphocyte identification (Figure 2.2b). Singlet lymphocytes were forward gated into CD19/CD3 plots and CLL cells were identified as CD19+/CD3- (Figure 2.2.c). CLL cells were forward gated for the volumetric quantification and phenotypic analysis of migrated and non-migrated CLL cells. Percentage positivity was determined using a FMO tube and MFI was based on the CD19+/CD3- gated population.

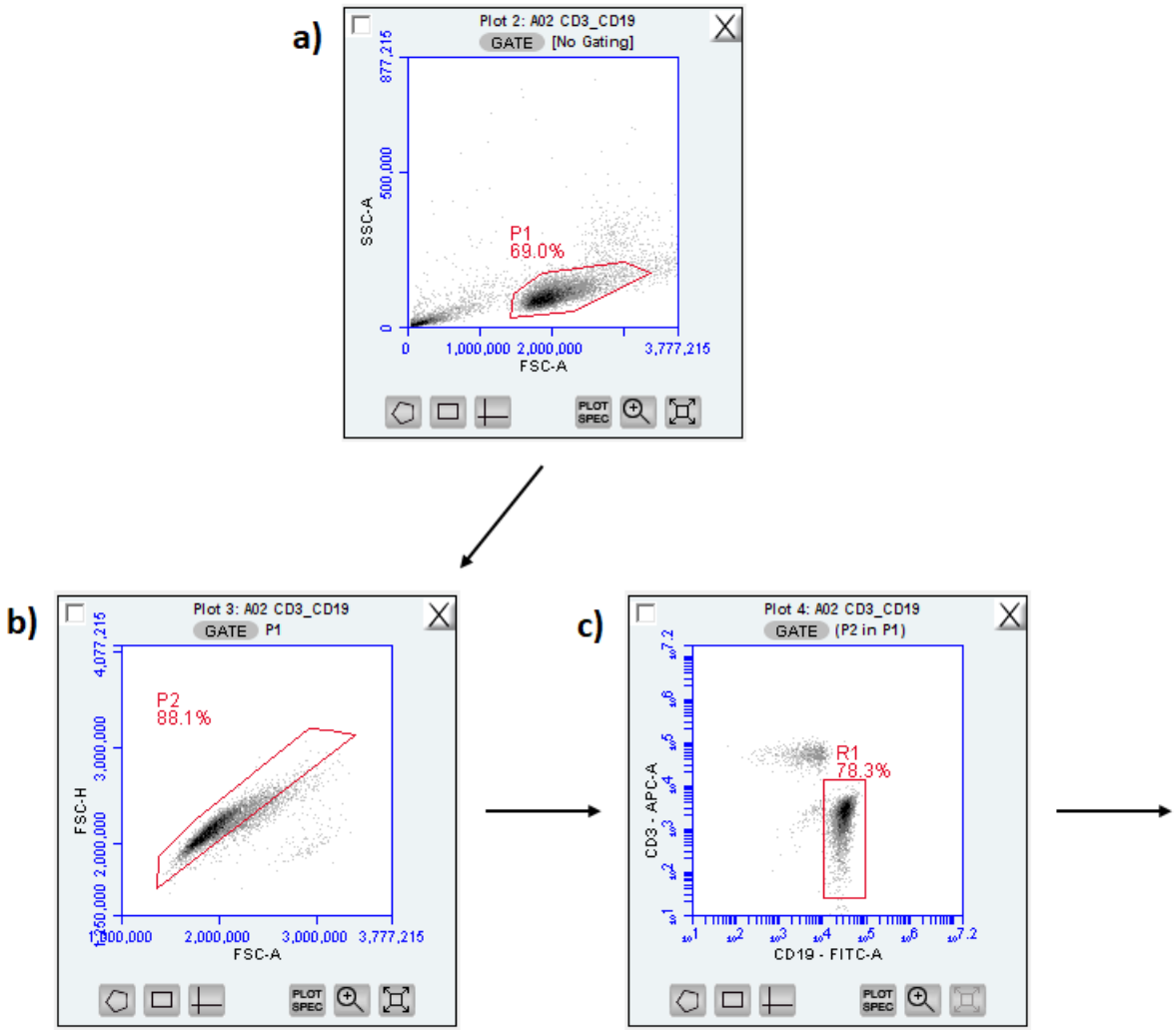

Figure 2.2: Gating Strategy for Multi-Colour Analysis on the Accuri Flow Cytometer.
a) Lymphocytes (P1) were identified from FSC-A/SSC-A scatter plots. b) Singlet lymphocytes (P2) were identified by FSC-A and FSC-H scatter plots. c) CLL cells (R1) were identified by CD19 and CD3 scatter plots. Phenotypic analysis was performed on CD19+/CD3- CLL cells (R1).

2.10.3: Flow Cytometry using a Beckman Coulter CytoFLEX LX

The Beckman Coulter CytoFLEX LX is a 21-colour flow cytometer and live CLL cells were identified as CD5+/CD19+/CD3-/FVD- (Figure 2.3).

Table 2.3: Antibody Panel C: CytoFLEX LX

Antibody	Clone	Fluorophore	Volume (For $\leq 1x10^6$ cells)
CD3	HIT3a	Alexa Fluor 488	2 μl
CD5	UCHT2	PE-Cy7	2 μl
CD19	HIB19	Pacific Blue	2 μl
CD38	HB-7	APC	2 μl
CD49d	9F10	PE	2 μl
CD62L	DREG-56	BV-650	2 μl
CD69	FN50	BV-785	2 μl
CXCR4	12G5	PerCP-Cy5.5	2 μl
FVD	-	eFluor™ 780	1 μl

Table 2.4: Antibody Panel D: CytoFLEX LX

Antibody	Clone	Fluorophore	Volume (For ≤1x10^6 cells)
CD3	HIT3a	Alexa Fluor 488	2 μl
CD5	UCHT2	PE-Cy7	2 μl
CD19	HIB19	Pacific Blue	2 μl
TLR9	eB72-1665	PE	2 μl
FVD	-	eFluor™ 780	1 μl

Table 2.5: Antibody Panel E: CytoFLEX LX

Antibody	Clone	Fluorophore	Volume (For ≤1x10^6 cells)
CD5	L17F12	PE-Cy7	2 μl
CD19	HIB	Pacific Blue	2 μl
Phospho-NF-κB p65 (ser529)	13A3-1	PE	5 μl

2.10.3.1: Extracellular Staining for the CytoFLEX LX

PBMCs were collected into FACS tubes at densities of 3x10^5-1x10^6 in 100μl PBS. The selected antibody panels (shown above) were added, and the tubes were vortexed before being incubated at 4°C for 20 minutes (the FVD was diluted 1:1000). Post-staining, the cells were washed twice in 1ml PBS (centrifuged at 300g for 7minutes)

and resuspended in 100μl of PBS for a) immediate FACS analysis or b) in preparation for intracellular staining.

2.10.3.2: Intracellular TLR9 Staining for the CytoFLEX LX

Prior to intracellular staining, PMBCs were stained for the CLL-cell identifying markers CD3, CD5 and CD19 and FVD as described above (Antibody Panel D: CytoFLEX LX, Table 2.4). Intracellular TLR9 staining was then achieved using the BD Cytofix/Cytoperm™ kit (as per the manufacturer's guidelines). The PBMCs were resuspended in 100μl PBS before being run on the CytoFLEX LX flow cytometer.

2.10.3.3: Antibody and Viability Compensations for the CytoFLEX-LX

Antibody compensations were performed as previously described in (methods section 2.10.1.2). Viability compensations were performed as previously described in (methods section 2.10.1.3). Compensations were calculated using CytExpert software.

2.10.3.4: Analysis using the CytoFLEX-LX

Cells were analysed by multicolour flow cytometry and results were analysed using CytExpert software. The gating strategy to identify live CLL cells from the PBMC population is shown in Figure 2.3. Lymphocytes were firstly identified from an FSC-A/SSC-A scatter plot and forward gated into an FSC-A/FSC-H scatter plot to determine the singlet lymphocyte population. T-cells were then excluded from the singlet lymphocytes using a CD3 histogram (T-cells are CD3 positive and so only CD3 negative cells were selected). Following this, viable cells were selected from a FVD/SSC-A scatter plot and finally live CLL cells were identified from CD5 (PE-Cy7)/CD19 (Pacific Blue) scatter plots as CD5/CD19 double positive. Percentage positivity was

determined using a FMO tube and MFI was based on the CD5+/CD19+/CD3-/FVD- gated population.

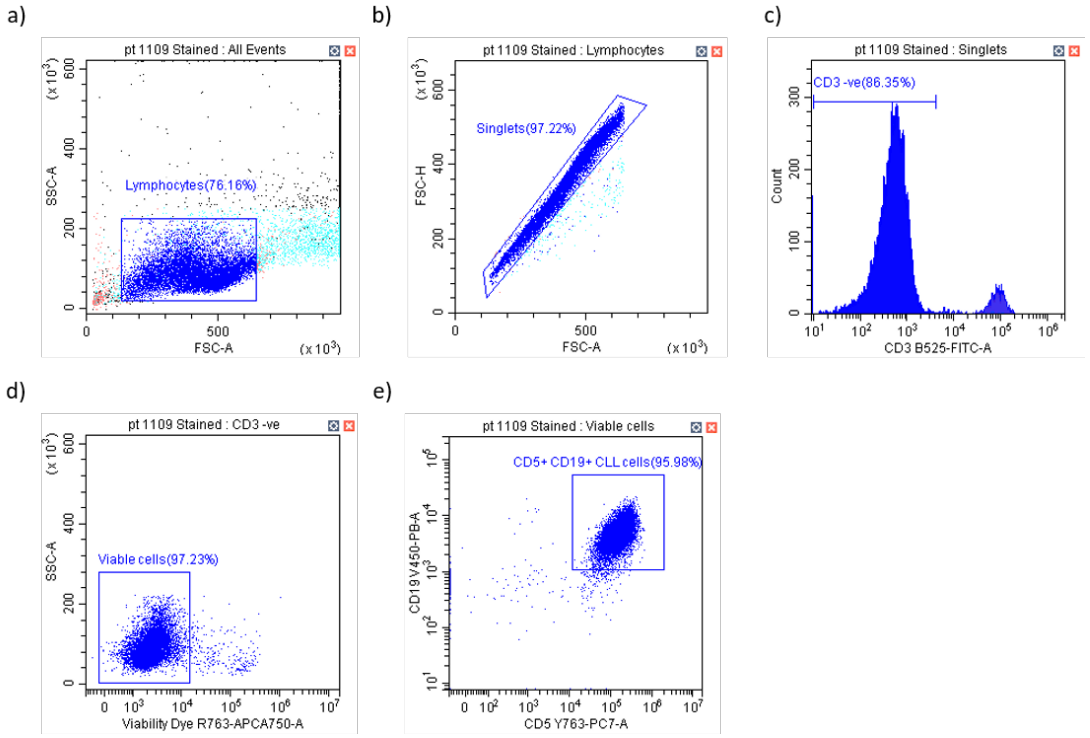

Figure 2.3: Gating Strategy for Multi-Colour Analysis on the CytoFLEX-LX Flow Cytometer. a) Lymphocytes were identified from FSC-A/SSC-A scatter plots. b) Singlet lymphocytes were identified from FSC-A/FSC-H scatter plots. c) T-cells (CD3 positive cells) were excluded from the singlet lymphocyte population from a CD3 histogram. d) Live cells were identified from SSC-A/FVD (eFluor™ 780) scatter plots. d) CLL cells were identified from CD5 (PE-Cy7)/CD19 (Pacific Blue) scatter plots. Phenotypic analysis was performed on CD5+/CD19+/CD3-/FVD- CLL cells.

2.11: Stimulation/Inhibition of TLR9 Signalling

2.11.1: TLR9 Agonist: ODN 2006

TLR9 was artificially activated using the commercially available TLR9 agonist, ODN 2006 (Invivogen). ODN 2006 is a synthetic and CpG-rich oligonucleotide, designed to mimic the presence of cell-free and circulating unmethylated CpG DNA.

ODN 2006 sequence: tcgtcgttttgtcgttttgtcgtt (24-mer)

PBMCs were seeded into a 96 well plate at a density of $3x10^6$ cells/well in 150µl complete media (materials section 2.5.1) + IL-4 (5µg/ml) and stimulated overnight with 1µM ODN 2006 at 37°C/5% CO_2.

2.11.2: TLR9 Antagonist: ODN INH-18

TLR9 was inhibited using the commercially available TLR9 antagonist, ODN INH-18 (Invivogen). ODN INH-18 contains TLR9-inhibitory CCT and GGG motifs (illustrated in red below) and it acts as a competitive inhibitor of ODN 2006.

ODN INH-18 sequence: 5'-cct gga tgg gaa ctt acc gct gca-3' (24mer).

PBMCs were seeded into a 96 well plate at a density of $3x10^6$ cells/well in 150µl complete media + IL-4 (5µg/ml) and pre-incubated with 5µM ODN INH-18 for 30 mins, prior to being incubated ± 1µM ODN 2006 at 37°C/5% CO_2.

2.12: Inhibition of B-Cell Receptor Signalling

BCR signalling was inhibited using the small molecule BCR-targeted kinase inhibitor, ibrutinib, which is specific for Bruton's Tyrosine Kinase (BTK), downstream of the BCR.

PBMCs were seeded into a 96 well plate at a density of $3x10^6$ cells/well in 150μl complete media + IL-4 (5μg/ml) and pre-incubated with 1μM ibrutinib for 30 mins, prior to being incubated with 1μM ODN 2006 at 37°C/5% CO_2.

2.13: Transwell Migration Assays

Transwell migration assays were performed using freeze-thawed liquid nitrogen banked PBMC aliquots (see Methods 2.7.3: Storage and Recovery of Peripheral Blood Mononuclear Cells). This was to ensure consistency between experiments as fresh (<24h post venesection) samples from some CLL patients, showed a higher basal level of CLL cell migration, relative to their corresponding freeze-thawed samples (see Appendix 7.3.4: Fresh vs Frozen PBMC Samples). The project relied upon the availability of frozen material, and it was therefore not practical to perform all transwell migration experiments using fresh material.

PBMCs were stimulated overnight in 96 well plates ± ODN 2006 (TLR9 agonist) ± ODN INH-18 (TLR9 antagonist) ± ibrutinib (BTK-inhibitor), as described above in methods section 2.11 (each experimental condition was performed in duplicate). A '0h live cell count' was then performed using an automated Countess II cell counter prior to the cells being transferred into 24 well transwell migration plates. Each transwell was divided into an apical and basal chamber, separated by a 6.5mm, 5 micron-pore

membrane and the cells were transferred into the apical chambers. A chemotactic gradient comprising complete media + 100ng/ml CXCL12 was established in the basal chambers to encourage the directional migration of PBMCs (Figure 2.4). The transwell migration plates were incubated for 4h at 37^{o}C/5% CO_2 to allow migratory cells to pass through the porous membrane and into the basal chambers. Post-incubation, PBMCs were collected from the basal (migrated) and apical (non-migrated) chambers into 1.5ml Eppendorf tubes and each side of the membrane was gently washed with PBS to ensure all cells were removed. Each Eppendorf tube was centrifuged at 300g for 8 minutes and PBMCs were resuspended in 100μl PBS prior to antibody staining with Antibody Panel B: Accuri (Table 2.2, method section 2.10.2), in preparation for volumetric quantification. Migrated and non-migrated cells were simultaneously phenotyped and counted using an Accuri flow cytometer. CLL cells were identified as CD19+/CD3- and CLL cell migration was calculated as a percentage of the 0h live cell count i.e., CLL cell migration = (Total number of migrated cells/0h live cell count) x100.

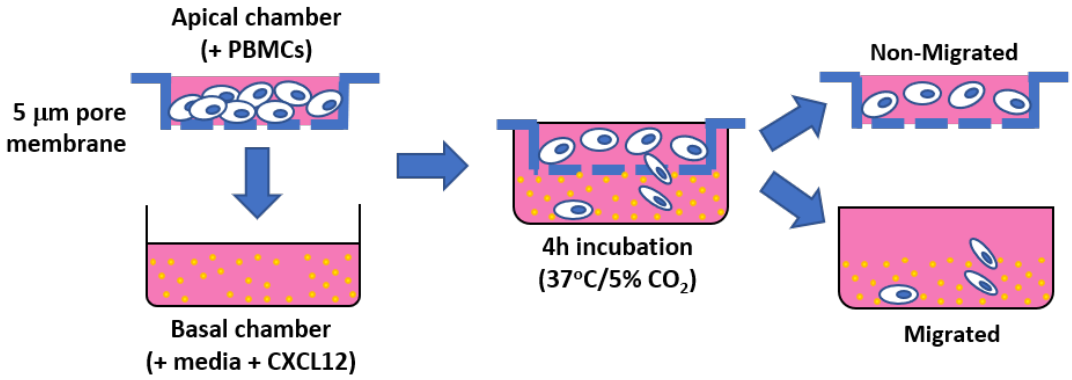

Figure 2.4: Transwell Migration Protocol. Primary patient PMBCs were cultured overnight ± ODN 2006 (TLR9 agonist) ± ODN INH-18 (TLR9 antagonist) ± ibrutinib (BTK-inhibitor) before being transferred into the apical chambers of 24 well, 5µm pore polycarbonate transwell migration plates; cell counts were performed at '0h migration' (i.e., prior to transfer) using a Countess II automated cell counter. A chemotactic gradient of CXCL12 (100ng/ml) in 600µl complete media was established in the basal chambers and plates were incubated at 37°C/5% $C0_2$ for 4h. At '4h migration' migrated and non-migrated PBMCs were collected and stained in preparation for volumetric quantification using an Accuri flow cytometer. CLL cells were identified as CD19+/CD3- and CLL migration was calculated as a percentage of the 0h live cell count.

2.14: Synergy Experiments using ODN INH-18 and Ibrutinib

Synergy experiments were performed using suboptimal concentrations of ODN INH-18 (TLR9 antagonist) and ibrutinib (BCR-targeted kinase inhibitor). This was to ensure that ODN 2006-stimulated CLL cell migration was not completely abrogated in the presence of either single-agent alone, enabling the quantification of additive/synergistic inhibition.

2.14.1: CLL Cell Migration

PBMCs were seeded into 96 well plates at a density of $3x10^5$ cells/well in 150μl complete media + IL-4 (5μg/ml) and pre-incubated for 30 minutes with ODN INH-18-alone, ibrutinib-alone or a combination of ODN INH-18 + ibrutinib. An uninhibited control was also incubated for 30 minutes alongside the experimental wells. Each condition was performed in duplicate and dose combinations were fixed at a molar ratio of 2:1 ODN INH-18: ibrutinib as follows:

- **Dose Combination 1**:
    - 0.5 μM ODN INH-18
    - 0.25 μM ibrutinib
    - 0.5 μM ODN INH-18 + 0.25 μM ibrutinib
- **Dose Combination 2**:
    - 1.0 μM ODN INH-18
    - 0.5 μM ibrutinib
    - 1.0 μM ODN INH-18 + 0.5 μM ibrutinib
- **Dose Combination 3**:
    - 2.0 μM ODN INH-18

- 1.0 μM ibrutinib
- 2.0 μM ODN INH-18 + 1.0 μM ibrutinib

Following the 30-minute incubation, the PBMCs in all wells (including the uninhibited control wells), were stimulated overnight with 1.0μM ODN 2006 at 37°C/5% CO_2. The PBMCs were then collected post-culture and transferred into the apical chambers of a 5μm pore, 24 well transwell migration plate. Transwell migration assays were then performed as described above in methods section 2.13. CLL cell migration was calculated as previously described and expressed relative to the (uninhibited) ODN 2006-stimulated control. These values were then used to calculate synergy using Compusyn software.

2.14.2: NF-κB Activation

PBMCs were seeded into 96 well plates at a density of $3x10^6$ cells/well in 150μl complete media + IL-4 and pre-incubated for 30 minutes with ODN INH-18-alone, ibrutinib-alone or a combination of ODN INH-18 + ibrutinib as above. For the NF-κB activation synergy experiments, only the optimised dose combination was used (i.e., Dose Combination 3).

Following the 30-minute incubation, the PBMCs were stimulated for 4 hours with 1.0μM ODN 2006 at 37°C/5% CO_2 before being collected into FACS tubes for fixation and staining using the BioLegend True-Phos fix and perm protocol (as per the manufacturer's guidelines). NF-κB activation was determined by the level of phosphorylated p65 (p-p65) (one of five NF-κB subunits). Briefly, PBMCs were firstly fixed for 15 minutes at 37°C/5% CO_2 using 0.5ml fixation buffer and then washed

twice in warm stain buffer. The cell pellet was then resuspended by pipetting and 1ml of ice-cold True-Phos perm buffer added drop by drop whilst vortexing the cells to permeabilise them. The cells were then incubated at -20^{o}C overnight. Cells were centrifuged at 1000g and then washed twice in stain buffer (also at 1000g) and then resuspended at 1x10^{7}/ml for staining. Cells were stained with Antibody Panel E: CytoFLEX LX (Table 2.5) incubated for 30 minutes at room temperature, protected from light. The cells were then washed twice in stain buffer (also at 1000g) and resuspended in 300μl of stain buffer for immediate FACS analysis. MFI values were taken from the CD5+/CD19+ population and expressed relative to the (uninhibited) ODN 2006-stimulated control. These values were then used to calculate synergy using Compusyn software.

2.14.3: Calculating Synergy using Compusyn Software

Synergy was calculated using Compusyn software which is a computer program for quantitation of synergism and antagonism in drug combinations and the determination of IC50 and ED50 values. All of the Data Entry Dialogs in CompuSyn are set up to enable simple result entry. For each experimental condition, CLL cell migration and NF-κB activation was expressed relative to the (uninhibited) ODN 2006-stimulated control and entered as values between 0-1.

2.15: Western Blotting

Western blotting was used to quantify IκBα expression in ODN 2006-stimulated CLL cells. IκBα is an inhibitory component of the canonical NF-κB activation pathway and sequesters NF-κB in the cytoplasm of inactive cells. Following upstream activation of

the NF-κB signalling pathway, IκBα is targeted for degradation, releasing NF-κB and enabling its translocation into the nucleus. The degradation/expression of IκBα can therefore be used as a marker of NF-κB responsiveness to stimuli. The temporal pattern of IκBα degradation was quantified at 0-6h post-stimulation with ODN 2006.

PBMCs were seeded into 12 well plates at a density of $2x10^6$ cells/well in 1ml complete media + IL-4 (5μg/ml) incubated with 1μM ODN 2006 at 37°C/5% CO_2. The cells were collected into 5ml FACS tubes at 0h, 0.5h, 1h, 4h and 6h post-stimulation and each timepoint was performed in triplicate. For each timepoint, cells were pooled into a single FACs tube to give a total of 6 million cells per timepoint and centrifuged at 300g for 7 minutes. The cells were then resuspended in 1ml ice cold PBS and transferred into a 1.5ml Eppendorf in preparation for cell lysis. The Eppendorf tubes were incubated on ice prior to lysis.

2.15.1: Cell Lysis

PBMCs were washed in ice cold PBS (centrifuging at 300g for 7 minutes) before being resuspended in 50μl RIPA buffer (materials section 2.6.2), vortexed and left to incubate on ice for 20 minutes. The resulting cell lysates were centrifuged at 10 000 rpm for 10 minutes and supernatants were transferred into clean Eppendorf tubes. Cell lysates were stored short-term at -20°C or longer term at -80°C.

2.15.2: Protein Quantification (BCA Assay)

The protein concentration of each cell lysate was determined using the Pierce™ BCA Protein Assay Kit. Albumin protein standards were prepared as suggested in the manufacturer's guidelines (using RIPA buffer as the diluent) then added in triplicate (12.5μl) to a 96 well plate; these standards were later used to calculate the standard

curve. The lysates were diluted 1:10 in RIPA buffer and added in duplicate (12.5μl) to the 96 well plate. 100μl working reagent (prepared following the manufacturer's guidelines) was added to each well and the plate was incubated for 30 minutes at 37^{o}C. Absorbance was read on a spectrophotometric plate reader (BioTek Synergy HT) at 540nm and the standard curve was calculated using Gen5 software. The final protein concentration of each sample was also calculated using Gen5 software.

2.15.3: Protein Electrophoresis

Cell lysates were defrosted on ice and diluted 1:4 in 4x SDS loading buffer. The samples were then placed on a heat block for 10 minutes at 96^{o}C to enable protein linearisation, replaced on ice to cool and centrifuged at 10 000 rpm for 10 minutes in preparation for protein electrophoresis. Samples were kept on ice before use.

TruPAGE pre-cast electrophoresis gels (4-12%) were inserted into a Novex Mini Cell protein electrophoresis tank (Invitrogen) filled with 1x TruPAGE TEA-Tricine SDS Running Buffer and 5μl protein standard ladder was added into the first well; these experiments used: Precision Plus Protein™ Kaleidoscope™ Prestained Protein Standards (a ladder ranging from 250-10 kDa). Samples were then loaded into the remaining wells and the protein electrophoresis was run at 150 volts for ~1.5 hour during which time the linearised proteins were separated in order of size.

2.15.4: Protein Transfer

Proteins were transferred from the gel onto an Immun-Blot® Low Fluorescence PVDF membrane. Prior to transference, the membrane was activated in 100% methanol for 10 seconds before being washed in distilled H_20 (dH_20) for 5 minutes and

equilibrated in 1x TruPage Transfer Buffer in dH_20 + 10% methanol for a further 5 minutes.

In preparation for protein transfer, the gel cassette was broken apart using a lever and the gel was rested in 1x TruPage Transfer Buffer in dH_20 + 10% methanol. Filter papers and sponges were also soaked in 1x TruPage Transfer Buffer in dH_20 + 10% methanol prior to transference. The transfer sandwich was then assembled as shown in Figure 2.5 and inserted alongside an ice pack into a Bio-Rad Mini-Protean® 3 electrophoresis tank filled with chilled 1x TruPage Transfer Buffer in dH_20 + 10% methanol. *(NB: air bubbles between the gel and the membrane were removed using a roller prior to the addition of the second filter paper).* The protein transfer was run at 4°C and 400mAmps for 90 minutes.

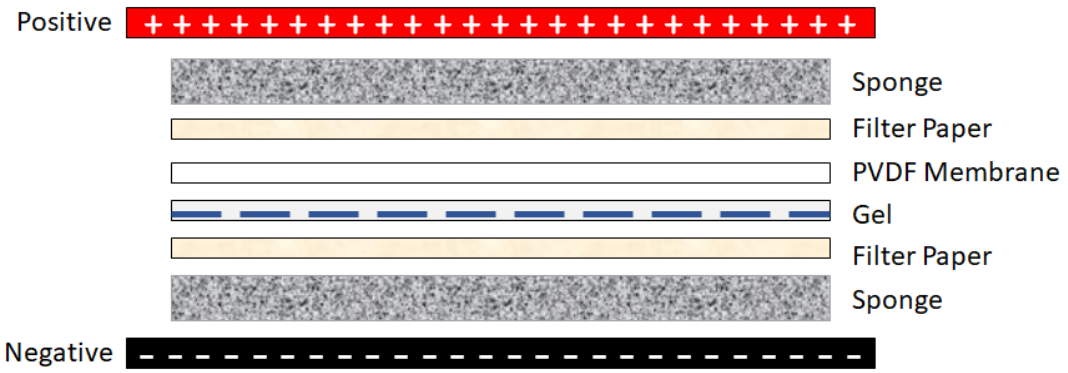

Figure 2.5: Western Blot Transfer. The western blot transfer sandwich was assembled on the black (negative charge) side of a transfer cassette as follows: Sponge; filter paper; gel; methanol-activated PVDF membrane; filter paper, sponge.

2.15.5: Membrane Blocking and Antibody Incubations

Following protein transfer, the membrane was fully immersed in 5% dried milk (Marvel) in PBS (i.e., blocking buffer) and incubated on a shaker for 1 hour at room temperature.

The blocking buffer was removed (by pouring off the membrane) and primary antibodies were diluted (as outlined in materials section 2.6.3) in fresh blocking buffer + 0.1% Tween-20 (blocking buffer-tween). The antibody dilutions were added to the membrane and incubated on a shaker at 4^{o}C overnight.

NB: antibodies for the target and housekeeping proteins were chosen to originate from unique host species and could therefore be incubated simultaneously. Secondary antibodies were specific to each host and were chosen to fluoresce in separate channels during imaging.

3x 5 minute membrane washes were performed on a shaker using PBS + 0.1% Tween 20 (PBS-T) before the addition of the fluorescent secondary antibodies. Secondary antibodies were diluted 1: 15000 in blocking buffer-tween + 0.01% SDS and incubated for 1 hour at room temperature on a shaker.

NB: secondary antibody incubations were protected from light in order to prevent fluorophore degradation i.e., membrane boxes were wrapped in tin foil whilst incubating.

A further 3x 5-minute membrane washes in PBS-T were performed in preparation for imaging (again protected from light).

2.15.6: Membrane Imaging

The membrane was blotted dry between two sheets of filter paper and sealed in a transparent plastic wallet; membranes were protected from light until imaged.

Membranes were imaged using the LI-COR Odyssey FC with exposure times set to:

- 600 channel (1 minute) – ladder
- 700 channel (4 minutes) – housekeeping protein
- 800 channel (4 minutes) – target protein

2.16: IGHV Mutational Status Identification

2.16.1: DNA Extraction

DNA extractions from freeze-thawed patient PBMC samples were performed using the DNeasy Blood & Tissue kit (Qiagen). Each extraction used $2x10^6$ cells and followed the protocol outlined in the manufacturers' handbook. DNA concentrations were quantified using the NanoDrop One (Thermo Scientific) as per the manufacturer instructions.

2.16.2: IGHV Sequencing

DNA extractions were sent for IGHV Sanger sequencing (Sseq) at The Royal Marsden Hospital (Centre for Molecular Pathology, Sutton).

2.16.3: IGHV Analysis

Nucleotide sequences were returned and viewed using SnapGene software.

IGHV analysis was performed using the ImMunoGeneTics (IMGT)/V-Quest tool of the international IMGT information system. Nucleotide sequences were entered and aligned against a Human Ig reference directory.

Patients were considered IGHV-unmutated (U-CLL) when displaying ≥98% homology to the reference directory and IGHV-mutated (M-CLL) when displaying <98% homology with the reference directory.

2.17 Statistical Analysis

Statistical analyses were performed using GraphPad Prism 8.0 (GraphPad Software, San Diego, CA). Data was assessed for normality and appropriate descriptive statistics and tests used. Unless otherwise stated, results are presented as mean (±SD) and paired t-test or Wilcoxon matched-pairs signed rank were used depending on whether the data were Gaussian. Correlation was determined using the Spearman's rank correlation coefficient.

3.0: Investigating the Effect of the TLR9 Agonist ODN 2006 on the Migration of CLL Cells *in vitro*

3.1: Introduction

Chronic Lymphocytic Leukaemia (CLL) is an incurable haematological malignancy characterised by an accumulation of clonal CD5+/CD19+ B-cells in the peripheral blood, bone marrow, lymph nodes and the spleen. CLL cells are highly dependent upon microenvironmental interactions and regularly traffic from the circulation into the secondary lymphoid tissues where they encounter a plethora of disease promoting stimuli. Strikingly, CLL cell proliferation occurs almost exclusively within the lymph node niche[40] whilst the vast majority of circulating CLL cells remain halted in the G0/G1 phase of the cell cycle[68]. CLL cell migration is therefore at the epicentre of CLL progression and is an extremely important target for therapeutic intervention; eliminating tissue-resident CLL cells would mark a huge step forward in the search for a curative treatment.

CLL cell trafficking is a complex process, orchestrated by a plethora of adhesion molecules and chemotactic gradients; CLL cells firstly undergo selectin and integrin-mediated transendothelial cell migration and then travel towards the LN and BM niche following chemokine receptor activation. A CLL cell-specific 'invadosome' structure has been identified on the membranes of migratory CLL cells, which contains the prognostic biomarkers CD49d and CD38[148,149]. CD49d is the alpha subunit of the $\alpha 4\beta 1$ integrin[74] and has been shown to be essential for CLL migration, and CD38 is a transmembrane glycoprotein associated with adhesion and cellular

activation; both markers correlate with lymphadenopathy, progressive disease and a poor clinical prognosis[27,42,74,75].

CXCR4 is the chemokine receptor for CXCL12: a chemokine secreted in high quantities by BM and LN stromal cells and its expression has been correlated with accelerated disease progression as a result of increased tissue-homing[76]. Gene expression profiling has revealed an overexpression of the chemokine receptor CXCR4 in circulating CLL cells[62] and Calissano et al.,[150] have reported CXCR4 to be most highly expressed in resting CLL cells preparing to migrate. CXCR4 expression has been suggested to cycle between $CXCR4^{bright}$ and $CXCR4^{dim}$ based on CXCL12-interactions and two distinct phenotypic subsets have been identified, which can distinguish recently egressed ($CXCR4^{dim}/CD5^{bright}$) from resting/circulating ($CXCR4^{bright}/CD5^{dim}$) CLL cells[150]. Recently egressed CLL cells have been in contact with high levels of CXCL12 in the lymphoid niche, which results in CXCR4 receptor internalisation and a lower surface expression of CXCR4; these CLL cells have been activated and express proliferative and anti-apoptotic markers. In contrast, CLL cells that have been circulating for a longer time have not been in contact with CXCL12 and CXCR4 is consequently recycled and re-expressed onto the cell surface. These CLL cells are non-proliferative and must traffic into the LN/BM to survive.

Although it is well established that CLL cells can be activated through Toll-like Receptor 9 (TLR9), chapter 3 postulates a role for TLR9 in the trafficking of CLL cells. TLR9 is an endosomal pattern recognition receptor of the innate immune system that is stimulated by unmethylated CpG DNA. Multiple studies have shown a link between TLR9 and the migratory potential of lung, breast, brain, prostate and gastric cancer

cell lines[141-145] and furthermore, Luo et al.,[144] reported a correlation between TLR9 and an increased propensity for lymph node metastasis in prostate cancer patients. As previously discussed, our group has identified a significantly higher level of unmethylated cell-free DNA in the plasma of CLL patients relative to healthy individuals and hypothesise that this has the potential to fuel CLL progression via the activation of TLR9[132]. Throughout this chapter, the effect of TLR9 activation upon the activation and migratory potential of primary peripheral blood-derived CLL cells was investigated. TLR9 activation was artificially stimulated using a commercially available TLR9 agonist. ODN 2006 is a 24-mer synthetic and CpG-rich oligonucleotide, designed to mimic the presence of cell-free and circulating unmethylated CpG DNA (5'- tcg tcg ttt tgt cgt ttt gtc gtt -3'). Artificial stimulation of TLR9 was required for the following reasons:

- Cell-free plasma DNA is highly labile and can rapidly degrade *ex vivo*.
- Cell-free unmethylated DNA levels vary between patients but activation with ODN 2006 allows a uniform and comparative stimulation across patient samples.
- ODN 2006-stimulated CLL cells can be phenotypically compared to matched unstimulated control CLL cells to identify the influence of TLR9 activation alone upon CLL cell migration.

A number of cell surface markers of CLL cell activation and migration were recurrently quantified throughout chapter 3, to act as an indicator of both activation and migratory potential ± stimulation; the biological relevance of each marker is outlined below in Table 3.1.

Table 3.1: Description of Cell Surface Markers used for CLL Cell Analysis

Marker	Marker Type	Marker Description
CD3	T-cell identifier	Co-receptor for the T-cell receptor (TCR). Used in these experiments to exclude T-cells from lymphocyte analysis.
CD5	CLL cell identifier/ BCR signalling	A T-cell associated marker, which is also expressed in a small subset of healthy B-cells. CD5 is consistently expressed in CLL and is thought to repress the BCR signalling response.
CD19	CLL cell identifier/ BCR signalling	Co-receptor of the BCR – enhancer of BCR signalling
CD38	Tissue-homing/ proliferation	A transmembrane glycoprotein with a diverse range of roles relating to cell metabolism, cell adhesion, activation, survival and proliferation. Associated with a poor prognosis in CLL. **Important for CLL cell homing (together with CD49d).**
CD49d	Tissue-homing	α-subunit of integrin $\alpha4\beta1$: involved in the transendothelial migration of CLL cells across HEVs. Associated with a poor prognosis. **Essential for CLL cell homing.**
CD62L	Tissue-homing	A selectin (adhesion molecule) implicated in CLL cell transendothelial migration.
CD69	Activation	B-cell/CLL cell activation marker

3.2: Confirming the Expression of TLR9 in Primary CLL Cells

This thesis explores the role of TLR9 in CLL cell activation and migration, and it was therefore fundamentally important to confirm the expression of TLR9 in the patient samples used throughout the project; both the percentage (%) positivity and mean fluorescent intensity (MFI) of TLR9 were quantified using flow cytometry. Live CLL cells were gated as CD5+/CD19+/CD3-/FVD- and TLR9 % positivity was found to exceed 50% in 32/33 of the tested samples. The remaining patient demonstrated a far lower expression of 18.3% and values ranged from 18.3% to 99.9%, with a mean (±SD) of 80.3% (±17.0). TLR9 MFI was similarly varied and ranged from 447.6 to 12448, with a mean (±SD) of 2388 (±2121). TLR9 was therefore confirmed to be expressed in the CLL cells of all 33 patient samples, with evident interpatient variability.

The lymphocyte population of CLL patients is largely monopolised by malignant B-CLL cells however in patients with earlier stage disease, CD3+ T-cells can constitute a significant proportion of the lymphocyte pool. In the above cohort, CD3+ T-cells comprised 1.5% to 37.1% of the singlet lymphocyte population, with a mean (±SD) of 12.8% (±9.1). Figure 3.1 illustrates the % positivity and MFI of TLR9 in CLL cells relative to CD3+ T-cells. Although marginally higher in the CD3+ T-cells, there was no significant difference between the % positivity of TLR9 in CLL cells relative to CD3+ T-cells ($P=0.090$, $n=33$); CD3+ T-cells demonstrated a mean (±SD) TLR9 % positivity of 84.3 (±13.0) with a range of 54.6% to 99.2%. There was however a significant difference between the MFI of TLR9 in CLL cells relative to CD3+ T-cells; CD3+ T-cells showed a significantly higher expression of 3456 (±2907) with a range of 910.7 to

10171 (P=0.002). These results suggest that ODN 2006 stimulation is likely to also affect CD3+ T-cells and emphasises the importance of removing the CD3+ lymphocytes from future phenotypic analyses. Figure 3.2 demonstrates the gating strategies used to analyse TLR9 expression in CLL cells and CD3+ cells and shows representative patient histograms compared with a fluorescent minus one (FMO) control i.e., a control sample stained with CD5, CD19, CD3 and FVD, but not TLR9. This gating strategy was utilised throughout the thesis.

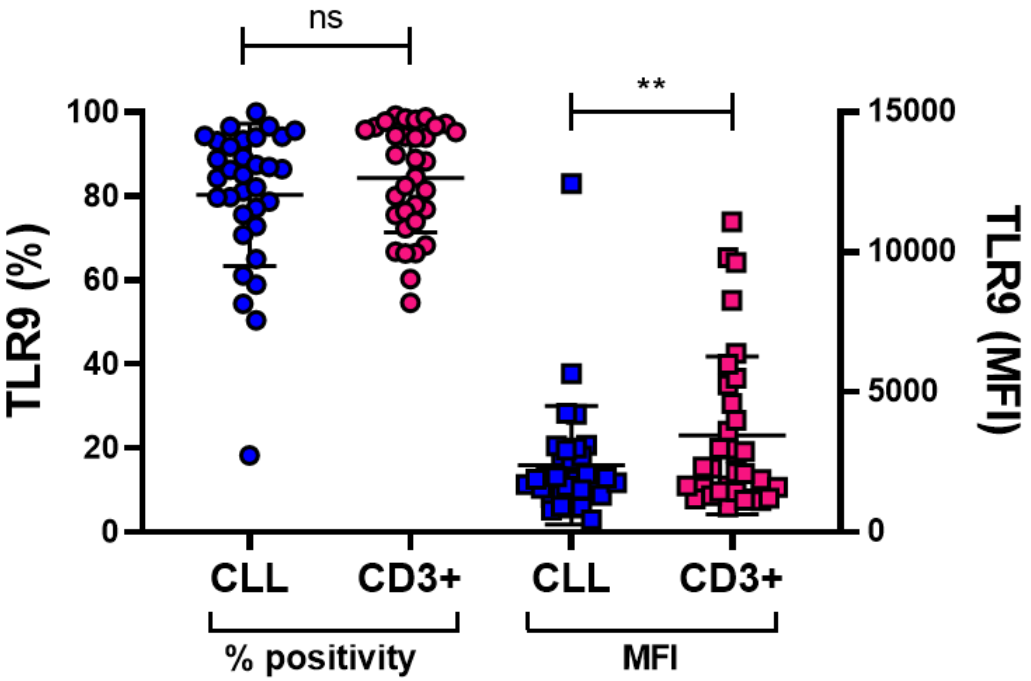

Figure 3.1: Primary CLL Cells and CD3+ T-Cells Express TLR9. Freeze-thawed primary PBMCs from 33 CLL patients were stained for extracellular expression of CD5, CD19 and CD3 and simultaneously incubated with a fixable viability dye (FVD). The cells were then permeabilised and stained for intracellular TLR9 before being processed by multicolour flow cytometry. Live CLL cells were gated as CD5+/CD19+/FVD-/CD3- and Live T-cells (CD3+ cells) were gated as FVD-/CD3+; analysis was performed using CytExpert software. There was no significant difference in the % positivity of TLR9 in CLL vs CD3+ T-cells (P=0.090, Wilcoxon Matched Pairs test). There was a significant difference between the MFI of TLR9 in CLL vs CD3+ T-cells (P=0.002, Wilcoxon Matched Pairs test); CD3+ T-cells displayed a significantly higher TLR9 MFI relative to CLL cells. Statistical analyses were performed using GraphPad Prism 8.0 and the Wilcoxon Matched Pairs test was used as the data were not Gaussian (as determined by the D'Agostino & Pearson omnibus normality test).

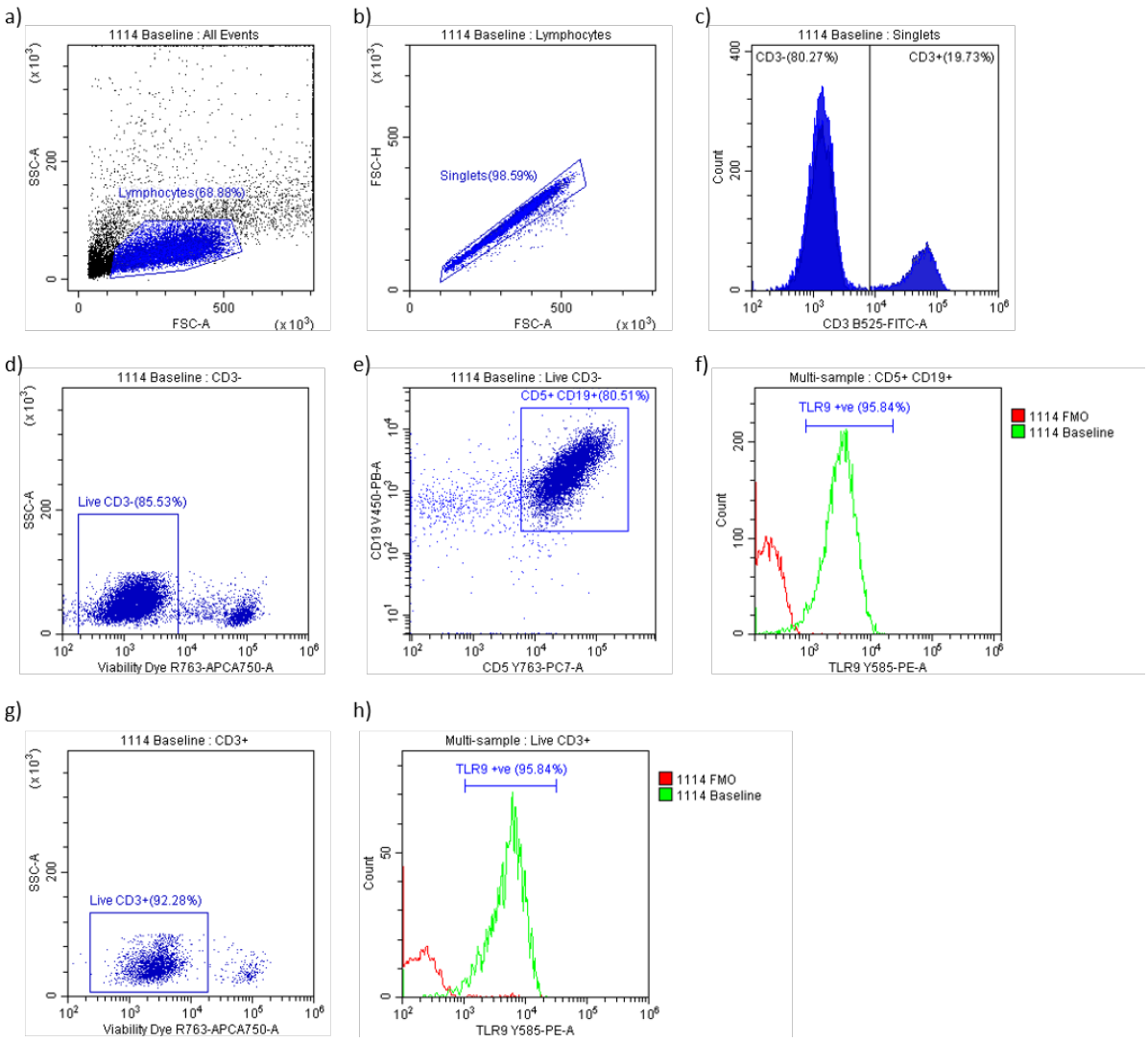

Figure 3.2: Representative Gating Strategy for the Analysis of TLR9 Expression in CLL and CD3+ Lymphocytes. Gating strategy using the CytoFLEX LX flow cytometer, showing representative patient 1114. a) The lymphocyte population was selected from a forward scatter-area (FSC-A)/side scatter-area (SSC-A) dot-plot. b) Singlet lymphocytes were then selected from a FSC-A/FSC-height (FSC-H) dot-plot. c) Either the CD3- or CD3+ population was selected from a CD3-histogram. For CLL cell analysis: the CD3- population was selected and live CD3- cells were then selected from (d): a FVD/SSC-A dot-plot and forward gated into (e) a CD5/CD19 dot-plot. TLR9 expression was then determined from a TLR9 histogram. (f) shows a CLL-cell specific TLR9 histogram overlay with both the FMO and stained baseline sample. For CD3+ T-cell analysis: the CD3+ population was selected from (c) and live CD3+ cells were selected from (g): a FVD/SSC-A dot plot. TLR9 expression was then determined from a TLR9 histogram. (h) shows a CD3+ cell specific TLR9 histogram overlay with both the FMO and stained baseline sample.

3.3: Stimulation of Primary CLL Cells with TLR9 Agonist ODN 2006 Induces a Migratory Phenotype

Having demonstrated the expression of TLR9 in primary CLL cells, the next step was to investigate their responsiveness to TLR9 stimulation. In physiological conditions, TLR9 responds to unmethylated CpG DNA, which has been shown to exist at up to 28-fold greater concentrations in the plasma of CLL patients relative to healthy individuals[132]. In the following experiments, CLL cells were artificially stimulated through TLR9 using the commercially available TLR9 agonist ODN 2006.

The potential impact of TLR9 activation on the migratory phenotype of CLL cells was firstly assessed by quantifying the response of the cell surface markers CD69, CD49d, CD38 and CD62L to stimulation with ODN 2006; the biological relevance of each marker is outlined in Table 3.1 above. The conditions for stimulating primary CLL cells were optimised prior to the following experiments and details of the optimisation experiments are presented in Appendix 7.1. In the below experiments, CLL cells were stimulated as outlined in methods section 2.11, and phenotypic analysis was performed using a CytoFLEX LX flow cytometer; both the percentage positivity and the MFI of each experimental marker was analysed. Live CLL cells were gated as CD5+/CD19+/CD3-/FVD-.

CLL Cell Activation:

CD69: CD69 is a B-cell activation marker and was included to infer the responsiveness of CLL cells to stimulation with ODN 2006.

Following stimulation with ODN 2006, the percentage positivity of CD69 (±SD) (in viable CLL cells) increased significantly from 39.4% (±22.8) to 69.1% (±19.7) ($P<0.001$, n=49) (Figure 3.3a-b). This level of activation was mirrored in the CD69 MFI (±SD) values where ODN 2006 was seen to increase the expression of CD69 from 2685 (±2215) to 7840 (±5201) ($P<0.001$, n=49) (Figure 3.3c). Interestingly, the percentage positivity of CD69 showed a significant correlation with the percentage positivity of TLR9 in both unstimulated ($P=0.039$, $R^2=0.14$, n=32) and ODN 2006-stimulated CLL cells ($P=0.003$, $R^2=0.25$, n=32) (Figure 3.3d-e). These data highlight an association between TLR9 expression and CLL cell activation, showing that patient samples with high TLR9 expression, display a more activated phenotype than patient samples with lower TLR9 expression. Furthermore, the P-value was lower and the R^2 value was higher in ODN 2006-stimulated CLL cells (relative to unstimulated CLL cells), showing that the observed correlation was stronger following activation of TLR9. Together, these data confirm that primary CLL cells are highly activated by stimulation with ODN 2006 and suggest a functional link between TLR9 and CD69 (i.e., CLL cell activation).

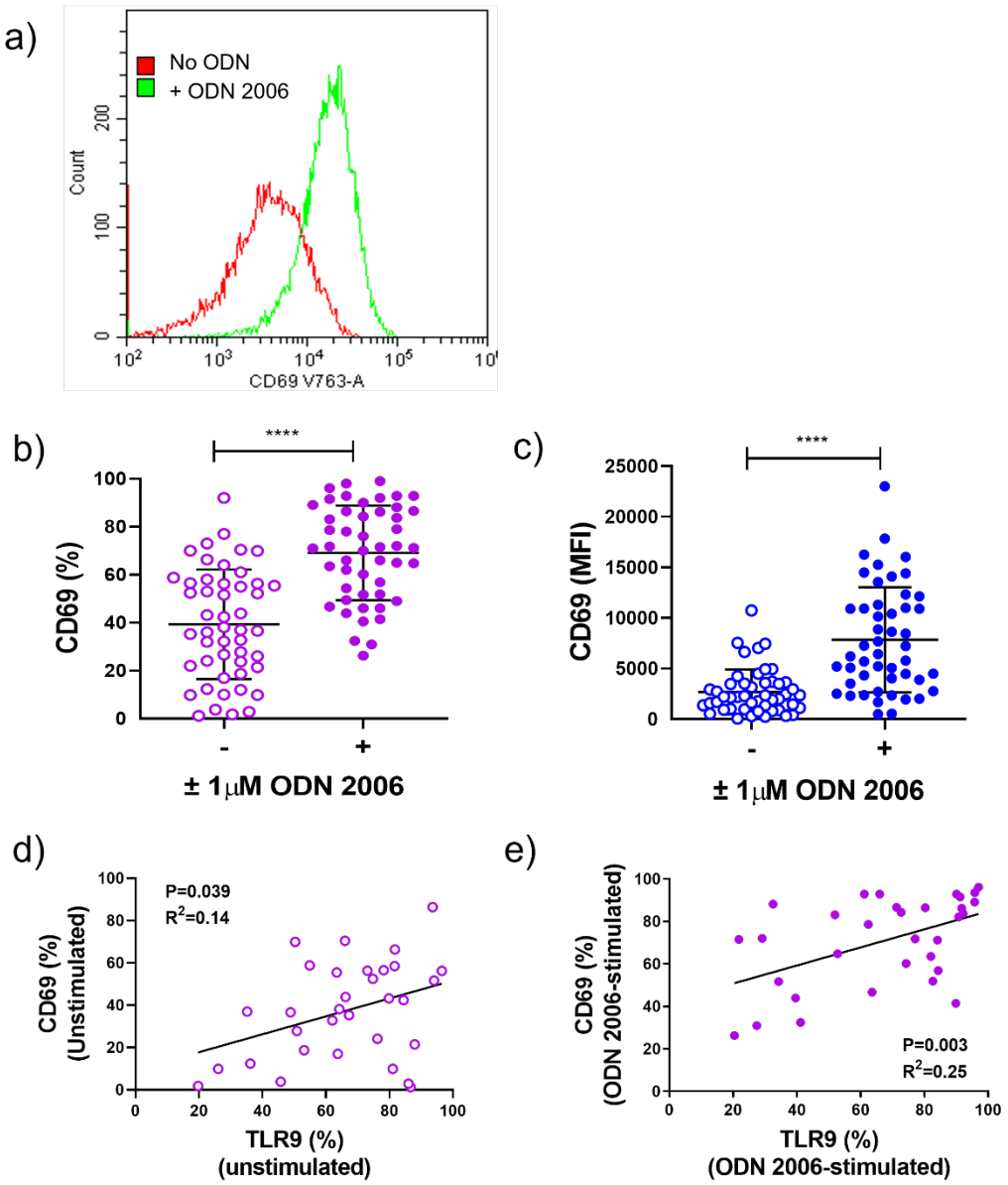

Figure 3.3: ODN 2006 Stimulates an Upregulation of CD69 in CLL Cells and CD69 Correlates with TLR9 in Both Unstimulated and ODN 2006-Stimulated CLL cells.
Primary PBMCs were cultured ± 1μM ODN 2006 in complete media (+IL-4) and incubated at 37°C/5% CO_2. Cells were collected at 24h post-stimulation and stained for flow cytometry (using the CytoFLEX LX flow cytometer); live CLL cells were identified as CD5+/CD19+/CD3-/FVD- and analysed using CytExpert software. a) a representative overlay histogram showing CD69 expression ± ODN 2006. b) ODN 2006 induced a significant increase in the percentage positivity of CD69 (P<0.001, n=49, Paired t-test). c) ODN 2006 stimulated a significant increase in CD69 MFI (P<0.001, n=49, Wilcoxon Matched Pairs test). d-e) There was a significant correlation between CD69 percentage positivity and TLR9 percentage positivity in unstimulated (P=0.039, R^2=0.14, n=32) and ODN 2006-stimulated CLL cells (P=0.003, R^2=0.25, n=32). Statistical analyses were performed using GraphPad Prism 8.0 and the Paired t-test or Wilcoxon Matched Pairs test was used depending on whether the data passed the D'Agostino & Pearson omnibus normality test. Correlation was determined using the Spearman's rank correlation coefficient.

CLL Cell Tissue Homing:

CD49d and CD38: CD49d and CD38 are components of the CLL 'invadosome' complex: an essential component of CLL cell homing.

Following stimulation with ODN 2006, the percentage positivity of CD49d (±SD) increased significantly from 49.5% (±39.2) to 56.7% (±41.8) ($P<0.001$, n=49) (Figure 3.4a-b) and CD49d MFI (±SD) significantly increased from 4604 (±7976) to 7631 (±11621) ($P<0.001$, n=49) (Figure 3.4c). Additionally, the percentage positivity of CD49d showed a significant correlation with the percentage positivity of TLR9 in ODN 2006-stimulated ($P=0.015$, $R^2=0.19$, n=31) but not unstimulated ($P=0.080$, $R^2=0.10$, n=31) CLL cells (Figure 3.4d-e).

Similarly, ODN 2006 stimulated a significant increase in both the percentage positivity and MFI of CD38. The percentage positivity (±SD) of CD38 significantly increased from 40.1% (±31.9) to 46.4% (±34.5) ($P=0.015$, n=49) (Figure 3.5a-b) and CD38 MFI significantly increased from 1206 (±2332) to 2159 (±4352) ($P=0.001$, n=49) (Figure 3.5c). As shown previously for CD69 (Figure 3.3d-e), the percentage positivity of CD38 showed significant correlation with the percentage positivity of TLR9 in **both** unstimulated ($P=0.011$, $R^2=0.20$, n=32) **and** ODN 2006-stimulated CLL cells ($P=0.005$, $R^2=0.24$, n=32) (Figure 3.5d-e). The P-value was lower and the R^2 value was higher in ODN 2006-stimulated CLL cells (relative to unstimulated CLL cells), showing that the observed correlation was stronger following activation of TLR9.

Together, these data suggest a functional link between TLR9 expression and the expression of both CD49d and CD38.

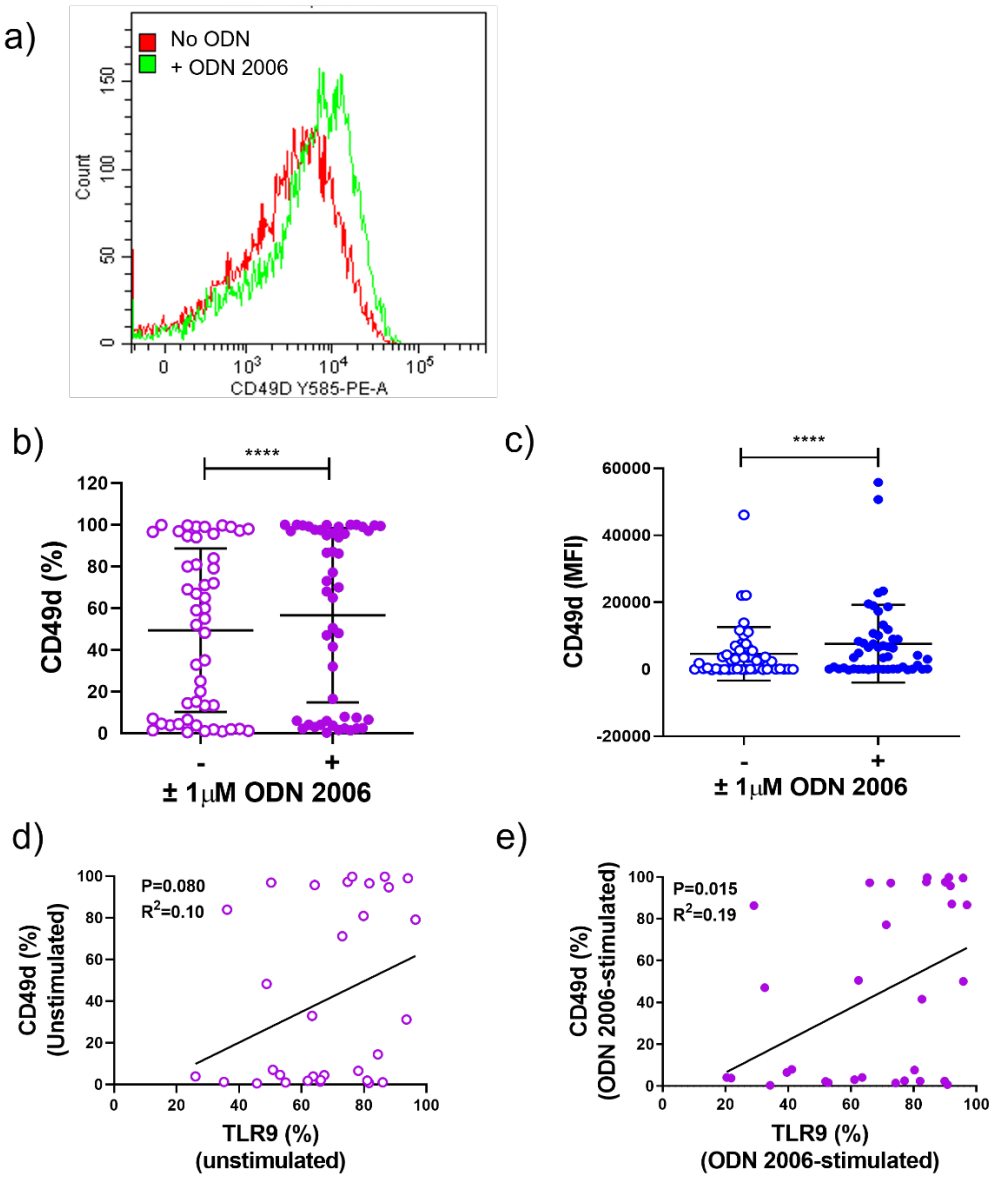

Figure 3.4: ODN 2006 Stimulates an Upregulation of CD49d in CLL Cells and CD49d Correlates with TLR9 in ODN 2006-Stimulated but Not Unstimulated CLL Cells.
Primary PBMCs were cultured ± 1μM ODN 2006 in complete media (+IL-4) and incubated at 37°C/5% CO_2. Cells were collected at 24h post-stimulation and stained for flow cytometry (using the CytoFLEX LX flow cytometer); live CLL cells were identified as CD5+/CD19+/CD3-/FVD- and analysed using CytExpert software. a) a representative overlay histogram showing CD49d expression ± ODN 2006. b) ODN 2006 induced a significant increase in the percentage positivity of CD49d (P<0.001, n=49, Wilcoxon Matched Pairs test). c) ODN 2006 induced a significant increase in CD49d MFI (P=0.001, n=49, Wilcoxon Matched Pairs test). d) There was no significant correlation between CD49d percentage positivity and TLR9 percentage positivity in unstimulated CLL cells (P=0.080, R^2=0.10, n=31). e) There was a significant correlation between CD49d percentage positivity and TLR9 percentage positivity in ODN 2006-stimulated CLL cells (P=0.015, R^2=0.18, n=31). Statistical analyses were performed using GraphPad Prism 8.0 and the Wilcoxon Matched Pairs test was used as the data was not Gaussian (as determined by the D'Agostino & Pearson omnibus normality test). Correlation was determined using the Spearman's rank correlation coefficient.

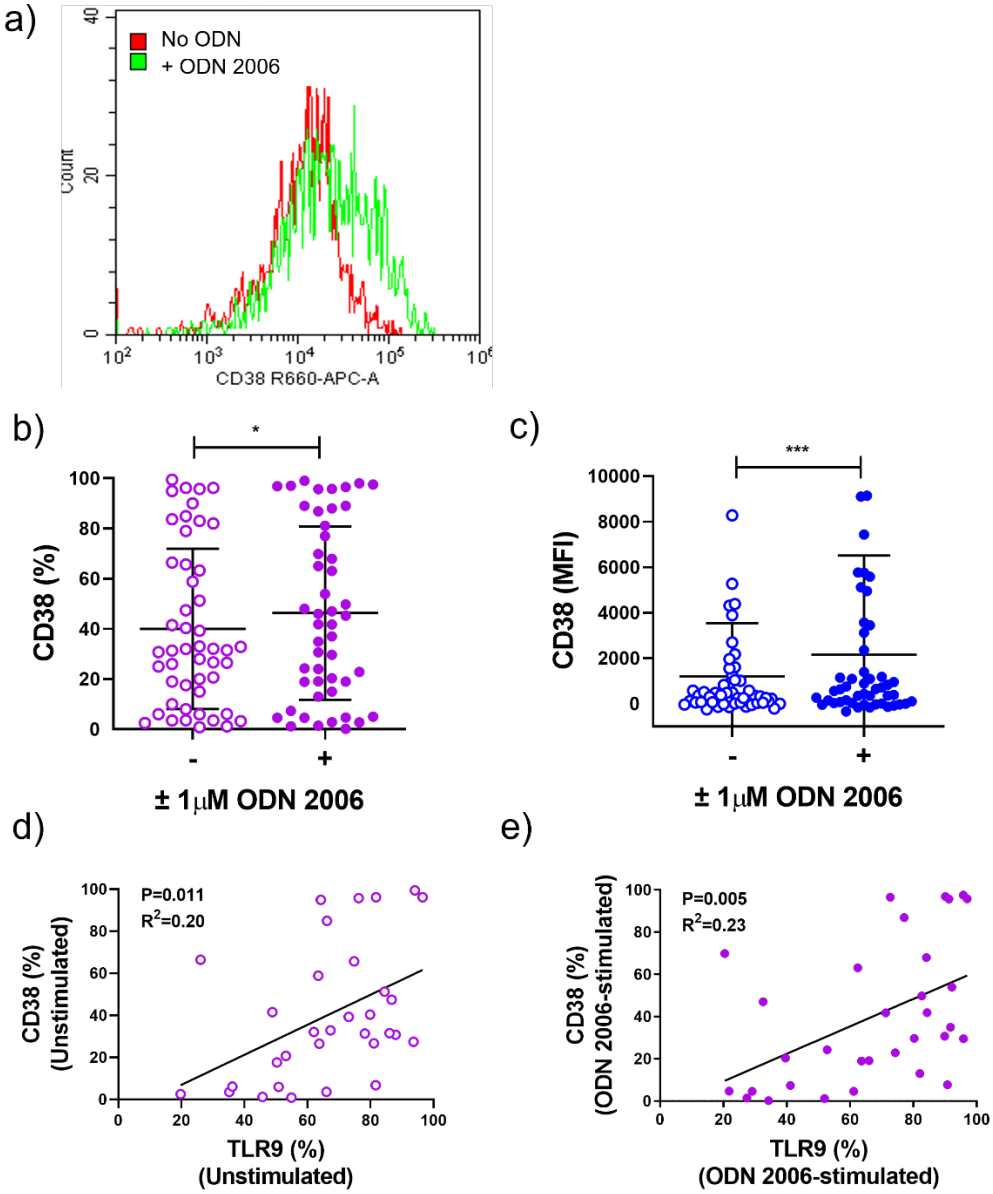

Figure 3.5: ODN 2006 Stimulates an Upregulation of CD38 in CLL Cells and CD38 Correlates with TLR9 in both Unstimulated and ODN 2006-Stimulated CLL Cells. Primary PBMCs were cultured ± 1μM ODN 2006 in complete media (+IL-4) and incubated at 37°C/5% CO_2. Cells were collected at 24h post-stimulation and stained for flow cytometry (using the CytoFLEX LX flow cytometer); live CLL cells were identified as CD5+/CD19+/CD3-/FVD- and analysed using CytExpert software. a) a representative overlay histogram showing CD38 expression ± ODN 2006. b) ODN 2006 induced a significant increase in the percentage positivity of CD38 (P=0.015), n=49, Wilcoxon Matched Pairs test). c) ODN 2006 induced a significant increase in CD49d MFI (P=0.001, n=49, Wilcoxon Matched Pairs test). d-e) There was a significant correlation between CD38 percentage positivity and TLR9 percentage positivity in both unstimulated (P=0.011, R^2=0.20, n=32) and ODN 2006-stimulated (P=0.005, R^2=0.23, n=32) CLL cells. Statistical analyses were performed using GraphPad Prism 8.0 and the Wilcoxon Matched Pairs test was used as the data was not Gaussian (as determined by the D'Agostino & Pearson omnibus normality test). Correlation was determined using the Spearman's rank correlation coefficient.

CD62L: CD62L is an adhesion molecule (selectin) implicated in the transendothelial migration of CLL cells.

There was no significant difference in the percentage positivity or antigen expression of CD62L following stimulation with ODN 2006 (P=0.488 and P=0.840, respectively, n=34) (Figure 3.6a-b). Unstimulated and stimulated CLL cells were 35.3% (±23.1) and 32.6% (±19.3) positive (±SD) for CD62L respectively and the MFIs for each condition were 984 (±1611) and 860 (±1327) (±SD). Furthermore, there was no significant correlation observed between the percentage positivity of CD62L and the percentage positivity of TLR9 in unstimulated (P=0.102, R^2=0.01, n=31) or ODN 2006-stimulated (P=0.096, R^2=0.09, n=31) CLL cells (Figure 3.6c-d). Taken together, these data suggest there to be no functional link between TLR9 and CD62L in primary CLL cells and consequently, this marker was not investigated any further in this study.

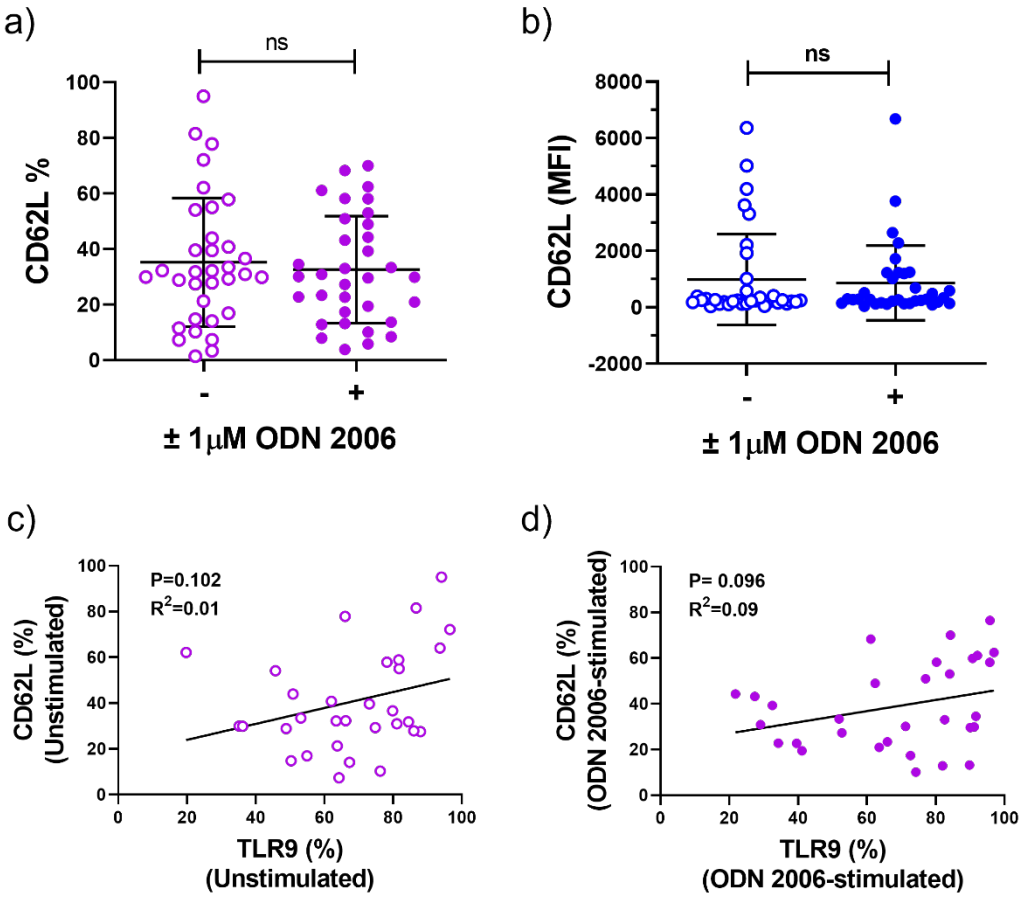

Figure 3.6: Stimulation of CLL Cells with ODN 2006 Does Not Significantly Alter the Expression of CD62L and CD62L Does Not Correlate with TLR9 in Unstimulated or ODN 2006-Stimulated CLL Cells. Primary CLL cells were stimulated ± 1μM ODN 2006. Cells were collected at 24h post-stimulation and stained for flow cytometry (using the CytoFLEX LX flow cytometer as previously described. a-b) There was no significant difference in the percentage positivity (P=0.488) or MFI (P=0.840) of CD62L post-stimulation with ODN 2006 (both n=34, both Wilcoxon Matched Pairs test). c) There was no significant correlation between the percentage positivity of CD62L and the percentage positivity of TLR9 in unstimulated CLL cells (P=0.102, R^2=0.01, n=31). d) There was no significant correlation between the percentage positivity of CD62L and the percentage positivity of TLR9 in ODN 2006-stimulated CLL cells (P=0.096, R^2=0.09, n=31). Statistical analyses were performed using GraphPad Prism 8.0 and the Wilcoxon Matched Pairs test was used as the data was not Gaussian (as determined by the D'Agostino & Pearson omnibus normality test). Correlation was determined using the Spearman's rank correlation coefficient.

Toll-Like Receptor 9 Signalling:

TLR9: Finally, the effect of ODN 2006 upon the expression of TLR9 itself was assessed. Both the percentage positivity and MFI of TLR9 were found to remain unchanged in the presence of ODN 2006 (n=30). In unstimulated and stimulated CLL cells respectively, TLR9 % positivity (±SD) was 65.7% (±19.8) and 66.2% (±24.5) and TLR9 MFI was 1785 (±1672) and 2148 (±2271) (Figure 3.7a-b).

Notably, both TLR9 percentage positivity and TLR9 MFI were significantly reduced following overnight culture in complete media (+IL-4), relative to the earlier presented pre-culture (baseline) TLR9 values. TLR9 % positivity (±SD) significantly reduced from 79.4% (±18.0) to 64.7% (±20.3) ($P<0.001$, n=28) (Figure 3.7c) and TLR9 MFI (±SD) significantly reduced from 2343 (±2236) to 1780 (±1746) ($P=0.006$, n=28) (Figure 3.7d). Since the migration assays in the following section were all performed on CLL cells that had been cultured overnight, any TLR9 vs cell surface marker/TLR9 vs CLL cell migration comparisons were performed using post-culture TLR9 values.

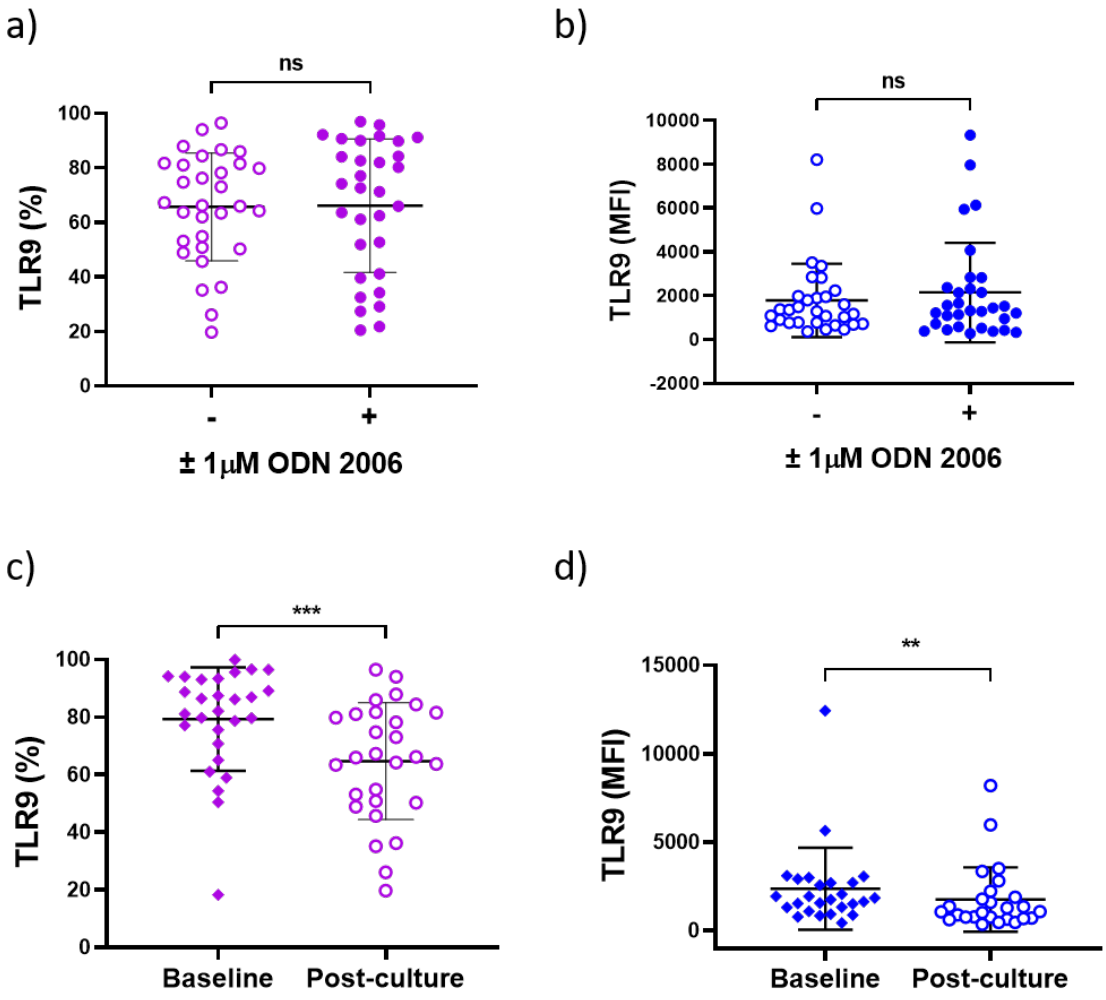

Figure 3.7: Stimulation of CLL Cells with ODN 2006 Does Not Alter Their Expression of TLR9. Primary PBMCs were cultured overnight ± 1μM ODN 2006 in complete media (+IL-4). PBMCs were then collected and stained for both extracellular CLL cell identification markers and intracellular TLR9 and analysed using a CytoFLEX LX flow cytometer (n=31); live CLL cells were gated as CD5+/CD19+/CD3-/FVD-. a) There was no significant difference in TLR9 % positivity post-stimulation with ODN 2006 (P=0.790, Paired t-test). b) There was no significant difference in TLR9 MFI post-stimulation with ODN 2006 (P=0.308, Wilcoxon Matched Pairs test). c) Following overnight culture in complete media (+IL-4), TLR9 % positivity was significantly reduced relative to baseline (pre-culture) levels (P<0.001, n=28, Wilcoxon Matched Pairs test). d) Following overnight culture in complete media (+IL-4), TLR9 MFI was significantly reduced relative to baseline (pre-culture) levels (P=0.006, n=28, Wilcoxon Matched Pairs test). Statistical analyses were performed using GraphPad Prism 8.0 and the Paired t-test or Wilcoxon Matched Pairs test was used depending on whether the data passed the D'Agostino & Pearson omnibus normality test.

3.4: The Observed ODN 2006-Stimulated Migratory Phenotype is TLR9-Dependent

In order to assess the specificity of the above identified ODN 2006-stimulated increase in CD69, CD38 and CD49d, the above experiments were repeated in the presence/absence of the TLR9 antagonist, ODN INH-18. ODN INH-18 is a commercially available inhibitor of TLR9 and would therefore be expected to limit any TLR9-mediated responses to ODN 2006. This oligonucleotide is of identical length to ODN 2006 but contains an inhibitory DNA motif consisting of two TLR9 inhibitory nucleotide triplets (i.e., a proximal cct and a more distal ggg, spaced four nucleotides apart) (5'-cct gga tgg gaa ctt acc gct gca-3'). A concentration of 5μM ODN INH-18 was chosen from a prior optimisation experiment outlined in Appendix 7.2. The below experiments were performed as outlined in methods section 2.11 and phenotypic analysis was performed using an Accuri flow cytometer. The Accuri flow cytometer is a small 4-colour instrument and in each experiment, two colours were used for CLL cell identification (i.e., CD3/CD19), leaving two colours available. Since CD62L was earlier shown to be non-responsive to ODN 2006 and CD38 showed a lesser response relative to CD69 and CD49d, CD69 and CD49d were chosen to complete the panel.

In the presence of ODN INH-18, the stimulatory effect of ODN 2006 was significantly reduced in terms of its ability to upregulate CD69 ($P=0.004$, $n=9$) and CD49d ($P=0.031$, $n=7$) (Figure 3.8). These results confirmed that the ODN 2006-induced upregulation of CD49d and CD69 was, at least in part, TLR9-dependent.

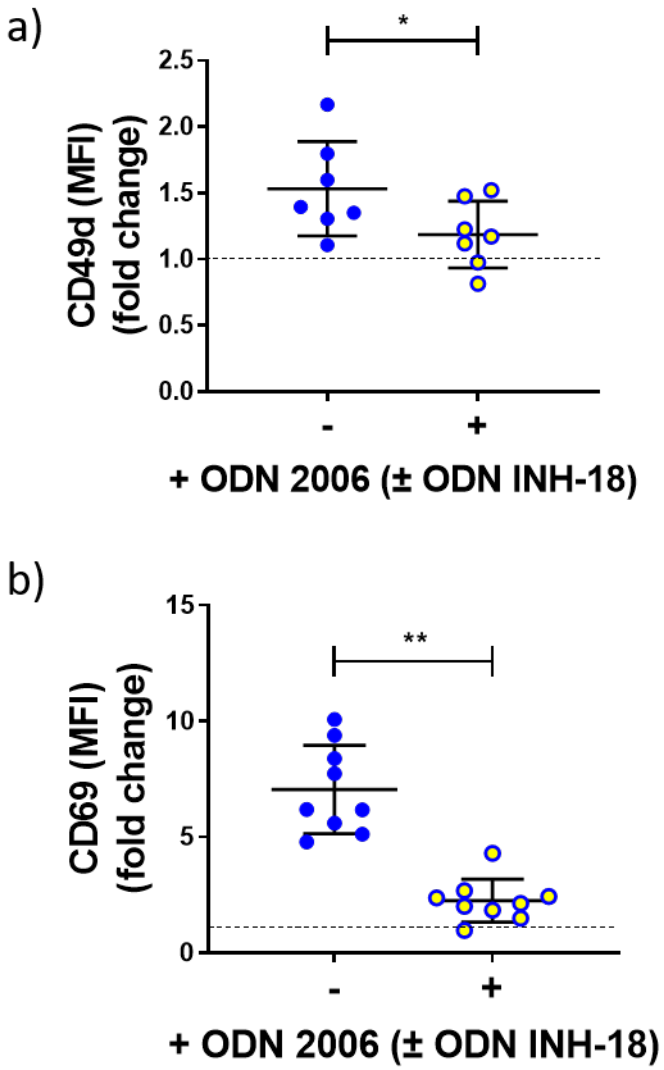

Figure 3.8: ODN 2006 Stimulates a TLR9-Dependent Upregulation of CD49d and CD69. Primary PBMCs were cultured in complete media (+IL-4) and pre-incubated for 30 minutes ± 5μM ODN INH-18 (TLR9 antagonist). The cells were then stimulated with 1μM ODN 2006 (TLR9 agonist) and incubated for 24h at 37°C/5% CO_2. Cells were harvested at 24h post-stimulation and stained for flow cytometry (using an Accuri flow cytometer); CLL cells were identified as CD3-/CD19+ and analysed using CFlow Plus software. a) ODN INH-18 significantly reduced the ODN 2006-stimulated upregulation of CD49d (P=0.031, n=7, Wilcoxon Matched Pairs test). b) ODN INH-18 significantly reduced the ODN 2006-stimulated upregulation of CD69 (P=0.004, n=9, Wilcoxon Matched Pairs test). The observed ODN 2006-stimulated upregulation of CD49d and CD69 appears to be TLR9-dependent. Statistical analyses were performed using GraphPad Prism 8.0 and the Wilcoxon Matched Pairs test was used as the data was not Gaussian (as determined by the D'Agostino & Pearson omnibus normality test).

3.5: Investigating the Effects of ODN 2006 upon CLL Cell Migration

Having established that ODN 2006-stimulation induces TLR9-dependent increases in phenotypic markers of both activation and migration in primary CLL cells, the project progressed to investigate the effects of ODN 2006 on CLL cell migration. It was hypothesised that TLR9 activation would promote the migration of CLL cells, and this was explored using a transwell migration assay where CLL cells (± ODN 2006) were prompted to migrate across the transwell insert by a CXCL12 chemotactic gradient.

3.5.1: Primary CLL Cells Express High Levels of CXCR4 which Correlate to the Expression of TLR9

In the following transwell migration experiments, CXCL12 was the chosen chemokine gradient used to assess CLL cell migration/homing. CXCL12 is secreted by stromal cells within the bone marrow and lymph node niche and is the ligand for the chemokine receptor CXCR4. CXCR4 is known to be overexpressed in CLL and has been associated with lymphadenopathy and disease progression[62,76]. As previously described for TLR9, it was important to confirm the expression of CXCR4 in the patient samples intended for use in the migration assays to ensure that they had the potential to respond to CXCL12. Figure 3.9a shows both the percentage positivity and MFI of CXCR4 in unstimulated CLL cells following an overnight culture in complete media (+IL-4); assessing the post-culture, rather than baseline (pre-culture), expression of CXCR4 was important for assessing the migratory potential of CLL cells as all transwell migration assays were performed on CLL cells after overnight culture. 36/36 patients were confirmed to express very high cell surface levels of CXCR4 ranging from 72.7% to 100%; the mean (+SD) percentage positivity of cell surface

CXCR4 was 98.1% (±4.7). There was a greater level of interpatient heterogeneity, however, between the MFI values of cell surface CXCR4, which ranged between 5218 and 56896 with a mean (±SD) of 24187 (±12040).

Interestingly, in unstimulated CLL cells, CXCR4 expression (MFI) showed a significant correlation with TLR9 (MFI) ($P=0.004$, $R^2=0.26$, $n=31$) suggesting that TLR9 is more highly expressed in CLL cells with a greater migratory potential (Figure 3.9b). Together, these data confirm CLL cells are primed for CXCL12-driven chemotaxis and CXCL12 is therefore an appropriate chemokine for the transwell migration assays.

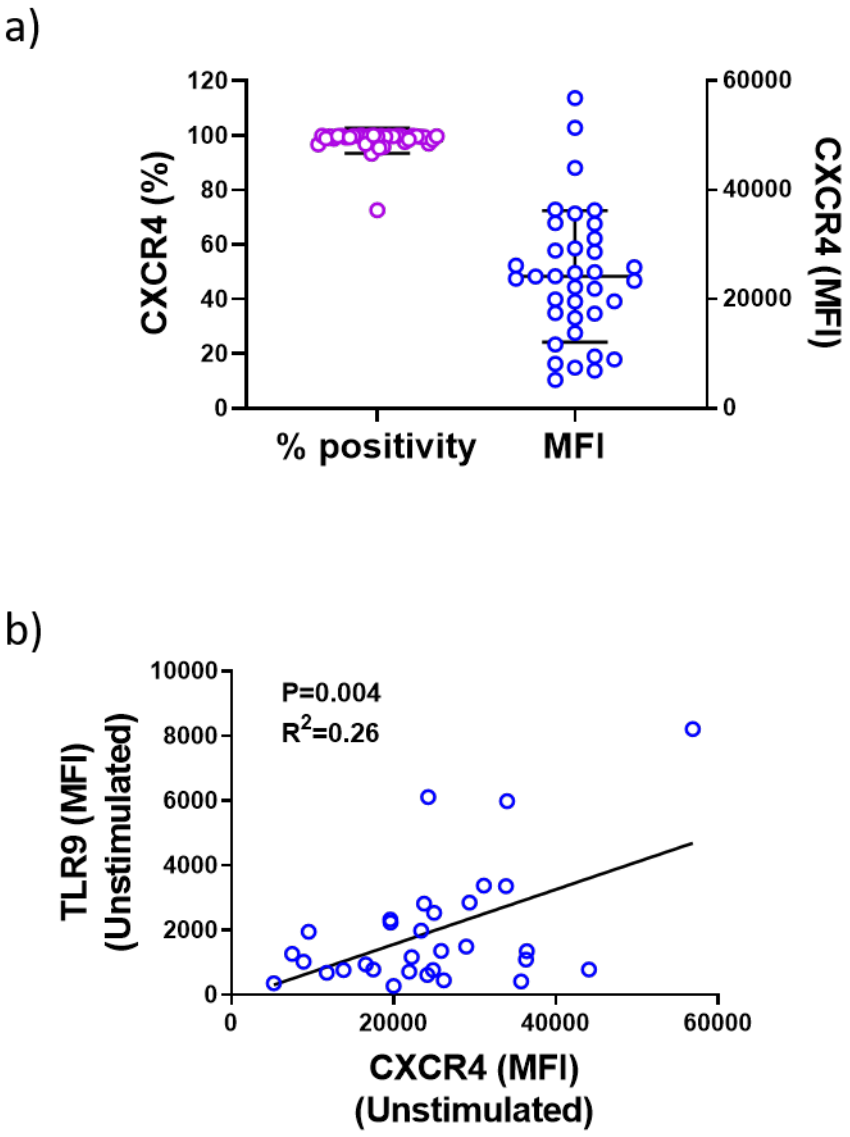

Figure 3.9: Primary CLL Cells Express High Levels of CXCR4 which Correlate to the Expression of TLR9. Primary PMBCs were cultured overnight in complete media (+IL-4) and collected and labelled for flow cytometry using a CytoFLEX LX flow cytometer as previously described. a) All 34 patients strongly expressed CXCR4 with the majority close to 100%, however there was a variation in CXCR4 MFI. b) CXCR4 expression (MFI) showed significant correlation with TLR9 expression (MFI) in unstimulated CLL cells (P=0.004 R^2=0.26, n=31). Statistical analysis was performed using GraphPad Prism 8.0. Correlation was determined using the Spearman's rank correlation coefficient.

3.6: Transwell Migration Optimisation

It was firstly necessary to optimise the transwell migration protocol to assess the effects of TLR9 activation upon CXCL12-driven CLL cell migration. The optimisation process was extensive and considered the following:

- The transwell migration membrane pore size
- CLL cell identification and quantification post-migration
- The transwell migration incubation period
- The effect of using fresh (i.e., <24h post-venesection) or frozen (i.e., freeze-thawed from liquid nitrogen) PBMC samples

The optimisation data for each point are detailed in Appendix 7.3.

3.7: Migrated CLL Cells Express Higher Levels of TLR9, CD69, CD49d and CD38

TLR9: Using the optimised transwell migration protocol (methods section 2.13), the expression of TLR9 was compared between migrated and non-migrated CLL cells. PBMCs from both the basal (migrated) and apical (non-migrated) chambers were collected post-incubation for analysis using the CytoFLEX LX flow cytometer and live CLL cells were gated as CD5+/CD19+/CD3-/FVD-. Migrated CLL cells showed a significantly higher expression of both TLR9 percentage positivity ($P<0.01$) and TLR9 MFI ($P<0.01$) (n=11); migrated and non-migrated CLL cells were 74.8% (±17.9) and 48.2% (±21.2) positive for TLR9 and showed respective MFI values of 7435 (±8994) and 3378 (±3078) Figure 3.10.

CD69, CD49d and CD38: To emphasise the importance of markers of CLL cell activation and adhesion, the expression of each marker was quantified in migrated vs non-migrated CLL cells. All three markers showed a higher expression in migrated relative to non-migrated CLL cells (CD69: P=0.02, n=7; CD49d: P=0.02; n=7 and CD38: P=0.01; n=8) Figure 3.11; MFI (±SD) values are shown in Table 3.2.

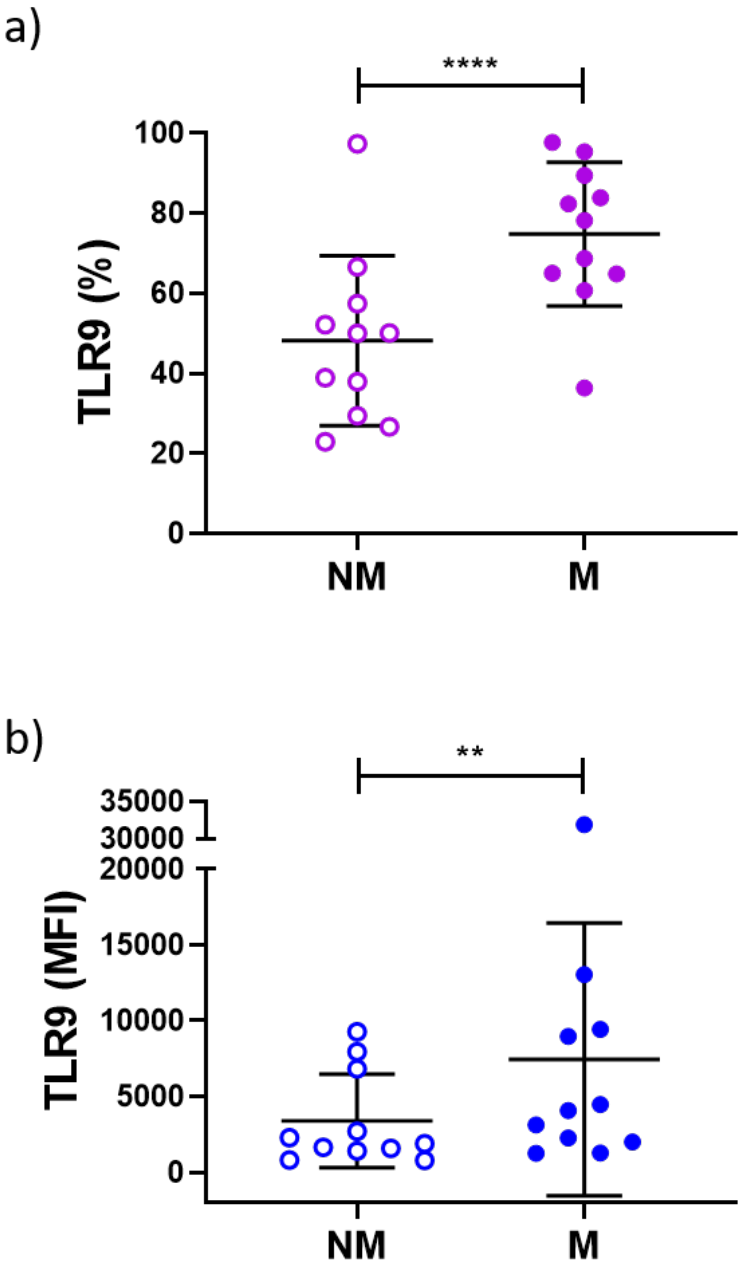

Figure 3.10: Migrated CLL Cells Express Higher Levels of TLR9 Relative to Non-Migrated CLL Cells. Unstimulated primary PBMCs were transferred into the apical chambers of 24-well, 5μm pore polycarbonate transwell migration plates and incubated for 4h at 37°C/5% $C0_2$; PBMCs migrated towards a chemotactic gradient (CXCL12). Cells from both the basal (migrated) and apical (non-migrated) chambers were collected after 4h of incubation and were analysed using a CytoFLEX LX flow cytometer. Live CLL cells were gated as CD5+/CD19+/CD3-/FVD-. TLR9 expression was determined using CytExpert software and statistical analysis was performed using GraphPad Prism; the Paired t-test or Wilcoxon Matched Pairs test was used depending on whether the data passed the D'Agostino & Pearson omnibus normality test. a-b) Migrated CLL cells showed a significantly higher TLR9 % positivity ($P<0.001$, Paired t-test) and TLR9 MFI ($P=0.02$, Wilcoxon Matched Pairs test) (n=11).

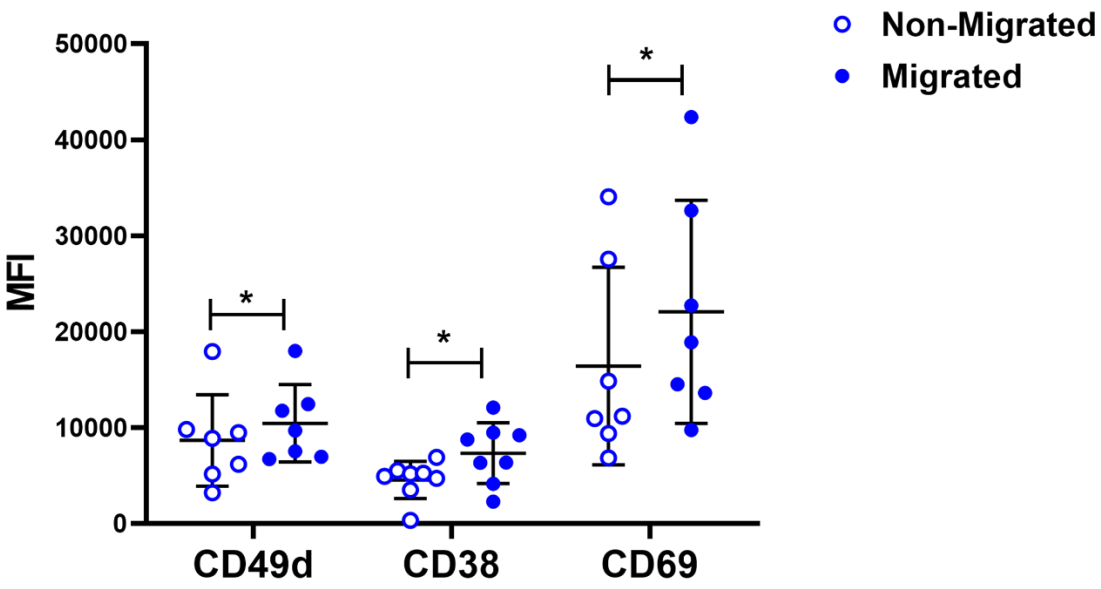

Figure 3.11: Migrated CLL Cells Express Higher Levels of CD69, CD49d and CD38 Relative to Non-Migrated CLL Cells. Unstimulated primary PBMCs were transferred into the apical chambers of 24-well, 5μm pore polycarbonate transwell migration plates and incubated for 4h at 37°C/5% $C0_2$; PBMCs migrated towards a chemotactic gradient (CXCL12). Cells from both the basal (migrated) and apical (non-migrated) chambers were harvested after 4h incubation prior to analysis using an Accuri flow cytometer. CLL cells were identified as CD3-/CD19+ and marker MFIs were determined using CFlow software. Each marker showed a significantly higher expression in migrated vs non-migrated CLL cells i.e., CD69: P=0.016 (Wilcoxon Matched Pairs test, n=7), CD49d: P=0.016 (Wilcoxon Matched Pairs test, n=7) and CD38: P=0.007 (Wilcoxon Matched Pairs test, n=8). Statistical analyses were performed using GraphPad Prism 8.0 and the Wilcoxon Matched Pairs test was used as the data was not Gaussian (as determined by the D'Agostino & Pearson omnibus normality test).

Table 3.2: The Expression of CD69, CD49d and CD38 in Migrated vs Non-Migrated CLL Cells

Marker	Migrated MFI (±SD)	Non-Migrated (±SD)
CD69	16414 (± 10297)	22077 (± 11645)
CD49d	8671 (± 4767)	10455 (± 4033)
CD38	4551 (± 1943)	7343 (± 3141)

CD69 (n=7); CD49d (n=7); CD38 (n=8).

Given that TLR9 is more highly expressed in migrated vs non-migrated CLL cells and earlier experiments have shown TLR9 activation to induce an upregulation of markers associated with a migrated CLL cell phenotype, these data provide further support for the involvement of TLR9 in CLL cell migration.

3.8: ODN 2006 Induces CLL Cell Migration in a Subset of CLL Patients

The effect of ODN 2006 upon CLL migration was investigated in a cohort of 32 patients. Figure 3.12a shows the percentage of basal (unstimulated) and ODN 2006-stimulated CLL migration for each patient. The migratory potential of CLL cells varied greatly between patients with basal migration ranging from 0.9% to 20.6% and ODN 2006-stimualted migration ranging from 1.4% to 27.2%; ODN 2006 increased the mean (±SD) percentage of CLL cell migration from 6.7% (±4.8) to 8.4% (±5.9) and although these changes appear modest, the observed increase reached statistical significance (P=0.018). It was evident that not all patients responded in the same way to stimulation with ODN 2006. Figure 3.12b shows the same migration data

expressed as fold change in migration (i.e., from basal to stimulated migration). Responses ranged from 0.20 to 3.89-fold meaning that a subset of patients (i.e., 11/32) showed either ***no change*** or a ***decrease*** rather than ***increase*** in CLL cell migration. These data suggest a dichotomous migratory response to stimulation with ODN 2006. Subsequently, patient samples will be referred to as 'Responders' (i.e., ≥1.2-fold) and 'Non/Reverse Responders (i.e., <1.2-fold).

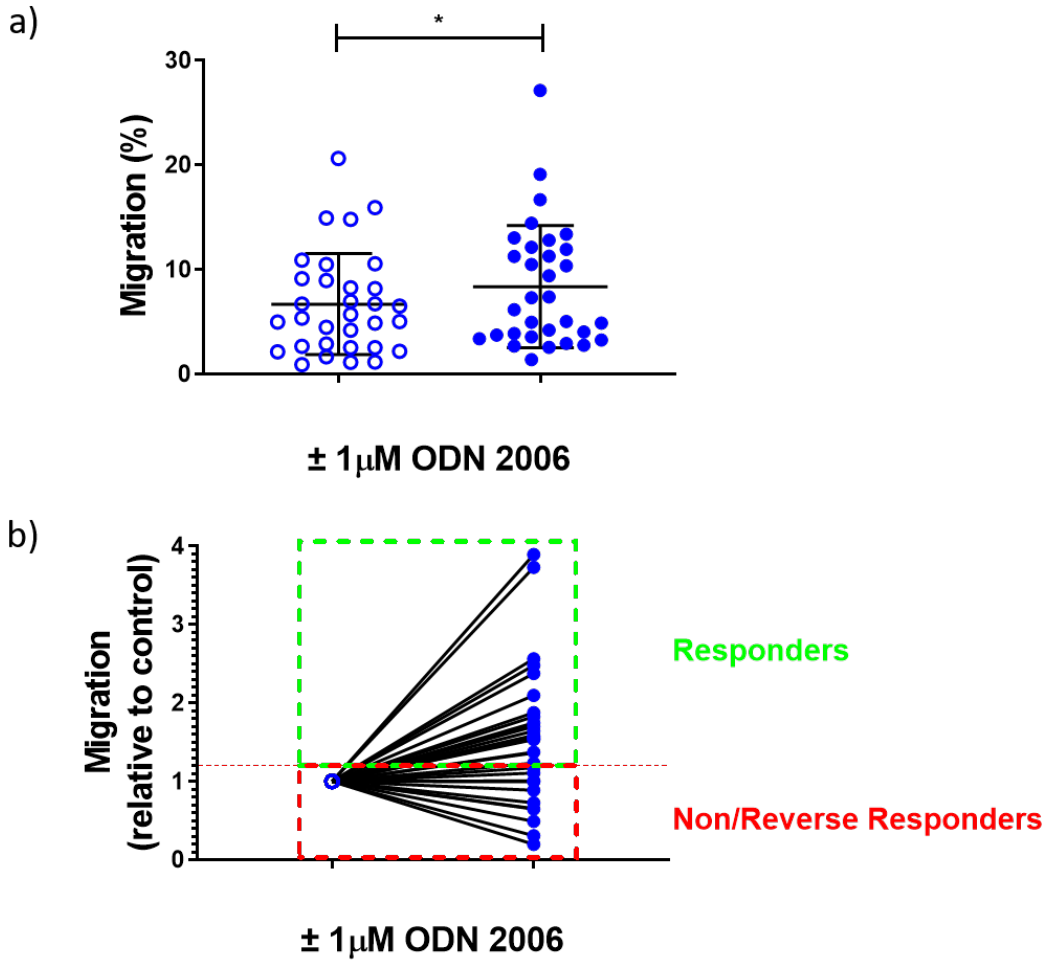

Figure 3.12: CLL Patient Samples Show a Dichotomous Migratory Response to Stimulation with the TLR9 Agonist, ODN 2006. Primary patient PMBCs were cultured overnight ± 1μM ODN 2006 (TLR9 agonist) before being transferred into the apical chambers of 24 well, 3-5μm pore polycarbonate transwell migration plates; cell counts were performed at '0h migration' i.e., prior to transfer using Countess II automated cell counter. A chemotactic gradient of CXCL12 (100ng/ml) in 600ml complete media was established in the basal chambers and plates were incubated at 37°C/5% $C0_2$ for 4h. At '4h migration' the migrated cells in the basal chambers of the transwell were collected and CLL cells were counted volumetrically using an Accuri flow cytometer. CLL cells were identified as CD3-/CD19+ and total migration was calculated as a percentage of the 0h live cell count. a) ODN 2006 stimulated a significant *increase* in CLL cell migration (P=0.04, n=33; Wilcoxon Matched Pairs test). b) The data from (a) is expressed as the fold change in migration following stimulation with ODN 2006: individual patients showed either an ***increase*** or ***decrease*** in CLL cell migration following stimulation with ODN 2006. Patients were considered 'Responders' if the fold change in migration was ≥1.2-fold and 'Non/Reverse Responders' if the fold change in migration was <1.2-fold. Statistical analyses were performed using GraphPad Prism 8.0 and the Wilcoxon Matched Pairs test was used as the data was not Gaussian (as determined by the D'Agostino & Pearson omnibus normality test).

It was important to determine the validity of the proposed dichotomous response and so further biological repeats were performed using 3 Responder and 3 Non/Reverse Responder patients; these experiments were designed to investigate the reproducibility of patient responses and were performed using freeze/thawed PBMC aliquots (stored in liquid nitrogen). Table 3.3 and Figure 3.13 show the percentage basal migration, percentage stimulated migration and the fold change in migration for each biological repeat. Responder and Non/Reverse Responder patients showed reproducible ***increases*** and ***decreases*** in CLL cell migration following stimulation with ODN 2006 and the migratory response of individual patients was therefore confirmed to be consistent.

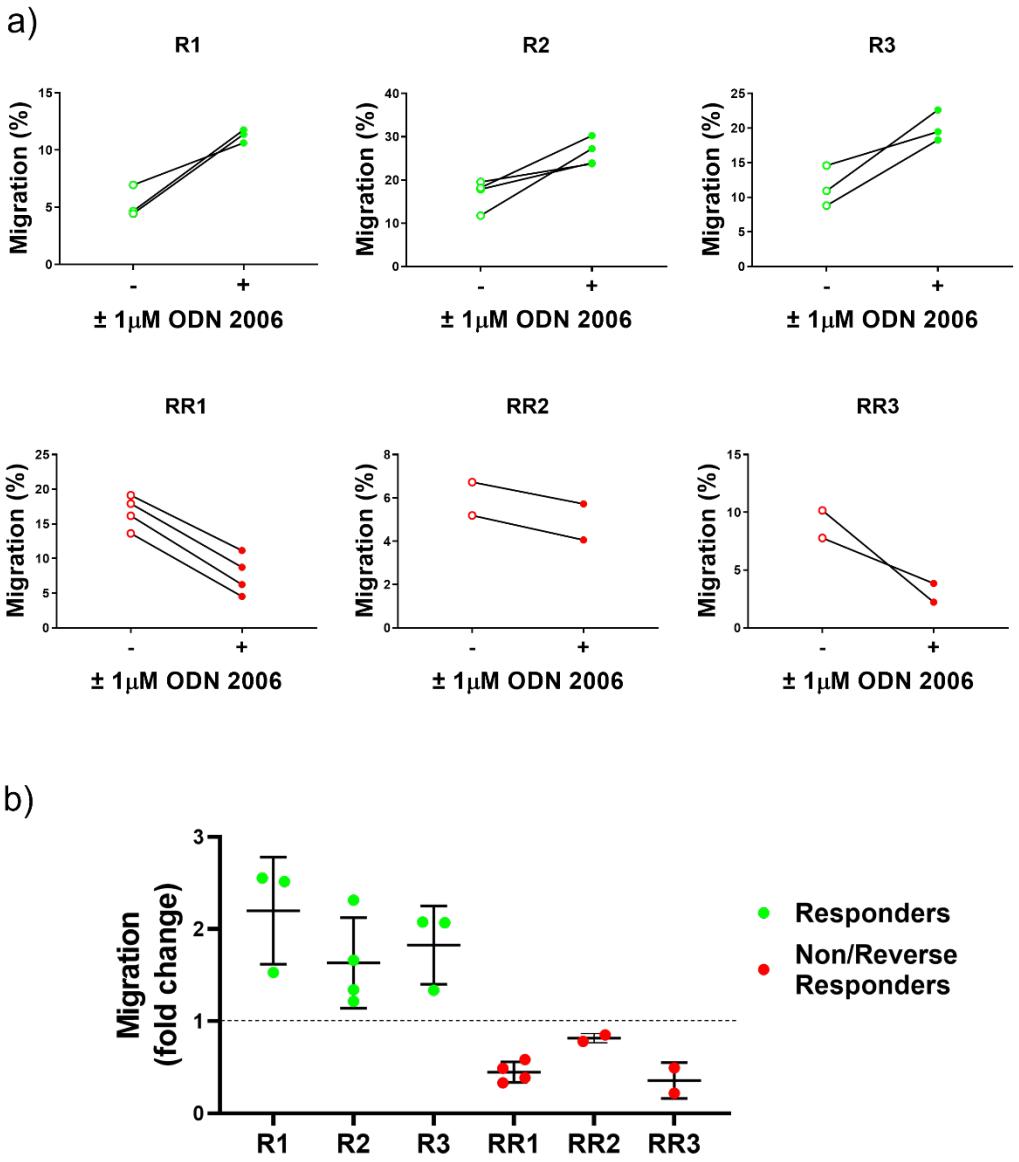

Figure 3.13: The Effect of ODN 2006-Stimulation on CLL Cell Migration was Consistent in Both the Responder and Reverse Responder subgroups. Biological repeats (2-4 repeats, depending on the availability of archived PBMCs) of transwell migration experiments were performed using freeze-thawed PBMC aliquots of 3 Responder and 3 Non/Reverse Responder patients; the transwell migration experiments were performed as previously described. Migration data is expressed both as a) % CLL migration and b) fold change (±SEM) in migration. The results confirmed the responses of Responder and Non/Reverse Responder patient samples were consistent.

Table 3.3: The Migratory Responses of Representative Responder and Reverse Responder Patients to Stimulation with ODN 2006

	Responder Migration		
Patient	Basal (%)	Stimulated (%)	Fold Change
R1	6.95	10.63	1.53
	4.76	11.77	2.52
	4.45	11.38	2.55
R2	19.54	23.77	1.22
	17.84	23.94	1.34
	18.22	30.25	1.66
	11.77	27.25	2.31
R3	14.58	19.47	1.34
	8.81	18.27	2.08
	10.92	22.61	2.07

	Non/Reverse Responder Migration		
	Basal (%)	Stimulated (%)	Fold Change
RR1	13.63	4.53	0.33
	19.13	11.16	0.58
	17.92	8.74	0.49
	16.18	6.24	0.39
RR2	5.19	4.05	0.78
	6.73	5.73	0.85
RR3	7.78	3.84	0.49
	10.17	2.22	0.22

3.9 The Migratory Response to ODN 2006 Does Not Correlate with Disease Burden

It was also important to identify whether the disease burden of individual CLL patients (i.e., the percentage of CLL cells present within the PBMC population), determined the outcome of the above transwell migration experiments. Since all transwell migration assays were performed using PBMCs, rather than isolated CLL cells, each patient sample had a unique composition; it was therefore vital to address this heterogeneity and technical variance. PBMCs from freeze-thawed aliquots were stained for flow cytometry and phenotyped using the CytoFLEX flow cytometer. CytExpert software was used to identify live CLL cells as CD5+/CD19+/CD3-/FVD-. The percentage of CLL cells in the PBMC population was noted for each patient. Figure 3.14) shows the disease burden of 29 CLL patients; in this cohort, disease burden ranged from 52.4% to 93.5%. Despite this clear heterogeneity however, disease burden was found not to correlate with either basal migration ($P=0.633$, $R^2=0.01$) or the fold change in migration in response to ODN 2006 ($P=0.281$, $R^2=0.04$). These results show that the percentage of CLL cells within the PBMC population does not influence the basal migration or migratory response to ODN 2006 and provide further support for the existence of a true bifurcated response to ODN 2006.

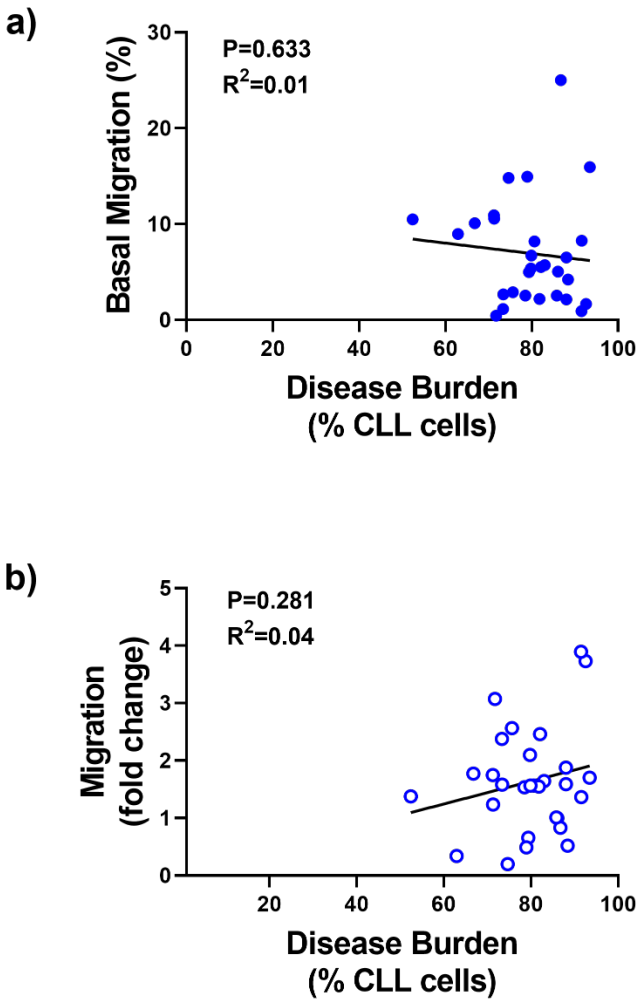

Figure 3.14: Disease Burden Does Not Correlate with Basal CLL Cell Migration or the Migratory Response to ODN 2006. Freeze-thawed primary PBMCs from 29 CLL patients were stained for flow cytometry and phenotyped using the CytoFLEX flow cytometer. CytExpert software was used to identify live CLL cells as CD5+/CD19+/CD3-/FVD- and the percentage of CLL cells in the PBMC population (i.e., disease burden) was noted for each patient. The disease burden of each individual was then compared with corresponding previously collected transwell migration data. Statistical analysis was performed using GraphPad Prism 8.0 and correlation was determined using the Spearman's rank correlation coefficient a) Disease burden showed no correlation with basal CLL cell migration (P=0.633, R^2=0.01). b) Disease burden showed no correlation with the migratory response to ODN 2006 (i.e., the fold change in CLL cell migration following stimulation with ODN 2006) (P=0.281, R^2=0.04).

3.10: The Migratory Response to ODN 2006 is TLR9-Dependent

Surprisingly, in the above patient cohort, the ODN 2006-stimulated changes in CLL cell migration showed no correlation with the expression of TLR9. Figure 3.15 shows TLR9 percentage positivity and TLR9 MFI vs CLL cell migration (%) and the fold change in migration in ODN 2006-stimulated CLL cells. It was therefore important to investigate the specificity of the observed changes for TLR9. Transwell migration experiments were repeated in the presence of the potent TLR9 antagonist ODN INH-18. PBMCs were cultured as previously described and pre-incubated ± 5μM ODN INH-18 for 30 minutes prior to stimulation with 1μM ODN 2006. Figure 3.16 shows the response of Responder (n=7) and Non/Reverse Responder (n=4) patients to ODN 2006 ± ODN INH-18; migration values are expressed relative to the unstimulated control (±SD). In the Responder subgroup, ODN 2006 induced a mean relative ***increase*** in CLL cell migration of 1.89 (± 0.60)-fold and in the presence of ODN INH-18, this effect was almost completely inhibited (to 1.1 [±0.16]-fold). In the Reverse Responder subgroup, ODN 2006 induced a relative ***decrease*** in CLL cell migration of 0.56 (±0.18)- fold and again, in the presence of ODN INH-18, this effect was almost entirely reversed (to 0.97 [±0.35]-fold). ODN INH-18 therefore reversed the effect of ODN 2006 in both the Responder and Non/Reverse Responder subgroups. These data confirm that although the dichotomous response to ODN 2006 could not be attributed to differences in the protein expression levels of TLR9, the observed migratory changes were TLR9-dependent.

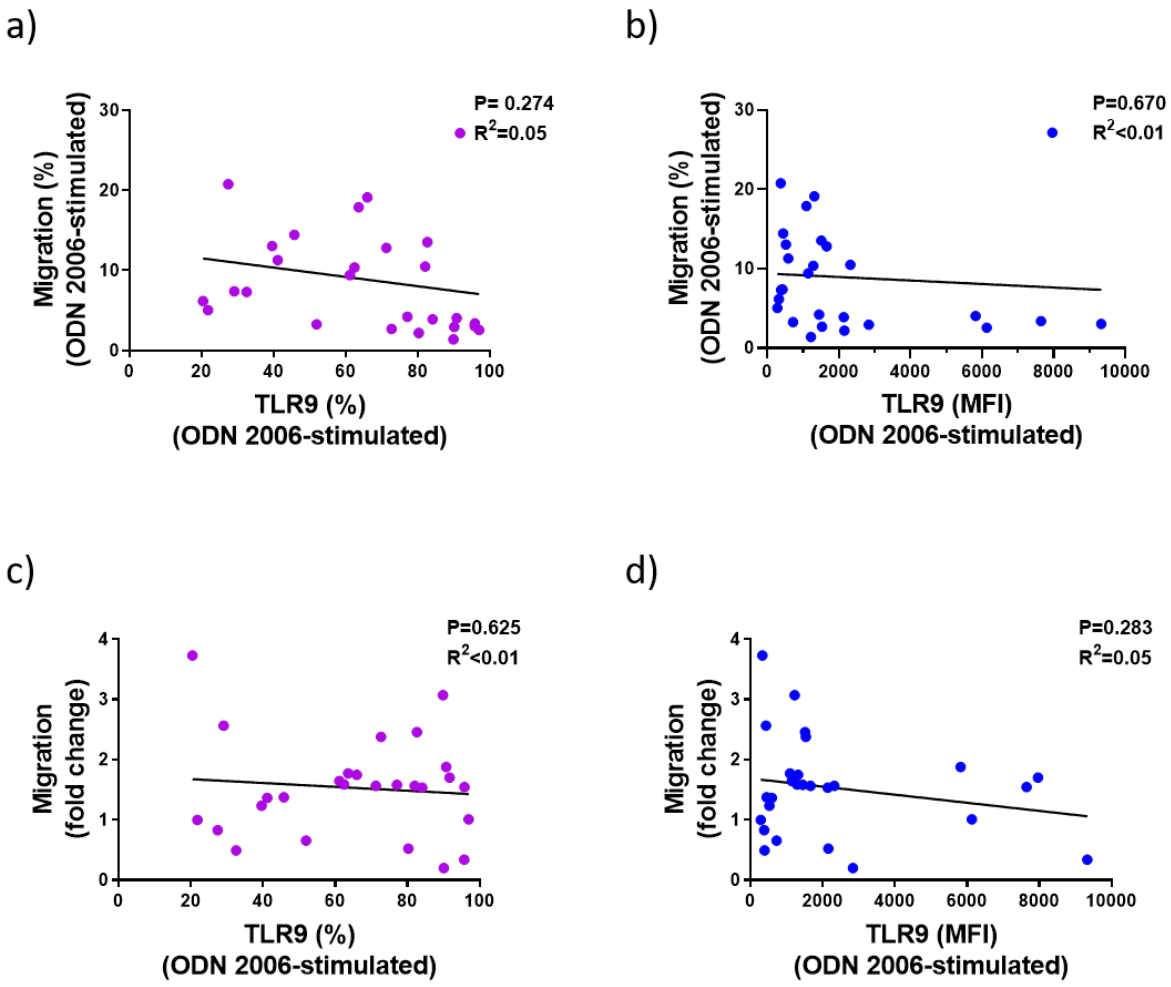

Figure 3.15: ODN 2006-Stimulated Changes in CLL Cell Migration Show No Correlation with the Expression of TLR9. Primary PBMCs were cultured overnight + 1μM ODN 2006 in complete media (+IL-4) and transferred into transwell migration chambers as previously described or stained for phenotypic analysis using a CytoFLEX LX flow cytometer. a) There was no correlation between TLR9 percentage positivity and CLL cell migration (%) in ODN 2006-stimulated CLL cells (P=0.274, R^2=0.05, n=27). b) There was no correlation between TLR9 MFI and CLL cell migration (%) in ODN 2006-stimulated CLL cells (P=0.670, R^2<0.01, n=27). c) There was no correlation between TLR9 percentage positivity and the fold change in CLL cell migration following stimulation with ODN 2006 P=0.625, R^2<0.01, n=27). d) There was no correlation between TLR9 MFI and the fold change in CLL cell migration following stimulation with ODN 2006 (P=0.283, R^2=0.05, n=27). Statistical analysis was performed using GraphPad Prism 8.0. Correlation was determined using the Spearman's rank correlation coefficient.

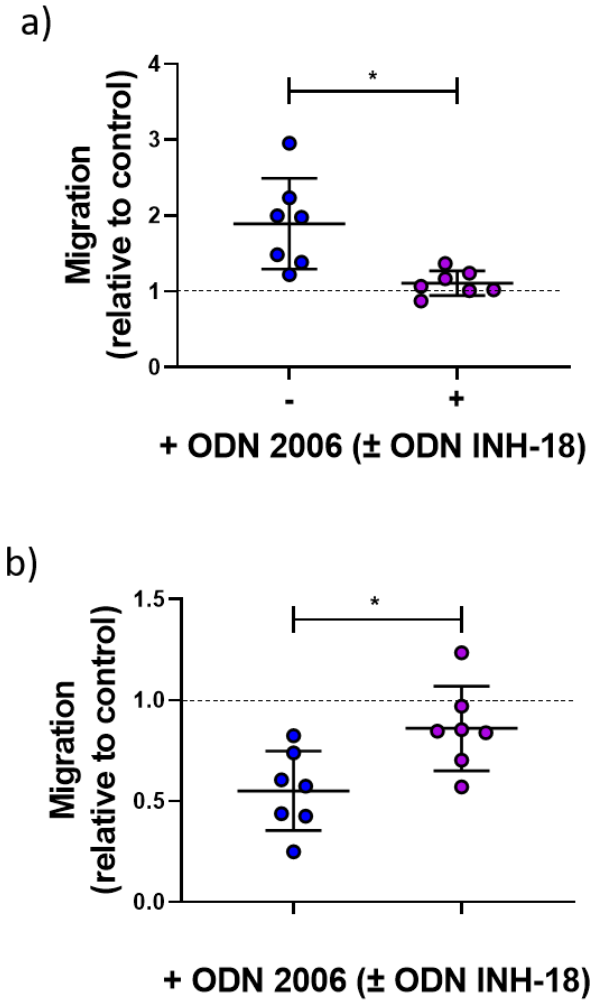

Figure 3.16: ODN INH-18 Inhibits ODN 2006-Induced Changes in CLL Cell Migration. PBMCs were pre-incubated for 30 minutes ± 5μM ODN INH-18 (TLR9 antagonist) before being stimulated overnight with 1μM ODN 2006 (TLR9 agonist) in complete media (+IL-4). Transwell migration experiments were performed as previously described. a) Responder patient samples: ODN INH-18 significantly inhibited the observed ODN 2006-stimulated increase in CLL cell migration (P=0.016, n=7, Wilcoxon Matched Pairs test). b) Non/Reverse Responder patient samples: ODN INH-18 reversed the observed ODN 2006-stimulated decrease in CLL cell migration (P=0.047, n=7 from 4 patients, Wilcoxon Matched Pairs test). Statistical analyses were performed using GraphPad Prism 8.0 and the Wilcoxon Matched Pairs test was used as the data were not Gaussian (as determined by the D'Agostino & Pearson omnibus normality test).

3.10.1: Confirming the Optimal Dose of ODN 2006 for the Promotion of CLL Cell Migration

Finally, a series of ODN 2006 dose response assays were performed to confirm the optimal concentration of ODN 2006 for the induction of CLL cell migration. A concentration of 1μM ODN 2006 was earlier optimised in the context of CLL cell surface marker expression and had been carried forward for use in subsequent transwell migration assays. In view of the dichotomy seen between patients, it was necessary to ensure that a concentration of 1μM ODN 2006 remained optimal for the stimulation of CLL cell migration, and that the dichotomy was not an artefact of incorrect dosing. Using a similar range to the original cell surface marker response optimisation, the migratory effect of: 0.1μM; 0.5μM; 1.0μM and 5.0μM ODN 2006 was analysed in 9 Responder and 5 Non/Reverse Responder patients. All 14 samples were taken from freeze/thawed PBMC aliquots and transwell migration experiments were performed as previously. Figure 3.17 and Table 3.4 show the response of each subgroup to stimulation with each of the tested concentrations of ODN 2006.

Table 3.4: Confirming the Optimal Dose of ODN 2006 for the Promotion of CLL Cell Migration

[ODN 2006] (μM)	CLL cell migration (fold change ±SD)	
	Responders	Non/Reverse Responders
0.1	2.12 (±0.96)	0.65 (±0.34)
0.5	2.74 (±0.88)	0.72 (±0.24)
1.0	2.83 (±1.02)	0.71 (±0.27)
5.0	2.58 (±0.84)	0.79 (±0.13)

Responders (n=9); Non/Reverse Responders (n=5).

In the 9 Responder patient samples, ODN 2006 induced a dose-dependent increase in CLL cell migration that peaked at 1μM ODN 2006, confirming this to be the optimal concentration to promote CLL cell migration in this subgroup. In contrast, in the 5 Non/Reverse Responder patients, CLL cell migration was not increased following stimulation with any of the tested concentrations of ODN 2006. This suggested that ODN 2006 was not able to induce CLL cell migration in these patients and the dichotomous migratory response to ODN 2006 was therefore confirmed not to be an artefact of sub-optimal dosing.

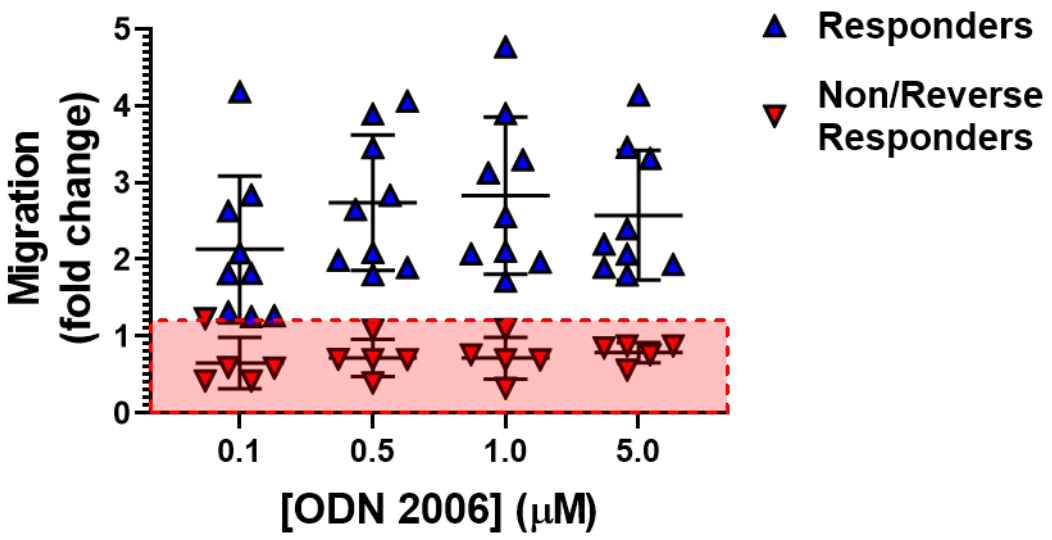

Figure 3.17: Stimulation with 1μM ODN 2006 Induced the Maximum Change in CLL Cell Migration. Freeze-thawed primary PMBCs from 9x Responder (blue triangle) and 5x Non/Reverse Responder (red triangle) patients were cultured overnight ± 0.1-5.0 μM ODN 2006 (TLR9 agonist). The PBMCs were then collected and transferred into the apical chambers of transwell migration plate; transwell migration assays were performed as previously described. Responder patient samples: CLL cell migration showed a dose-dependent response to stimulation with ODN 2006; a concentration of 1μM ODN 2006 was shown to be optimal. Non/Reverse Responder patient samples: CLL cell migration did not increase at any of the tested concentrations of ODN 2006. The dichotomous response was confirmed not to be an artifact of sub-optimal dosing.

3.11: Discussion

The aim of Chapter 3 was to investigate the potential role of Toll-like Receptor 9 (TLR9) in CLL cell migration, and it was hypothesised that activation of TLR9 would promote CLL cell migration. Throughout the chapter, TLR9 was stimulated using the commercially available TLR9 agonist ODN 2006. Firstly, the effect of ODN 2006 stimulation was investigated with regard to the expression of a panel of CLL cell activation and migration markers. ODN 2006 was found to stimulate significant increases in the expression of CD69, CD38 and CD49d and these responses were confirmed to be TLR9 dependent in the presence of a TLR9-specific antagonist. CD69 is a B-cell activation marker and CD49d and CD38 are components of the CLL specific 'invadosome' structure involved in the tissue-homing of CLL cells[148,149]. Taken together, these data indicate that ODN 2006-stimulated CLL cells are primed for activation and migration.

In a cohort of 32 patients, ODN 2006 induced a significant increase in CLL cell migration. It was evident however that this was not a uniform effect across all CLL patient samples the data appeared to suggest a bifurcated migratory response to ODN 2006; in a subset of patient samples, stimulation with ODN 2006 induced a ***decrease*** rather than ***increase*** in CLL cell migration. The two potentially distinct subgroups were tentatively named 'Responders' and 'Non/Reverse Responders' and follow-up biological repeat experiments were performed to investigate the reproducibility of responses; these experiments were performed using freeze/thawed aliquots of 3 Responder and 3 Non/Reverse Responder patient samples. Each individual sample showed a consistent increase or decrease in CLL cell

migration in response to ODN 2006, therefore confirming the experimental reproducibility.

It was firstly important to consider disease burden (i.e., the percentage of CLL cells present within the PBMC population) as a potential confounding variable. Since the transwell migration experiments were performed using PBMCs, rather than isolated CLL cells, it was important to identify whether the variation in PBMC composition between patients was accountable for the observed variation in migratory responses in unstimulated and ODN 2006-stimulated CLL cells. Disease burden was found not to correlate with either basal migration or the fold change in migration following stimulation with ODN 2006 and was therefore confirmed not to influence the migratory response to ODN 2006. Additionally, the migratory response to ODN 2006 was investigated using a range of concentrations of ODN 2006 to ensure the observed dichotomy was not due to suboptimal dosing. Results from these experiments confirmed a dose-dependent migratory response to ODN 2006 in 9/14 patients and confirmed 1μM ODN 2006 to be optimal. They also illustrated that the 5/14 patient samples that did not show an increase in CLL cell migration in response to 1μM ODN 2006 also failed to induce migration following stimulation with any of the tested concentrations. Together these data support the existence of a dichotomous migratory response to ODN 2006.

The migratory responses to ODN 2006 were confirmed to be, at least in part, TLR9-dependent in a series of transwell migration experiments using the potent TLR9 antagonist ODN INH-18. A 30-minute pre-incubation with 5μM ODN INH-18 almost entirely reversed the observed ODN 2006-stimulated changes in CLL migration in

both the Responder and Non/Reverse Responder subgroups. Curiously however, the migratory response could not be attributed to the protein expression of TLR9; neither the percentage positivity nor mean fluorescent intensity of TLR9 correlated with the fold change in CLL cell migration. Interestingly, previous studies identifying TLR9-dependent effects of CpG ODN upon CLL cell proliferation and survival have also shown there to be no correlation between proliferative/apoptotic responses and the mRNA or protein expression levels of TLR9[138,151]. In our recently published manuscript however we showed that CLL cells from patients with higher levels of TLR9 mRNA, engrafted better in a murine xenograft model[132].

It is possible that the intracellular location of TLR9 holds a greater significance to TLR9 compared to total protein expression. In physiological resting conditions, TLR9 is sequestered within the endoplasmic reticulum (ER) and transported to the endosomal membrane in its inactive pre-receptor form following the endocytosis of CpG DNA into early endosomes[128,129,152]; TLR9 functionality is not enabled until the pre-protein is successfully integrated within the endosomal membrane and PH-dependent proteolytic cleavage has occurred[130]. It could be that the spatial expression or conformation of TLR9 is distinct in different subgroups of CLL following stimulation with ODN 2006 and that these differences influence the migratory response. In this study, there were no significant changes observed in the expression levels of TLR9 following stimulation with ODN 2006 however it is again unclear whether spatial/conformational changes were induced. The non-responsiveness of TLR9 expression to stimulation with CpG ODN has also been previously reported in HeLa cells but again, the intracellular localisation of TLR9 was not determined[153].

Interestingly, the above-mentioned publications investigating the effect of ODN 2006 stimulation upon the proliferation and survival of CLL cells have also reported a clear dichotomous response[138,139,151]; primary CLL cells have been described to either proliferate or undergo apoptosis following stimulation with ODN 2006 and this has been found to depend upon the mutational status of the B-cell receptor. CLL can be divided into two main prognostic subtypes according to the IGHV-locus of the BCR: IGHV-unmutated (U-CLL) patients usually experience an aggressive disease course with a poor clinical outcome, whilst IGHV-mutated cases (M-CLL), normally experience a far more indolent disease course. Following stimulation with ODN 2006, U-CLL patient samples have been shown to respond in a proliferative and anti-apoptotic manner whilst M-CLL patient samples respond in a non-proliferative and pro-apoptotic manner[138,139,151]. The experiments in Chapter 3 identified a dichotomous migratory response to stimulation with ODN 2006 in a currently undefined subgroup of patients; it is possible that IGHV-mutational status relates to these patterns. Since IGHV-sequencing is not routinely performed on pre-treatment CLL patients at The Royal Sussex County Hospital, the IGHV-mutational status of the patient cohort of Chapter 3 was unknown at the time of data collection. Chapter 4 aims to further define the dichotomous response to ODN 2006. It is hypothesised that the bifurcation exists between the M-CLL and U-CLL patient subgroups.

4.0: Bifurcation of the Migratory Responses to ODN 2006

4.1: Introduction

Chapter 3 identified that CLL cells have a dichotomous migratory response to TLR9 activation. In a cohort of 32 patient samples the TLR9 agonist ODN 2006 was shown to induce either an increase ***or*** decrease in CLL cell migration and the response of individual samples was found to be consistent following biological repeats. This led to the hypothesis that IGHV-mutational status may contribute to the dichotomous migratory response to ODN 2006 as multiple studies have reported differing sensitivities of U-CLL and M-CLL patient samples to stimulation with TLR9 agonistic CpG DNA (in the context of proliferation and survival) [138,139,151]. The work detailed in this chapter set out to establish whether this was also the determining factor of the dichotomous migratory response following TLR9 agonism with ODN 2006.

In healthy individuals the B-cell population is polyclonal, meaning that each naïve B-cell expresses a BCR with unique antigen specificity. Following antigen exposure, activated B-cells can further increase their affinity for the recognised antigen through a process called somatic hypermutation. During somatic hypermutation, a succession of point mutations are introduced into the variable regions of the both the heavy and light immunoglobulin chains, resulting in conformational changes in the antigen-binding domain[37]. In contrast, CLL cells are almost always monoclonal with each malignant cell having a common cell of origin and consequentially identical BCR specificity. For each patient, the mutational status of the BCR provides great prognostic value. Patients with U-CLL generally experience a more aggressive disease course with rapid progression and an inferior response to chemotherapeutic agents

whilst patients with M-CLL predominately experience a far more indolent disease course[3,17-19]; the average TTFT of U-CLL vs M-CLL patients is 3.5 years vs 9.2 years[19].

U-CLL cells are known to have a higher dependency upon microenvironmental signals and are more responsive to stimulation via the BCR than M-CLL patients[83]; M-CLL patients have been shown not to respond to BCR-stimulation *in vitro* and are largely considered to be anergic[80,84,85]. It is possible the same could be true for CLL cell activation via TLR9. This chapter investigates the relationship between IGHV-mutational status and the migratory response to ODN 2006 and aims to identify a phenotype for the Non/Reverse-Responder patient samples.

4.2: Determining the IGHV-Mutational Status of the CLL Patient Cohort

The phenotypic and migratory data presented in Chapter 3 were collected blind to the IGHV-mutational status of each sample. The Brighton and Sussex University Hospital trust do not routinely test for the IGHV-mutational status of their patients and this information was therefore unavailable in the majority of cases. To address this missing data, DNA was retrospectively extracted from frozen PBMC aliquots of 31 patient samples from the Chapter 3 cohort; this was achieved using the DNeasy Blood & Tissue Kit (Qiagen) and samples were sent for IGHV-sequencing at The Royal Marsden Hospital (Sutton) (see methods section 2.16). The resulting IGHV nucleotide sequences were read using SnapGene software (Figure 4.1a) and aligned to the ImMunoGeneTics (IMGT) reference directory of naïve B-cell IGHV sequences (Figure 4.1b). Samples were considered IGHV-*unmutated* (U-CLL) when displaying ≥98% homology to the reference directory of naïve B-cell IGHV sequences and IGHV-

mutated (M-CLL) when displaying <98% homology with the reference directory (Figure 4.1c).

Of the 31 patient samples, 14 were identified as IGHV-*unmutated* (U-CLL) and 17 were identified as IGHV-*mutated* (M-CLL) (See Appendix 7.4, Table 7.6). Additionally, the IGHV-mutational status of a further 7 patient samples from the chapter 3 cohort, was provided at the time of sample receipt i.e., 6 U-CLL and 1 M-CLL (See Appendix 7.4, Table 7.7).

a)

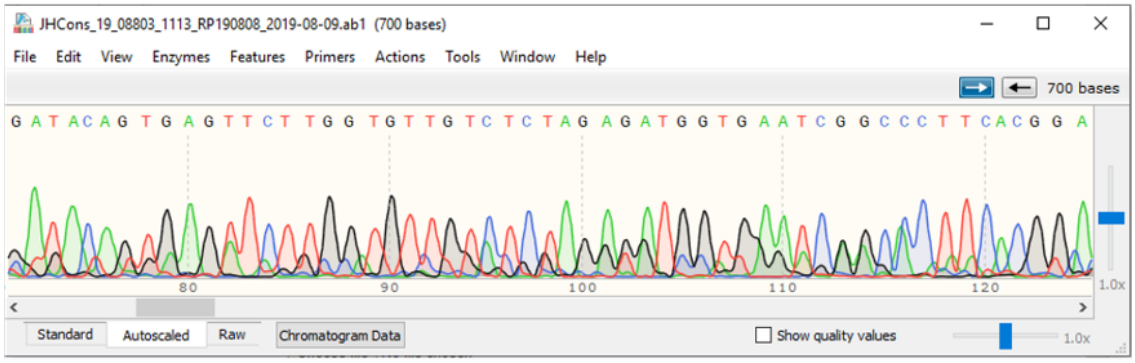

b)

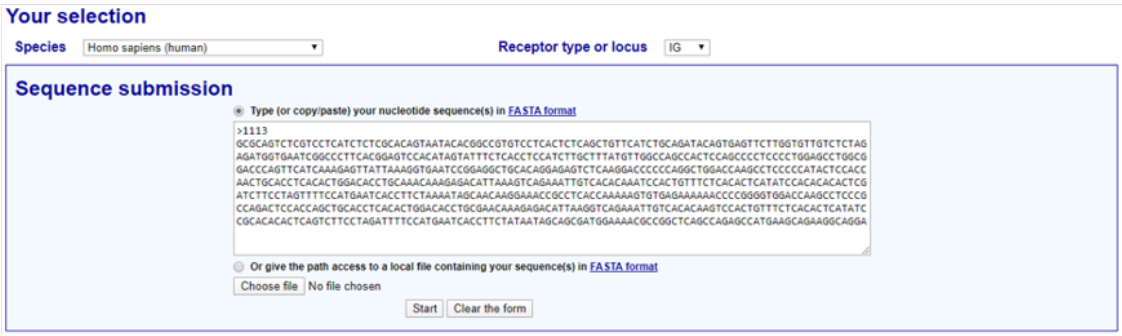

c)

Analysed sequence length: 700.
Sequence analysis category: 3 (complementay reverse_no indel search).
Complementary reverse sequence compared with the *Homo sapiens* (human) IG set from the IMGT reference directory

```
>1113  (complementary reverse)
tcctgccttctgcttcatggctctggctgagccggcgttttccatcgctgctattataga
aggtgattcatggaaaatctaggaagactgagtgtgtgcggatatgagtgtgagaaacag
tggacttgtgtgacaatttctgaccttaatgtctctttgttcgcaggtgtccagtgtgag
gtgcagctggtggagtctggcgggaggcttggtccaccccggggttttttctcacacttt
ttggtgaggcggtttccttgttgctattttagaaggtgattcatggaaaactaggaagat
cgagtgtgtgtggatatgagtgtgagaaacagtggatttgtgtgacaatttctgacttta
atgtctctttgtttgcaggtgtccagtgtgaggtgcagttggtggagtatgggggaggct
tggtccagcctgggggtccttgagactctcctgtgcagcctccggattcacctttaata
actctttgatgaactgggtccgccaggctccaggggaggggctggagtggctggccaaca
taaagcaagatggaggtgagaaatactatgtggactccgtgaagggccgattcaccatct
ctagagacaacaccaagaactcactgtatctgcagatgaacagctgagagtgaggacacg
gccgtgtattactgtgcgagagatgaggacgagactgcgc
```

Result summary:	No rearrangement found (stop codons)		
V-GENE and allele	Homsap IGHV3-7*01 F	score = 1084	identity = 86.11% (248/288 nt)
FR-IMGT lengths, CDR-IMGT lengths	[8.8.X]		

Figure 4.1: IGHV Sequence Alignment. a) IGHV nucleotide sequences were read using Snapgene viewer. b) IGHV nucleotide sequences were entered into the IMGT/V-QUEST tool of the online IMGT information system. c) IGHV nucleotide sequences were aligned with the IMGT reference directory to identify the percentage homology to germline sequences. In this representative example, patient 1113 showed 86.11% homology to the closest germline sequence (IGHV3-7 gene) and is therefore classified as IGHV-mutated (M-CLL).

4.3: A Bifurcated Migratory Response to Stimulation with ODN 2006 Occurs between M-CLL and U-CLL and a Further Bifurcation Occurs within the U-CLL Subgroup

Having identified the IGHV-mutational status of all previously unassigned patients, the migratory data from Chapter 3 were re-visited. Patient samples were divided into M-CLL and U-CLL subgroups and the data was re-analysed accordingly. A strikingly clear divide in the migratory responses of M-CLL and U-CLL samples was observed. Surprisingly, ODN 2006 induced a significant ***increase*** in the migration but only in the ***M-CLL*** subset (Figure 4.2a). In this subgroup, CLL cell migration (mean ±SD) significantly increased from 7.7% (±3.5) to 12.8% (±5.5) ($P<0.001$, n=14) following stimulation with ODN 2006 whilst in the ***U-CLL*** subgroup, CLL cell migration was not significantly altered following exposure to ODN 2006 (i.e., from 5.9% (±5.6) to 5.0% (±3.3); $P=0.932$, n=18). ODN 2006 therefore appeared to promote CLL cell migration in the M-CLL but not U-CLL subgroup. Interestingly, compared to the U-CLL subgroup, the M-CLL patients also had marginally higher basal migration in the absence of any stimulation ($P=0.049$). Although initially surprising, these results were in keeping with a previous study suggesting U-CLL cells to be less migratory, relative to M-CLL cells[154]; in this study, Eagle et al., concluded that U-CLL cells were better primed for lymph node retention, rather than chemotaxis[154].

When analysing the responses of individual samples however, a clear bifurcation in the U-CLL subgroup was evident; Figure 4.2b, shows the same data expressed as fold change in migration (relative to the unstimulated control) and illustrates the wider range of responses in U-CLL samples relative to M-CLL samples. U-CLL responses to

ODN 2006 ranged from a 0.20 to 3.89-fold change, with a mean of 1.34 (±0.92). Using a threshold of ≥1.2-fold to categorise 'Responder' and 'Non/Reverse Responder' samples, 10/18 (55.6%) U-CLL samples were identified as 'Non/Reverse Responders' and 8/19 (44.4%) as 'Responders'.

In contrast, the M-CLL subgroup displayed a mean fold change of 1.80 (±0.67) with a range of 1.00 to 3.73-fold; 13/14 (92.9%) samples were identified as 'Responders' and no samples showed a decrease in migration in response to ODN 2006. The previously identified Non/Reverse Responder subgroup was therefore almost exclusively comprised of U-CLL samples: i.e., 10/11 Non/Reverse Responder samples were U-CLL. Additionally, the responses of M-CLL and U-CLL samples were significantly different from each other (P=0.034) (Figure 4.2b). Table 7.6 and 7.7 in Appendix 7.4, shows the mutational status and responder status of each patient sample. Together, these results show that the earlier identified dichotomy in the migratory response to ODN 2006 is caused by the differential responses of the M-CLL and U-CLL subgroups.

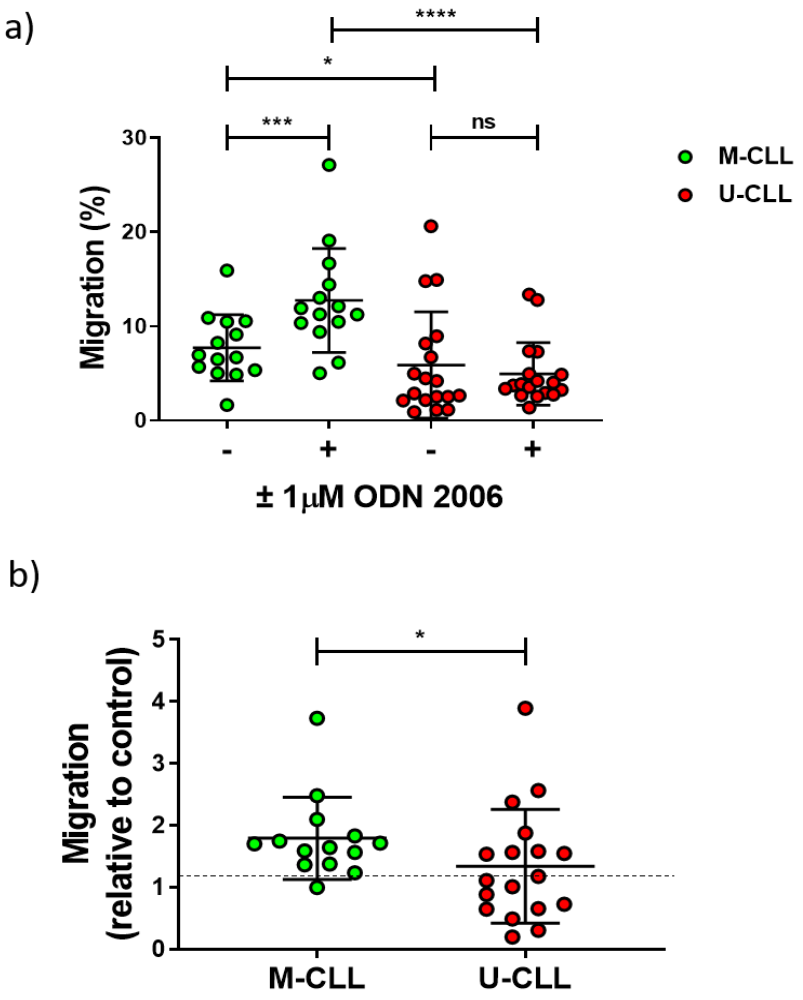

Figure 4.2: M-CLL and U-CLL Patient Samples Show Distinct Migratory Responses to Stimulation with ODN 2006. Migratory data from Chapter 3 was re-analysed and patients were grouped according to their IGHV mutational status. Transwell migration data from 32 CLL patient samples was divided into M-CLL (n=14) and U-CLL (n=18) subgroups and analysed accordingly. a) Migration values were expressed as a percentage of the 0h live cell input count. Following stimulation with 1μM ODN 2006, the M-CLL subgroup showed a significant increase in CLL cell migration compared to their unstimulated control (P<0.001, Wilcoxon Matched Pairs test) but the U-CLL subgroup showed no significant difference in CLL cell migration (P=0.932, Wilcoxon Matched Pairs test). In addition, in the M-CLL subgroup the basal and ODN 2006-stimulated percentage of CLL cell migration was significantly higher than the U-CLL subgroup (P=0.049 and P<0.001 respectively, Mann-Whitney test). b) Migration values were expressed as fold change relative to the unstimulated control. 13/14 M-CLL patients showed an increase in CLL cell migration following stimulation with ODN 2006 (i.e., >1.2-fold increase). 8/18 U-CLL patients showed an increase in CLL cell migration following stimulation with ODN 2006 and 10/18 showed either no change or a reversed response. Statistical analysis was performed using GraphPad Prism and statistical tests were selected depending on whether the data passed the D'Agostino-Pearson omnibus normality test.

4.4: TLR9 Expression Correlates with the Migratory Responses of Both the M-CLL and U-CLL Subgroup

Chapter 3 described a surprising lack of correlation between the protein expression of TLR9 and the migratory response to ODN 2006. This data was re-visited in the context of M-CLL vs U-CLL to determine whether the dichotomous migratory response to ODN 2006 could be attributed to differential TLR9 expression between the two groups. Figure 4.3 and Tables 4.1 and 4.2 show both the basal and ODN 2006-stimulated expression of TLR9 in M-CLL (n=16) and U-CLL (n=14) patient samples. Expression of TLR9 (both percentage positivity and MFI) was higher in the U-CLL relative to the M-CLL subgroup. TLR9 expression also increased following stimulation with ODN 2006 in the U-CLL but not the M-CLL subgroup. These results show that surprisingly, the U-CLL subgroup have both higher basal and ODN 2006-stimulated TLR9 expression, despite showing the lowest basal and TLR9-induced migration.

Table 4.1: TLR9 Expression (Percentage Positivity) in M-CLL vs U-CLL Patient Samples

	TLR9 Percentage Positivity (%)		
	M-CLL	**U-CLL**	**P-value (M-CLL vs U-CLL)**
Unstimulated	63.7 (±19.2)	75.4 (±14.2)	P=0.072
+ ODN 2006	60.6 (±23.6)	80.1 (±18.5)	P=0.019
P- value (±ODN 2006)	P=0.185	P=0.073	

M-CLL (n=16); U-CLL (n=14).

Table 4.2: TLR9 Expression (Mean Fluorescence Intensity) in M-CLL vs U-CLL Patient Samples

	TLR9 Mean Fluorescence Intensity		
	M-CLL	**U-CLL**	**P-value (M-CLL vs U-CLL)**
Unstimulated	1376 (±869.8)	2727 (±2376)	P=0.085
+ ODN 2006	1639 (±1848)	3364 (±2799)	P=0.028
P- value (±ODN 2006)	P=0.669	P=0.042	

M-CLL (n=16); U-CLL (n=14).

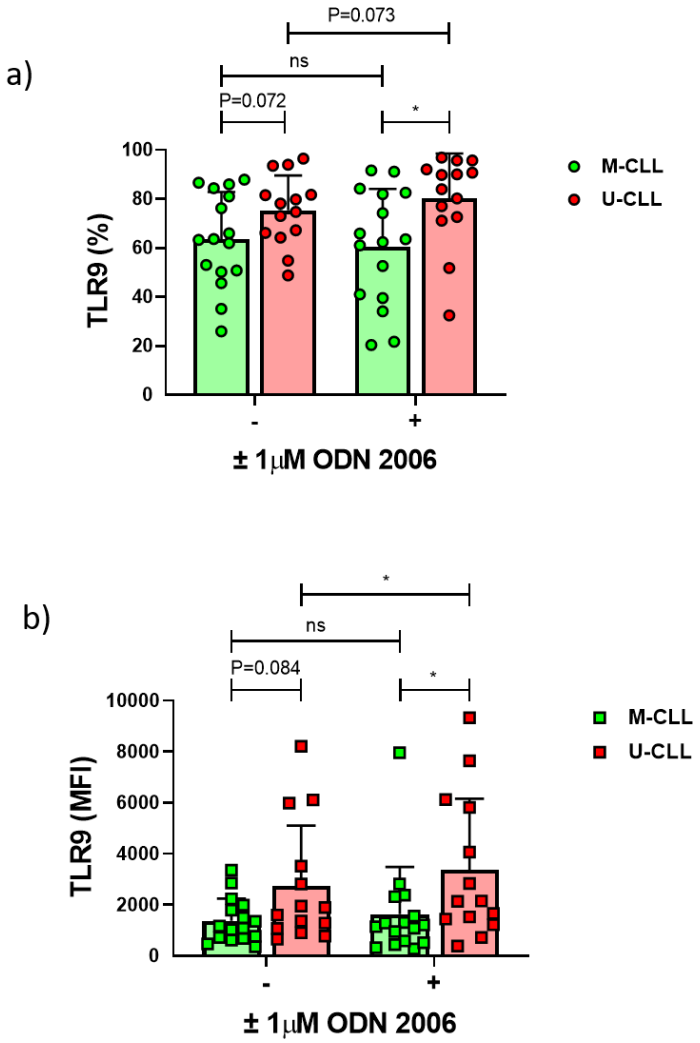

Figure 4.3: TLR9 Expression is Higher in the U-CLL Subgroup. TLR9 expression data earlier presented in Chapter 3, was re-visited and divided into M-CLL and U-CLL subgroups. Primary CLL cells were stimulated ± 1μM ODN 2006, stained for both extracellular CLL cell identification markers and intracellular TLR9 and analysed using CytExpert software on a Cytoflex LX flow cytometer. Live CLL cells were gated as CD5+/CD19+/CD3-/FVD-. a) In the U-CLL subgroup, TLR9 percentage positivity was higher in both unstimulated and ODN 2006-stimulated CLL cells compared to the M-CLL subgroup (P=0.072 [trend] and P=0.028 respectively, both Unpaired t-test). Following stimulation with ODN 2006 there was no significant change in TLR9 percentage positivity in the M-CLL subgroup but there was an increase trend in the U-CLL subgroup (P=0.185 and P=0.073 respectively, both Paired t-test). b) In the U-CLL subgroup, TLR9 MFI was higher in both unstimulated and ODN 2006-stimulated CLL cells compared to the M-CLL subgroup (P=0.084 [trend] and P=0.028 respectively, both Mann-Whitney test). Following stimulation with ODN 2006 there was no significant change in TLR9 MFI in the M-CLL (P=0.669) but a significant increase in the U-CLL subgroup (P=0.042), both Wilcoxon Matched pairs test). Statistical analyses were performed using GraphPad Prism and statistical tests were selected depending on whether the data passed the D'Agostino-Pearson omnibus normality test.

In view of these surprising results, the relationship between CLL cell migration and expression levels of TLR9 was investigated. Although ODN 2006 had no effect on TLR9 expression in the M-CLL subgroup, TLR9 levels were variable between patients and showed a significant ***positive*** correlation with ODN 2006-stimulated M-CLL cell migration (P=0.022, R^2=0.42, n=12) (Figure 4.4a); this suggested a functional link between TLR9 and the pro-migratory response of M-CLL samples to ODN 2006. Additionally, after the removal of a clear outlier (which had levels of migration that were too low to allow meaningful analysis), TLR9 was found to strongly correlate with the observed fold increase in M-CLL cell migration following stimulation with ODN 2006 (P=0.006, R^2=0.59, n=11) (Figure 4.4b). These results implicate TLR9 in the migratory response of M-CLL patients to stimulation with ODN 2006.

In striking contrast to the M-CLL subgroup, ODN 2006 increased TLR9 expression in the U-CLL subgroup (shown above) and yet despite this, TLR9 levels showed a significant ***negative*** correlation with the percentage of ODN 2006-stimulated migration (P=0.008, R^2=0.43, n=15) (Figure 4.5a); this suggested an inverse functional link between TLR9 levels and the migratory response of U-CLL cells to ODN 2006. There was however no correlation observed between U-CLL TLR9 levels and the fold change in CLL cell migration following stimulation with ODN 2006 (P=0.835, R^2<0.01, n=15) (Figure 4.5b). These results suggest that whilst U-CLL patients with higher levels of TLR9 migrate less in response to stimulation with ODN 2006, this is not determined by TLR9 expression.

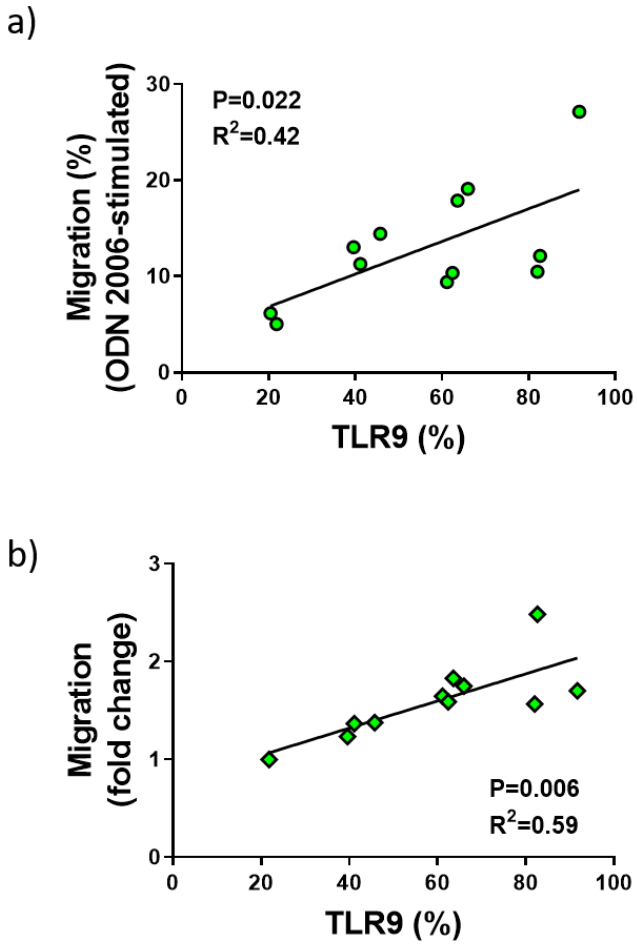

Figure 4.4: TLR9 Positively Correlates with ODN 2006-Stimulated M-CLL Cell Migration. Primary PBMCs from 12 M-CLL patients were cultured ± 1μM ODN 2006 and either transferred into the apical chambers of a 24-well, 5μM pore polycarbonate, transwell migration plate to assess CLL cell migration or stained for intracellular TLR9 and analysed using a CytoFLEX LX flow cytometer; live CLL cells were gated as CD5+/CD19+/CD3-/FVD-. a) TLR9 (percentage positivity) showed a strong positive correlation with ODN 2006-stimulated migration (P=0.022, R^2=0.42). b) TLR9 (percentage positivity) showed strong positive correlation with the fold change in migration in response to ODN 2006 (P=0.006 R^2=0.59, n=11). Statistical analysis was performed using GraphPad Prism 8.0. Correlation was determined using the Spearman's rank correlation coefficient.

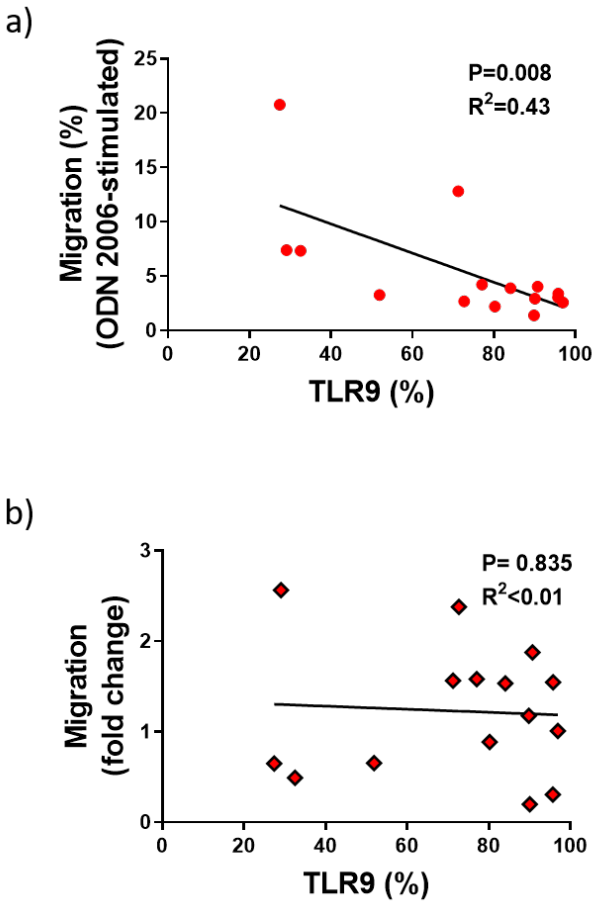

Figure 4.5: TLR9 Negatively Correlates with ODN 2006-Stimulated U-CLL Cell Migration. Primary PBMCs from 15 U-CLL patients were cultured ± 1μM ODN 2006 and either transferred into the apical chambers of a 24-well, 5μM pore polycarbonate, transwell migration plate to assess CLL cell migration or stained for intracellular TLR9 and analysed using a CytoFLEX LX flow cytometer; live CLL cells were gated as CD5+/CD19+/CD3-/FVD-. a) TLR9 (percentage positivity) showed a strong negative correlation with ODN 2006-stimulated migration (P=0.008, R^2=0.43). b) TLR9 (percentage positivity) (n=12) did not correlate with the fold change in migration in response to ODN 2006 (P=0.835, R^2<0.01). Statistical analysis was performed using GraphPad Prism 8.0. Correlation was determined using the Spearman's rank correlation coefficient.

4.5: Delineating the Dichotomous Migratory Response of U-CLL Patients to ODN 2006

A clear dichotomous migratory response to ODN 2006 has been observed between the M-CLL and U-CLL subgroups and a further bifurcation appears to exist within the U-CLL subgroup. Whilst M-CLL samples demonstrated a uniform positive migratory response to ODN 2006, U-CLL samples were divided and either demonstrated an increase in CLL cell migration in the presence of ODN 2006 (similar to M-CLL) or a decrease in CLL cell migration. The migratory responses of the M-CLL and U-CLL subgroups were found to be functionally but oppositely, linked with the expression of TLR9 however the mechanisms behind these observations were unknown. The phenotypic data from chapter 3 was re-visited and re-analysed in the context of M-CLL vs U-CLL in order to identify any potential differences which may account for the migratory dichotomy.

4.5.1: ODN 2006 Induces the Same Migratory Phenotype in Both M-CLL and U-CLL Patient Samples

Chapter 3 described the effect of ODN 2006 on the expression of a panel of CLL cell surface markers. The panel was chosen to include markers of CLL cell activation and adhesion/migration and comprised CD69, CD49d, CD38 and CD62L. ODN 2006 was found to induce a significant upregulation of CD69, CD49d and CD38 but not CD62L. The response of each marker to stimulation with ODN 2006 was re-analysed in turn.

CD69 is a B-cell activation marker shown in Chapter 3 to respond strongly to stimulation with ODN 2006. Both groups showed a strong and significant upregulation of CD69 in response to ODN 2006. In the M-CLL subgroup (n=18), CD69

percentage positivity significantly increased from 27.5% (±21.0) to 61.5% (±20.4) (P<0.001) and CD69 MFI significantly increased from 1865 (±1493) to 6756 (±5260) (P<0.001). In the U-CLL subgroup (n=18), CD69 percentage positivity significantly increased from 45.2% (±19.3) to 74.9% (±19.9) (P<0.001) and CD69 MFI significantly increased from 3023 (±1897) to 10029 (±5683) (P<0.001). The basal expression of CD69 (both percentage positivity and MFI) was significantly higher in the U-CLL relative to M-CLL subgroup however there was no significant difference in the ODN 2006-stimulated expression of CD69 between the two subgroups (Figure 4.6 and Table 4.3). Together these results show that that ODN 2006 can strongly promote CLL cell activation in both the M-CLL and U-CLL subgroups and that the U-CLL subgroup exhibits a higher basal level of activation, relative to the M-CLL subgroup.

Table 4.3: The U-CLL Subgroup Expressed Significantly Higher Basal Levels of CD69 and CD49d, Relative to the M-CLL Subgroup

	Cell Surface Marker Expression U-CLL vs M-CLL (P-value)			
	Basal		ODN 2006-Stimulated	
	% Positivity	MFI	% Positivity	MFI
CD69	P=0.013	P=0.040	P=0.054	P=0.081
CD49d	P=0.089	P=0.029	P=0.149	P=0.118
CD38	P=0.226	P=0.425	P=0.161	P=0.293
CD62L	P=0.425	P=0.563	P=0.071	P=0.143

M-CLL (n=18), U-CLL (n=18).

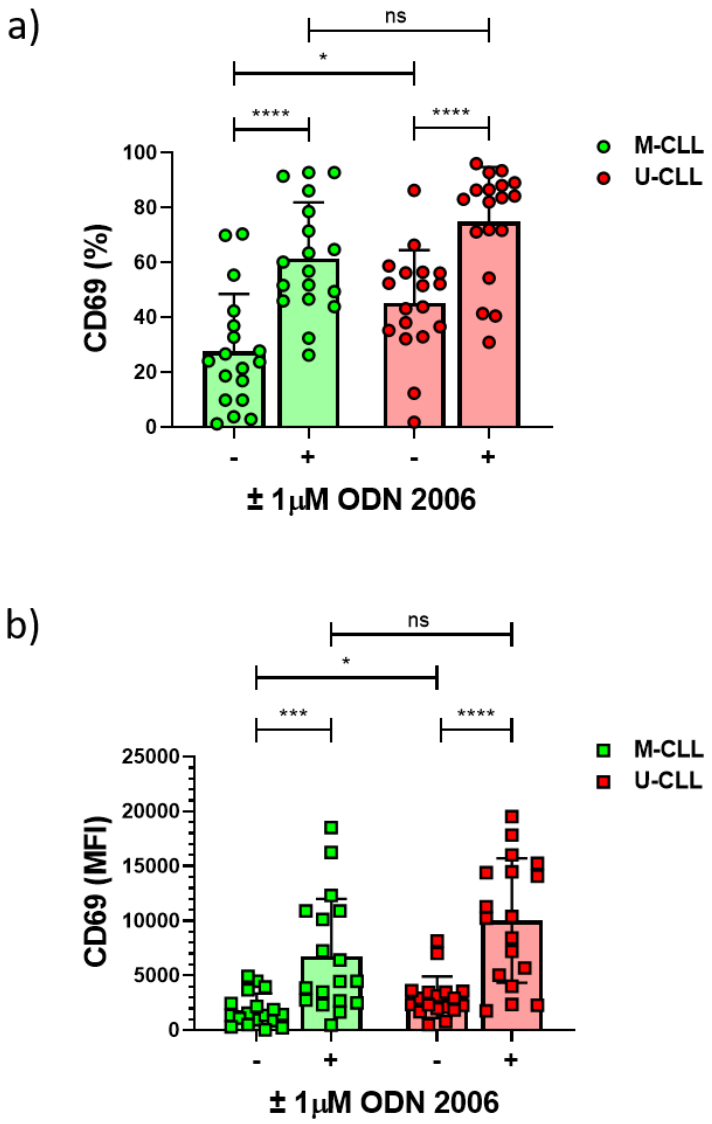

Figure 4.6: ODN 2006 Induced an Upregulation of CD69 in Both U-CLL and M-CLL. Primary PBMCs were cultured in complete media (+IL-4) ± 1μM ODN 2006 at 37°C/5% CO_2. Cells were collected at 24h post-stimulation and stained for flow cytometry; live CLL cells were identified as CD5+/CD19+/CD3-/FVD- and analysed using CytExpert software on a Cytoflex LX flow cytometer. a) ODN 2006 induced a significant increase in the percentage positivity of CD69 in both the M-CLL (P<0.001, n=18) and U-CLL (P<0.001, n=18) subgroups (both Paired t-test). Basal expression of CD69 (percentage positivity) was significantly higher in the U-CLL relative to the M-CLL subgroup (P=0.013, Unpaired t-test). b) ODN 2006 induced a significant increase in CD69 MFI in both the M-CLL (P<0.001, n=18, Paired t-test) and U-CLL (P<0.001, n=18, Wilcoxon Matched Pairs test) subgroups. Basal expression of CD69 (MFI) was significantly higher in the U-CLL relative to the M-CLL subgroup (P=0.040, Mann-Whitney test). Statistical analyses were performed using GraphPad Prism and statistical tests were selected depending on whether the data passed the D'Agostino-Pearson omnibus normality test.

CD49d and CD38 are components of the CLL cell 'invadosome' complex involved in CLL cell transendothelial migration. In the M-CLL subgroup (n=18), whilst there was no significant difference in the percentage positivity of CD49d following stimulation with ODN 2006 (i.e., 27.4% (±39.5) to 30.13% (±39.8) (P=0.143), CD49d MFI significantly increased from 2034 (±3998) to 3640 (±6768) (P<0.001) (Figure 4.7). In the U-CLL subgroup (n=18), both CD49d percentage positivity and CD49d MFI were significantly increased following stimulation with ODN 2006. CD49d percentage positivity increased from 56.2 (±41.5) to 58.1% (±42.5) (P=0.039) and CD49d MFI increased from 5648 (±10704) to 7304 (±12050) (P<0.001). As found for CD69, the basal expression of CD49d was higher in the U-CLL relative to the M-CLL subgroup however this trend reached statistical significance for CD49d MFI only (Table 4.3). The ODN 2006-stimulated expression of CD49d was also higher in the U-CLL relative to the M-CLL subgroup however again these trends did not reach statistical significance (Table 4.3). Together, these results suggest that ODN 2006 can promote the upregulation of CD49d in both the M-CLL and U-CLL subgroup and that U-CLL cells generally express higher basal levels of CD49d. Expression and upregulation of CD49d therefore does not appear to be driving the increase in ODN 2006-stimulated increase in M-CLL migration.

In chapter 3, ODN 2006 was shown to induce a statistically significant increase in CD38 in a larger cohort of 49 patient samples, however this was a smaller increase relative to the changes observed for CD69 and CD49d. In this cohort of 18 M-CLL and 18 U-CLL samples, increases in ODN 2006-stimulated CD38 did not reach statistical significance. In the M-CLL subgroup, CD38 percentage positivity changed from 32.6% (±26.6) to 29.9% (±26.5) (P=0.090) and CD38 MFI increased from 590.6 (±1040) to

1067 (±2419) (P=0.766) (Figure 4.8). In the U-CLL subgroup, CD38 percentage positivity changed from 47.4% (±37.0) to 48.5% (±37.1) (P=0.442) and CD38 MFI increased from 2064 (±3468) to 3151 (± 6518) (P=0.142). Whilst both the basal and ODN 2006-stimulated levels of CD38 expression (both percentage positivity and MFI) were higher in the U-CLL relative to the M-CLL subgroup, these trends did not reach statistical significance and it was not possible to draw any meaningful conclusions (Table 4.3).

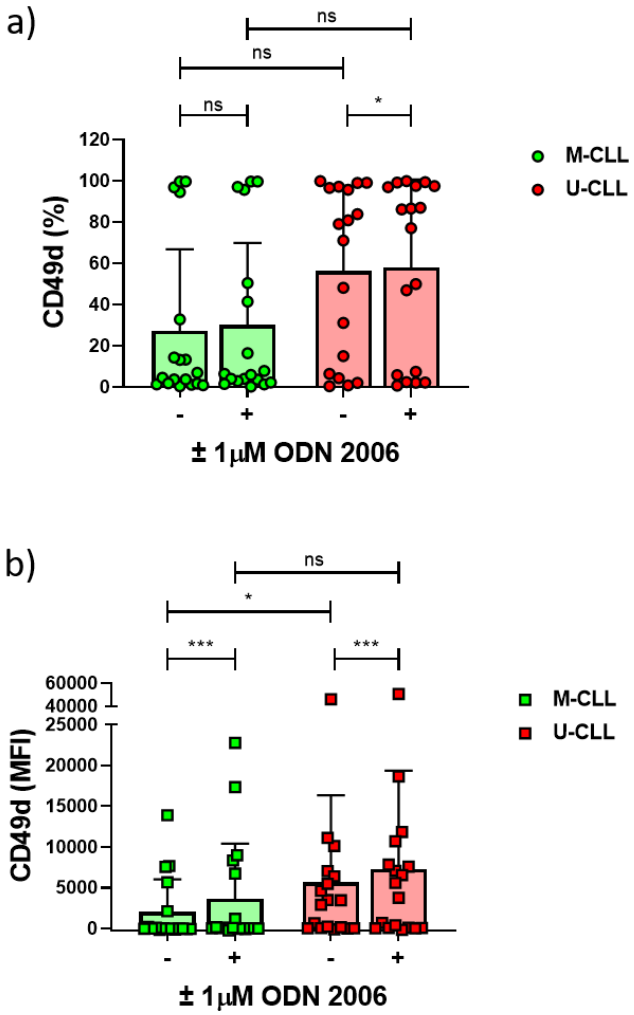

Figure 4.7: ODN 2006 Induced an Upregulation of CD49d in Both U-CLL and M-CLL. Primary PBMCs were cultured in complete media (+IL-4) ± 1μM ODN 2006 at 37°C/5% CO_2. Cells were collected at 24h post-stimulation and labelled for flow cytometry; live CLL cells were identified as CD5+/CD19+/CD3-/FVD- and analysed using CytExpert software on a Cytoflex LX flow cytometer. a) ODN 2006 induced a significant increase in the percentage positivity of U-CLL (P=0.039, n=18, Wilcoxon Matched Pairs test) but not M-CLL (P=0.143, n=18, Paired t-test). The basal and ODN 2006-stimulated expression of CD49d (percentage positivity) was higher in the U-CLL relative to the M-CLL subgroup however this did not reach statistical significance (P=0.089 and P= 0.149 respectively, Mann-Whitney test). b) ODN 2006 induced a significant increase in CD49d MFI in both the M-CLL (P<0.001, n=18) and U-CLL (P<0.001, n=18) subgroups (both Wilcoxon Matched Pairs test). The basal but not ODN 2006-stimulated expression of CD49d (MFI) was significantly higher in the U-CLL relative to the M-CLL subgroup (P=0.029 and P=0.118 respectively) (both Unpaired t-test). Statistical analyses were performed using GraphPad Prism and statistical tests were selected depending on whether the data passed the D'Agostino-Pearson omnibus normality test.

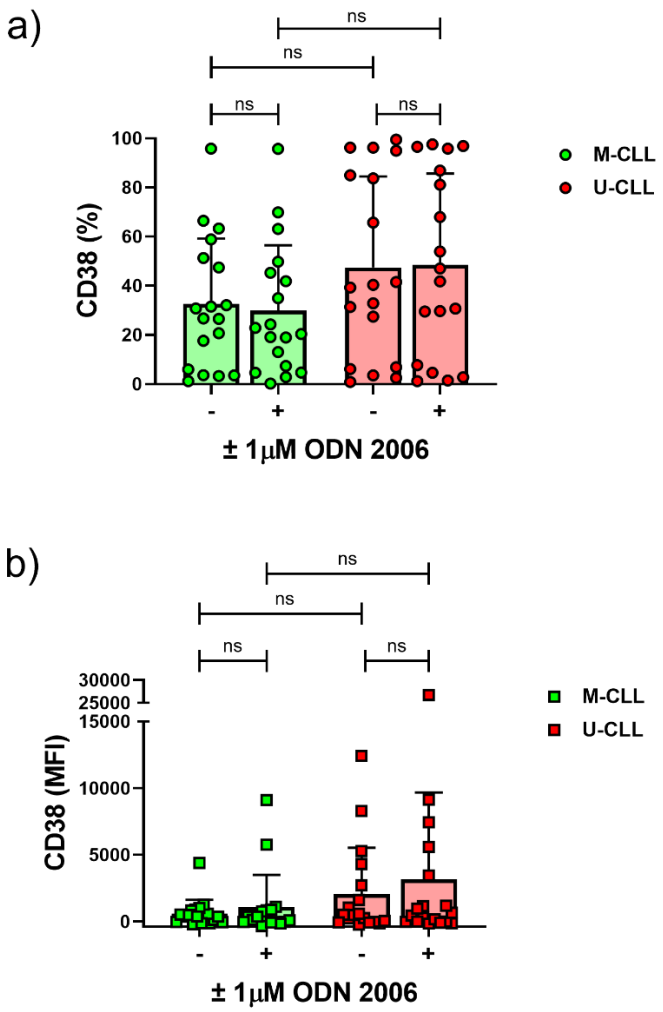

Figure 4.8: CD38 was More Highly Expressed in the U-CLL Subgroup Relative to the M-CLL Subgroup, Although This Trend Did Not Reach Statistical Significance. Primary PBMCs were cultured in complete media (+IL-4) ± 1μM ODN 2006 at 37°C/5% CO_2. Cells were collected at 24h post-stimulation and stained for flow cytometry; live CLL cells were identified as CD5+/CD19+/FVD-/CD3- and analysed using CytExpert software on a Cytoflex LX flow cytometer. a) Following stimulation with ODN 2006 there was no significant increase in the percentage positivity of CD38 in either the M-CLL (P=0.090, n=18, Paired t-test) or U-CLL (P=0.442, n=18, Wilcoxon Matched Pairs test). Both the basal and ODN 2006-stimulated CD38 percentage positivity were highest in the U-CLL subgroup although this trend did not reach statistical significance (P=0.226 and P=0.161 respectively, both Mann-Whitney test). b) Following stimulation with ODN 2006 there was no significant increase in the MFI of CD38 in either the M-CLL (P=0.766, n=18) or U-CLL (P=0.142, n=18) (both Wilcoxon Matched Pairs test). Both the basal and ODN 2006-stimulated CD38 MFI were highest in the U-CLL subgroup although this trend did not reach statistical significance (P=0.425 and P=0.293 respectively, both Mann-Whitney test). Statistical analyses were performed using GraphPad Prism and statistical tests were selected depending on whether the data passed the D'Agostino-Pearson omnibus normality test.

CD62L is an adhesion molecule (selectin) involved in transendothelial migration and was shown in chapter 3 not to induce any significant changes in expression following stimulation with ODN 2006. Here, these findings were confirmed to be true of both M-CLL (n=18) and U-CLL (n=18) samples; there were no significant changes in the percentage positivity or MFI of CD62L in either subgroup (Figure 4.9). CD62L percentage positivity decreased from 33.5% (±21.6) to 28.5% (± 19.1) (P=0.179) in the M-CLL subgroup and increased from 39.8% (±24.8) to 40.76% (±20.6) (P=0.803) in the U-CLL subgroup. CD62L MFI increased from 766.7 (±1206) to 865.9 (±1625) (P=0.580) in the M-CLL subgroup and decreased from 1498 (±2168) to 1028 (± 1029) in the U-CLL subgroup (P=0.640). Basal CD62L was higher in the U-CLL relative to the M-CLL subgroup however this trend did not reach statistical significance (Table 4.3).

Together, these data show that for each of the described markers, U-CLL and M-CLL samples showed similar phenotypic responses following stimulation with ODN 2006, despite the significantly different migratory responses of these subgroups. This is particularly surprising for CD49d, which is known to play an important role in CLL migration[42].

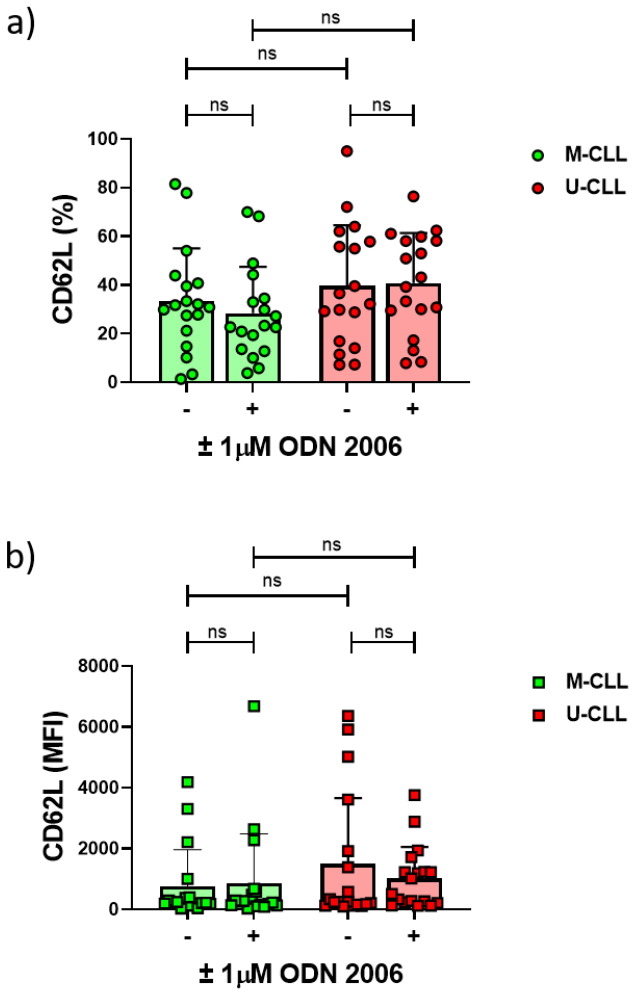

Figure 4.9: ODN 2006 Does Not Induce CD62L Expression in Either the U-CLL or M-CLL Subgroup. Primary PBMCs were cultured in complete media (+IL-4) ± 1μM ODN 2006 at 37°C/5% CO_2. Cells were collected at 24h post-stimulation and stained for flow cytometry; live CLL cells were identified as CD5+/CD19+/CD3-/FVD- and analysed using CytExpert software on a Cytoflex LX flow cytometer. a) Following stimulation with ODN 2006 there was no significant change in the percentage positivity of M-CLL (P=0.179) or U-CLL (P=0.803) (both n=18, Paired t-test). There was also no significant difference between the basal percentage positivity or the ODN 2006-stimulated percentage positivity of CD62L between the M-CLL and U-CLL subgroups (P=0.425 and P=0.071 respectively, Unpaired t-test). b) Following stimulation with ODN 2006 there was no significant change in the MFI of M-CLL (P=0.580) or U-CLL (P=0.640) (both n=18, Wilcoxon Matched Pairs test). Basal CD62L (MFI) was higher in the U-CLL, relative to M-CLL subgroup although this trend did not reach statistical significance (P=0.563, Mann-Whitney test). There was no significant difference between the ODN 2006-stimulated MFI of CD62L between the M-CLL and U-CLL subgroups (P=0.143, Mann-Whitney test). Statistical analyses were performed using GraphPad Prism and statistical tests were selected depending on whether the data passed the D'Agostino-Pearson omnibus normality test.

4.5.2: TLR9 Expression Positively Correlates with the Basal Expression of CD69 and CD38 in the U-CLL Subgroup

The U-CLL subgroup have shown to express the highest basal levels of CD69, CD49d and CD38 and also the highest basal and ODN 2006-stimulated expression of TLR9. Surprisingly, despite their migratory phenotype, U-CLL samples have shown the lowest levels of basal and ODN 2006-induced migration. The observation of lower basal migration in U-CLL is in keeping with previous studies[154] and it is possible that these cells are primed to migrate but are functionally unable to do so; it may be that these cells are already highly basally activated and in the presence of ODN 2006, migration cannot be induced any further. In the U-CLL subgroup, TLR9 has shown an inverse relationship with ODN 2006-stimulated CLL cell migration and if high basal activation were driving these reduced responses, then TLR9 expression may be expected to correlate with the basal levels of activation markers.

In this subgroup, basal TLR9 expression showed a strong positive correlation with the basal expression of CD69 ($P<0.001$, $R^2=0.61$, $n=16$) and CD38 ($P=0.034$, $R^2=0.28$, $n=16$) but surprisingly not CD49d ($P=0.766$, $R^2=0.01$, $n=16$) (Figure 4.10a-c). As the strongest basal TLR9 expression correlations were with CD69, its expression was then correlated to the fold difference in CD69 following ODN 2006 stimulation. As expected, in the U-CLL subgroup, TLR9 expression ***negatively*** correlated with the fold change in CD69 following stimulation with ODN 2006 ($P=0.007$, $R^2=0.44$, $n=15$) (Figure 4.10d). This data shows that U-CLL samples expressing higher levels of TLR9 and CD69, are the least responsive to ODN 2006 stimulation and support the hypothesis that these cells cannot be further activated in the presence of additional stimuli. The lack of correlation with CD49d was interesting considering that CD49d is

important for CLL cell migration[42] and indicates that CD49d expression is likely not the cause of the functional defect.

In contrast, the M-CLL subgroup have the lowest basal expression of TLR9, CD69, CD49d and CD38 but the highest basal and ODN 2006 induced migration. The trends described above for the U-CLL subgroup were therefore not mirrored in M-CLL samples. In the M-CLL subgroup, there was no correlation between the basal expression of TLR9 and the basal expression of CD69 ($P=0.596$, $R^2=0.02$, $n=16$), CD49d ($P=0.78$, $R^2=0.01$, $n=16$) or CD38 ($P=0.313$, $R^2=0.07$, $n=16$) (Figure 4.11a-c). There was also no correlation between the basal expression of TLR9 and the ODN 2006-stimulated fold change in CD69 ($P=0.313$, $R^2=0.07$). (Figure 4.11d). These results indicate that M-CLL cells are signalling differently to U-CLL both in the resting state and following activation through TLR9.

It is recognised that this interpretation of these results is very hypothetical and that there are many other possible explanations for the findings described. However, taken together, they identify a population of U-CLL samples that are highly activated in the absence of ODN 2006 that potentially cannot be activated any further; these high TLR9-expressing samples are less responsive to activation and migration following TLR9 activation. It is possible therefore that the reduction in CLL cell migration seen in some of the TLR9/CD69 high expressing U-CLL patients may indicate overactivation i.e., CLL cell exhaustion, akin to the well characterised BCR-induced anergic state of M-CLL cells.

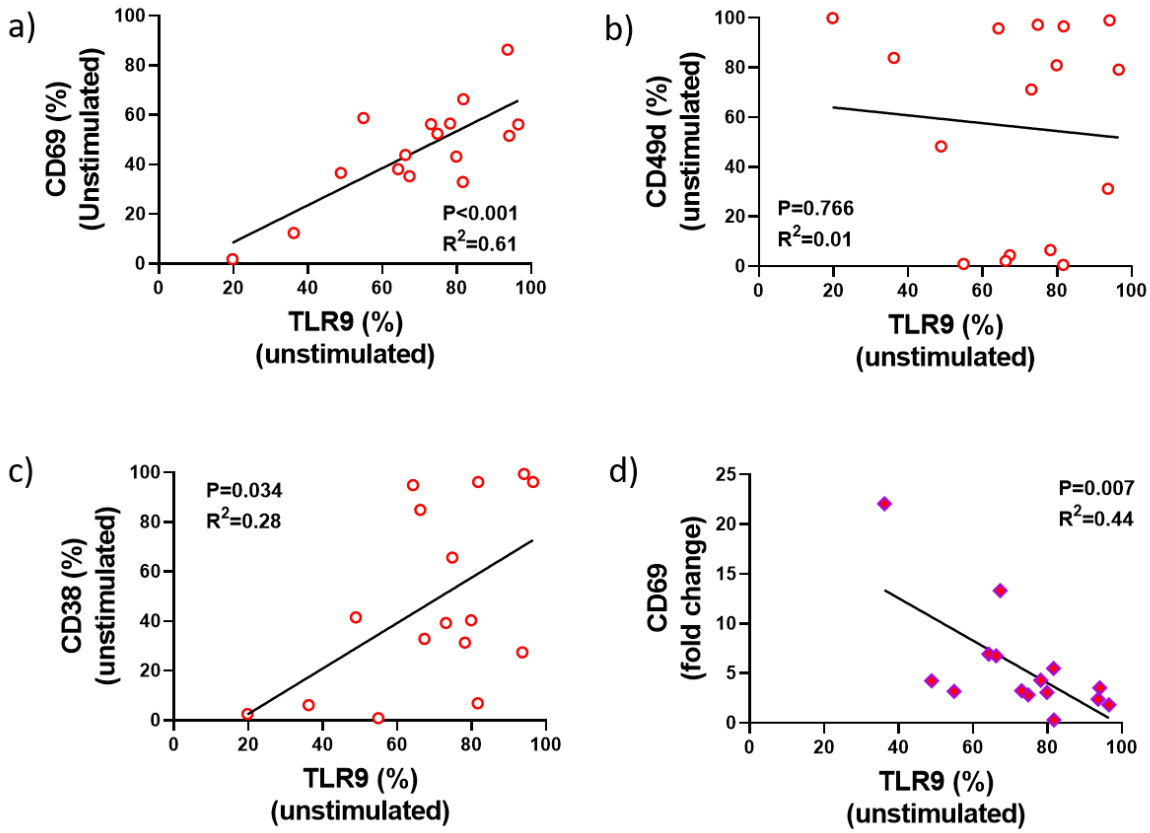

Figure 4.10: TLR9 Expression Correlates with Basal Levels of CD69 and CD38 but Not CD49d in U-CLL Patient Samples. Unstimulated primary PBMCs from 16 U-CLL patients were collected and stained for flow cytometry using a CytoFLEX LX flow cytometer and analysed using CytExpert software. Live cells were gated as CD5+/CD19+/CD3-/FVD- prior to marker analysis. a) Basal TLR9 percentage positivity shows strong positive correlation with basal CD69 percentage positivity (P<0.001, R^2=0.61). b) Basal TLR9 percentage positivity shows no correlation with basal CD49d percentage positivity (P=0.766, R^2=0.01). c) Basal TLR9 percentage positivity shows positive correlation with basal CD38 percentage positivity (P=0.034, R^2=0.28) d) Basal TLR9 percentage positivity shows strong negative correlation with the ODN 2006-stimulated fold change in CD69 expression (P=0.007, R^2=0.44, n=15). U-CLL patients expressing higher levels of TLR9 show greater basal activation relative to U-CLL patients with lower TLR9 expression. Statistical analysis was performed using GraphPad Prism 8.0 and correlation was determined using the Spearman's rank correlation coefficient.

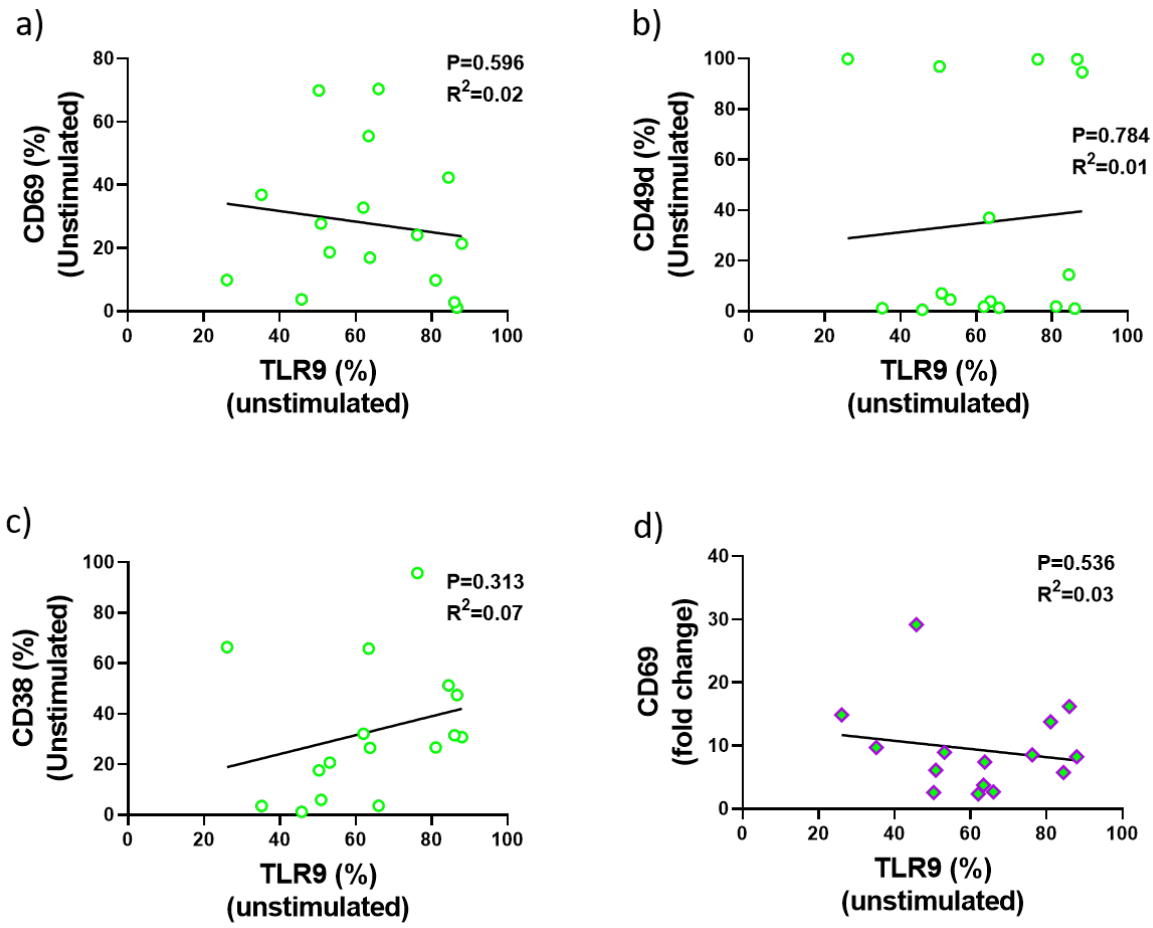

Figure 4.11: TLR9 Expression Does Not Correlate with Basal Levels of CD69, CD49d or CD38 in M-CLL Patient Samples. Unstimulated primary PBMCs from 16 M-CLL patients were collected and stained for flow cytometry using a CytoFLEX LX flow cytometer and analysed using CytExpert software. Live cells were gated as CD5+/CD19+/CD3-/FVD- prior to marker analysis. a-c) There was no correlation between the basal TLR9 percentage positivity and the basal percentage positivity of CD69 (P=0.596, R^2=0.02), CD49d (P=0.784, R^2=0.01) or CD38 (P=0.313, R^2=0.07). d) there was no correlation between basal TLR9 (percentage positivity) and the ODN 2006-stimulated fold change in CD69 expression (P=0.536, R^2=0.03, n=15). Statistical analysis was performed using GraphPad Prism 8.0 and correlation was determined using the Spearman's rank correlation coefficient.

4.5.3: Basal Activation Influences the Migratory Response of U-CLL Cells to Stimulation with ODN 2006

The basal expression of activation and adhesion/migration markers have been shown to be higher in U-CLL vs M-CLL samples and in U-CLL this has been associated with TLR9 expression. A plausible hypothesis for the observed bifurcated migratory response to ODN 2006 is therefore that the U-CLL subgroup are less responsive to TLR9 stimulation as they are already operating at maximum activation. This would be in keeping with a study by Eagle et al.,[154] which identified clear defects in the migratory capabilities of U-CLL cells relative to M-CLL cells. As previously shown in Figure 4.2, the U-CLL subgroup demonstrate significantly lower basal and ODN 2006-stimulated levels of CLL cell migration relative to the M-CLL subgroup.

The **range** of basal migration was however greater in the U-CLL subgroup (i.e., 19.7% vs 14.3% in the M-CLL subgroup) and when comparing the responses of the U-CLL subgroup-alone, the migratory response was found to negatively correlate with basal migration ($P=0.008$, $R^2=0.36$, $n=18$) (Figure 4.12a). These findings support the hypothesis that U-CLL cells with higher basal migration, migrate less in response to ODN 2006 and showed that U-CLL samples with low basal migration were ODN 2006 'Responders' and U-CLL samples with high basal migration were ODN 2006 'Non/Reverse Responders'. Interestingly, in the M-CLL subgroup a similar trend was seen (although it did not reach statistical significance), and the migratory response to ODN 2006 appears to be dependent on low levels of basal migration ($P=0.075$, $R^2=0.24$, $n=14$) (Figure 4.12b). Unlike in the U-CLL subgroup however, the migratory responses of M-CLL patients with the highest levels of basal migration, did not fall below 1.2-fold. The only M-CLL patient sample displaying a migratory response <1.2-

fold was the earlier identified single M-CLL Non-Responder, with a basal migration value of 5.0% and a migratory response of 1.0-fold. Together, this data supports the hypothesis that TLR9 induced migration could be an alternative signalling pathway utilised by CLL cells that are not already being stimulated to their maximal capacity by other signalling pathways such as the BCR.

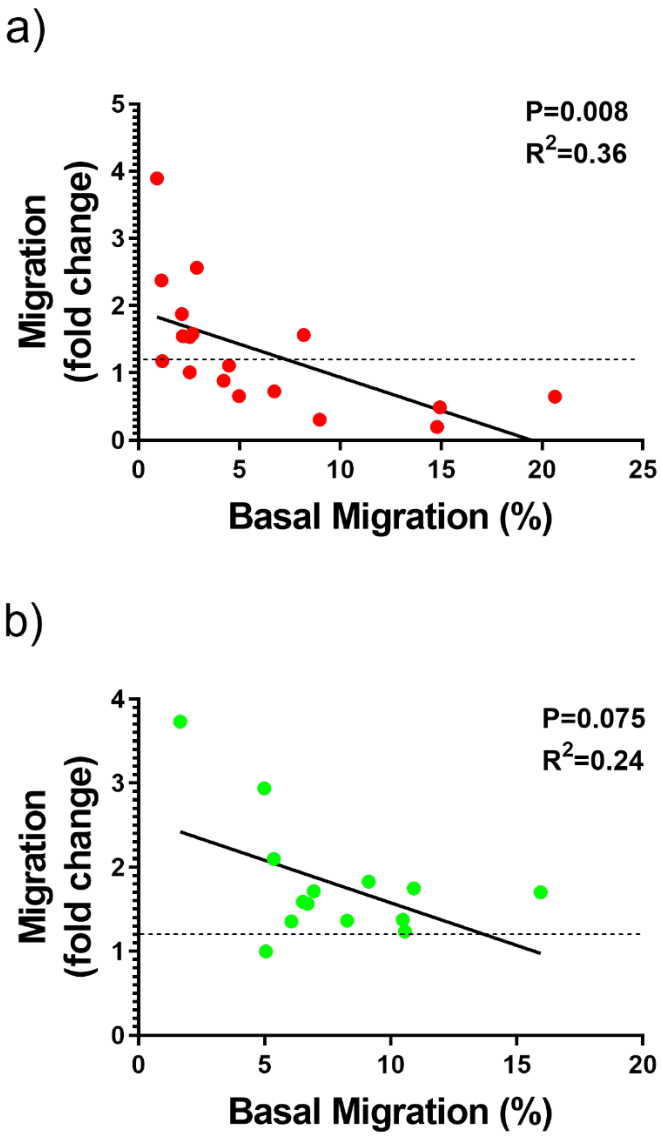

Figure 4.12: Basal CLL Cell Migration Negatively Correlates with the Migratory Response to ODN 2006 in the U-CLL Subgroup and Shows a Similar Trend in the M-CLL Subgroup. Primary patient PMBCs were cultured overnight ± 1 μM ODN 2006 (TLR9 agonist) before being transferred into the apical chambers of a 24-well, 5μM pore polycarbonate, transwell migration plate; transwell migration assays were performed as previously described. a) U-CLL: basal CLL cell migration shows a strong negative correlation with the migratory response to ODN 2006 (P=0.008, R^2=0.36, n=18). b) M-CLL: there is trend in correlation between basal CLL cell migration and the migratory response to ODN 2006 (P=0.075, R^2=0.24, n=14). Statistical analysis was performed using GraphPad Prism 8.0 and correlation was determined using the Spearman's rank correlation coefficient.

4.6: U-CLL Responder Samples Show a Reduced Migratory Response to 10-Fold Higher Concentrations of ODN 2006

Finally, to test the hypothesis that the Non/Reverse Responder subgroup are in a state of CLL cell exhaustion/overactivation, and that their poor responses are not due to insufficient stimulation, the ODN 2006 dose response curve presented in Chapter 3 was revisited and extended to include 10μM ODN 2006 (i.e., a concentration 10x greater than the optimised 1μM ODN 2006). In the extended dose response experiments, the U-CLL subgroup were grouped into Responders and Non/Reverse Responders and their migratory responses to each dose were assessed. Figure 4.13 and Table 4.4 show the migratory response of 3x U-CLL Responder and 3x U-CLL Non/Reverse Responder patients to stimulation with 0.1μM, 0.5μM, 1.0μM, 5.0μM and 10μM ODN 2006. In this cohort a clear dose dependent migratory response was observed in the U-CLL Responder subgroup. In conjunction with previous experiments, a concentration of 1μM ODN 2006 induced the greatest fold-change in CLL cell migration. At the higher doses of 5.0μM and 10μM ODN 2006, the migratory response was reduced relative to 1μM ODN 2006 indicating that these concentrations are too high. In comparison, the U-CLL Non/Reverse Responder subgroup remained consistent and CLL cell migration was not induced at any of the tested concentrations. This demonstrates that 1μM ODN 2006 is the optimal concentration and U-CLL Non/Reverse Responders maintain these responses regardless of ODN 2006 concentration. Together, this data suggests that within the U-CLL subgroup there is a TLR9 Non/Reverse Responder subgroup that do not

respond to TLR9 stimulation (regardless of concentration) and a TLR9 Responder subgroup that have similar responses to the M-CLL subgroup.

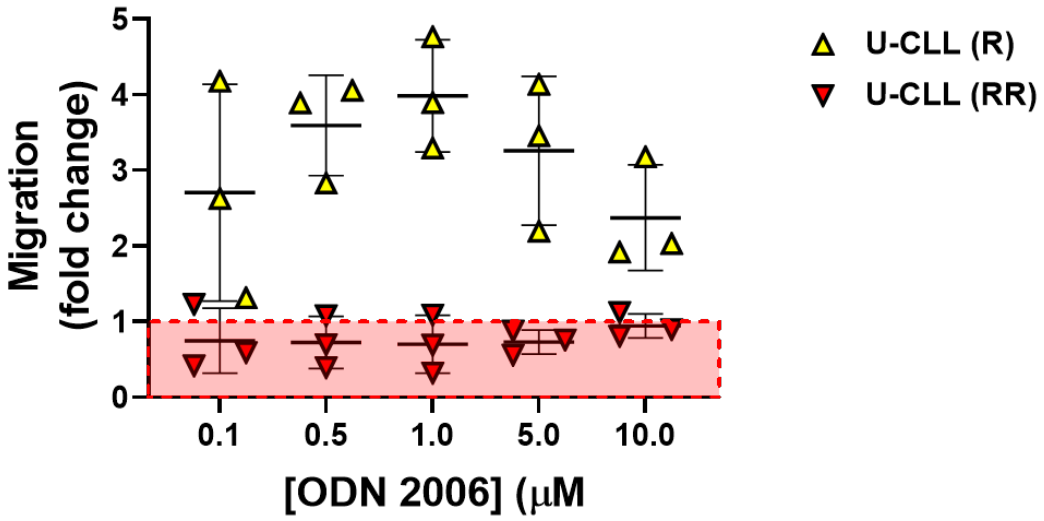

Figure 4.13: U-CLL Responder Samples Show a Reduced Migratory Response in the Presence of High Concentrations of ODN 2006. Primary patient PMBCs from 3 U-CLL Responders (yellow) and 3 U-CLL Non/Reverse Responders (red) were cultured overnight with 0.0μM, 0.1μM, 0.5μM, 1.0μM, 5.0μM or 10μM ODN 2006 before being transferred into the apical chambers of a 24-well, 5μM pore polycarbonate, transwell migration plate; transwell migration assays were performed as previously described. The U-CLL Responder samples showed a dose dependent migratory response to stimulation with ODN 2006 which reached a maximum at 1.0μM; migration increased by: 2.71 (±1.43); 3.59 (±0.66); 3.99 (+0.74); 3.26 (±0.98) and 2.38 (±0.70)-fold, respectively. The U-CLL Non/Reverse Responder subgroup did not show a dose dependent migratory response to stimulation with ODN 2006 and CLL cell migration reduced by 0.75 (±0.43); 0.73 (±0.34); 0.70 (±0.38); 0.73 (±0.16) and 0.94 (±0.16)-fold, respectively.

Table 4.4: The Migratory Response of U-CLL Responder and Non/Reverse Responder Samples to Stimulation with 0.1μM, 0.5μM, 1.0μM, 5.0μM and 10μM ODN 2006

	CLL Cell Migration (Fold Change ±SD)	
[ODN 2006] (μM)	**U-CLL Responders**	**U-CLL Non/Reverse Responders**
0.1	2.71 (±1.43)	0.75 (±0.43)
0.5	3.59 (±0.66)	0.73 (±0.34)
1.0	3.99 (+0.74)	0.70 (±0.38
5.0	3.26 (±0.98)	0.73 (±0.16)
10.0	2.38 (±0.70)	0.94 (±0.16)

U-CLL Responders (n=3); U-CLL Non/Reverse Responders (n=3).

4.7: Discussion

The phenotypic and migratory data presented in Chapter 3 were collected blindly of the IGHV-mutational status and presented as a single cohort. In order to identify whether the bifurcated migratory response to stimulation with ODN 2006 was dependent upon the IGHV-mutational status, DNA was retrospectively extracted from archived PBMC aliquots and sent for sequencing at The Royal Marsden Hospital. The data from Chapter 3 were then re-analysed as two distinct subgroups: M-CLL and U-CLL.

ODN 2006 was found to stimulate a significant increase in CLL cell migration in the M-CLL subgroup-only; there was no significant difference in the CLL cell migration of the U-CLL subgroup. This finding was rather surprising and seemed to conflict with previous findings from other groups regarding the sensitivity of M-CLL and U-CLL to TLR9 activation. In these studies, U-CLL patients have been reported to be highly responsive to CpG ODN, resulting in an intense activation of ERK, AKT and JNK followed by cell cycle initiation and CLL cell proliferation[138,139]. In contrast, M-CLL patients have been reported to be far less responsive to CpG ODN, inducing only a weak activation of ERK, AKT and JNK and consequently failing to exit the G1 phase of the cell cycle; M-CLL cells do not proliferate in response to CpG ODN and are conversely induced to undergo apoptosis[138,151]. When considering the migratory responses of individual patients however, a further bifurcation within the U-CLL subgroup was evident. U-CLL samples showed a heterogeneous migratory response to ODN 2006 with 10/18 being categorised as Non/Reverse Responders and 8/18 being categorised as Responders. In comparison, the M-CLL subgroup samples

demonstrated a uniform positive migratory response to ODN 2006, with 13/14 being categorised as Responders and the remaining M-CLL sample showing a fold change in migration of 1.0. None of the M-CLL samples showed a reduction in CLL cell migration following stimulation with ODN 2006.

The expression of TLR9 was higher in the U-CLL subgroup relative to the M-CLL subgroup appearing to suggest that the bifurcated migratory response between the two groups was inversely TLR9-dependent. Furthermore, when comparing within the individual subgroups, differences between the two subgroups were apparent. In ODN 2006-stimulated M-CLL cells, TLR9 expression showed a strong ***positive*** correlation with both the percentage of CLL cell migration and the fold change in migration in response to ODN 2006. In ODN 2006-stimulated U-CLL cells however, TLR9 expression showed a ***negative*** correlation with the percentage of CLL cell migration but not the fold change in migration in response to ODN 2006. This suggested there to be additional factors influencing the responses of U-CLL samples to ODN 2006.

It is possible that non-responsive U-CLL samples are harbouring activating mutations in components of the TLR signalling pathway; mutations within the adaptor protein MyD88 or the downstream IRAK 1/2/4 kinases for example may result in constitutive TLR-signalling in these samples, rendering them unable to respond to further TLR9 stimulation. A recurrent activating mutation (L265P) within the TIR domain of MyD88 for example is known to result in increased NF-κB phosphorylation and enhanced NF-κB-DNA binding[86]. Given that MyD88 mutations occur almost exclusively in M-CLL patients however[3,86-88], this scenario seems unlikely and there appears to be a selective pressure upon TLR-signalling in M-CLL-only; perhaps the identified pro-

migratory effect of TLR9 activation could account for this pressure. Furthermore, the re-analysed phenotypic data from Chapter 3 show that all U-CLL cells **DO** phenotypically respond to ODN 2006 but that this is not reflected in their migratory response. U-CLL and M-CLL samples showed a comparative upregulation of CD69 and CD49d suggesting an uncoupling of the phenotypic and migratory responses to ODN 2006 (there was no significant change in CD38 or CD62L expression in either subgroup). U-CLL cells are known to be less migratory that M-CLL cells and proteomic analysis has revealed U-CLL cells to underexpress components of migratory pathways relative to M-CLL cells. A comparative study by Eagle et al.,[154] identified clear defects in the migratory capabilities of U-CLL cells relative to M-CLL cells, involving a lesser expression of proteins involved in lymphocyte chemotaxis. Whilst this may appear counterintuitive, given that U-CLL is associated with lymphadenopathy and a progressive disease course, the study revealed U-CLL cells to express comparatively higher levels of proteins involved in lymph node retention. This means that whilst U-CLL cells may migrate less readily towards the lymph nodes, they will remain protected within the lymph node microenvironment longer. The data presented in this chapter, showed basal CLL cell migration to be significantly lower in the U-CLL relative to the M-CLL subgroup and additionally that the basal migration of U-CLL samples negatively correlated with the migratory response to ODN 2006. In the M-CLL subgroup there was a similar trend towards an inverse relationship between basal migration and migratory response to ODN 2006 but even samples with the highest levels of basal migration showed an increase in CLL cell migration following TLR9 stimulation. This suggests that M-CLL samples have a higher threshold for TLR9 activation and emphasises that the signalling machinery in M-CLL and U-CLL samples

is distinct. It could be that the non-responsive U-CLL cells are not equipped to respond to further pro-migratory signals, and this could account for there being heterogeneous changes in U-CLL migration following stimulation with ODN 2006. It is also possible that the Reverse Responder U-CLL cells are exhibiting overactivation/exhaustion, akin to the well characterised BCR-induced anergic state of M-CLL cells[80].

Anergy occurs as a result of sustained antigen ligation and is associated with the onset of negative regulatory pathways[80]. In M-CLL patients, the BCR has undergone somatic hypermutation and has a high affinity for its cognate antigen. BCR stimulation in M-CLL cells is chronic and prolonged and results in a state of CLL cell exhaustion. In U-CLL patients however, the BCR have **not** undergone somatic hypermutation and therefore remain polyreactive to a range of stimuli (with lower affinity). Consequently, the resulting signals are more transient and U-CLL cells are highly responsive to BCR activation[85]. As earlier described, the opposite appears true of TLR9 activation with CpG activation inducing a seemingly anergic signal in U-CLL cells and a responsive signal in M-CLL cells. Perhaps each subgroup is differentially tolerant to BCR/TLR9 activation.

The U-CLL subgroup showed a higher basal expression of CD69, CD49d and CD38 (although statistical significance was reached for CD69 and CD49d only) and TLR9 strongly correlated with the basal expression of CD69 and CD38 (but not CD49d) in U-CLL samples. These results suggested high TLR9-expressing U-CLL samples to be activated and primed for migration in the absence of ODN 2006 and it was hypothesised that, despite this, they are functionally unable to migrate any further.

Perhaps these samples have a lower migratory threshold and had already reached their maximum potential. In support of this hypothesis, U-CLL Responder samples showed reduced migratory responses following exposure to higher concentrations of ODN 2006. An extended dose response curve showed a dose dependent migratory response to ODN 2006 up to the optimised concentration of 1μM ODN 2006; at concentrations 5-fold and 10-fold higher, this response was reduced. This supports the idea that reduced responses to ODN 2006 could be due to overactivation/exhaustion.

This data identifies TLR9 as a promising target for the inhibition of CLL cell tissue-homing in the M-CLL Responder and U-CLL Responder subgroups. It may also be a promising target in U-CLL Non/Reverse Responders in the presence of BCR-inhibitors if basal activation is reduced. Currently used BCR-targeted agents (such as ibrutinib and idelalisib) have been shown to reduce CLL cell migration and to redistribute tissue-resident CLL cells back into the peripheral blood[105], however, not all cells are 'ejected' from these protective microenvironments and so these agents are non-curative[101]. It is possible that previously non-responsive U-CLL Non/Reverse Responders could have their basal activation reduced by BCR-targeted agents and this could sensitise them to signalling through TLR9. It would therefore be interesting to establish whether the inhibition of the TLR9 signalling pathway can synergise with currently available BCR-targeted therapeutics to further reduce CLL cell tissue-homing and potentially promote a complete clearance of the lymphoid tissues and bone marrow in all subgroups. Chapter 5 aims to investigate the relationship between TLR9 signalling and the efficacy of ibrutinib (in the context of CLL cell migration) and hypothesises that dual targeting of the TLR9 and BCR signalling

pathway will result in a greater reduction in CLL cell migration as compared with each single pathway alone.

5.0: Investigating Dual Targeting of BTK and TLR9 Signalling

5.1: Introduction

Chapters 3 and 4 identified a bifurcated migratory response to CpG ODN 2006. In the 'TLR9 Responder' subgroup, ODN 2006 stimulated a TLR9-dependent ***increase*** in CXCL12-driven CLL cell migration whilst in the 'TLR9-Non/Reverse-Responder' subgroup, ODN 2006 either induced ***no change*** or a TLR9-dependent ***decrease*** in CXCL12-driven CLL cell migration. The Non/Reverse-Responder subgroup was almost exclusively comprised of U-CLL patients and was associated with high basal activation and CLL cell migration. Cells from these patients appeared unresponsive to ODN 2006 and so migration could not be increased any further. U-CLL is highly responsive to BCR-activation[83,84] indicating that the high levels of basal migration in the Non/Reverse-Responder subgroup may be BCR-dependent. BCR activation stimulates the upregulation of a number of adhesion molecules an induces chemotaxis towards CXCL12 and CXCL13 and CLL cells are known to have heterogenous levels of constitutive BCR signalling[155,156]. Given that the levels of circulating unmethylated cell-free CpG-DNA are significantly higher in CLL patients relative to healthy controls[132], the potential for TLR9 to play an important role in tissue-homing in the TLR9-Responder subgroup is a credible hypothesis.

Currently available BCR-targeted therapeutics inhibit downstream kinases of the BCR (i.e., ibrutinib and idelalisib inhibit BTK and PI3K, respectively). Of the two agents, ibrutinib has proven to be the least toxic and is widely utilised as a front-line therapeutic for poor-prognosis CLL, whilst idelalisib is approved as a second-line therapeutic only[102,104]. Although both of these drugs have proven extremely

successful at inhibiting CLL cell migration and re-distributing CLL cells from the lymphoid tissue microenvironments into the peripheral blood, they cannot be considered as curative agents and the vast majority of patients achieve only a partial response to treatment[101]. Patients remain on treatment for as long as can be tolerated and over time, many patients develop acquired resistance and disease progression. Resistance to ibrutinib for example, has been partially attributed to genetic mutations within the ibrutinib-binding site of BTK or the downstream, kinase PLCγ2[109]. In a recent real-world study investigating the genetic landscape of a cohort of 30 ibrutinib-treated patients, 57% and 13% of patients had developed BTK and PLCγ2-mutations respectively following 3 years on therapy; these mutations were found to be indicative of a future relapse[111]. Curiously however, BTK and PLCγ2-mutations are typically found at extremely low frequencies (i.e., in small subclones of the disease), bringing into question the ability of such low frequency events to drive the observed resistance alone[112]. Furthermore, 15-30% of ibrutinib-resistant cases are not associated with known mutations, suggesting there to be other unidentified mechanisms at play[110,111]. One such mechanism may be the sensitivity to alternate external microenvironmental stimuli. In a recent *in vitro* study, Jayappa et al.,[97] reported that an 'agonist mix' of environmental stimuli conferred resistance to a combination of ibrutinib and Venetoclax by activating NF-κB independently of the BCR.

TLR9 may offer a compensatory mechanism for NF-κB activation via the BCR-independent MyD88/IRAK4 signalling pathway; it is possible that the earlier identified pro-migratory effects of ODN 2006 could antagonise the effects of ibrutinib

by promoting CLL cell migration in the absence of BTK. It is important to consider however that TLR9 does not only signal independently of the BCR and that a complex cross-talk of interaction occur between the two pathways e.g.:

- In healthy B-cells, BCR and TLR9 act together to respond to DNA-containing antigens; following antigen-binding and BCR internalisation, the BCR can translocate into autophagosome-like compartments, which can then fuse with TLR9-containing endosomes and result in synergistic BCR/TLR9 signalling.[156b]
- TLR9 can activate an alternate (B-cell specific) signalling pathway via the BCR co-receptor CD19. This mechanism is independent from antigen-binding and activates PI3K, BTK and AKT[157].
- In ZAP-70 positive CLL cells, TLR9 can stimulate the secretion of BCR-activating autoantigens. CpG DNA can therefore induce BCR-signalling via an auto-stimulatory positive feedback loop[158].

In order for TLR9 to promote ibrutinib-resistance, CpG-driven CLL cell migration must operate independently of BTK. Chapter 5 investigated whether BCR-proximal signalling components and/or BTK play a role in ODN 2006-stimulated CLL cell migration and the effects of a dual inhibition of BTK/TLR9. Finally, it will explore potential differences in NF-κB-signalling which could account for the dichotomous migratory response to ODN 2006.

5.2: Investigating the Role of CD19/BTK in ODN 2006-Stimulated Phenotypic and Migratory Changes

Given the evident crosstalk between BCR and TLR9 signalling, it was firstly important to investigate whether the BCR/BTK activation plays a role in the phenotypic/migratory responses of CLL cells to stimulation with ODN 2006. As discussed earlier, TLR9 is both capable of initiating BCR-signalling via an autocrine positive feedback loop and of activating the BCR co-receptor CD19 to initiate a CD19/PI3K/BTK-dependent signalling cascade[157,158]. The former mechanism was reported to be ZAP-70-dependent however unfortunately, the ZAP-70 status of the patients used in this project is unknown. If the migratory response to ODN 2006 is BCR/BTK-***dependent***, a dual targeted BCR/TLR9 combinational approach to therapy would be futile as all TLR9-dependent migration would be eliminated in the presence of ibrutinib. If the migratory response to ODN 2006 is BCR/BTK-***independent***, BCR and TLR9-inhibition will have the potential to synergise.

5.2.1: ODN 2006 Induces Phenotypic Changes in the Expression of BCR-Associated Markers

TLR9 effect of ODN 2006-stimulation upon BCR-signalling was firstly assessed on CLL cells from a large cohort of patients using the BCR associated markers CD5 and CD19. CLL cells are characteristically CD5/CD19 double positive, and both have functional roles in CLL cell maintenance. CD19 is a co-receptor for the BCR complex and acts to enhance BCR-signalling. Following stimulation with the TLR9 agonist ODN 2006, the surface expression of CD19 (MFI [±SD]) was shown to significantly ***increase*** from 2121 (±826.1) to 2554 (±1188) (P=0.007, n=35) (Figure 5.1a). Conversely, CD5 is a negative

regulator of BCR signalling and is acts to dampen the signalling response to BCR action; expression of CD5 is associated with B-cell anergy and a favourable prognosis; patients expressing lower levels of CD5 were found to experience a comparatively shorter time to first treatment than patients expressing higher levels of CD5[159]. Following stimulation with ODN 2006, the surface expression of CD5 MFI [±SD]) was found to significantly ***decrease*** from 70382 (±39607) to 56216 (±34793) ($P<0.001$, $n=35$) (Figure 5.1b). Taken together, these results imply that in addition to initiating TLR9 signalling, ODN 2006 triggers an increased capacity for BCR signalling.

The expression of TLR9 (percentage positivity) was also shown to significantly correlate with the fold change in CD19 expression (MFI) following stimulation with ODN 2006 ($P=0.016$, $R^2=0.14$, $n=32$) (Figure 5.1c). The same was not true of CD5; TLR9 (percentage positivity) was not found to correlate with the fold change in CD5 expression (MFI) following stimulation with ODN ($P=0.636$, $R^2=0.01$, $n=32$) (Figure 5.1d). These results suggest a functional link between TLR9 and CD19 but not CD5.

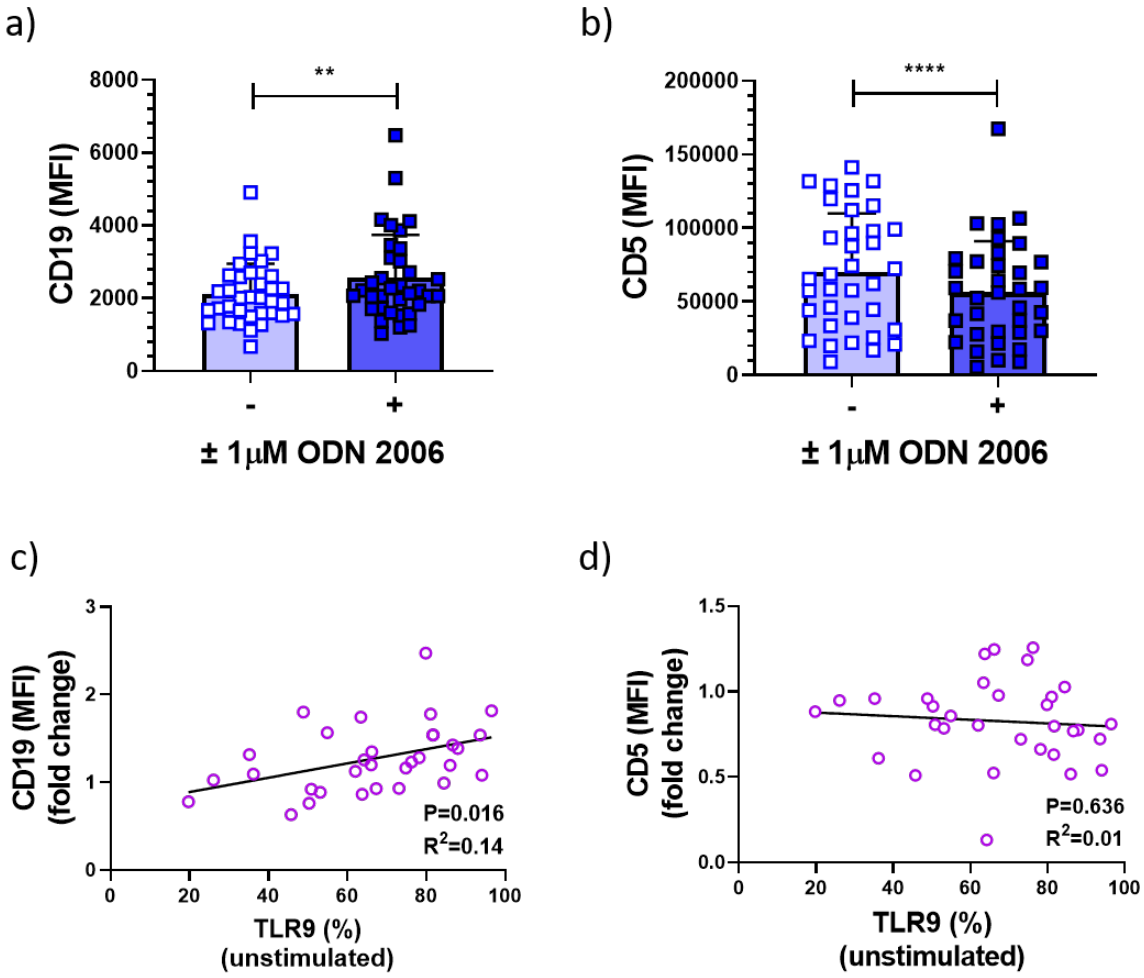

Figure 5.1: ODN 2006 Stimulates an Upregulation of CD19 and Downregulation of CD5, and TLR9 Correlates with the Fold Change in CD19 Expression. Primary PBMCs were cultured ± 1μM ODN 2006 in complete media (+IL-4) and incubated at 37°C/5% CO_2. Cells were collected at 24h post-stimulation and stained for flow cytometry (using the CytoFLEX LX flow cytometer); live CLL cells were identified as CD5+/CD19+/CD3-/FVD- and analysed using CytExpert software. Statistical analyses were performed using GraphPad Prism 8.0 and the Wilcoxon Matched Pairs test was used as the data was not Gaussian (according to the D'Agostino & Pearson omnibus normality test). Correlation was determined using the Spearman's rank correlation coefficient. a) ODN 2006 stimulated a significant increase in CD19 MFI (P=0.007, n=35, Wilcoxon Matched Pairs Test). b) ODN 2006 stimulated a significant decrease in CD5 MFI (P<0.001, n=35, Wilcoxon Matched Pairs Test). c) TLR9 (percentage positivity) showed significant correlation with ODN 2006-stimulated fold change in CD19 expression (MFI) (P=0.016, R^2=0.14, n=32). d) There was no correlation between TLR9 (percentage positivity) and the ODN 2006-stimulated fold change in CD5 expression (MFI) (P=0.636, R^2=0.01, n=32).

5.2.2: ODN 2006 Induces CLL Cell Activation Independently of BTK

Having shown a clear link between TLR9 activation and the potential for BCR signalling, the next step was to determine whether the observed ODN 2006-stimulated CLL cell activation was BCR-independent. In previous chapters, the cell surface protein CD69 was used as a marker of CLL cell activation and ODN 2006 was shown to stimulate a significant upregulation of CD69 in all CLL patients. This effect could be significantly reduced in the presence of the TLR9 antagonist ODN INH-18 and was therefore confirmed to be TLR9 dependent. It is currently unclear, however, if the mechanism of CD69 upregulation is independent from BCR-signalling. Figure 5.2 depicts the positive correlation between CD19 and ODN 2006-stimulated CLL cell activation. In basal (unstimulated) conditions, CD19 expression (MFI) showed no significant correlation with CD69 percentage positivity ($P=0.105$, $R^2=0.08$, $n=35$) or MFI ($P=0.052$, $R^2=0.11$, $n=35$); there was a trend in correlation with CD69 MFI however this did not reach statistical significance. Following stimulation with ODN 2006 however, CD19 showed a strong correlation with both CD69 percentage positivity ($P=0.003$, $R^2=0.23$, $n=35$) and MFI ($P<0.001$, $R^2=0.30$, $n=35$). These results indicate a potential functional link between CD19 and the ODN 2006-stimulated upregulation of CD69.

As previously described, CpG DNA can stimulate a B-cell specific and lesser described BTK-***dependent*** pathway via CD19-PI3K/AKT [157]. In order to determine whether the ODN 2006-stimulated upregulation of CD69 is via BTK, CLL cells were pre-incubated with 1μM ibrutinib for 30 minutes before being stimulated overnight with 1μM ODN 2006. This was to identify whether ODN 2006 could increase the expression of CD69 in the absence of functional BTK. Figure 5.3 shows duplicate experiments from 5

individual CLL patients (n=10). Following an incubation with ODN 2006-alone, the percentage positivity of CD69 increased from 54.80% (±12.02) to 79.64% (±12.11) ($P<0.001$) and this response was not diminished in the presence of ibrutinib ($P=0.232$). In CLL cells stimulated with ODN 2006 + ibrutinib, the percentage positivity of CD69 increased to from 54.80% (±12.02) to 84.69% (±9.90). Furthermore, the same pattern was observed for CD69 MFI which increased by 3.56-fold (±1.20) following stimulation with ODN 2006-alone and 3.08-fold (±1.30) following stimulation with ODN 2006 + ibrutinib. These results show that ODN 2006 can induce CLL cell activation independently of BTK.

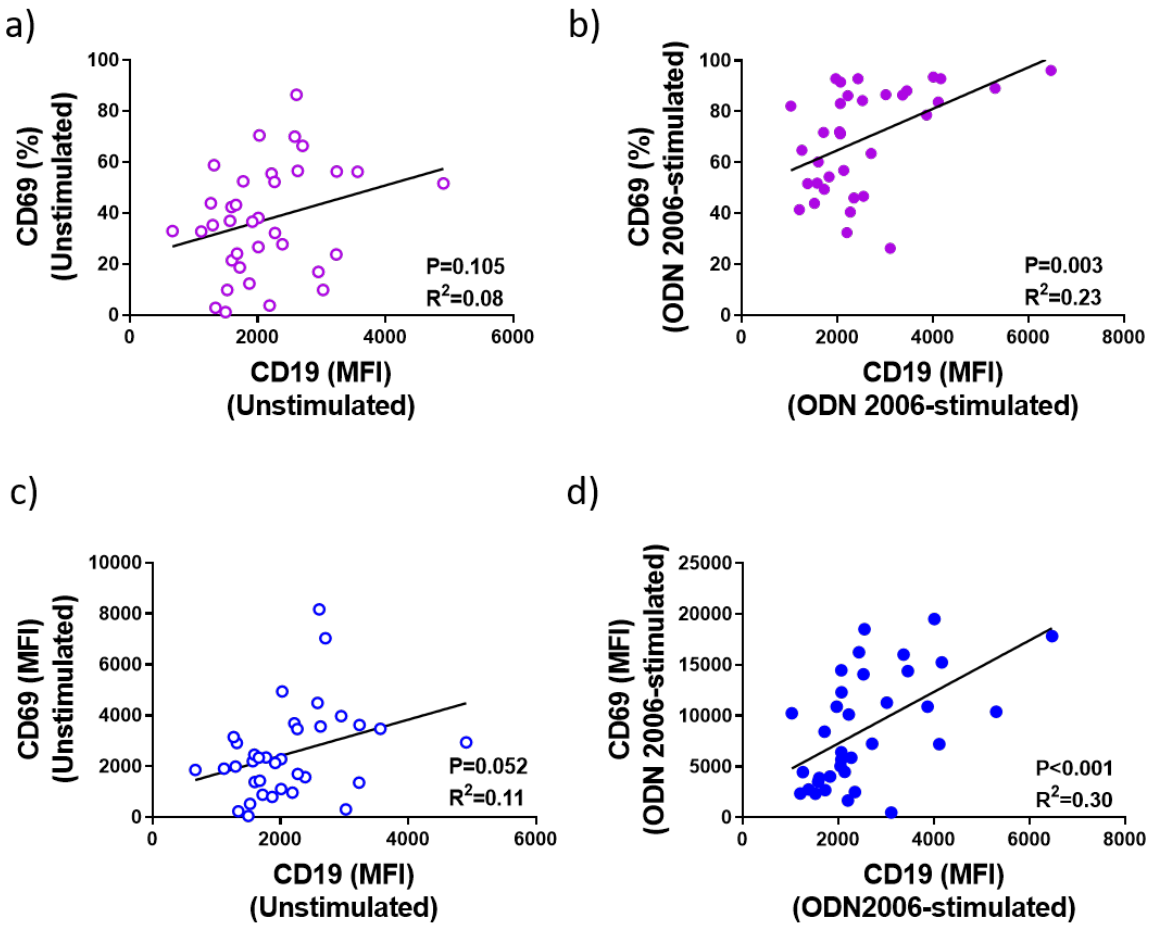

Figure 5.2: CD19 Correlates with CD69 in ODN 2006-Stimulated CLL Cells. Primary PBMCs were cultured ± 1μM ODN 2006 in complete media (+IL-4) and incubated at 37°C/5% CO_2. Cells were collected at 24h post-stimulation and stained for flow cytometry (using the CytoFLEX LX flow cytometer); live CLL cells were identified as CD5+/CD19+/CD3-/FVD- and analysed using CytExpert software. Statistical analyses were performed using GraphPad Prism 8.0 and correlation was determined using the Spearman's rank correlation coefficient. a) There was no correlation between the expression of CD19 (MFI) and CD69 (% positivity) in unstimulated CLL cells (P=0.105, R^2=0.08, n=35). b) There was a significant correlation between the expression of CD19 (MFI) and CD69 (% positivity) in ODN 2006-stimulated CLL cells (P=0.003, R^2=0.23, n=35). c) There was a trend in correlation between the expression of CD19 (MFI) and CD69 (MFI) in unstimulated CLL cells, but statistical significance was not reached (P=0.052, R^2=0.11, n=35). b) There was a significant correlation between the expression of CD19 (MFI) and CD69 (MFI) in ODN 2006-stimulated CLL cells (P<0.001, R^2=0.30, n=35).

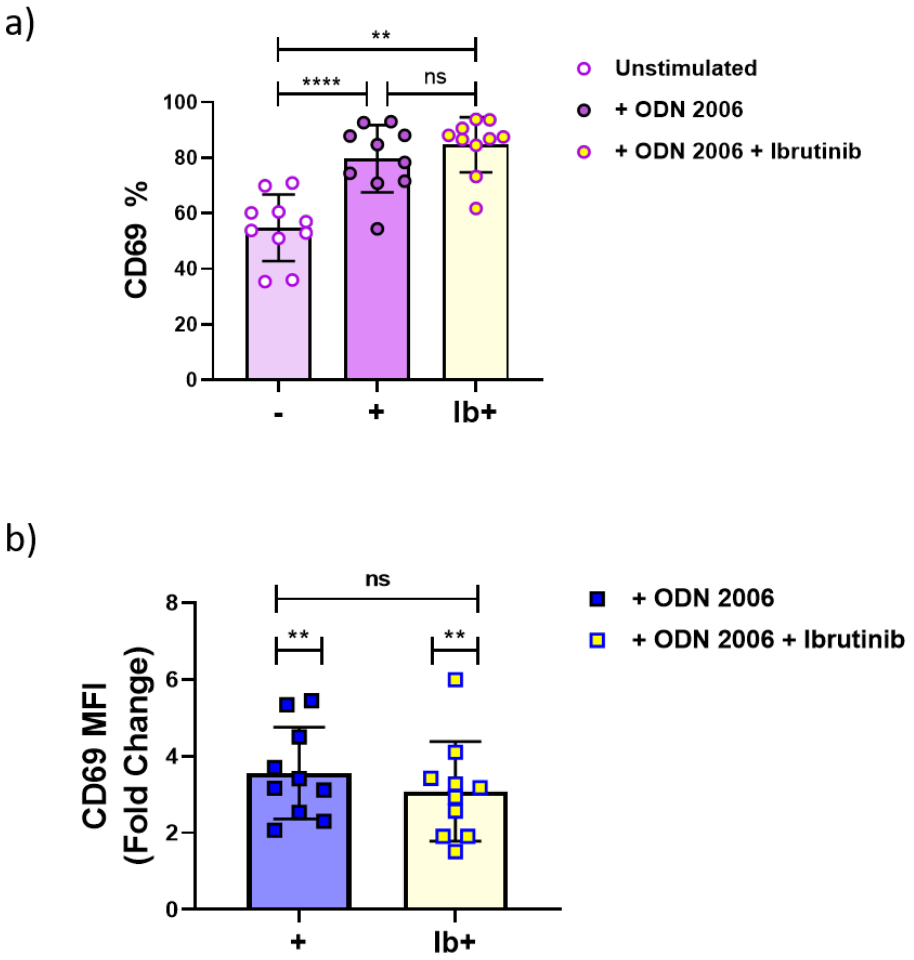

Figure 5.3: ODN 2006 Induces CLL Cell Activation Independently of BTK. Primary PBMCs were pre-incubated ± 1μM ibrutinib for 30 minutes prior to being stimulated with 1μM TLR9 agonist ODN 2006 and cultured overnight in complete media +IL-4 at 37°C/5% CO_2 (n=10 from 5 CLL individual patients). The cells were then collected and stained for phenotypic analysis using the CytoFLEX LX flow cytometer (live CLL cells were gated as CD5+/CD19+/CD3-/FVD-). Phenotypic analysis was performed using CytExpert software and statistical analysis was performed using GraphPad Prism 8.0; the Paired t-test or Wilcoxon Matched Pairs test was used depending on whether the data passed the D'Agostino & Pearson omnibus normality test. a) ODN 2006 stimulated a significant increase in CD69 percentage positivity both alone (P<0.001, Paired t-test) and in the presence of ibrutinib (P=0.002, Wilcoxon Matched Pairs test). There was no significant difference in the response of CD69 percentage positivity to stimulation with ODN 2006 or ODN 2006 + ibrutinib (P=0.232, Wilcoxon Matched Pairs test). b) ODN 2006 stimulated a significant increase in CD69 MFI (fold change, relative to the unstimulated control) both alone (P=0.002, Wilcoxon Matched Pairs test) and in the presence of ibrutinib (P=0.002, Wilcoxon Matched Pairs test). There was no significant difference in the response of CD69 (MFI) to stimulation with ODN 2006 ± ibrutinib (P=0.197, Paired t-test). ODN 2006 can therefore upregulate CD69 independently of BTK.

5.2.3 CD19 Correlates with CD49d and CD38 and is More Highly Expressed in Migrated Relative to Non-Migrated CLL Cells

Having established that ODN 2006-stimulated CLL cell activation is independent from BTK, the relationship between CD19/BTK and CLL cell migration was explored. CD49d and CD38 are components of the 'invadosome' structure, involved in CLL cell tissue-homing and were shown in earlier chapters to be upregulated in response to stimulation with ODN 2006. As found for CD69, the percentage positivity of CD49d showed a significant correlation with CD19 in ODN 2006-stimulated CLL cells ($P=0.008$, $R^2=0.19$, $n=35$) but not unstimulated CLL cells ($P=0.090$, $R^2=0.08$, $n=35$) (Figure 5.4a-b). This suggested a functional link between CD19 and the ODN 2006-stimulated upregulation of CD49d. Although there was no statistically significant correlation between CD19 and CD49d MFI in ODN 2006-stimulated ($P=0.078$, $R^2=0.09$, $n=35$) or unstimulated ($P=0.146$, $R^2=0.06$, $n=35$) CLL cells (Figure 5.4c-d), there was a trend. Similarly, the percentage positivity of CD38 showed a significant correlation with CD19 in ODN 2006-stimulated CLL cells ($P=0.003$, $R^2=0.24$, $n=35$) but not unstimulated CLL cells ($P=0.71$, $R^2=0.10$, $n=35$); although there was a trend, this did not reach statistical significance (Figure 5.5a-b). This again suggested a functional link between CD19 and the ODN 2006-stimulated upregulation of CD38, however CD38 MFI correlated with CD19 in both ODN 2006-stimulated ($P=0.001$, $R^2=0.27$, $n=35$) and unstimulated CLL cells ($P=0.011$, $R^2=0.18$) (Figure 5.5d). It was therefore unclear from these results whether a functional link exists between CD19 and the ODN 2006-stimulated upregulation of the adhesion/migration markers CD49d and CD38.

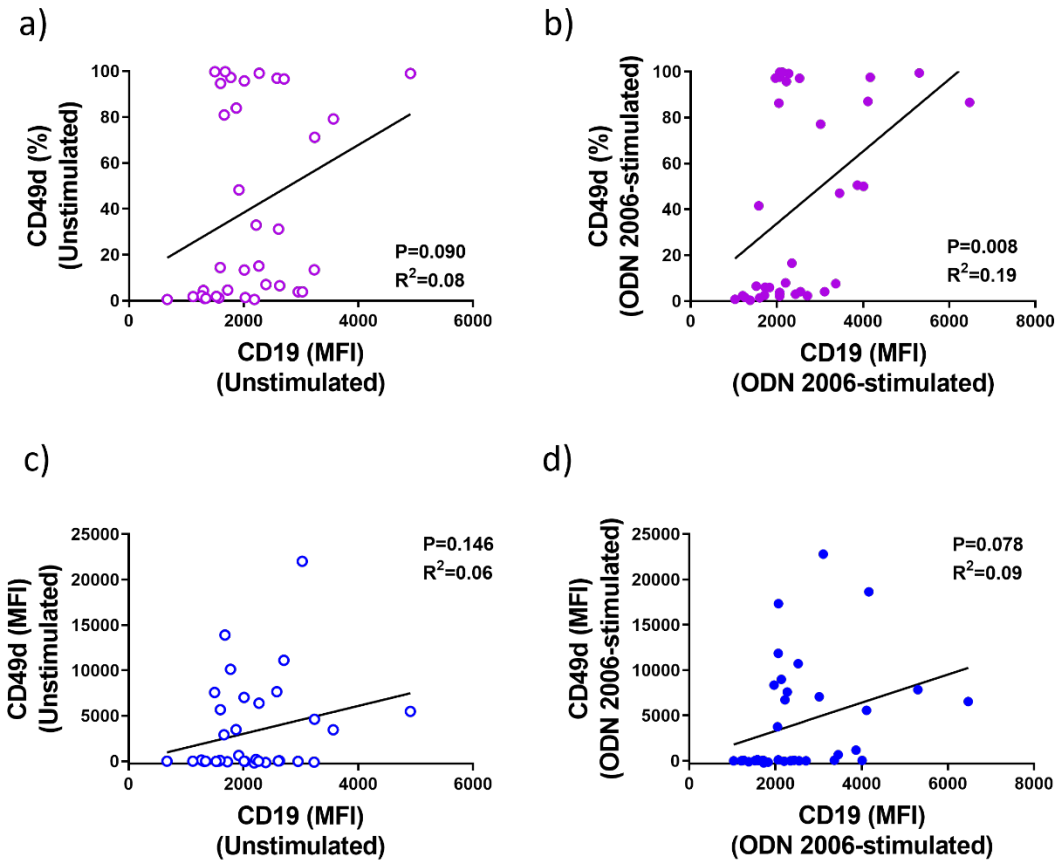

Figure 5.4: CD19 Correlates with CD49d Percentage Positivity in ODN 2006-Stimulated CLL Cells. Primary PBMCs from 35 patients were cultured ± 1μM ODN 2006 in complete media (+IL-4) and incubated overnight at 37°C/5% CO_2. Cells were collected at 24h post-stimulation and stained for flow cytometry (using the CytoFLEX LX flow cytometer); live CLL cells were identified as CD5+/CD19+/CD3-/FVD- and analysed using CytExpert software. Statistical analyses were performed using GraphPad Prism 8.0 and correlation was determined using the Spearman's rank correlation coefficient. a) There was no correlation between CD19 (MFI) and CD49d percentage positivity in unstimulated CLL cells (P=0.090, R^2=0.08). b) CD19 (MFI) significantly correlated with CD49d percentage positivity in ODN 2006-stimulated CLL cells (P=0.008, R^2=0.19). c) There was no statistically significant correlation between CD19 (MFI) and CD49d MFI in unstimulated CLL cells (P=0.146, R^2=0.06). d) There was no statistically significant correlation between CD19 (MFI) and CD49d MFI in ODN 2006-stimulated CLL cells (P=0.078, R^2=0.09).

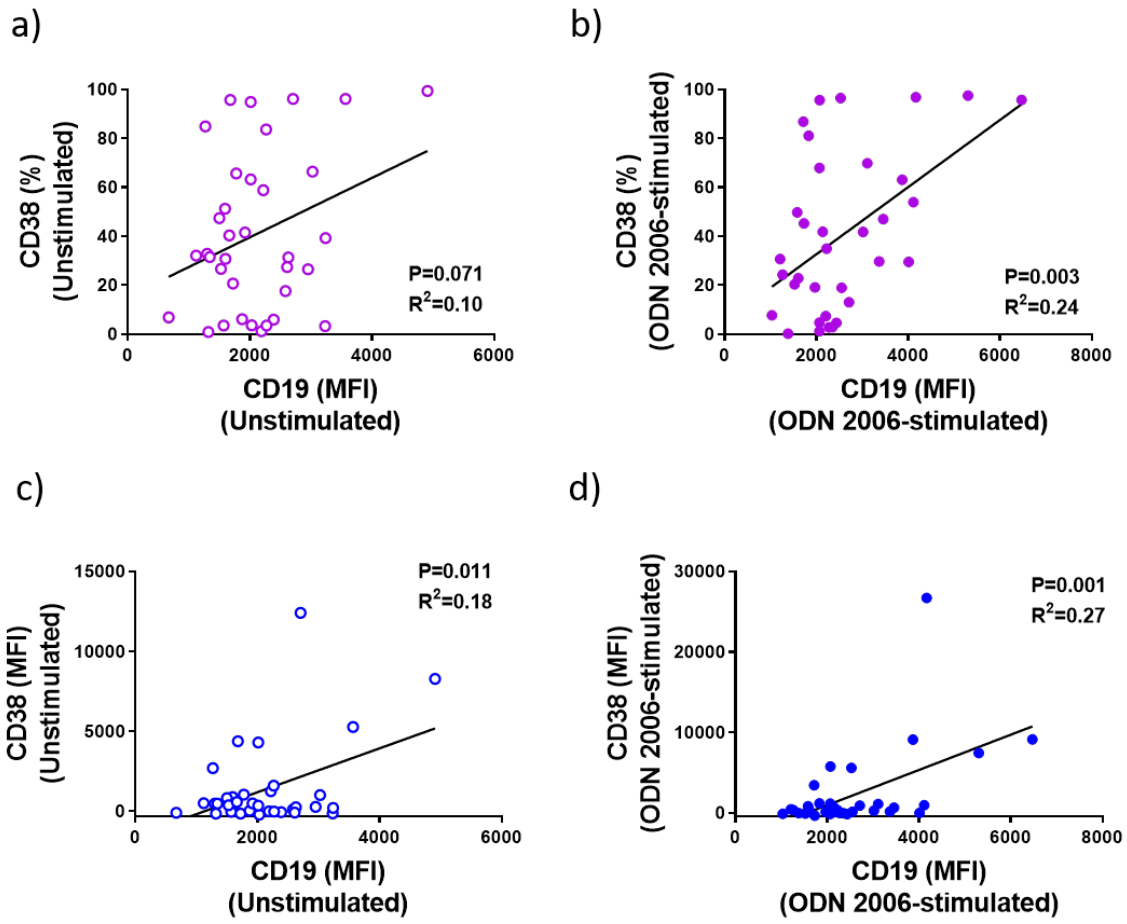

Figure 5.5: CD19 Shows Weak but Statistically Significant Correlation with CD38 in ODN 2006-Stimulated CLL Cells. Primary PBMCs from 35 patients were cultured ± 1μM ODN 2006 in complete media (+IL-4) and incubated overnight at 37°C/5% CO_2. Cells were collected at 24h post-stimulation and stained for flow cytometry (using the CytoFLEX LX flow cytometer); live CLL cells were identified as CD5+/CD19+/CD3-/FVD- and analysed using CytExpert software. Statistical analyses were performed using GraphPad Prism 8.0 and correlation was determined using the Spearman's rank correlation coefficient. a) There was no correlation between CD19 (MFI) and CD38 percentage positivity in unstimulated CLL cells (P=0.071, R^2=0.10). b) CD19 (MFI) significantly correlated with CD38 percentage positivity in ODN 2006-stimulated CLL cells (P=0.003, R^2=0.24). c) CD19 (MFI) significantly correlated with CD38 MFI in unstimulated CLL cells (P=0.011, R^2=0.18). d) CD19 (MFI) significantly correlated with CD38 MFI in ODN 2006-stimulated CLL cells (P=0.001, R^2=0.27).

In order to elucidate whether the ODN 2006-stimulated upregulation of CD49d and CD38 was BTK-dependent, phenotyping experiments were performed in the presence of ibrutinib as described for CD69. In a small cohort of CLL patient samples, ODN 2006-alone stimulated a 1.78 (±0.81)-fold increase in the expression (MFI) of CD49d (P=0.016) (n= 8 from 6 individual patients). This was not significantly altered by the presence of ibrutinib (P=0.750), and ODN 2006 stimulated a 1.96 (±0.87)-fold increase in CD49d (MFI) (P= 0.008); there was no significant difference between the response of CD49d (MFI) to ODN 2006 ± ibrutinib (P=0.75) (Figure 5.6). Based upon the CD49d MFI values alone, these results suggest that ODN 2006 can induce an upregulation in CD49d expression ***independently*** of BTK.

Unfortunately, it was not possible to draw meaningful conclusions from the CD38 data collected from this small patient cohort. All 6 patients expressed very low levels of CD38 and ODN 2006 consequently failed to upregulate CD38 to a statistically significant level in these patients. Further repeats were intended to expand the cohort however due to the restrictions placed upon laboratory access during the COVID-19 lockdown period, priority was given to migration experiments.

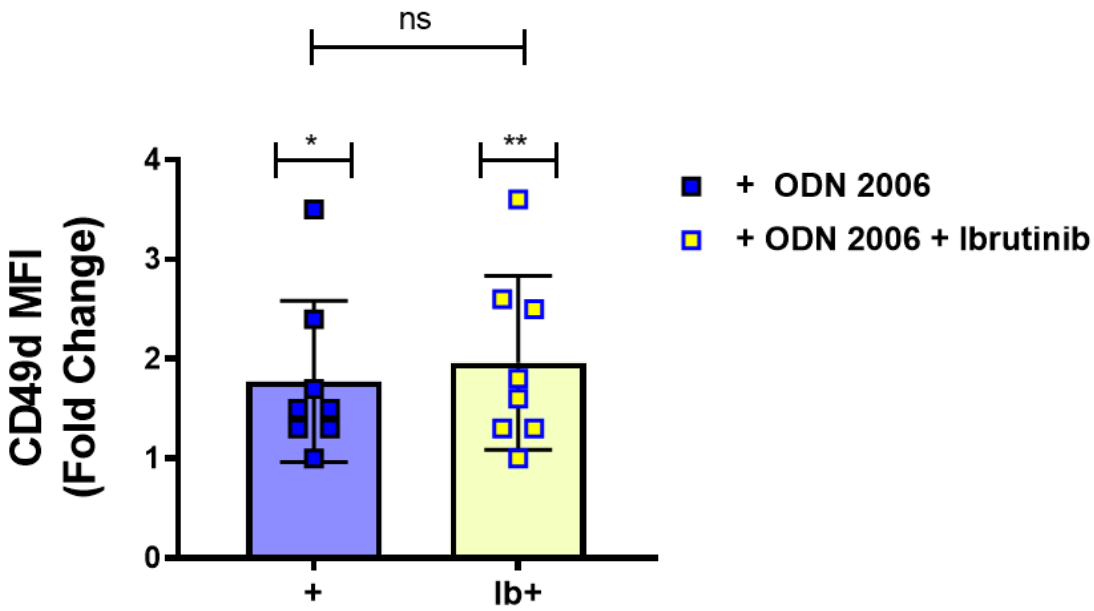

Figure 5.6: ODN 2006 Upregulates the Expression of CD49d Independently of BTK. Primary PBMCs were pre-incubated ± 1μM ibrutinib for 30 minutes prior to being stimulated with 1μM TLR9 agonist ODN 2006 and cultured overnight in complete media +IL-4 at 37°C/5% CO_2 (n=8 from 6 CLL patients). The cells were then collected and stained for phenotypic analysis using the CytoFLEX LX flow cytometer (live CLL cells were gated as CD5+/CD19+/CD3-/FVD-. Phenotypic analysis was performed using CytExpert software and statistical analysis was performed using GraphPad Prism 8.0. The Wilcoxon Matched Pairs test was used as the data was not Gaussian (according to the D'Agostino & Pearson omnibus normality test). ODN 2006 stimulated a significant increase in CD49d (MFI) positivity both alone (P=0.016, Wilcoxon Matched Pairs test) and in the presence of ibrutinib (P=0.008, Wilcoxon Matched Pairs test). There was no significant difference in the response of CD49d (MFI) to stimulation with ODN 2006 ± ibrutinib (P=0.750, Wilcoxon Matched Pairs test). ODN 2006 can therefore upregulate CD49d independently of BTK.

The expression of CD19 was quantified in migrated vs non-migrated CLL cells. In both unstimulated and ODN 2006-stimulated CLL cells, CD19 showed a significantly higher expression in migrated CLL cells relative to non-migrated CLL cells. (Unstimulated: 33367 (±15248) vs 25803 (±12776) and ODN 2006-stimulated: 44479 (±18160) vs 33958 (±17600) (for both conditions, $P<0.001$, $n=14$) (Figure 5.7a). Despite the highest CD19 MFI being in the ODN 2006 stimulated migrated CLL cells, CD19 MFI did ***not*** show any correlation with the migratory response to ODN 2006 (basal: $P=0.289$, $R^2=0.04$; ODN 2006-stimulated $P=0.056$, $R^2=0.13$, $n=29$); there was however a strong trend in ODN 2006-stimulated CLL cells, although this did not reach statistical significance. (Figure 5.7b-c). Together, these results suggest that CD19 may be implicated in TLR9-dependent CLL cell migration.

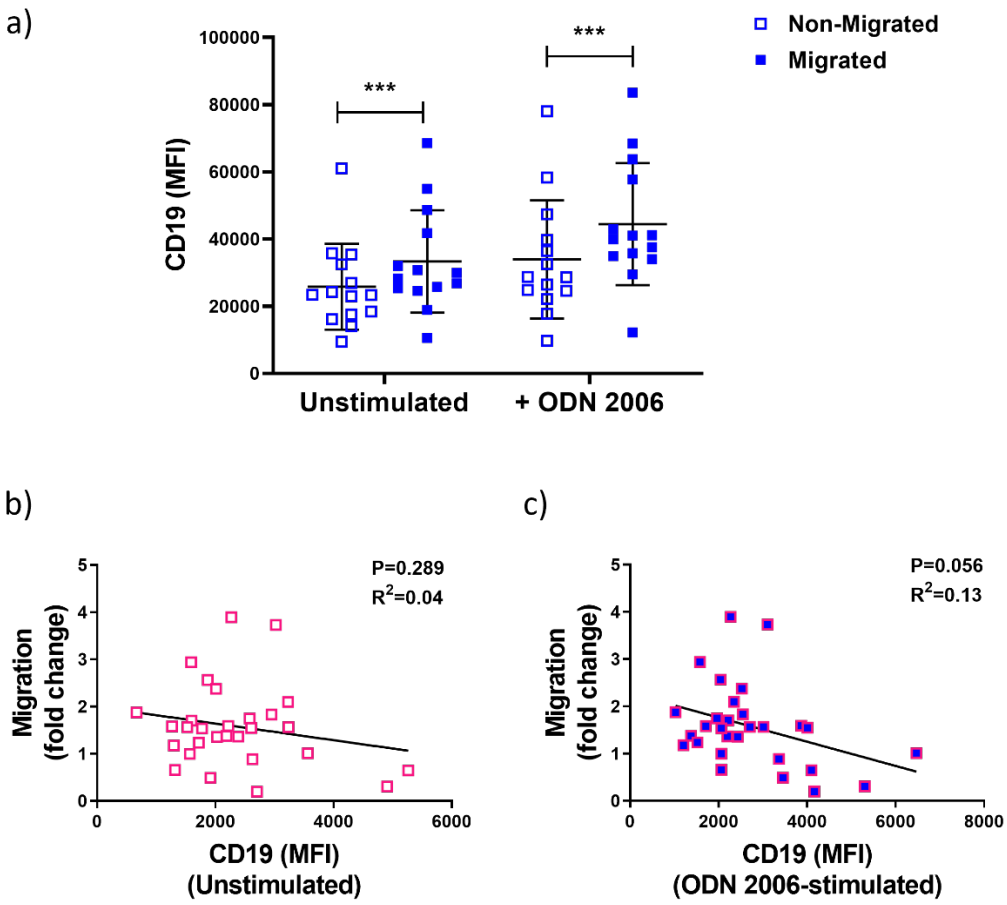

Figure 5.7: CD19 is More Highly Expressed in Migrated vs Non-Migrated CLL Cells but it Does Not Correlate to the Migratory Response to ODN 2006. Primary PBMCs were cultured ± 1μM ODN 2006 in complete media (+IL-4) and incubated overnight at 37°C/5% CO_2. a) PBMCs were transferred into the apical chambers of 24-well, 5μm pore transwell migration plates and incubated for 4h at 37°C/5% CO_2; PBMCs migrated towards a chemotactic gradient (CXCL12). At 4h migration, PBMCs from both the basal (migrated) and apical (non-migrated) chambers were collected for analysis using the Accuri flow cytometer and CLL cells were identified and gated as CD19+/CD3-. CD19 expression was determined using CFlow software and statistical analysis was performed using GraphPad Prism 8.0. The Wilcoxon Matched Pairs test was used as the data was not Gaussian (according to the D'Agostino & Pearson omnibus normality test). Correlation was determined using the Spearman's rank correlation coefficient. a) CD19 expression (MFI) was higher in migrated vs non-migrated CLL cells in both unstimulated ($P<0.001$, n=14) and ODN 2006-stimulated ($P<0.001$, n=14) conditions (both Wilcoxon Matched Pairs test). b-c) Transwell migration assays were performed as above, and analysis was performed using the CytoFLEX LX flow cytometer and CytExpert software; live CLL cells were gated as CD5+/CD19+/CD3-/FVD-. There was no correlation between the unstimulated (basal) expression of CD19 (MFI) and the migratory response to ODN 2006 ($P=0.289$, $R^2=0.04$, n=29). There was no correlation between the ODN 2006-stimulated expression of CD19 (MFI) and the migratory response to ODN 2006 ($P=0.056$, $R^2=0.13$, n=29).

5.2.4: The Bifurcated Migratory Response to ODN 2006 is CD19/BTK-Dependent

The above phenotyping data suggest ODN 2006 to be operating independently of BTK, inferring that TLR9 may be able to promote CLL cell migration in the presence of ibrutinib. Using the same methodology as above, the effect of ibrutinib upon ODN 2006-stimulated CLL cell migration was investigated. PBMCs were stimulated ± ODN 2006 ± ibrutinib and transferred into transwell migration chambers to migrate against a CXCL12-gradient. The data is presented independently for Responder and Non/Reverse Responder subgroups.

Responders: In a cohort of 17 Responder patients, stimulation with ODN 2006 alone resulted in a 2.55 (±1.23)-fold increase in CLL cell migration ($P<0.001$). In the presence of ibrutinib, ODN 2006 stimulated a 2.23 (±1.22)-fold increase in CLL cell migration ($P<0.001$). There was no significant difference between the migratory response of Responder CLL cells following stimulation with ODN 2006-alone or ODN 2006 + ibrutinib ($P=0.159$). These results suggest that in the Responder subgroup, ODN 2006 can stimulate an increase in CLL cell migration independently of BTK (Figure 5.8).

Non/Reverse-Responders: In a smaller cohort of Non/Reverse-responder patients, stimulation with ODN 2006-alone stimulated a 0.66 (±0.25)-fold ***decrease*** in CLL cell migration ($P=0.008$, n=9 from 6 individual patients). Strikingly, in the presence of ibrutinib, this effect was ***reversed*** and ODN 2006 no longer caused a reduction in CLL cell migration; following stimulation with ODN 2006 + ibrutinib, CLL cell migration was 1.15 (± 0.34)-fold that of the unstimulated control ($P=0.25$); there **was** a significant difference between ODN 2006-stimulated and ODN 2006 + ibrutinib-

stimulated CLL cell migration (P=0.010) (Figure 5.9a). BTK therefore appears to play a role in the migratory response of Non/Reverse Responder subgroup to stimulation with ODN 2006.

In Chapter 3, biological repeats were performed on a small cohort of patients to determine whether the proposed bifurcated migratory response to ODN 2006 was a consistent and reproducible trend. Within the above data are biological repeats for 3 of the 6 patients in the cohort; the repeats are individually presented in Figure 5.9b to again determine the reproducibility of this trend. Patient responses were confirmed to be reproducible; in each case, the presence of ibrutinib reversed the observed ODN 2006-stimulated decrease in CLL cell migration.

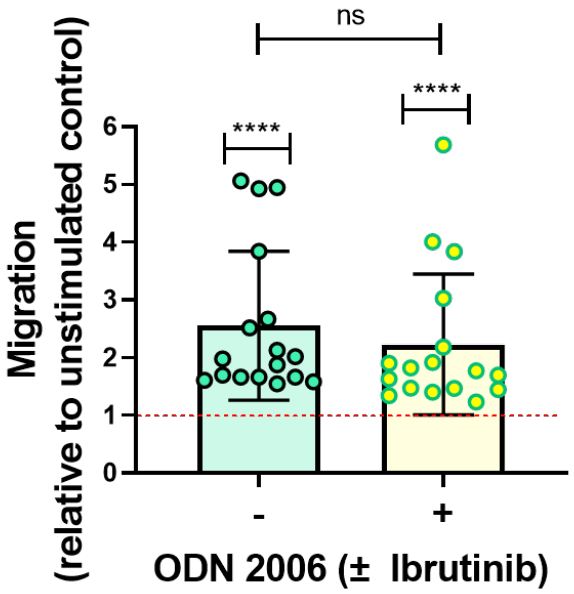

Figure 5.8: The Migratory Response of Responder Patient Samples is Independent of BTK. Primary PBMCs from 17 TLR9-Responder patients were pre-incubated ± 1μM ibrutinib for 30 minutes prior to an overnight stimulation with 1μM ODN 2006 in complete media +IL-4 at 37°C/5% CO_2. The PBMCs were then counted at 0h migration, transferred into the apical chambers of a 5μm pore polycarbonate transwell migration plate and incubated for 4h; a CXCL12-driven chemotactic gradient was established in the basal transwell chamber. At 4h migration, the migrated PBMCs were collected and stained for CLL cell identification; live CLL cells were identified as CD19+/CD3- and counted volumetrically using the Accuri flow cytometer using CFlow software. CLL cell migration was calculated as a percentage of the 0h cell count. Statistical analysis was performed using Graphpad Prism 8.0 and the Wilcoxon Matched Pairs test was used as the data was not Gaussian (according to the D'Agostino & Pearson omnibus normality test). Stimulation with ODN 2006 alone resulted in a significant increase in CLL cell migration ($P<0.001$, Wilcoxon Matched Pairs test). Stimulation with ODN 2006 + ibrutinib also resulted in a significant increase in CLL cell migration ($P<0.001$, Wilcoxon Matched Pairs test). There was no significant difference between the migratory response of TLR9-Responder CLL cells stimulated with ODN 2006 alone or ODN 2006 + ibrutinib ($P=0.159$, Wilcoxon Matched Pairs test). ODN 2006 therefore stimulates a ***BTK-independent increase*** in CLL cell migration in the Responder subgroup.

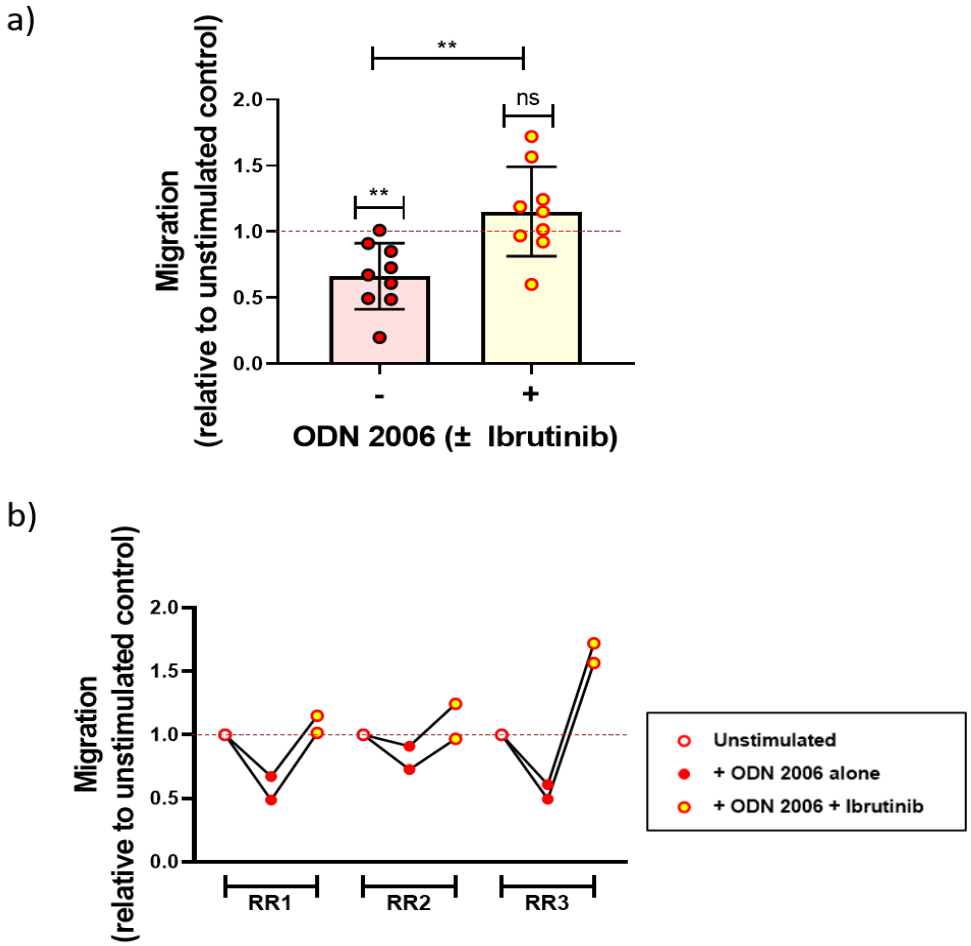

Figure 5.9: The Migratory Response of Non/Reverse Responder Patient Samples is BTK-Dependent. Primary PBMCs TLR9 Non/Reverse Responder patients were pre-incubated ± 1μM ibrutinib for 30 minutes prior to an overnight stimulation with 1μM ODN 2006 in complete media +IL-4 at 37°C/5% CO_2. Transwell migration experiments were then performed as previously described and statistical analysis was performed using GraphPad Prism 8.0. The Wilcoxon Matched Pairs test was used as the data was not Gaussian (according to the D'Agostino & Pearson omnibus normality test). a) As previously shown, stimulation with ODN 2006 alone resulted in a significant *decrease* in CLL cell migration compared to the unstimulated control (P=0.008, Wilcoxon Matched Pairs test, n=9 from 6 individual patients). There was no significant change in CLL cell migration following stimulation with ODN 2006 + ibrutinib compared to the unstimulated control (P=0.25, Wilcoxon Matched Pairs test, n=9, from 6 individual patients). There **was** a significant difference between the migratory response of TLR9 Responder CLL cells stimulated with ODN 2006-alone or ODN 2006 + ibrutinib (P=0.010). b) For each of 3 patients (RR1-RR3) responses were plotted individually as biological duplicates and demonstrated that ODN 2006 stimulated migration was consistently reduced in the absence of ibrutinib (red dots) and comparatively raised in the presence of ibrutinib (yellow dots). ODN 2006 therefore stimulates a ***BTK-dependent decrease*** in CLL cell migration in the Non/Reverse-Responder subgroup.

The above presented CD19 correlative data were revisited in the light of this seemingly BTK-dependent mechanism of migratory bifurcation. Strikingly, when divided into Responder and Non/Reverse-Responder subgroups, CD19 appeared to be strongly functionally linked to the Non/Reverse-Responder subgroup only. Figure 5.10 shows correlative data for Responder and Non/Reverse-Responders in ODN 2006-stimulated CLL cells. Here, CD19 is shown to significantly correlate with CD69 (%) (P=0.026, R^2=0.59), CD49d (%) (P=0.006, R^2=0.74) and CD38 (%) (P=0.007, R^2=0.73) in the Non/Reverse-Responder subgroup-only (n=8). There was no correlation between CD19 and CD69 (%) P=0.208, R^2=0.09), CD49d (%) (P=0.488, R^2=0.03) or CD38 (%) (P=0.285, R^2=0.06) in the Responder subgroup (n=20).

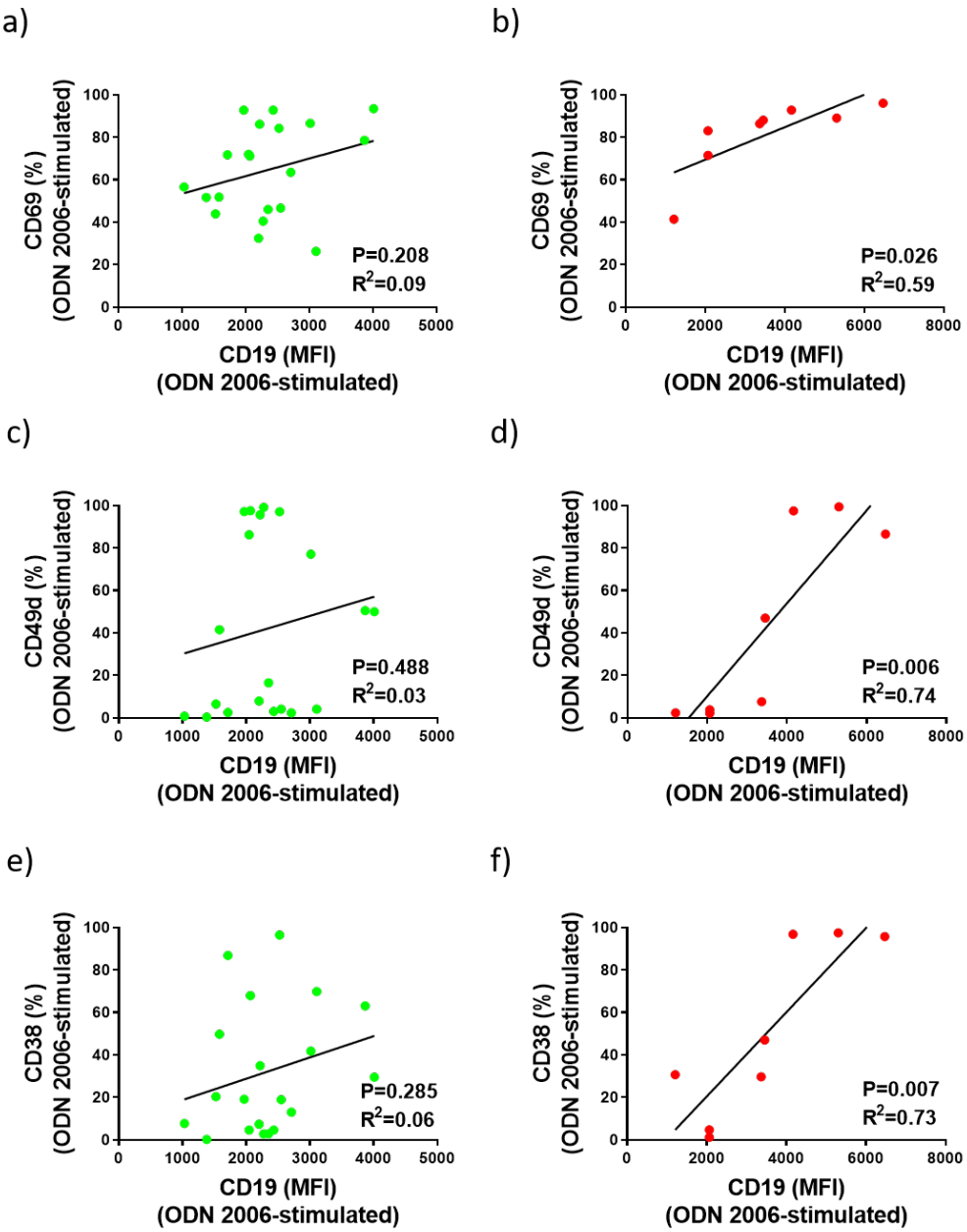

Figure 5.10: CD19 Correlates with CD69, CD49d and CD38 in the Non/Reverse-Responder Subgroup Only. This figure presents reanalysed CytoFLEX LX flow cytometry data from Figure 5.2, Figure 5.4 and Figure 5.5; patients were divided into Responder (green, n=20) and Non/Reverse Responder (red, n=8) and all of the presented data is from ODN 2006-stimulated CLL cells. a) CD19 significantly correlated with CD69 (% positivity) in Non/Reverse Responder (P=0.026, R^2=0.59) but not Responder (P=0.208, R^2=0.09) patients. b) CD19 significantly correlated with CD49d (% positivity) in Non/Reverse Responder (P=0.006, R^2=0.74) but not Responder (P=0.488, R^2=0.03) patients. c) CD19 significantly correlated with CD38 (% positivity) in Non/Reverse Responder (P=0.007, R^2=0.73) but not Responder (P=0.285, R^2=0.06) patients. Statistical analysis was performed using GraphPad Prism 8.0 and correlation was determined using the Spearman's rank correlation coefficient.

Furthermore, the trend appeared to extend to the migratory response to ODN 2006. When reanalysed to consider the Responder and Non/Reverse Responder subgroup division, CD19 expression levels appeared to be associated with Non/Reverse Responder but not Responder CLL cell migration (Figure 5.11). There was no correlation between CD19 (MFI) and the migratory response to ODN 2006 in the Responder subgroup ($P=0.62$, $R^2=0.02$, $n=18$) and a strong ***negative*** correlation with the migratory response to ODN 2006 in the Non/Reverse Responder subgroup ($P=0.013$, $R^2=0.67$, $n=8$). Together, these results suggest that ODN 2006 ***promotes*** CLL cell migration in the Responder subgroup, independently of both CD19 and BTK and that ODN 2006 appears to ***inhibit*** CLL cell migration in the Non/Reverse Responder subgroup, in a CD19/BTK dependent manner.

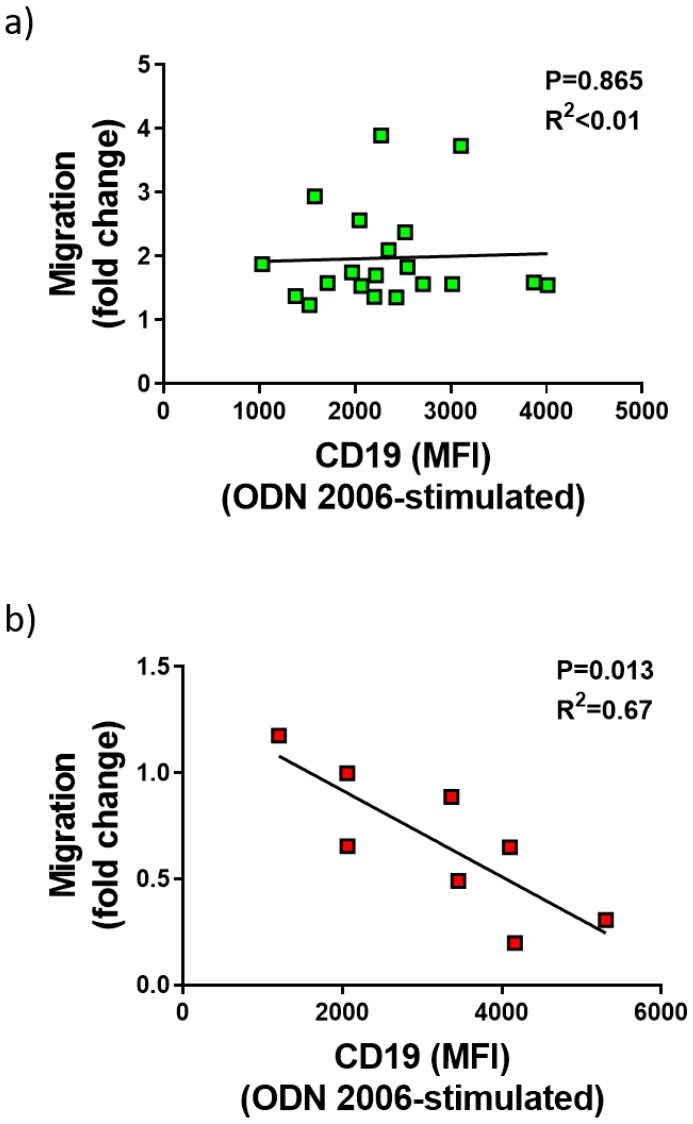

Figure 5.11: CD19 May Negatively Correlate with the Migratory Response to ODN 2006 in the Non/Reverse-Responder Subgroup Only. This figure presents reanalysed CytoFLEX LX flow cytometry data from Figure 5.7; patients have been divided into Responder (n=18) and Non/Reverse-Responder patients (n=8). In ODN 2006-stimulated CLL cells, there was (a) no correlation between CD19 (MFI) and the migratory response to ODN 2006 in the Responder subgroup (P=0.62, R^2=0.02) and (b) a strong negative correlation between CD19 (MFI) and the migratory response to ODN 2006 in the Non/Reverse-Responder subgroup (P=0.013, R^2=0.67). Statistical analysis was performed using GraphPad Prism 8.0 and correlation was determined using the Spearman's rank correlation coefficient.

5.3: Dual Targeting of TLR9 and BTK Induces a Synergistic Reduction in CLL Cell Migration in the Responder Subgroup

In the Responder subgroup, ODN 2006 was found to induce a BTK-independent increase in CLL cell migration. This suggests that a dual targeted inhibition of BCR and TLR9 has the potential to synergise since TLR9 is operating independently of BCR-signalling. A series of transwell migration assays were performed to investigate TLR9 inhibition as a potential novel combinational therapy with ibrutinib. The TLR9 antagonist ODN INH-18 was used to inhibit ODN 2006-stimulated TLR9 activation.

In order to investigate the effects of TLR9 **inhibition** in conjunction with ibrutinib, it was important to culture the cells in the presence of TLR9-stimulatory ODN. Ideally, CLL cells would be cultured and activated using autologous plasma containing cell-free CpG DNA. Indeed, in our recent publication[132], our group used short term assays to demonstrate that autologous patient plasma contains elevated levels of CpG DNA, which activates CLL cells in an identical way to ODN 2006. However, as previously discussed, this plasma-derived CpG DNA is both labile and difficult to dose-standardise for longer experiments and stocks of frozen PBMCs are isolated and banked away from their CpG DNA-containing plasma. Figure 5.12 shows the importance of performing these experiments in ODN 2006-activated CLL cells rather than unstimulated CLL cells as in the absence of ODN 2006, CLL cell migration was not affected by TLR9 inhibition. In a cohort of 11 patients, PBMCs were cultured ± 5μM ODN INH-18-alone (TLR9 inhibitor) and CLL cell migration i.e., the percentage of CLL cell migration with/without 5μM ODN INH-18 was 8.14% (±5.62) and 8.41% (±6.20), respectively (P=0.467).

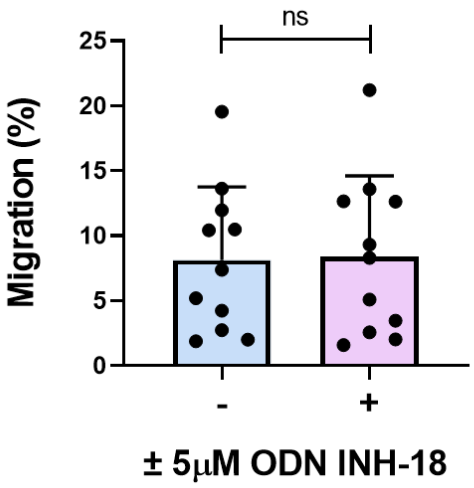

Figure 5.12: ODN INH-18 Has No Effect upon CLL Cell Migration in the Absence of ODN 2006. Primary PBMCs from 11 'Responder' patients were incubated overnight with the TLR9 antagonist ODN INH-18 in complete media +IL-4 at 37°C/5% CO_2 transwell migration assays were then performed as previously described. Statistical analysis was performed using GraphPad Prism 8.0. A Paired t-test was used as the data was Gaussian (according to the D'Agostino & Pearson omnibus normality test). In the absence of a TLR9 agonist, ODN INH-18 had no effect on CLL cell migration (P=0.467, Paired t-test, n=11).

The synergy experiments were therefore performed on ODN 2006 stimulated CLL cells and were performed using suboptimal doses of each inhibitor. Suboptimal doses were used to ensure that ODN 2006-stimulated CLL cell migration was not completely abrogated in the presence of either single-agent alone and allow for the quantification of additive or synergistic inhibition when used in combination.

PBMCs were pre-incubated with either ibrutinib-alone **or** ODN INH-18-alone **or** ibrutinib + ODN INH-18 for 30 minutes prior to an overnight stimulation with ODN 2006. Three dose combinations were chosen, each at a ratio of 2:1 ODN INH-18: ibrutinib as follows:

- **Dose Combination 1**:
    - 0.25 μM ibrutinib-alone
    - 0.50 μM ODN INH-18-alone
    - 0.25 μM ibrutinib + 0.5 μM ODN INH-18
- **Dose Combination 2**:
    - 0.50 μM ibrutinib-alone
    - 1.0 μM ODN INH-18-alone
    - 0.50 μM ibrutinib + 0.50 μM ODN INH-18
- **Dose Combination 3**:
    - 1.0 μM ibrutinib -alone
    - 2.0 μM ODN INH-18-alone
    - 1.0μM ibrutinib + 2.0 μM ODN INH-18

Table 5.1 and Figure 5.13 compare the inhibitory effects of each dose combination with the corresponding single-agent incubations. For each experimental condition, the fold change in CLL cell migration is calculated relative to the ODN 2006-**stimulated** control (i.e., an uninhibited control) (n=8).

- **Dose Combination 1:**

A combined dose of 0.25μM ibrutinib and 0.5μM ODN INH-18 resulted in a significantly greater reduction in CLL cell migration compared with 0.25μM ibrutinib-alone (P=0.049) but **not** 0.5μM ODN INH-18-alone (P=0.482) Figure 5.13a.

- **Dose Combination 2:**

A combined dose of 0.5μM ibrutinib and 1.0μM ODN INH-18 resulted in a significantly greater reduction in CLL cell migration compared with 0.5μM ibrutinib-alone (P=0.015) but **not** 0.5μM ODN INH-18-alone (P=0.062) Figure 5.13b.

- **Dose Combination 3:**

A combined dose of 1.0μM ibrutinib and 2.0μM ODN INH-18 resulted in a significantly greater reduction in CLL cell migration compared with both 1.0μM ibrutinib alone (P=0.008) **AND** 2.0μM ODN INH-18 alone (P=0.002) Figure 5.13c.

It therefore appeared that at the highest tested dose combination (i.e., dose combination 3), ibrutinib and ODN INH-18 was potentially acting synergistically; it was unclear at this point however whether the induced differences were additive or synergistic. Table 5.2 lists the changes in CLL cell migration (relative to the ODN 2006-stimulated control) for each individual patient at each tested dose combination. These values were entered into CompuSyn software to determine whether the observed changes could be considered additive or synergistic. Combination Index (CI) analysis demonstrated that the ODN INH-18 and ibrutinib were synergistic in 6/8 samples (i.e., CI<1) (Figure 5.13d and Table 5.3). The mean CI at the half maximal effective dose (ED50) for the combination of the two drugs was 0.2 indicating a strong synergistic effect. Of the two patients who did not demonstrate synergy, one (patient 4) had a very good response to ibrutinib alone but not to ODN INH-18 and the other (patient 5) had a good response to ODN INH-18 alone but not to ibrutinib. This further highlights the heterogeneity of CLL as a disease and the importance of identifying the best drug or drug combination for each patient.

Table 5.1: Fold Change in ODN 2006-Stimulated CLL Cell Migration, in Responder Patients, Following a Pre-Incubation with Ibrutinib, ODN INH-18 or a Combination of Both Ibrutinib AND ODN INH-18

	Fold Change in Migration (±SD) (Relative to ODN 2006-Stimulated Control)		
	Dose Combination 1	**Dose Combination 2**	**Dose Combination 3**
Ibrutinib	0.89 (±0.12)	0.91 (±0.18)	0.84 (±0.22)
ODN INH-18	0.70 (±0.24)	0.72 (±0.27)	0.72 (±0.25)
Ibrutinib + ODN INH-18	0.66 (±0.31)	0.58 (±0.26)	0.48 (±0.20)

All conditions: (n=8).

Table 5.2: Individual Patient Fold Change Values for the Calculation of Ibrutinib/ODN INH-18 Synergy (CLL Cell Migration)

Pt	Fold Change in Migration (Relative to ODN 2006-Stimulated Control)								
	Ibrutinib (μM)			ODN INH-18 (μM)			Dose Combination		
	0.25	0.5	1.0	0.5	1.0	2.0	1	2	3
1	0.93	0.97	0.87	0.99	0.96	0.90	0.80	0.84	0.67
2	0.92	0.95	1.07	0.85	0.92	0.86	0.88	0.62	0.49
3	0.92	0.95	1.07	0.85	0.92	0.86	0.88	0.62	0.49
4	0.96	0.65	0.53	0.85	1.02	1.03	1.02	0.88	0.73
5	1.09	1.15	0.98	0.48	0.45	0.56	0.56	0.60	0.56
6	0.73	0.62	0.49	0.55	0.58	0.55	0.17	0.17	0.17
7	0.72	0.98	0.86	0.77	0.64	0.75	0.67	0.68	0.56
8	0.92	0.99	0.81	0.29	0.30	0.27	0.26	0.21	0.20

Table 5.3: Combination Index Values for Ibrutinib/ODN INH-18 Synergy Experiments (CLL Cell Migration)

	Median Effective Dose (ED)			
Pt	**ED50**	**ED75**	**ED90**	**ED95**
1	1.38E-04	0.001	0.009	0.040
2	0.004	0.017	0.069	0.179
3	0.883	0.941	1.027	1.145
4	33.963	14.124	5.874	3.243
5	1.923	1.664	1.440	1.306
6	0.087	0.180	0.374	0.614
7	0.307	0.416	0.575	0.754
8	0.635	0.713	0.800	0.867

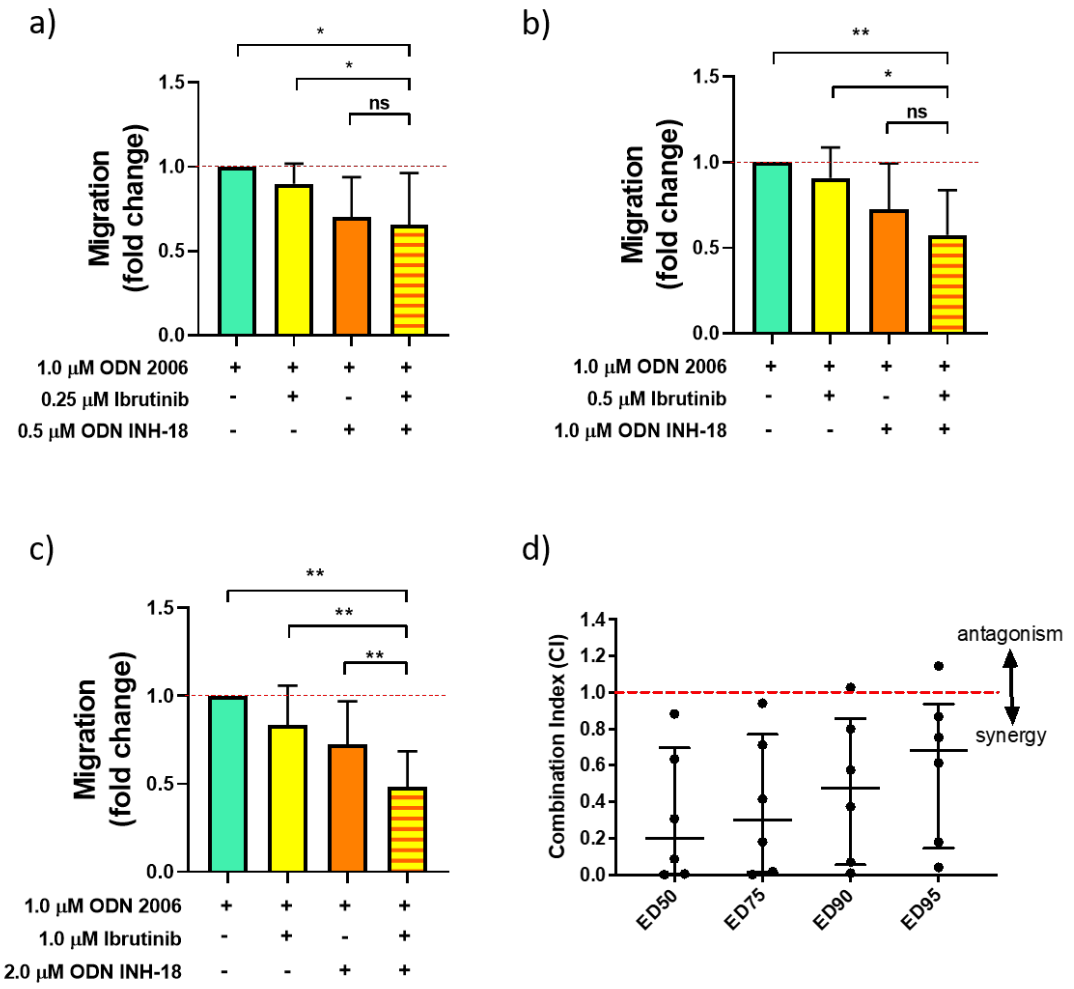

Figure 5.13: Dual Inhibition of TLR9 and BTK Induces a Synergistic Decrease in CLL Cell Migration. Primary PBMCs from 8 CLL patients were pre-incubated for 30 minutes with ODN INH-18-alone, ibrutinib-alone or ODN INH-18 + ibrutinib (at a ratio of 2:1) before being stimulated overnight with 1μM ODN 2006. Transwell migration assays were performed as previously described. a) A combination of 0.25μM ibrutinib + 0.5μM ODN INH-18 did not reduce migration any more than 0.5μM ODN INH-18-alone (P=0.482, Paired t-test). b) Although the combination of 0.5μM ibrutinib + 1.0μM ODN INH-18 appeared to reduce migration more than either agent alone, this was not statistically significant compared with ODN INH-18-alone (P=0.0624, Paired t-test). c) The combination of 1.0 μM ibrutinib and 2.0μM ODN INH-18 reduced migration more than either agent alone and this was statistically significant compared with both ibrutinib-alone (P=0.008, Paired t-test) and ODN INH-18 alone (P=0.002, Paired t-test). Statistical analysis was performed using GraphPad Prism 8.0 and the Paired t-test was used as the data was Gaussian (according to the D'Agostino & Pearson omnibus normality test). d) Combination Index (CI) analysis demonstrated that the ODN INH-18 and ibrutinib were synergistic in 6/8 samples (i.e., CI<1). The mean CI at the half maximal effective dose (ED50) for the combination of the two drugs was 0.2 indicating a strong synergistic effect.

5.4 Dual Targeting of BTK and TLR9 in TLR9 Non/Reverse-Responder Patient Samples

CD19 and BTK appear to play a role in the migratory response of Non/Reverse Responder patients to stimulation with ODN 2006. As previously discussed, this could be a result of Non/Reverse Responder CLL cells having already reached their maximal migratory potential through BCR/BTK signalling. It is possible that within these samples, CLL cell migration cannot be further increased and that perhaps a negative regulatory mechanism is instead initiated following stimulation with ODN 2006. The BTK-inhibitor ibrutinib was earlier shown to reverse the effect of ODN 2006 in the Non/Reverse Responder subgroup suggesting that in the absence of BCR/BTK-signalling, these patient CLL cells may become sensitised to ODN 2006 as a result of reduced basal activation/migration. TLR9-signalling could therefore be acting as a mechanism of resistance to ibrutinib in the Non/Reverse Responder subgroup. The effect of a dual inhibition of BTK and TLR9 was investigated in the TLR9 Non/Reverse Responder patients however due to the laboratory restrictions placed during the COVID-19 induced lockdown period, these experiments remain a work in progress. The data presented in Figures 5.14 and 5.15 are preliminary findings and depict duplicate experiments from 3 Non/Reverse Responder patients (i.e., n=6 from 3 patients, numbers are too low for statistical analysis).

Figure 5.14 confirms that ibrutinib reverses the negative migratory effects of ODN 2006 in this cohort of Non/Reverse Responder patients at each of the tested concentrations. In the presence of ODN 2006-alone, CLL cell migration was reduced to 0.75 ± 0.21-fold (±SD) that of the unstimulated control. This was rescued back to

0.96 (± 0.16); 1.10 (± 0.18) and 0.95 (±0.30)-fold in the presence of 0.25μM, 0.5μM and 1.0μM ibrutinib respectively. Having confirmed this trend in these patients, dual inhibition was executed as described above for the Responder subgroup; the same dose combinations of ODN INH-18 and ibrutinib were used.

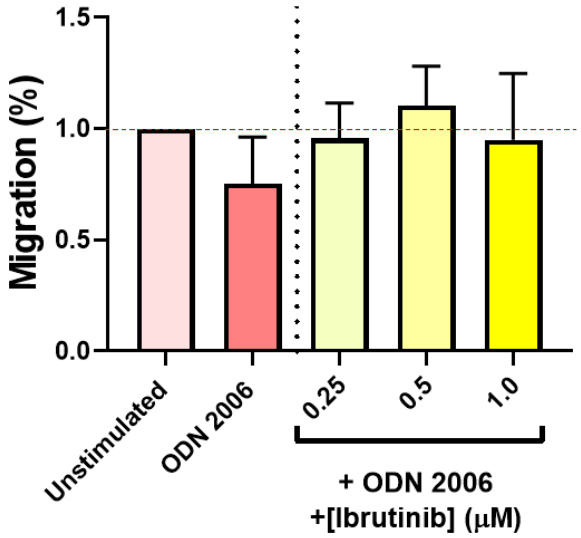

Figure 5.14: Ibrutinib Reverses the ODN 2006-Induced Reduction in CLL Cell Migration in the Non/Reverse-Responder Patient Subgroup. Primary PBMCs from Non/Reverse Responder patients were pre-incubated for 30 minutes with a range of concentrations of ibrutinib before being stimulated overnight with 1μM ODN 2006 (n=6 from 3 patients). Transwell migration assays were performed as previously. ODN 2006-alone stimulated a reduction in CLL cell migration and in the presence of 0.25μM, 0.5μM and 1μM ibrutinib, migration was rescued close to or above basal levels.

Figure 5.15 shows each dose combination relative to the (uninhibited) ODN 2006-stimulated control and the fold change values (±SD) are shown in Table 5.4 below. For dose combinations no. 1 and no. 2, dual targeting of BTK and TLR9 showed no benefit and CLL cell migration remained increased relative to the (uninhibited) ODN 2006-stimulated control. For dose combination no.3 however, the addition of ODN

INH-18 resulted in migration values closest to the (uninhibited) ODN 2006-stimulated control and reversed the migration increase induced by ibrutinib alone. These preliminary results suggest that at the correct concentration, dual inhibition of BTK and TLR9 may counteract the observed pro-migratory effects of ibrutinib-alone. Patient numbers are currently very low for these experiments and further repeats would be required to confirm this trend. If confirmed, this would suggest that in addition to TLR9 Responder patients, TLR9 inhibition could also benefit ibrutinib-treated, TLR9 Non/Reverse Responder patients.

Table 5.4: Fold Change in ODN 2006-Stimulated CLL Cell Migration, in Non/Reverse Responder Patients, Following a Pre-Incubation with Ibrutinib, ODN INH-18 or a Combination of Both Ibrutinib AND ODN INH-18

	Migration (Fold Change ± SD)		
Dose Combination	**Ibrutinib**	**ODN INH-18**	**Ibrutinib + ODN INH-18**
1	1.41 ±0.60	1.28 ±0.47	1.59 ±0.50
2	1.64 ±0.77	1.40 ±0.16	1.53 ±0.15
3	1.40 ±0.70	1.30 ±0.36	1.17 ±0.25

All conditions: n=6 from 3 patients.

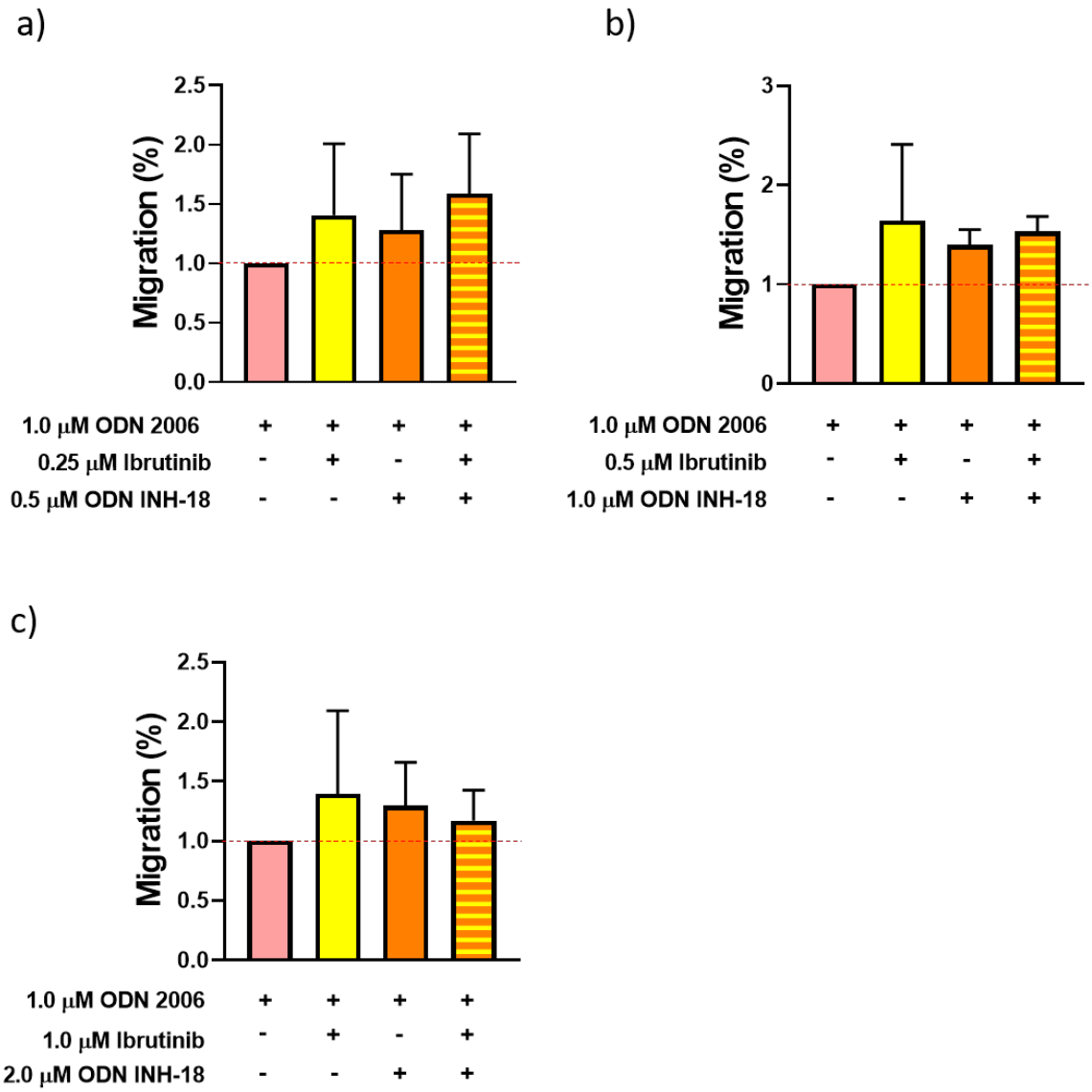

Figure 5.15: Dual Targeting of BTK and TLR9 in Non/Reverse-Responder Patients. Primary PBMCs were pre-incubated for 30 minutes with ODN INH-18-alone, ibrutinib alone or ODN INH-18 + ibrutinib (at a ratio of 2:1) before being stimulated overnight with 1μM ODN 2006 (n=6 from 3 patients). Transwell migration assays were performed as previously. At each concentration ODN INH-18-alone and ibrutinib-alone showed increased CLL cell migration relative to the ODN 2006-stimulated control. a-b) With combinations of 0.25μM ibrutinib + 0.5μM ODN INH-18 and 0.5μM ibrutinib + 1.0μM ODN INH-18, dual inhibition had no effect on CLL cell migration relative to ibrutinib-alone. c) With a combination of 0.5μM ibrutinib + 1.0μM ODN INH-18, the increase in CLL cell migration induced by ibrutinib-alone was inhibited by ODN INH-18.

5.5: Dual Targeting of BTK and TLR9 Induces a Synergistic Inhibition of Transcription Factor NF-κB

Both BCR and TLR9 signalling converge to induce the phosphorylation and nuclear translocation of NF-κB which in turn has the potential to drive CLL cell activation and migration. As the dual inhibition of TLR9 and BCR was shown to reduce CLL cell migration in the Responder subgroup, it is possible that inhibition of NF-κB may be a potential single-agent therapy to simultaneously block both signalling pathways. To investigate whether NF-kB inhibition may be implicated in the synergistic reductions in CLL cell migration observed with ibrutinib + ODN INH-18, synergy experiments were repeated to assess intracellular levels of p-p65 NF-κB. The optimal synergistic doses (identified in the migration assays i.e., dose combination 3) were used and intracellular p-p65 NF-κB was analysed by flow cytometry. PBMCs from 12 Responder patients were pre-incubated for 4 hours with either ODN INH-18, ibrutinib or ODN INH-18 + ibrutinib before being analysed on a CytoFLEX LX flow cytometer. In the presence of ibrutinib-alone, p-p65 NF-κB MFI (±SD) reduced from 1623 (±1194) to 1437 (±812.7) (P=0.009). In the presence of ODN INH-18-alone, p-p65 NF-κB MFI (±SD) reduced from 1623 (±1194) to 1231 (±853.5) (P=0.001). In the presence of both ibrutinib **AND** ODN INH-18, p-p65 NF-κB MFI (±SD) reduced from 1623 (±1194) to 1015 (±655.6) (P=0.001); the combination of ibrutinib and ODN INH-18 therefore induced the strongest inhibition of p-p65 NF-κB and was significantly reduced relative to either ibrutinib-alone (P=0.001) or ODN INH-18-alone (P=0.001) (Figure 5.16a).

Combination Index (CI) analysis demonstrated that the two drugs were synergistic at reducing p-p65 NF-κB in all 12 patients using 1μM ibrutinib + 2μM ODN INH-18 (i.e., CI<1). The mean CI at the half maximal effective dose (ED50) for the combination of the two drugs was 0.4, indicating a strong synergistic effect (Figure 5.16b). TLR9 signalling provides a compensatory mechanism of NF-κB activation in the absence of BCR signalling. These results strongly support the rationale for targeting NF-κB activation as a therapeutic strategy for CLL.

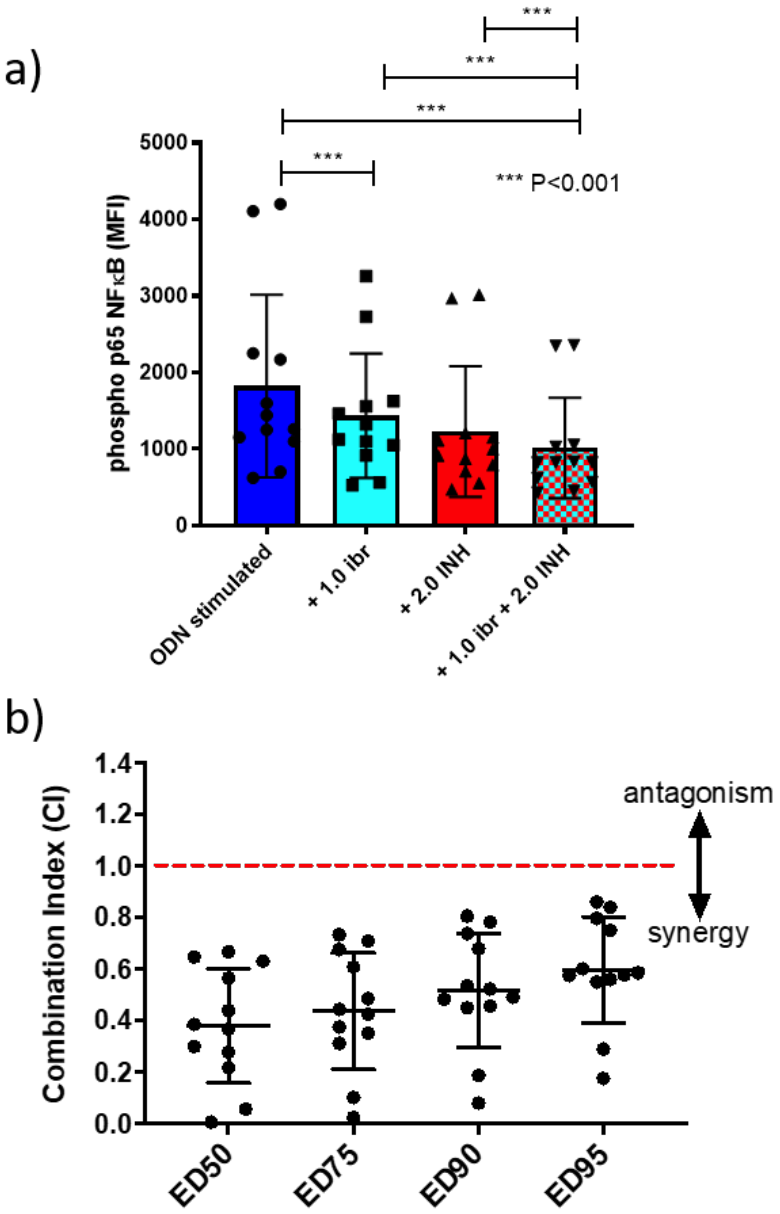

Figure 5.16: Dual Inhibition of TLR9 and BTK Results in a Synergistic Reduction in p-p65 NF-κB Activation. CLL cells from 12 different patients were pre-incubated with either 2μM ODN INH-18 (TLR9 antagonist) **OR** 1μM ibrutinib (BTK-inhibitor) **OR** 2μM ODN INH-18 + 1μM ibrutinib for 30 minutes prior to stimulation with 1μM ODN 2006 for 4 hours. Following activation, cells were harvested and stained for CD5, CD19 and intracellular p-p65 NF-κB or an isotype matched control (IMC) and then assessed by flow cytometry and the MFI values were recorded. Statistical analysis was performed using GraphPad Prism 8.0. The Paired t test was used as the data was Gaussian (according to the D'Agostino & Pearson omnibus normality test). a) The combination of ODN INH-18 and ibrutinib gave the maximum inhibition of p-p65 NF-κB ($P<0.01$, Paired t test). **b)** Combination Index (CI) analysis demonstrated that the two agents were synergistic at reducing p-p65 NF-κB in all 12 patients using 1μM ibrutinib + 2μM ODN INH-18 (i.e., $CI<1$). The mean CI at the half maximal effective dose (ED50) for the combination of the two agents was 0.4, indicating a strong synergistic effect.

5.6: The Bifurcated Migratory Response to ODN 2006 is also Seen in Canonical NF-κB-Signalling

ODN INH-18 has proven to be a potent inhibitor of TLR9 activation *in vitro* and has shown to induce synergistic reductions in CLL cell migration in combination with the BTK-inhibitor ibrutinib. The use of ODN INH-18 in a clinical setting however would not be practical since an unprotected oligonucleotide sequence would be vulnerable to nuclease degradation and therefore very labile *in vivo*. Further development of this dual targeted approach is therefore required. It would be beneficial to identify a targetable downstream component of the TLR9-signalling pathway and one such candidate is the transcription factor NF-κB. In fact, since both the TLR9 and BCR signalling pathways culminate in the activation of NF-κB, this approach could potentially achieve a dual targeted result from a single molecular agent. Furthermore, multiple NF-κB inhibitors are already in existence, rendering this an extremely practical target to consider.

In order to investigate NF-κB signalling in TLR9 activated CLL cells, I-kappa-Bα (IκBα) degradation was used as a quantifiable marker of NF-κB-activation. IκBα is an inhibitory component of the canonical NF-κB activation pathway which sequesters NF-κB in the cytoplasm of inactive cells. Following activation, IκBα is targeted for degradation, releasing NF-κB and enabling its translocation into the nucleus; here, active NF-κB can initiate the transcription of NF-κB target genes. IκBα degradation therefore directly correlates with NF-κB activation and its expression can be used to illustrate the responsiveness of NF-κB to different stimuli. In the following

experiments, the degradation/expression levels of IκBα following stimulation with ODN 2006 was tracked over a period of 6h.

Figure 5.17 shows the temporal pattern of IκBα degradation (from 0-6h) following stimulation with ODN 2006 in 6 Responder 4 Non/Reverse Responder CLL samples (IκBα is shown relative to the housekeeping protein β-actin). In the Responder subgroup, IκBα was rapidly degraded following stimulation with ODN 2006, with a maximal reduction at 1h post-stimulation, and was replenished by 4h post-stimulation (Table 5.5). In the Non/Reverse Responder subgroup, a greater heterogeneity was observed. Maximal IκBα degradation was slower post-stimulation and took longer to recover, compared with the Responder subgroup (Table 5.5). The mean IκBα expression had not returned to resting levels by 6h post-stimulation in 2/4 Non/Reverse Responder patients. Further repeats are required to better assess the responses of IκBα to stimulation with ODN 2006 in this subgroup however these preliminary results suggest there may be subgroup-specific differences in the temporal activation patterns of canonical NF-κB activation in Responder and Non/Reverse Responder samples.

Table 5.5: IκBα Degradation Patterns in Responder and Non/Reverse Responder Patient Samples in Response to Stimulation with ODN 2006

	IκBα (Relative to β-actin) (±SD)	
Timepoint (hours)	**Responders**	**Non/Reverse Responders**
0	0.07 (±0.05)	0.09 (±0.06)
0.5	0.05 (±0.41)	0.05 (±0.04)
1	0.03 (±0.03)	0.07 (±0.09)
4	0.06 (±0.03)	0.05 (±0.03)
6	0.08 (±0.05)	0.05 (±0.02)

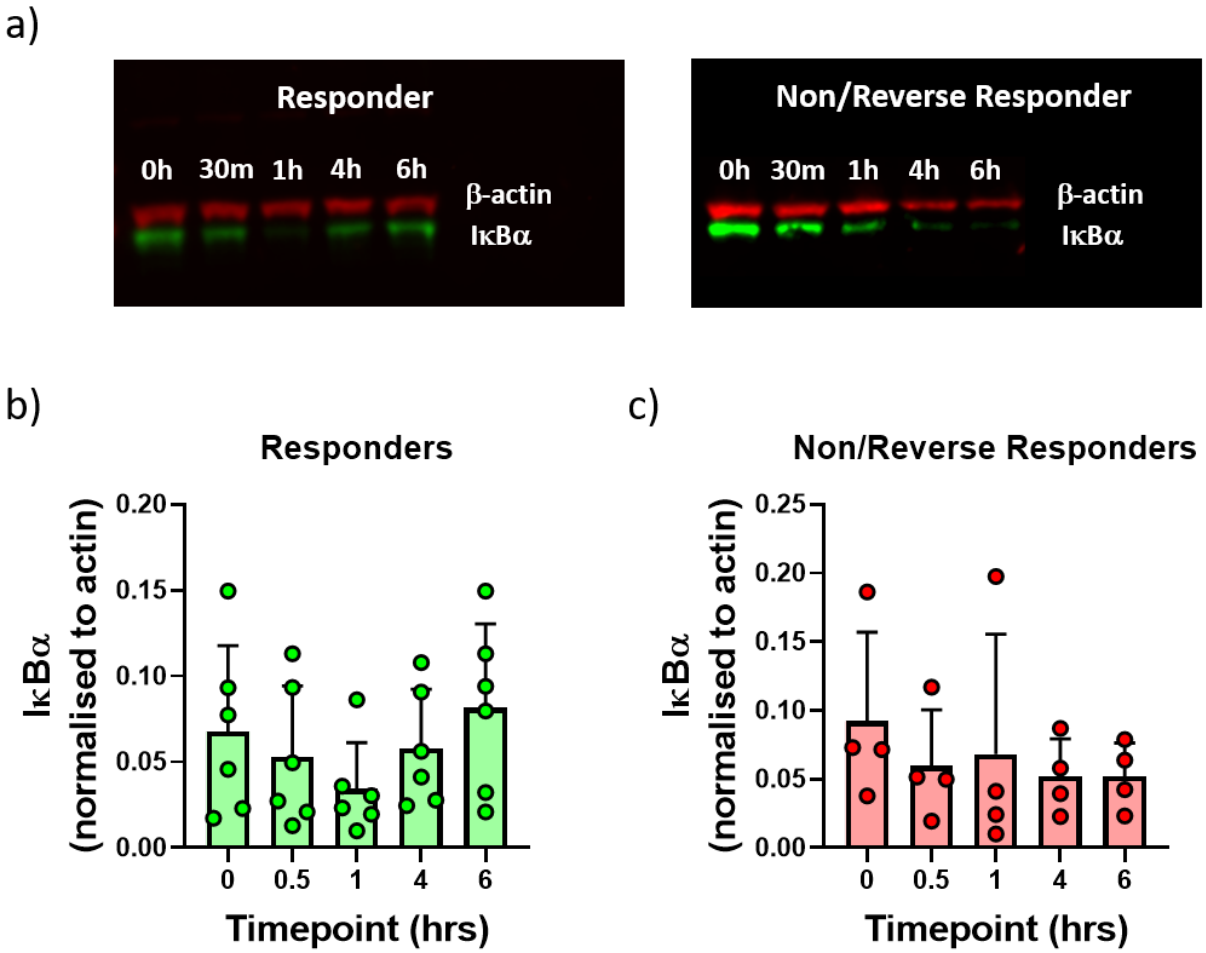

Figure 5.17: The Bifurcated Migratory Response to ODN 2006 is Observed in Canonical NF-κB Signalling. PBMCs from 6 Responder and 4 Non/Reverse Responder samples were stimulated with 1μM ODN 2006 and incubated in complete media +IL-4 at 37°C/5% CO_2 for 0-6h; 6 million cells were plated per well. At each timepoint, PBMCs were lysed in 50μl RIPA buffer and quantified using a BCA assay in preparation for western blotting. 20-40μg protein was loaded for electrophoresis. IκBα degradation was the target protein for these blots and was used as a marker of canonical NF-κB activation. IκBα was detected simultaneously with the housekeeping protein, β-actin, by immunofluorescence and membrane imaging was performed using a Li-COR Odyssey FC and Image Studio Lite software (version 5.2). IκBα expression is shown normalised to β-actin. a) Representative western blot images from a Responder and Non/Reverse Responder patient sample. b) Responders: IκBα was rapidly degraded following stimulation with ODN 2006, with a maximal reduction at 1h post-stimulation. IκBα expression was replenished by 4h post-stimulation. c) Non/Reverse Responders: a greater heterogeneity was observed in this subgroup compared with the Responder subgroup and maximal IκBα degradation was slower post-stimulation with ODN 2006. IκBα was slower to recover in the Non/Reverse Responder subgroup.

5.7 Discussion

The data presented in this chapter demonstrates that TLR9 signalling can activate NF-κB independently of BCR-signalling and is therefore a potential mechanism of resistance to BCR-targeted therapeutics such as ibrutinib. In addition to operating independently however, a great deal of cross-talk exists between the two pathways and TLR9 has previously been shown to stimulate BCR-signalling via the secretion of autoantibodies in ZAP-70 positive CLL[158]. Additionally, in parallel to the BCR-independent TLR9-MyD88-IRAK4/1/2 pathway, TLR9 can stimulate a B-cell specific TLR9-CD19-PI3K-BTK-AKT pathway[157]. The interaction between TLR9 and BCR signalling following stimulation with ODN 2006 was explored to elucidate whether ODN 2006-stimulated phenotypic/migratory changes are independent of CD19/BTK; in order for TLR9 to be a plausible mechanism of resistance to ibrutinib, ODN 2006 must be operating independently of BTK.

ODN 2006 upregulated the surface expression of the BCR co-receptor CD19 and downregulated the surface expression of the BCR-signalling negative regulator CD5; this suggests the propensity of CLL cells for BCR-signalling is increased following TLR9 activation. TLR9 is known to upregulate following BCR-activation in naïve B-cells[91,124] and so this effect therefore appears mutual, further highlighting the functional cross-over between BCR and TLR9 signalling. Furthermore, the expression of TLR9 was found to correlate with the fold change in CD19 expression following ODN 2006, suggesting a functional link between TLR9 and CD19; this was however not true of CD5. Since CD19 has been implicated in TLR9-signalling, it was important to identify whether the previously described phenotypic and migratory effects of ODN 2006

were operating via CD19. CD19 showed no correlation with CD69 expression in resting (unstimulated) CLL cells and a strong correlation with CD69 expression in ODN 2006-stimulated CLL cells; this suggested the CD19/BTK-dependent TLR9 signalling may be involved in mediating ODN 2006-stimulated increases in CD69 (i.e., CLL cell activation). In the presence of the BTK-inhibitor ibrutinib however, there was found to be no difference in the ODN 2006-stimulated upregulation of CD69, relative to ODN 2006-alone. It was therefore concluded that TLR9 could stimulate CLL cell activation independently of BTK. These findings are in keeping with a study by Morbach et al.,[157] in which BTK-inhibition was found to inhibit BCR-stimulated but not TLR9-stimulated increases in CD69; whilst aspects of CLL cell activation were found to be inhibited by ibrutinib i.e., increases in CD86 (a co-stimulatory protein involved in T-cell activation), CD69 was unaffected.

The migratory story was more complex and the migratory markers CD49d and CD38 were found to correlate with CD19 expression in the Non/Reverse Responder subgroup only. Non/Reverse Responder patients with high activated levels of CD19 therefore appear to be the most primed for CLL cell migration. Despite their seemingly increased potential for tissue-homing, samples with the highest levels of CD19 showed the greatest reductions in TLR9-induced CLL cell migration. It is possible that Non/Reverse Responder CLL cells have already reached their maximum migratory potential via BCR/CD19 signalling and that TLR9 cannot stimulate further migration in these samples. These findings were in keeping with the results from chapter 4, which suggested a subpopulation of highly basally activated U-CLL samples. The Non/Reverse Responder subgroup primarily consists of U-CLL patient samples and U-CLL is known to be highly responsive to BCR signalling[83,84]. BCR

activation is known to induce CLL cell migration and CLL cells are known to have heterogenous levels of constitutive BCR signalling[155,156]. The Non/Reverse Responder samples may therefore have reached their activation/migration potential in basal conditions through constitutive BCR signalling. Alternately, these samples may be exhibiting auto-activation of the BCR as described by Wagner et al.,[158] in 2016. This study reported ZAP70 positive CLL cells to secrete auto-stimulatory anti-bodies. Additionally, TLR9 and BCR have been shown to signal together in the presence of DNA-containing antigens and in this context, TLR9 has been implicated in B-cell tolerance and the inhibition of autoimmunity[160]. Chronic stimulation of TLR9 has also been shown to initiate a negative regulatory feedback mechanism, including the inhibition of NF-κB target gene expression[161]. The induction of such a negative feedback mechanism may account for the reduction in CLL cell migration in some Non/Reverse Responders i.e., perhaps in these patients, additional stimulation with ODN 2006 induces a negative regulatory anergic state reminiscent of B-cell anergy. Further work is required to delineate these interactions and to identify the mechanisms behind the Non/Reverse-Responder response to ODN 2006. Interestingly, in support of these hypotheses, BTK-inhibition was shown to reverse ODN 2006-stimulated decreases in CLL cell migration in the Non/Reverse Responder subgroup; Non/Reverse Responder patients therefore became sensitised to TLR9 signalling in the absence of BTK activation.

TLR9 Responder patients were shown to induce CLL cell migration independently of BTK indicating that TLR9 is a potential mechanism of resistance to ibrutinib in this subset of patients. Transwell migration experiments were performed to investigate whether the dual inhibition of TLR9 (ODN INH-18) and BTK (ibrutinib) could induce

synergistic reductions in CLL cell migration. A strongly synergistic effect was observed in 6/8 Responder patients, providing further evidence for the role of TLR9 in ibrutinib-resistance; a dual targeted TLR9/BTK approach to treatment holds the potential for clinical benefit. Furthermore, in the Responder subgroup, ODN INH-18 and ibrutinib were also shown to synergistically inhibit NF-κB activation. This is in keeping with a study by Dadashian et al.,[93] in which the simultaneous inhibition of BTK (BCR-signalling) and IRAK1/4 (TLR9 signalling) showed a synergistic downregulation of NF-κB signalling and a synergistic decrease in CLL cell survival. Since the TLR9 and BCR pathways converge at the point of NF-κB activation, therapeutic inhibition of NF-κB is a promising approach to simultaneously eliminate both pathways.

Preliminary results from an NF-κB activation time-course experiment identified a potential difference between the temporal activation patterns of Responder and Non/Reverse Responder samples in response to ODN 2006. For these experiments NF-κB subunits were not measured directly, but through IκBα degradation. In the Responder subgroup, a greater heterogeneity was observed and maximal IκBα degradation was slower following stimulation with ODN 2006. IκBα was also slower to recover in this subgroup. Further repeats are required to confirm and strengthen these findings as the patient numbers are currently small for these experiments. It is also important to consider that NF-κB is not a single entity and is in fact a family of five related subunits belonging to both the canonical and non-canonical signalling pathways (i.e., p65, p52, p50, RelB and c-Rel)[96]. The above experiments do not take into consideration potential differences in the ratios of NF-κB subunits being translocated into the nucleus; perhaps discrete sets of NF-κB target genes are being

transcribed following ODN 2006-stimulation in Responder and Non/Reverse Responder patients. In a study by Jayappa et al.,[97] stimulation of CLL cells with an 'agonist mix' containing CpG ODN, CD40L and IL-10 was reported to preferentially initiate non-canonical NF-κB signalling i.e., an alternate mechanism of NF-κB activation, which is independent from IκBα degradation. It would therefore be of interest to identify which subunits are being translocated into the nucleus following stimulation with ODN 2006 and whether there are observable differences between the two patient subgroups. Nuclear fractionation experiments and subsequent NF-κB subunit analysis (by ELISA) have been planned to complement the existing data and remain a work in progress.

Alternatively, the migratory response to ODN 2006 may in some cases be independent from the activation of NF-κB and instead dependent upon the activation of a separate transcription factor. In addition to NF-κB, our group has identified a synergistic reduction in the activation of ODN 2006-stimulated pSTAT3 following a pre-incubation with both ODN INH-18 and ibrutinib. Activated STAT3 has been associated with CXCL12-driven chemotaxis in *ex vivo* CLL cells[162]. These results were again in keeping with Dadashian et al.,[93] who identified a synergistic reduction of CpG-stimulated pSTAT3 in the

presence of ibrutinib and an IRAK1/4 inhibitor. Together these data support the rationale for the inhibition of TLR9 in combination with BTK as a dual targeted therapeutic strategy for subgroups of CLL. Although further investigation into the downstream transcription factors involved in TLR9/BCR mediated CLL cell migration is required, preliminary results suggest that NF-κB may be a promising target for the

simultaneous inhibition of both pathways. Finally, these data further highlight the heterogeneity of signalling in CLL and the need to move towards a more 'personalised medicine' approach to treatment.

6.0: Final Discussion

This thesis investigated the role of TLR9 in CLL cell migration, hypothesising that TLR9 signalling may promote CLL cell migration, independently of BCR-signalling, and act as a mechanism of resistance to BCR-targeted therapies. The trafficking of CLL cells to the BM and secondary lymphoid tissues is integral to disease maintenance and progression and this is best exemplified by the clinical effects of BTK and PI3Kδ inhibitors on lymphocyte redistribution. Circulating and tissue-resident CLL cells exhibit distinct phenotypic signatures, reflective of their different microenvironmental encounters and for this reason, CLL has been described as a disease of two compartments[40,60]. CLL cell proliferation occurs almost exclusively within the LN niche[40] and exposure to a plethora of cytokines, chemokines and cell:cell interactions with tissue-resident accessory cells promotes CLL cell survival[62,66,70-72]. In contrast, PB-CLL cells are relatively inactive and non-proliferative and are able to survive for prolonged periods of time due to an upregulation of the anti-apoptotic protein BCL-2[40,62,140]. TLR9 signalling is already known to induce CLL cell proliferation, survival, immunogenicity and resistance to therapy[138-140,151,163], however the role of TLR9 in CLL cell migration was undefined prior to this study. Components of TLR signalling are expressed at higher levels in the LN compartment relative to the PB[93], although it is unclear whether these pathways are activated before or after entry into the LN niche. TLR9-stimulatory mtDNA has been found to be 28.1-fold higher in the plasma of CLL patients, relative to healthy individuals[132], rendering TLR9 activation within the PB, a potential mechanism of CLL cell tissue-homing.

6.1: Overview of Main Findings

CLL Cell Migration: The TLR9 agonist ODN 2006 was found to induce a TLR9-dependent cellular activation and a migratory phenotype in all CLL samples. Following stimulation with ODN 2006 the activation marker CD69 and two components of the CLL-specific 'invadosome' structure (involved in the tissue-homing of CLL cells)[148,149] were significantly increased in all CLL samples. Interestingly, an uncoupling was observed between phenotypic activation and migratory changes as not all samples showed an increase in CLL cell migration following stimulation with ODN 2006. Consequently, patient samples were categorised into Responder and Non/Reverse Responder subgroups. Responder samples showed consistent ***increases*** in CLL cell migration following stimulation with ODN 2006, whilst Non/Reverse Responder samples either showed ***no change*** or a ***decrease*** in CLL cell migration following stimulation with ODN 2006. The migratory responses of both groups were confirmed to be TLR9-dependent (in the presence of the TLR9 antagonist ODN INH-18) and were therefore suggestive of a dichotomous functional response to TLR9 stimulation.

Previous groups have also reported dichotomous proliferative and apoptotic responses to CpG ODN, depending on the mutational status of the BCR; U-CLL patient samples have been shown to respond in a proliferative and anti-apoptotic manner, whilst M-CLL patient samples have been shown to respond in a non-proliferative and pro-apoptotic manner[138,139,151].

Strikingly, and in contrast to what may be expected, 13/14 M-CLL samples were categorised as TLR9 Responders and ODN 2006 appeared to induce a significant

increase in CLL cell migration in the ***M-CLL*** subgroup-only. A more detailed analysis revealed a further bifurcation within the ***U-CLL*** subgroup, with 8/18 U-CLL samples showing comparable fold changes in CLL cell migration to the M-CLL subgroup; these samples were categorised as Responders and the remaining 10/18 U-CLL samples were categorised as Non/Reverse Responders. U-CLL Non/Reverse Responder samples exhibited higher basal levels of activation and migration, relative to U-CLL Responders, and it was hypothesised that these samples were not able to be further activated by ODN 2006; this could explain how these samples failed to show an increase in migratory capacity. U-CLL cells are highly dependent upon BCR signalling and it could be hypothesised that in some cases they are already signalling to their maximum potential through the BCR[40,80,83-85].

Published data regarding the effects of TLR9 activation on CLL migration and tissue engraftment is currently extremely limited. In a study by Liang et al.,[163] CpG-stimulated CLL cells were reported to show ***decreased*** rates of engraftment within the peritoneal cavity and spleen of NOD-*scid* mice, which the group attributed to increased levels of apoptosis. A more recent study by Dampmann et al.,[164] however, reported that CpG ODN stimulated an increase in CLL cell polarisation with a redistribution of CXCR4 to the leading edge and an ***increase*** in CLL cell BM engraftment in NSG mice but not spleen engraftment. It is possible that these seemingly contradictory findings identify the preferential homing of CpG-stimulated CLL cells to the BM niche rather than intraperitoneal cavity or spleen and it is also possible that differences may be due to IGHV-status. The IGHV-status of CLL cells used in these engraftment experiments was not determined. In our recent Blood publication, we identified a link between TLR9 expression levels and CLL cell

engraftment in NSG mice[132]. In further support of a pro-migratory role for TLR9, an association between TLR9 and increased lymph node metastasis has been identified in a number of solid tumours[141-145].

TLR9 as a Potential Mechanism of Ibrutinib Resistance: In the Responder subgroup, ODN 2006 stimulated a significant increase in CLL cell migration in the presence of ibrutinib. This implied that in this subgroup, TLR9 promotes CLL cell migration independently of BTK and implicates TLR9 signalling as a potential mechanism of resistance to ibrutinib. The Responder subgroup consisted mainly of M-CLL patient samples and interestingly, in striking contrast to chemo(immuno)therapy, M-CLL patients have shown slower and less complete clinical responses to ibrutinib, relative to U-CLL patients; M-CLL patients show a slower clearance of malignant cells from both the peripheral blood and the bone marrow niche[165,166]. As previously discussed, M-CLL has a reduced responsiveness and lower dependency upon BCR signalling compared with U-CLL[40,83,84] and it therefore seems likely that alternative signalling pathways are operating in this subgroup. It is therefore possible that TLR9 could be a contributing factor to these clinical differences. M-CLL patients show reduced rates of ibrutinib-induced death in both the peripheral blood and tissue-compartments[165,166] and perhaps the persistence of these cells is supported by TLR9 driven trafficking into and out of the protective LN/BM niches.

The observation that driver mutations in the TLR signalling adaptor protein MyD88 are almost exclusively found in M-CLL patients[3,86-88], signifies an unidentified selective pressure for this mutation in M-CLL but not U-CLL patients. MyD88-mutated M-CLL patients have a considerably shorter TTFT[87] and an OS comparable to U-CLL

patients[88], which appears to conflict with their apoptotic-response to CpG ODN. Perhaps the identified pro-migratory effect of TLR9 activation could account for this selective pressure and counteract the apoptotic responses observed *in vitro*. CpG induced apoptosis has been reported from day 3-4 onwards[151,163]; it is therefore plausible that if CpG DNA were to promote the earlier trafficking of these cells to the LN/BM *in vivo*, these apoptotic signals may be nullified by entry into these tissue microenvironments. Exposure to pro-survival signals within these protective niches may render *in vitro* apoptotic responses biologically irrelevant.

Interestingly, ibrutinib was able to reverse ODN 2006-stimulated decreases in CLL cell migration in TLR9 Non/Reverse Responder patient samples. This supports the idea that this subgroup of samples has high levels of basal activation that is mediated, at least in part, by BCR signalling. Exposure to ibrutinib blocks these signals, which allows the cells to be activated via the TLR9 signalling pathway. This implies that all CLL cells probably have functional TLR9 signalling machinery, but this only becomes evident in CLL cells with high basal BCR signalling in the context of BCR inhibition. Logically, this leads to the suggestion that TLR9 signalling may provide a potential mechanism of ibrutinib resistance in this subgroup of patients. Despite initially rapid responses of aggressive U-CLL to treatment with ibrutinib[165,166], U-CLL patients with Chr.17p deletions showed significantly lower rates of PFS at 30 months post-treatment initiation[167]. Given that all Non/Reverse Responder patients in this cohort were U-CLL samples with high levels of basal activation, it is possible that the presence of ibrutinib sensitises them to TLR9-driven migration, which contributes to the shorter duration of responses in these patients. We now plan to investigate a larger cohort of Non/Reverse Responder patient samples derived from the UK FLAIR

study. In addition to performing our migration assay on this cohort of samples, we will perform whole genome sequencing analysis to determine whether U-CLL Reverse Responders are genetically distinct from U-CLL Responders.

BCR/TLR9 Synergy: In the Responder subgroup, dual inhibition of BCR and TLR9 signalling was found to be highly synergistic. In ODN 2006-stimulated cells, both NF-κB activation and CLL cell migration showed greater reductions in the presence of ibrutinib + ODN INH-18, relative to each single agent alone. BCR and TLR9 signalling therefore appear to be mutually compensatory in the Responder subgroup, suggesting that these patients may benefit from a BTK/TLR9 dual targeted approach to therapy. This is in keeping with the recent observation that dual inhibition of BTK and IRAK1/4 (downstream of TLR activation) showed a synergistic downregulation of both NF-κB signalling and CLL cell survival[93]. It also supports the earlier mentioned publication by Jayappa et al.,[97] in which CpG ODN was found to promote the survival of CLL cells treated with a combination of ibrutinib + venetoclax. TLR9 therefore appears to be a promising target for the prevention of microenvironment-mediated treatment resistance. The NF-κB signalling pathway is activated downstream of both the BCR and TLR9 and is a potential molecular target for the dual inhibiton of BCR and TLR9 signalling. Preliminary results have identified potential differences in the temporal activation patterns of NF-κB in ODN 2006-stimulated Responder and Non/Reverse Responder samples, however further repeats are required to confirm and strengthen these findings.

6.2: Limitations and Future Work

A significant limitation to this thesis has been the restrictions placed on laboratory usage during the COVID-19 pandemic. University closures and subsequent social distancing regulations and reduced working hours have substantially impacted upon the feasibility of data collection over the past year. For this reason, some experiments have been completed with smaller than intended patient sample cohorts and others have been regrettably rendered unfeasible. A further contributor to this problem has been the prolonged reduction in the accessibility of patient material. Since the beginning of the COVID-19 pandemic, the regular CLL clinic at The Royal Sussex County Hospital in Brighton has been closed. Given that CLL patients have a compromised immune system and are deemed clinically vulnerable, they have instead been having routine blood samples taken by community nurses. Our group relies heavily on this clinic and throughout this time, we have been limited to opportunistic samples from CLL inpatients admitted onto the haematology ward. This was particularly difficult considering our requirement for treatment-naïve samples.

The cohort of patient samples used in this thesis is particularly short of Non/Reverse Responder patients. Given that the vast majority of Non/Reverse responder samples were derived from U-CLL patients, this perhaps reflects the CLL patient demographics attending haematology clinics at The Royal Sussex County Hospital in Brighton. This is a general hospital and often patients with the most severe/aggressive disease are referred to specialist centres elsewhere. Our samples may therefore not be representative of the Responder vs Non/Reverse Responder split seen in tertiary referral centres.

A further limitation of the study is that the suggested role of BCR/BTK-signalling in the determination of the U-CLL migratory response to ODN 2006, was based on correlative phenotypic rather than mechanistic data. Given more time, it would be preferential to provide a more in-depth and mechanistic view of the bifurcated migratory response to ODN 2006. Basal and ODN 2006-stimulated levels of BTK activation (phospho-BTK) could be quantified in Responder and Non/Reverse Responder samples by western blotting. This would give an indication of the constitutive levels of BCR activation and confirm whether U-CLL Non/Reverse Responders are indeed operating at maximal activation. BCR activation could also be induced in U-CLL Responder samples via stimulation with IgM, to observe whether this has any effect on the migratory response of U-CLL cells to TLR9 activation and inhibition. Furthermore, it would be highly informative to complete the work started on ODN 2006-stimulated NF-κB activation. Prior to the COVID-19 restrictions, nuclear fractionation experiments had been optimised in preparation for planned NF-κB subunit analysis (by ELISA). The intended aim of these experiments was to identify potential differences in NF-κB subunit usage in Responder and Non/Reverse Responder samples following stimulation with ODN 2006. NF-κB comprises five related subunits (i.e., RelA (p65), p52, p50, RelB and c-Rel) and NF-κB activation can be induced following stimulation of the canonical or non-canonical NF-κB signalling pathway. NF-κB can translocate into the nucleus in a combination of 15 different homo/heterodimer arrangements to elicit distinct signal-specific patterns of gene expression[98]. It would be interesting to identify whether Responder and Non/Reverse Responder patients stimulate differences in NF-κB activation.

Additionally, whilst Non/Reverse Responder migration was found not to alter in the presence of different concentrations of ODN 2006, earlier timepoints of activation have not been investigated. Given the assumption of overstimulation/overactivation in these patients, it is possible that a shorter incubation with ODN 2006 (before transfer into the transwell migration chambers), may yield different responses. Perhaps an overnight stimulation leads to chronic activation and CLL cell exhaustion, akin to the well-characterised BCR-induced anergy in the M-CLL subgroup[80]. It is also unclear if U-CLL responses are static or whether they may change with disease progression. It would be interesting to track the migratory responses of U-CLL patients over time to identify whether sensitivity to TLR9 activation diminishes as the disease becomes more activated and more aggressive.

6.3: The Clinical Relevance of TLR9-Dependent CLL Cell Migration

Current BCR-targeted agents, such as ibrutinib, induce a large-scale redistribution of tissue-resident CLL cells into the peripheral blood and promote CLL cell apoptosis[165-167]. These agents however fail to achieve a complete systemic disease clearance and require an open-ended commitment to therapy[101]. This implies that targeting a single activation pathway is inadequate to eradicate disease and a dual targeted approach to treatment may be a more promising strategy. The identification of novel candidates for combinational therapies is therefore of paramount importance. This thesis presents evidence for the potential clinical benefit of TLR9 inhibition in conjunction with BCR inhibition. Such an approach may be of particular therapeutic benefit to the M-CLL Responder subgroup who show BTK-independent increases in CLL migration in response to TLR9 activation.

The Responder subgroup was comprised predominantly of M-CLL patients who demonstrate slower and less complete responses to treatment with ibrutinib relative to the U-CLL subgroup[165,166]. In a phase 1b-2 multicentre study, 33% of M-CLL and 77% of U-CLL patients achieved a partial or complete response (in the absence of lymphocytosis) after 24 months of follow-up[165]. If TLR9-driven migration was confirmed to be contributing factor to the reduced responses of M-CLL patients to ibrutinib, a combinational therapy targeted towards both BTK and TLR9 may enhance the lymphocyte redistribution and cytotoxicity of ibrutinib in this patient subgroup. M-CLL patients may therefore achieve deeper responses to ibrutinib-containing regimens.

Although the kinetics of ibrutinib-induced CLL cell death is relatively slow, circulating cellular debris is likely to be higher in plasma of ibrutinib-treated patients. Cellular debris contains TLR9-agonistic mtDNA[132], and therefore has the potential to promote TLR9-dependent CLL cell migration in a self-propagating manner. This effect will be true of all cytotoxic agents suggesting that TLR9 inhibition may be beneficial to a range of therapeutic combinations. In addition to migratory changes, TLR9 has been shown to antagonise the cytotoxic effect of Fludarabine[140] and a combination of ibrutinib + venetoclax[97] *in vitro*. Combinational therapies with TLR9 inhibition may therefore also improve the clinical efficacy of the current therapeutics.

The data also suggested a potentially latent mechanism of treatment resistance in the subpopulation of U-CLL Reverse Responder patients, where ODN 2006-stimulated **decreases** in CLL migration were reversed in the presence of ibrutinib; these patients may become TLR9 sensitised and therefore also benefit from TLR9-

inhibition. Patients who do not respond to TLR9 activation in the absence OR presence of ibrutinib, however, may represent a subgroup most likely to have an optimal response to single agent ibrutinib-containing treatments. These patients may not require additional targeted intervention. The ability to prospectively identify patients who will not completely respond to therapy would greatly aid clinical disease management and allow a more rational approach to treatment selection.

6.4: Medical Research Council-Funded Grant

Based on the data presented in this thesis, our group have been awarded funding from the Medical Research Council (MRC) to continue our investigations into TLR9 as a potential mechanism of resistance to targeted therapies in CLL. The project is entitled 'Overcoming ibrutinib and venetoclax resistance in Chronic Lymphocytic Leukaemia'. The project has three experimental aims which are briefly described below:

1. **Validation of an *in-vitro* Screening Tool to Predict Clinical Response to Ibrutinib ± Venetoclax.**

Migratory responses to TLR9 activation may influence the clinical outcome of CLL patients on treatment with current targeted therapeutics. We aim to test this hypothesis in a clinical trial setting and establish whether TLR9 responses can prospectively predict for post-treatment minimal residual disease (MRD) and clinical response (progression-free survival [PFS]). In order to carry out this work, we have been granted access to 200 treatment-naïve patient samples from the UK CLL FLAIR study, in which samples were collected prior to treatment-initiation and patients were randomised to one of four treatment arms i.e.,

- ibrutinib-alone
- ibritinib + rituximab
- ibrutinib + venetoclax
- fludarabine + cycloclophosphamide + rituximab.

Our research will focus on the three ibrutinib-containing arms of the study i.e., patients treated with ibrutinib alone or in combination with venetoclax or rituximab. The migratory response of each baseline sample to stimulation with ODN 2006 (± ibrutinib) will be assessed *in vitro* (as described throughout the thesis) and compared with clinical response data. This presents an exciting opportunity to observe the clinical outcome and MRD status of TLR9 Responder and Non/Reverse Responder groups and may help us to confirm the role of TLR9-stimulated migration in treatment-resistance. If successful, this would provide a simple stratification tool to identify patients most likely to achieve optimal responses to single agent therapy and those who may need additional targeted intervention.

2. <u>Identification of the Qualitative and Quantitative Differences in NF-κB Signalling in Drug Resistant CLL</u>

TLR9, BTK and BCL-2 all converge on NF-κB signalling, making NF-κB an attractive target candidate for the inhibition of all three pathways. As earlier described, Responder and Non/Reverse Responder patients may potentially differ in their activation of NF-κB signalling (i.e., either by distinct IκBα degradation patterns or subtype-specific subunit-usage). Initially, we will establish whether TLR9-induced canonical or non-canonical NF-κB activation occurs in the Responder and Non/Reverse Responder patients, when activated alone or in the presence of

ibrutinib (± venetoclax). The basal NF-κB dimer repertoire will also be assessed, as the level of NF-κB inhibition may depend on basal BCR signalling resulting in temporally distinct responses to the same stimuli. This will help us to link heterogeneous migratory responses with differential NF-κB signalling and potentially identify subgroup-specific druggable candidates. RNA sequencing will also be performed to compare the transcriptomic changes in ibrutinib (± venetoclax)-treated CLL cells to pinpoint mechanisms of TLR9-induced resistance.

3. **Rational Therapeutic Targeting of Drug Resistant CLL Through Systems Biology**

Our final aim is to integrate the data from our functional assays (Aim 1), signalling assays and gene expression experiments (Aim 2) through mechanistic mathematical modelling, with the help and expertise of Dr. Simon Mitchell. Inhibition of NF-κB itself would induce significant and intolerable toxicities and is therefore necessary to employ a more targeted approach and to identify promising downstream target genes. Using mathematical simulations, it is possible to computationally predict the efficacy of potential candidate genes, based on basal/inducible NF-κB patterns inferred from aim 2 above. The most promising candidates will then be subsequently verified in the laboratory.

It is hoped that this project will validate a clinically useful response predictor for ibrutinib ± venetoclax and also identify promising therapeutic strategies for drug-resistant patients. CLL is the most common leukaemia in the western world and although targeted therapies have revolutionised treatment, they are expensive, non-curative and some patients develop resistance. In the era of personalised medicine,

the challenge is to identify the right drugs for the right patients. This will ensure that patients get the best treatments whilst reducing healthcare costs associated with treatment failure.

References

1. Jaffe E. Pathology And Genetics Of Tumours Of Haematopoietic And Lymphoid Tissues: IARC Press; 2001.
2. van der Straten L, Levin MD, Visser O, et al. Survival continues to increase in chronic lymphocytic leukaemia: a population-based analysis among 20 468 patients diagnosed in the Netherlands between 1989 and 2016. *Br J Haematol*. 2020;189(3):574-577.
3. Puente XS, Bea S, Valdes-Mas R, et al. Non-coding recurrent mutations in chronic lymphocytic leukaemia. *Nature*. 2015;526(7574):519-524.
4. UK Cr. Chronic Lymphocytic Leukaemia (CLL) statistics; 2020.
5. Diehl LF, Karnell LH, Menck HR. The American College of Surgeons Commission on Cancer and the American Cancer Society. The National Cancer Data Base report on age, gender, treatment, and outcomes of patients with chronic lymphocytic leukemia. *Cancer*. 1999;86(12):2684-2692.
6. Redaelli A, Laskin BL, Stephens JM, Botteman MF, Pashos CL. The clinical and epidemiological burden of chronic lymphocytic leukaemia. *Eur J Cancer Care (Engl)*. 2004;13(3):279-287.
7. Hallek M, Cheson BD, Catovsky D, et al. iwCLL guidelines for diagnosis, indications for treatment, response assessment, and supportive management of CLL. *Blood*. 2018;131(25):2745-2760.
8. Rawstron AC, Kreuzer KA, Soosapilla A, et al. Reproducible diagnosis of chronic lymphocytic leukemia by flow cytometry: An European Research Initiative on CLL (ERIC) & European Society for Clinical Cell Analysis (ESCCA) Harmonisation project. *Cytometry B Clin Cytom*. 2018;94(1):121-128.
9. Rai KR, Sawitsky A, Cronkite EP, Chanana AD, Levy RN, Pasternack BS. Clinical staging of chronic lymphocytic leukemia. *Blood*. 1975;46(2):219-234.
10. Binet JL, Leporrier M, Dighiero G, et al. A clinical staging system for chronic lymphocytic leukemia: prognostic significance. *Cancer*. 1977;40(2):855-864.
11. Binet JL, Auquier A, Dighiero G, et al. A new prognostic classification of chronic lymphocytic leukemia derived from a multivariate survival analysis. *Cancer*. 1981;48(1):198-206.
12. Baliakas P, Mattsson M, Stamatopoulos K, Rosenquist R. Prognostic indices in chronic lymphocytic leukaemia: where do we stand how do we proceed? *J Intern Med*. 2016;279(4):347-357.
13. International CLLIPIwg. An international prognostic index for patients with chronic lymphocytic leukaemia (CLL-IPI): a meta-analysis of individual patient data. *Lancet Oncol*. 2016;17(6):779-790.
14. Eichhorst B, Fink AM, Bahlo J, et al. First-line chemoimmunotherapy with bendamustine and rituximab versus fludarabine, cyclophosphamide, and rituximab in patients with advanced chronic lymphocytic leukaemia (CLL10): an international, open-label, randomised, phase 3, non-inferiority trial. *Lancet Oncol*. 2016;17(7):928-942.
15. Montserrat E, Sanchez-Bisono J, Vinolas N, Rozman C. Lymphocyte doubling time in chronic lymphocytic leukaemia: analysis of its prognostic significance. *Br J Haematol*. 1986;62(3):567-575.
16. Pepper C, Majid A, Lin TT, et al. Defining the prognosis of early stage chronic lymphocytic leukaemia patients. *Br J Haematol*. 2012;156(4):499-507.
17. Damle RN, Wasil T, Fais F, et al. Ig V gene mutation status and CD38 expression as novel prognostic indicators in chronic lymphocytic leukemia. *Blood*. 1999;94(6):1840-1847.

18. Hamblin TJ, Davis Z, Gardiner A, Oscier DG, Stevenson FK. Unmutated Ig V(H) genes are associated with a more aggressive form of chronic lymphocytic leukemia. *Blood*. 1999;94(6):1848-1854.
19. Rassenti LZ, Huynh L, Toy TL, et al. ZAP-70 compared with immunoglobulin heavy-chain gene mutation status as a predictor of disease progression in chronic lymphocytic leukemia. *N Engl J Med*. 2004;351(9):893-901.
20. Fischer K, Bahlo J, Fink AM, et al. Long-term remissions after FCR chemoimmunotherapy in previously untreated patients with CLL: updated results of the CLL8 trial. *Blood*. 2016;127(2):208-215.
21. Dohner H, Stilgenbauer S, Benner A, et al. Genomic aberrations and survival in chronic lymphocytic leukemia. *N Engl J Med*. 2000;343(26):1910-1916.
22. Rossi D, Terzi-di-Bergamo L, De Paoli L, et al. Molecular prediction of durable remission after first-line fludarabine-cyclophosphamide-rituximab in chronic lymphocytic leukemia. *Blood*. 2015;126(16):1921-1924.
23. Landau DA, Tausch E, Taylor-Weiner AN, et al. Mutations driving CLL and their evolution in progression and relapse. *Nature*. 2015;526(7574):525-530.
24. Hallek M, Wanders L, Ostwald M, et al. Serum beta(2)-microglobulin and serum thymidine kinase are independent predictors of progression-free survival in chronic lymphocytic leukemia and immunocytoma. *Leuk Lymphoma*. 1996;22(5-6):439-447.
25. Del Poeta G, Maurillo L, Venditti A, et al. Clinical significance of CD38 expression in chronic lymphocytic leukemia. *Blood*. 2001;98(9):2633-2639.
26. Riches JC, O'Donovan CJ, Kingdon SJ, et al. Trisomy 12 chronic lymphocytic leukemia cells exhibit upregulation of integrin signaling that is modulated by NOTCH1 mutations. *Blood*. 2014;123(26):4101-4110.
27. Bulian P, Shanafelt TD, Fegan C, et al. CD49d is the strongest flow cytometry-based predictor of overall survival in chronic lymphocytic leukemia. *J Clin Oncol*. 2014;32(9):897-904.
28. Pepper C, Buggins AG, Jones CH, et al. Phenotypic heterogeneity in IGHV-mutated CLL patients has prognostic impact and identifies a subset with increased sensitivity to BTK and PI3Kdelta inhibition. *Leukemia*. 2015;29(3):744-747.
29. Herling CD, Cymbalista F, Gross-Ophoff-Muller C, et al. Early treatment with FCR versus watch and wait in patients with stage Binet A high-risk chronic lymphocytic leukemia (CLL): a randomized phase 3 trial. *Leukemia*. 2020;34(8):2038-2050.
30. Landau DA, Carter SL, Stojanov P, et al. Evolution and impact of subclonal mutations in chronic lymphocytic leukemia. *Cell*. 2013;152(4):714-726.
31. Burger JA, Landau DA, Taylor-Weiner A, et al. Clonal evolution in patients with chronic lymphocytic leukaemia developing resistance to BTK inhibition. *Nat Commun*. 2016;7:11589.
32. Levin TT, Li Y, Riskind J, Rai K. Depression, anxiety and quality of life in a chronic lymphocytic leukemia cohort. *Gen Hosp Psychiatry*. 2007;29(3):251-256.
33. Agrawal D, Sarode R. Complete Blood Count or Complete Blood Count with Differential: What's the Difference? *Am J Med*. 2017;130(8):915-916.
34. Watson CT, Glanville J, Marasco WA. The Individual and Population Genetics of Antibody Immunity. *Trends Immunol*. 2017;38(7):459-470.
35. Pilzecker B, Jacobs H. Mutating for Good: DNA Damage Responses During Somatic Hypermutation. *Front Immunol*. 2019;10:438.
36. Roth DB. V(D)J Recombination: Mechanism, Errors, and Fidelity. *Microbiol Spectr*. 2014;2(6).
37. Teng G, Papavasiliou FN. Immunoglobulin somatic hypermutation. *Annu Rev Genet*. 2007;41:107-120.

38. Dal Porto JM, Gauld SB, Merrell KT, Mills D, Pugh-Bernard AE, Cambier J. B cell antigen receptor signaling 101. *Mol Immunol*. 2004;41(6-7):599-613.
39. Girard JP, Moussion C, Forster R. HEVs, lymphatics and homeostatic immune cell trafficking in lymph nodes. *Nat Rev Immunol*. 2012;12(11):762-773.
40. Herishanu Y, Perez-Galan P, Liu D, et al. The lymph node microenvironment promotes B-cell receptor signaling, NF-kappaB activation, and tumor proliferation in chronic lymphocytic leukemia. *Blood*. 2011;117(2):563-574.
41. Lafouresse F, Bellard E, Laurent C, et al. L-selectin controls trafficking of chronic lymphocytic leukemia cells in lymph node high endothelial venules in vivo. *Blood*. 2015;126(11):1336-1345.
42. Till KJ, Spiller DG, Harris RJ, Chen H, Zuzel M, Cawley JC. CLL, but not normal, B cells are dependent on autocrine VEGF and alpha4beta1 integrin for chemokine-induced motility on and through endothelium. *Blood*. 2005;105(12):4813-4819.
43. Seifert M, Sellmann L, Bloehdorn J, et al. Cellular origin and pathophysiology of chronic lymphocytic leukemia. *J Exp Med*. 2012;209(12):2183-2198.
44. Kulis M, Heath S, Bibikova M, et al. Epigenomic analysis detects widespread gene-body DNA hypomethylation in chronic lymphocytic leukemia. *Nat Genet*. 2012;44(11):1236-1242.
45. Oakes CC, Seifert M, Assenov Y, et al. DNA methylation dynamics during B cell maturation underlie a continuum of disease phenotypes in chronic lymphocytic leukemia. *Nat Genet*. 2016;48(3):253-264.
46. Cimmino A, Calin GA, Fabbri M, et al. miR-15 and miR-16 induce apoptosis by targeting BCL2. *Proc Natl Acad Sci U S A*. 2005;102(39):13944-13949.
47. Klein U, Lia M, Crespo M, et al. The DLEU2/miR-15a/16-1 cluster controls B cell proliferation and its deletion leads to chronic lymphocytic leukemia. *Cancer Cell*. 2010;17(1):28-40.
48. Fabbri M, Bottoni A, Shimizu M, et al. Association of a microRNA/TP53 feedback circuitry with pathogenesis and outcome of B-cell chronic lymphocytic leukemia. *JAMA*. 2011;305(1):59-67.
49. Brady CA, Attardi LD. p53 at a glance. *J Cell Sci*. 2010;123(Pt 15):2527-2532.
50. Van Dyke DL, Shanafelt TD, Call TG, et al. A comprehensive evaluation of the prognostic significance of 13q deletions in patients with B-chronic lymphocytic leukaemia. *Br J Haematol*. 2010;148(4):544-550.
51. Parker H, Rose-Zerilli MJ, Parker A, et al. 13q deletion anatomy and disease progression in patients with chronic lymphocytic leukemia. *Leukemia*. 2011;25(3):489-497.
52. Dohner H, Stilgenbauer S, James MR, et al. 11q deletions identify a new subset of B-cell chronic lymphocytic leukemia characterized by extensive nodal involvement and inferior prognosis. *Blood*. 1997;89(7):2516-2522.
53. Rossi D, Gaidano G. The clinical implications of gene mutations in chronic lymphocytic leukaemia. *Br J Cancer*. 2016;114(8):849-854.
54. Austen B, Skowronska A, Baker C, et al. Mutation status of the residual ATM allele is an important determinant of the cellular response to chemotherapy and survival in patients with chronic lymphocytic leukemia containing an 11q deletion. *J Clin Oncol*. 2007;25(34):5448-5457.
55. Rossi D, Fangazio M, Rasi S, et al. Disruption of BIRC3 associates with fludarabine chemorefractoriness in TP53 wild-type chronic lymphocytic leukemia. *Blood*. 2012;119(12):2854-2862.
56. Zucchetto A, Caldana C, Benedetti D, et al. CD49d is overexpressed by trisomy 12 chronic lymphocytic leukemia cells: evidence for a methylation-dependent regulation mechanism. *Blood*. 2013;122(19):3317-3321.

57. Liso V, Capalbo S, Lapietra A, Pavone V, Guarini A, Specchia G. Evaluation of trisomy 12 by fluorescence in situ hybridization in peripheral blood, bone marrow and lymph nodes of patients with B-cell chronic lymphocytic leukemia. *Haematologica*. 1999;84(3):212-217.
58. Till KJ, Lin K, Zuzel M, Cawley JC. The chemokine receptor CCR7 and alpha4 integrin are important for migration of chronic lymphocytic leukemia cells into lymph nodes. *Blood*. 2002;99(8):2977-2984.
59. Walsby E, Buggins A, Devereux S, et al. Development and characterization of a physiologically relevant model of lymphocyte migration in chronic lymphocytic leukemia. *Blood*. 2014;123(23):3607-3617.
60. Pasikowska M, Walsby E, Apollonio B, et al. Phenotype and immune function of lymph node and peripheral blood CLL cells are linked to transendothelial migration. *Blood*. 2016;128(4):563-573.
61. Gonzalez-Gascon YMI, Hernandez-Sanchez M, Rodriguez-Vicente AE, et al. A high proportion of cells carrying trisomy 12 is associated with a worse outcome in patients with chronic lymphocytic leukemia. *Hematol Oncol*. 2016;34(2):84-92.
62. Mittal AK, Chaturvedi NK, Rai KJ, et al. Chronic lymphocytic leukemia cells in a lymph node microenvironment depict molecular signature associated with an aggressive disease. *Mol Med*. 2014;20:290-301.
63. Plander M, Seegers S, Ugocsai P, et al. Different proliferative and survival capacity of CLL-cells in a newly established in vitro model for pseudofollicles. *Leukemia*. 2009;23(11):2118-2128.
64. Buggins AG, Pepper C, Patten PE, et al. Interaction with vascular endothelium enhances survival in primary chronic lymphocytic leukemia cells via NF-kappaB activation and de novo gene transcription. *Cancer Res*. 2010;70(19):7523-7533.
65. Hamilton E, Pearce L, Morgan L, et al. Mimicking the tumour microenvironment: three different co-culture systems induce a similar phenotype but distinct proliferative signals in primary chronic lymphocytic leukaemia cells. *Br J Haematol*. 2012;158(5):589-599.
66. Mangolini M, Gotte F, Moore A, et al. Notch2 controls non-autonomous Wnt-signalling in chronic lymphocytic leukaemia. *Nat Commun*. 2018;9(1):3839.
67. Chiorazzi N. Cell proliferation and death: forgotten features of chronic lymphocytic leukemia B cells. *Best Pract Res Clin Haematol*. 2007;20(3):399-413.
68. Andreeff M, Darzynkiewicz Z, Sharpless TK, Clarkson BD, Melamed MR. Discrimination of human leukemia subtypes by flow cytometric analysis of cellular DNA and RNA. *Blood*. 1980;55(2):282-293.
69. Ten Hacken E, Burger JA. Microenvironment interactions and B-cell receptor signaling in Chronic Lymphocytic Leukemia: Implications for disease pathogenesis and treatment. *Biochim Biophys Acta*. 2016;1863(3):401-413.
70. Burger JA, Quiroga MP, Hartmann E, et al. High-level expression of the T-cell chemokines CCL3 and CCL4 by chronic lymphocytic leukemia B cells in nurselike cell cocultures and after BCR stimulation. *Blood*. 2009;113(13):3050-3058.
71. Buggins AG, Patten PE, Richards J, Thomas NS, Mufti GJ, Devereux S. Tumor-derived IL-6 may contribute to the immunological defect in CLL. *Leukemia*. 2008;22(5):1084-1087.
72. Park E, Chen J, Moore A, et al. Stromal cell protein kinase C-beta inhibition enhances chemosensitivity in B cell malignancies and overcomes drug resistance. *Sci Transl Med*. 2020;12(526).
73. Buggins AG, Pepper CJ. The role of Bcl-2 family proteins in chronic lymphocytic leukaemia. *Leuk Res*. 2010;34(7):837-842.
74. Brachtl G, Pinon Hofbauer J, Greil R, Hartmann TN. The pathogenic relevance of the prognostic markers CD38 and CD49d in chronic lymphocytic leukemia. *Ann Hematol*. 2014;93(3):361-374.

75. Majid A, Lin TT, Best G, et al. CD49d is an independent prognostic marker that is associated with CXCR4 expression in CLL. *Leuk Res*. 2011;35(6):750-756.
76. Burger JA. Chemokines and chemokine receptors in chronic lymphocytic leukemia (CLL): from understanding the basics towards therapeutic targeting. *Semin Cancer Biol*. 2010;20(6):424-430.
77. Redondo-Munoz J, Jose Terol M, Garcia-Marco JA, Garcia-Pardo A. Matrix metalloproteinase-9 is up-regulated by CCL21/CCR7 interaction via extracellular signal-regulated kinase-1/2 signaling and is involved in CCL21-driven B-cell chronic lymphocytic leukemia cell invasion and migration. *Blood*. 2008;111(1):383-386.
78. Rosen A, Murray F, Evaldsson C, Rosenquist R. Antigens in chronic lymphocytic leukemia--implications for cell origin and leukemogenesis. *Semin Cancer Biol*. 2010;20(6):400-409.
79. Herve M, Xu K, Ng YS, et al. Unmutated and mutated chronic lymphocytic leukemias derive from self-reactive B cell precursors despite expressing different antibody reactivity. *J Clin Invest*. 2005;115(6):1636-1643.
80. Packham G, Krysov S, Allen A, et al. The outcome of B-cell receptor signaling in chronic lymphocytic leukemia: proliferation or anergy. *Haematologica*. 2014;99(7):1138-1148.
81. Chen L, Widhopf G, Huynh L, et al. Expression of ZAP-70 is associated with increased B-cell receptor signaling in chronic lymphocytic leukemia. *Blood*. 2002;100(13):4609-4614.
82. Rosenwald A, Alizadeh AA, Widhopf G, et al. Relation of gene expression phenotype to immunoglobulin mutation genotype in B cell chronic lymphocytic leukemia. *J Exp Med*. 2001;194(11):1639-1647.
83. Coscia M, Pantaleoni F, Riganti C, et al. IGHV unmutated CLL B cells are more prone to spontaneous apoptosis and subject to environmental prosurvival signals than mutated CLL B cells. *Leukemia*. 2011;25(5):828-837.
84. Lanham S, Hamblin T, Oscier D, Ibbotson R, Stevenson F, Packham G. Differential signaling via surface IgM is associated with VH gene mutational status and CD38 expression in chronic lymphocytic leukemia. *Blood*. 2003;101(3):1087-1093.
85. Guarini A, Chiaretti S, Tavolaro S, et al. BCR ligation induced by IgM stimulation results in gene expression and functional changes only in IgV H unmutated chronic lymphocytic leukemia (CLL) cells. *Blood*. 2008;112(3):782-792.
86. Puente XS, Pinyol M, Quesada V, et al. Whole-genome sequencing identifies recurrent mutations in chronic lymphocytic leukaemia. *Nature*. 2011;475(7354):101-105.
87. Baliakas P, Hadzidimitriou A, Agathangelidis A, et al. Prognostic relevance of MYD88 mutations in CLL: the jury is still out. *Blood*. 2015;126(8):1043-1044.
88. Qin SC, Xia Y, Miao Y, et al. MYD88 mutations predict unfavorable prognosis in Chronic Lymphocytic Leukemia patients with mutated IGHV gene. *Blood Cancer J*. 2017;7(12):651.
89. Muzio M, Scielzo C, Bertilaccio MT, Frenquelli M, Ghia P, Caligaris-Cappio F. Expression and function of toll like receptors in chronic lymphocytic leukaemia cells. *Br J Haematol*. 2009;144(4):507-516.
90. De Nardo D. Toll-like receptors: Activation, signalling and transcriptional modulation. *Cytokine*. 2015;74(2):181-189.
91. Ruprecht CR, Lanzavecchia A. Toll-like receptor stimulation as a third signal required for activation of human naive B cells. *Eur J Immunol*. 2006;36(4):810-816.
92. Gimenez N, Schulz R, Higashi M, et al. Targeting IRAK4 disrupts inflammatory pathways and delays tumor development in chronic lymphocytic leukemia. *Leukemia*. 2020;34(1):100-114.

93. Dadashian EL, McAuley EM, Liu D, et al. TLR Signaling Is Activated in Lymph Node-Resident CLL Cells and Is Only Partially Inhibited by Ibrutinib. *Cancer Res*. 2019;79(2):360-371.
94. Bertilaccio MT, Simonetti G, Dagklis A, et al. Lack of TIR8/SIGIRR triggers progression of chronic lymphocytic leukemia in mouse models. *Blood*. 2011;118(3):660-669.
95. Chan TS, Lee YS, Del Giudice I, et al. Clinicopathological features and outcome of chronic lymphocytic leukaemia in Chinese patients. *Oncotarget*. 2017;8(15):25455-25468.
96. Mansouri L, Papakonstantinou N, Ntoufa S, Stamatopoulos K, Rosenquist R. NF-kappaB activation in chronic lymphocytic leukemia: A point of convergence of external triggers and intrinsic lesions. *Semin Cancer Biol*. 2016;39:40-48.
97. Jayappa KD, Portell CA, Gordon VL, et al. Microenvironmental agonists generate de novo phenotypic resistance to combined ibrutinib plus venetoclax in CLL and MCL. *Blood Adv*. 2017;1(14):933-946.
98. Shih VF, Tsui R, Caldwell A, Hoffmann A. A single NFkappaB system for both canonical and non-canonical signaling. *Cell Res*. 2011;21(1):86-102.
99. Rai KR, Jain P. Chronic lymphocytic leukemia (CLL)-Then and now. *Am J Hematol*. 2016;91(3):330-340.
100. Thompson PA, Tam CS, O'Brien SM, et al. Fludarabine, cyclophosphamide, and rituximab treatment achieves long-term disease-free survival in IGHV-mutated chronic lymphocytic leukemia. *Blood*. 2016;127(3):303-309.
101. O'Brien S, Furman RR, Coutre S, et al. Single-agent ibrutinib in treatment-naive and relapsed/refractory chronic lymphocytic leukemia: a 5-year experience. *Blood*. 2018;131(17):1910-1919.
102. Sharma S, Rai KR. Chronic lymphocytic leukemia (CLL) treatment: So many choices, such great options. *Cancer*. 2019;125(9):1432-1440.
103. Anderson MA, Deng J, Seymour JF, et al. The BCL2 selective inhibitor venetoclax induces rapid onset apoptosis of CLL cells in patients via a TP53-independent mechanism. *Blood*. 2016;127(25):3215-3224.
104. Yosifov DY, Wolf C, Stilgenbauer S, Mertens D. From Biology to Therapy: The CLL Success Story. *Hemasphere*. 2019;3(2):e175.
105. Robak T, Robak P. BCR signaling in chronic lymphocytic leukemia and related inhibitors currently in clinical studies. *Int Rev Immunol*. 2013;32(4):358-376.
106. Shanafelt TD, Wang XV, Kay NE, et al. Ibrutinib-Rituximab or Chemoimmunotherapy for Chronic Lymphocytic Leukemia. *N Engl J Med*. 2019;381(5):432-443.
107. Hampel PJ, Call TG, Rabe KG, et al. Disease Flare During Temporary Interruption of Ibrutinib Therapy in Patients with Chronic Lymphocytic Leukemia. *Oncologist*. 2020;25(11):974-980.
108. Lampson BL, Yu L, Glynn RJ, et al. Ventricular arrhythmias and sudden death in patients taking ibrutinib. *Blood*. 2017;129(18):2581-2584.
109. Woyach JA, Furman RR, Liu TM, et al. Resistance mechanisms for the Bruton's tyrosine kinase inhibitor ibrutinib. *N Engl J Med*. 2014;370(24):2286-2294.
110. Woyach JA, Ruppert AS, Guinn D, et al. BTK(C481S)-Mediated Resistance to Ibrutinib in Chronic Lymphocytic Leukemia. *J Clin Oncol*. 2017;35(13):1437-1443.
111. Quinquenel A, Fornecker LM, Letestu R, et al. Prevalence of BTK and PLCG2 mutations in a real-life CLL cohort still on ibrutinib after 3 years: a FILO group study. *Blood*. 2019;134(7):641-644.
112. Sedlarikova L, Petrackova A, Papajik T, Turcsanyi P, Kriegova E. Resistance-Associated Mutations in Chronic Lymphocytic Leukemia Patients Treated With Novel Agents. *Front Oncol*. 2020;10:894.

113. Berglof A, Hamasy A, Meinke S, et al. Targets for Ibrutinib Beyond B Cell Malignancies. *Scand J Immunol*. 2015;82(3):208-217.
114. Awan FT, Schuh A, Brown JR, et al. Acalabrutinib monotherapy in patients with chronic lymphocytic leukemia who are intolerant to ibrutinib. *Blood Adv*. 2019;3(9):1553-1562.
115. Bose P, Gandhi V. Managing chronic lymphocytic leukemia in 2020: an update on recent clinical advances with a focus on BTK and BCL-2 inhibitors. *Fac Rev*. 2021;10:22.
116. Woyach J, Huang, Y., Rogers, K., Bhat, S., Grever, M., Lozanski, A., Doong, T., Blachly, J., Lozanski, G., Jones, D. and Byrd, J. Resistance to Acalabrutinib in CLL Is Mediated Primarily By BTK Mutations. *Blood*. 2019;134:504.
117. Naeem A, Nguy, W., Tyekucheva, S., Fernandes, S., Rai, V., Ebata, K., Gomez, E., Brandhuber, B., Rothenberg, S. and Brown, J. LOXO-305: Targeting C481S Bruton Tyrosine Kinase in Patients with Ibrutinib-Resistant CLL. *Blood*. 2019;134:478.
118. Mato AR, Flinn, I.W., Pagel, J.M., Brown, J.R., Cheah, C.Y., Coombs, C.C., Patel, M.R. Rothenberg,S.M., Tsai, D.E., Ku, N.C., Wang, M.L. Results from a First-in-Human, Proof-of-Concept Phase 1 Trial in Pretreated B-Cell Malignancies for Loxo-305, a Next-Generation, Highly Selective, Non-Covalent BTK Inhibitor. *Blood*. 2019;134 501.
119. Durani U, Hogan WJ. Emergencies in haematology: tumour lysis syndrome. *Br J Haematol*. 2020;188(4):494-500.
120. Roberts AW, Davids MS, Pagel JM, et al. Targeting BCL2 with Venetoclax in Relapsed Chronic Lymphocytic Leukemia. *N Engl J Med*. 2016;374(4):311-322.
121. Jain N, Keating M, Thompson P, et al. Ibrutinib and Venetoclax for First-Line Treatment of CLL. *N Engl J Med*. 2019;380(22):2095-2103.
122. Hemmi H, Takeuchi O, Kawai T, et al. A Toll-like receptor recognizes bacterial DNA. *Nature*. 2000;408(6813):740-745.
123. Bekeredjian-Ding I, Doster A, Schiller M, et al. TLR9-activating DNA up-regulates ZAP70 via sustained PKB induction in IgM+ B cells. *J Immunol*. 2008;181(12):8267-8277.
124. Bernasconi NL, Onai N, Lanzavecchia A. A role for Toll-like receptors in acquired immunity: up-regulation of TLR9 by BCR triggering in naive B cells and constitutive expression in memory B cells. *Blood*. 2003;101(11):4500-4504.
125. Lanzavecchia A, Bernasconi N, Traggiai E, Ruprecht CR, Corti D, Sallusto F. Understanding and making use of human memory B cells. *Immunol Rev*. 2006;211:303-309.
126. Grandjenette C, Kennel A, Faure GC, Bene MC, Feugier P. Expression of functional toll-like receptors by B-chronic lymphocytic leukemia cells. *Haematologica*. 2007;92(9):1279-1281.
127. Barton GM, Kagan JC, Medzhitov R. Intracellular localization of Toll-like receptor 9 prevents recognition of self DNA but facilitates access to viral DNA. *Nat Immunol*. 2006;7(1):49-56.
128. Latz E, Schoenemeyer A, Visintin A, et al. TLR9 signals after translocating from the ER to CpG DNA in the lysosome. *Nat Immunol*. 2004;5(2):190-198.
129. Ahmad-Nejad P, Hacker H, Rutz M, Bauer S, Vabulas RM, Wagner H. Bacterial CpG-DNA and lipopolysaccharides activate Toll-like receptors at distinct cellular compartments. *Eur J Immunol*. 2002;32(7):1958-1968.
130. Ewald SE, Lee BL, Lau L, et al. The ectodomain of Toll-like receptor 9 is cleaved to generate a functional receptor. *Nature*. 2008;456(7222):658-662.
131. Lee BL, Moon JE, Shu JH, et al. UNC93B1 mediates differential trafficking of endosomal TLRs. *Elife*. 2013;2:e00291.
132. Kennedy E, Coulter EM, Halliwell E, et al. TLR9 expression in Chronic Lymphocytic Leukemia identifies a pro-migratory subpopulation and novel therapeutic target. *Blood*. 2021.

133. Riley JS, Tait SW. Mitochondrial DNA in inflammation and immunity. *EMBO Rep*. 2020;21(4):e49799.
134. Yeh P, Hunter T, Sinha D, et al. Circulating tumour DNA reflects treatment response and clonal evolution in chronic lymphocytic leukaemia. *Nat Commun*. 2017;8:14756.
135. Karlin S, Ladunga I, Blaisdell BE. Heterogeneity of genomes: measures and values. *Proc Natl Acad Sci U S A*. 1994;91(26):12837-12841.
136. Liu B, Du Q, Chen L, et al. CpG methylation patterns of human mitochondrial DNA. *Sci Rep*. 2016;6:23421.
137. Ingelsson B, Soderberg D, Strid T, et al. Lymphocytes eject interferogenic mitochondrial DNA webs in response to CpG and non-CpG oligodeoxynucleotides of class C. *Proc Natl Acad Sci U S A*. 2018;115(3):E478-E487.
138. Longo PG, Laurenti L, Gobessi S, et al. The Akt signaling pathway determines the different proliferative capacity of chronic lymphocytic leukemia B-cells from patients with progressive and stable disease. *Leukemia*. 2007;21(1):110-120.
139. Tarnani M, Laurenti L, Longo PG, et al. The proliferative response to CpG-ODN stimulation predicts PFS, TTT and OS in patients with chronic lymphocytic leukemia. *Leuk Res*. 2010;34(9):1189-1194.
140. Fonte E, Apollonio B, Scarfo L, et al. In vitro sensitivity of CLL cells to fludarabine may be modulated by the stimulation of Toll-like receptors. *Clin Cancer Res*. 2013;19(2):367-379.
141. Xu L, Zhou Y, Liu Q, et al. CXCR4/SDF-1 pathway is crucial for TLR9 agonist enhanced metastasis of human lung cancer cell. *Biochem Biophys Res Commun*. 2009;382(3):571-576.
142. Merrell MA, Ilvesaro JM, Lehtonen N, et al. Toll-like receptor 9 agonists promote cellular invasion by increasing matrix metalloproteinase activity. *Mol Cancer Res*. 2006;4(7):437-447.
143. Ilvesaro JM, Merrell MA, Swain TM, et al. Toll like receptor-9 agonists stimulate prostate cancer invasion in vitro. *Prostate*. 2007;67(7):774-781.
144. Luo Y, Jiang QW, Wu JY, et al. Regulation of migration and invasion by Toll-like receptor-9 signaling network in prostate cancer. *Oncotarget*. 2015;6(26):22564-22574.
145. Qin XR, Wu J, Yao XY, Huang J, Wang XY. Helicobacter pylori DNA promotes cellular proliferation, migration, and invasion of gastric cancer by activating toll-like receptor 9. *Saudi J Gastroenterol*. 2019;25(3):181-187.
146. Parikh SA, Rabe KG, Kay NE, et al. Chronic lymphocytic leukemia in young (</= 55 years) patients: a comprehensive analysis of prognostic factors and outcomes. *Haematologica*. 2014;99(1):140-147.
147. Excellence NIfHaC. Appraisal consultation document – Ibrutinib for treating chronic lymphocytic leukaemia; 2016.
148. Redondo-Munoz J, Ugarte-Berzal E, Garcia-Marco JA, et al. Alpha4beta1 integrin and 190-kDa CD44v constitute a cell surface docking complex for gelatinase B/MMP-9 in chronic leukemic but not in normal B cells. *Blood*. 2008;112(1):169-178.
149. Buggins AG, Levi A, Gohil S, et al. Evidence for a macromolecular complex in poor prognosis CLL that contains CD38, CD49d, CD44 and MMP-9. *Br J Haematol*. 2011;154(2):216-222.
150. Calissano C, Damle RN, Marsilio S, et al. Intraclonal complexity in chronic lymphocytic leukemia: fractions enriched in recently born/divided and older/quiescent cells. *Mol Med*. 2011;17(11-12):1374-1382.
151. Jahrsdorfer B, Wooldridge JE, Blackwell SE, et al. Immunostimulatory oligodeoxynucleotides induce apoptosis of B cell chronic lymphocytic leukemia cells. *J Leukoc Biol*. 2005;77(3):378-387.

152. Brinkmann MM, Spooner E, Hoebe K, Beutler B, Ploegh HL, Kim YM. The interaction between the ER membrane protein UNC93B and TLR3, 7, and 9 is crucial for TLR signaling. *J Cell Biol*. 2007;177(2):265-275.
153. Droemann D, Albrecht D, Gerdes J, et al. Human lung cancer cells express functionally active Toll-like receptor 9. *Respir Res*. 2005;6:1.
154. Eagle GL, Zhuang J, Jenkins RE, et al. Total proteome analysis identifies migration defects as a major pathogenetic factor in immunoglobulin heavy chain variable region (IGHV)-unmutated chronic lymphocytic leukemia. *Mol Cell Proteomics*. 2015;14(4):933-945.
155. Ziegler CGK, Kim J, Piersanti K, et al. Constitutive Activation of the B Cell Receptor Underlies Dysfunctional Signaling in Chronic Lymphocytic Leukemia. *Cell Rep*. 2019;28(4):923-937 e923.
156. Quiroga MP, Balakrishnan K, Kurtova AV, et al. B-cell antigen receptor signaling enhances chronic lymphocytic leukemia cell migration and survival: specific targeting with a novel spleen tyrosine kinase inhibitor, R406. *Blood*. 2009;114(5):1029-1037.
156b. Chaturvedi A, Dorward D, Pierce SK. The B cell receptor governs the subcellular location of Toll-like receptor 9 leading to hyperresponses to DNA-containing antigens. *Immunity*. 2008;6:799-809.
157. Morbach H, Schickel JN, Cunningham-Rundles C, et al. CD19 controls Toll-like receptor 9 responses in human B cells. *J Allergy Clin Immunol*. 2016;137(3):889-898 e886.
158. Wagner M, Oelsner M, Moore A, et al. Integration of innate into adaptive immune responses in ZAP-70-positive chronic lymphocytic leukemia. *Blood*. 2016;127(4):436-448.
159. Friedman DR, Guadalupe E, Volkheimer A, Moore JO, Weinberg JB. Clinical outcomes in chronic lymphocytic leukaemia associated with expression of CD5, a negative regulator of B-cell receptor signalling. *Br J Haematol*. 2018;183(5):747-754.
160. Nickerson KM, Christensen SR, Cullen JL, Meng W, Luning Prak ET, Shlomchik MJ. TLR9 promotes tolerance by restricting survival of anergic anti-DNA B cells, yet is also required for their activation. *J Immunol*. 2013;190(4):1447-1456.
161. Butcher SK, O'Carroll CE, Wells CA, Carmody RJ. Toll-Like Receptors Drive Specific Patterns of Tolerance and Training on Restimulation of Macrophages. *Front Immunol*. 2018;9:933.
162. Brophy S, Quinn, F.M., O'Brien D., Browne, P., Vandenberghe, E., McElligott, A. The Regulation of STAT3 and Its Role in the Adhesion and Migration of Chronic Lymphocytic Leukaemia Cells. *Blood*. 2016;128(2).
163. Liang X, Moseman EA, Farrar MA, et al. Toll-like receptor 9 signaling by CpG-B oligodeoxynucleotides induces an apoptotic pathway in human chronic lymphocytic leukemia B cells. *Blood*. 2010;115(24):5041-5052.
164. Dampmann M, Gorgens A, Mollmann M, et al. CpG stimulation of chronic lymphocytic leukemia cells induces a polarized cell shape and promotes migration in vitro and in vivo. *PLoS One*. 2020;15(2):e0228674.
165. Byrd JC, Furman RR, Coutre SE, et al. Targeting BTK with ibrutinib in relapsed chronic lymphocytic leukemia. *N Engl J Med*. 2013;369(1):32-42.
166. Burger JA, Li KW, Keating MJ, et al. Leukemia cell proliferation and death in chronic lymphocytic leukemia patients on therapy with the BTK inhibitor ibrutinib. *JCI Insight*. 2017;2(2):e89904.
167. Byrd JC, Furman RR, Coutre SE, et al. Three-year follow-up of treatment-naive and previously treated patients with CLL and SLL receiving single-agent ibrutinib. *Blood*. 2015;125(16):2497-2506.
168. Kuse R, Schuster S, Schubbe H, Dix S, Hausmann K. Blood lymphocyte volumes and diameters in patients with chronic lymphocytic leukemia and normal controls. *Blut*. 1985;50(4):243-248.

7.0: Appendices

7.1: Optimisation of TLR9 Agonist ODN 2006

An initial optimisation was required to identify the correct conditions for the stimulation of primary CLL cells with ODN 2006; these experiments were performed in duplicate using isolated PBMCs from three CLL patients. For each patient, PBMC aliquots were split into two fractions: fresh (i.e., <24h post venesection) and frozen (i.e., freeze-thawed aliquots from liquid nitrogen). It was important to confirm the reproducibility of results in frozen samples since many of the experiments in this project were performed using archived PBMC samples.

PBMCs were stimulated with 0μM (unstimulated); 0.5μM; 1.0μM; 2.0μM or 5.0μM ODN 2006 and incubated for 24h or 48h (see methods section 2.11) before being collected and stained for phenotypic analysis. PBMCs were stained for the cell surface markers: CD5 and CD19 (CLL cell identification), CD69 (CLL cell activation), CD49d and CD38 (CLL cell adhesion/migration); a fixable viability dye (FVD) was also included to assess changes in CLL cell viability (Antibody Panel A: LSR II, Table 2.1). These optimisation experiments were performed using the LSR II flow cytometer and were analysed using FACsDiva software. Live CLL cells were gated as CD5+/CD19+/FVD-.

At 24h post-stimulation, ODN 2006 had no effect on the viability of fresh or frozen CLL samples at any of the tested concentrations (Figure 7.1). At 48h post stimulation, both fresh and frozen samples showed a decline in viability relative to the 24h timepoint and this was most marked in the frozen cohort for which the viability of

one patient sample had decreased from ~50% (24h) to ~25% (48h). For each condition, the mean viability (± SD) is outlined in Table 7.1.

Given the reduced viability observed at the 48h timepoint, further experiments were designed to terminate within a 24h period.

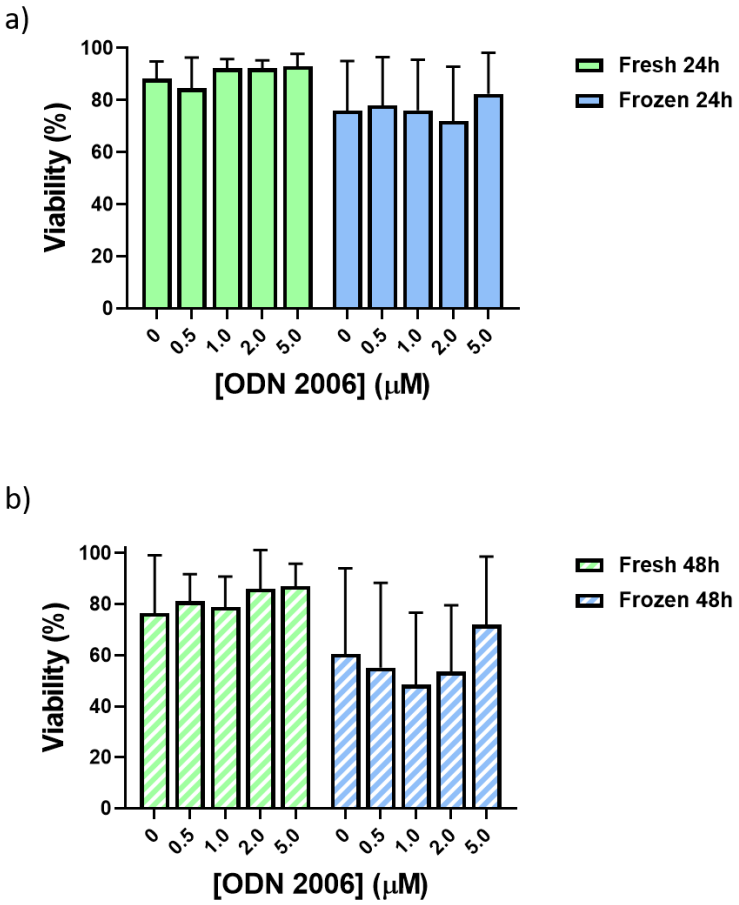

Figure 7.1: ODN 2006 Optimisation: The Effect of ODN 2006 on CLL Cell Viability. Primary PBMCs were stimulated with 0-5μM ODN 2006 (TLR9 agonist) in complete media + IL-4 and incubated for 24h or 48h at 37°C/5% CO_2. These experiments were performed in both fresh (i.e., <24h post-venesection) and frozen (i.e., freeze-thawed from liquid nitrogen) PBMCs to enable matched comparisons (n=5, from 3 individual patients). Post stimulation, the cells were stained with a fixable viability dye (FVD) and CLL cell viability was assessed by flow cytometry using an LSR II flow cytometer; viable CLL cells were gated as CD5+/CD19+/FVD- and phenotypic analysis was performed using FACs Diva software. a) At 24h, ODN 2006 did not show a dose dependent effect upon cell viability in either the fresh or frozen samples. b) At 48h incubation, viability was reduced relative to the 24h timepoint.

Table 7.1: Optimisation of ODN 2006: CLL Cell Viability

	Viability (Mean % ±SD)			
[ODN 2006] (μM)	**Fresh (24h)**	**Frozen (24h)**	**Fresh (48h)**	**Frozen (48h)**
0	88.2 (±6.7)	76.0 (±19.0)	76.5 (±22.6)	60.6 (±33.5)
0.5	84.6 (±11.8)	78.0 (±18.5)	81.2 (±10.6)	55.1 (±33.2)
1.0	92.3 (±3.5)	76.2 (±9.4)	79.0 (±11.9)	48.5 (±28.2)
2.0	92.3 (±3.0)	72.0 (±20.9)	86.1 (±15.1)	53.5 (± 26.1)
5.0	92.0 (±4.7)	82.5 (±15.8)	87.1 (±8.7)	72.1 (± 26.6)

All conditions: n=5 from 3 individual patients.

The observed changes in cell surface marker expression appeared very similar across all of the tested concentrations of ODN 2006 (Figure 7.2 and Tables 7.2-7.4). Marker expression values are expressed as the fold change in mean fluorescent intensity (MFI) relative to the unstimulated control. This was to enable a more accurate interpatient comparison since the range of raw MFI values was too great in this small group of patients. All of the different concentrations caused upregulation to some extent, however there is no clear pattern. The concentration of 1μM ODN 2006 was chosen as it marginally induced the greatest changes in the expression of CD49d and CD38 in frozen (freeze-thawed) samples. As earlier stated, many of the samples used throughout this project were freeze-thawed PBMC aliquots and so the responses of frozen PBMCs were of particular importance. Furthermore, our group has had previous experience of using ODN 2006 in a much larger patient cohort and has also previously identified 1μM as the optimum concentration for the stimulation of CLL cells.

Table 7.2: Optimisation of ODN 2006: CD69

CD69	MFI Fold Change ±SD)	
[ODN 2006]	**24h Fresh**	**24h Frozen**
0.5	9.81 (±11.07)	5.31 (±1.07)
1.0	9.88 (±11.52)	5.12 (±0.68)
2.0	11.81 (±12.40)	1.74 (± 0.78)
5.0	11.07 (±8.34)	2.31 (±1.03)

Tables 7.2-7.4: n=5 from 3 individual patients.

Table 7.3: Optimisation of ODN 2006: CD49d

CD49d	MFI (Fold Change ±SD)	
[ODN 2006]	**24h Fresh**	**24h Frozen**
0.5	1.30 (±0.27)	1.28 (±0.28)
1.0	1.30 (±0.29)	1.45 (±0.51)
2.0	1.19 (±0.26)	1.43 (±0.31)
5.0	1.23 (±0.20)	1.45 (± 0.36)

Table 7.4: Optimisation of ODN 2006: CD38

CD38	MFI (Fold Change ±SD)	
[ODN 2006]	**24h Fresh**	**24h Frozen**
0.5	1.49 (±0.76)	2.25 (±0.75)
1.0	1.65 (±0.47)	2.94 (±1.68)
2.0	1.78 (±0.90)	2.48 (± 1.17)
5.0	1.40 (± 0.39)	2.57 (±1.15)

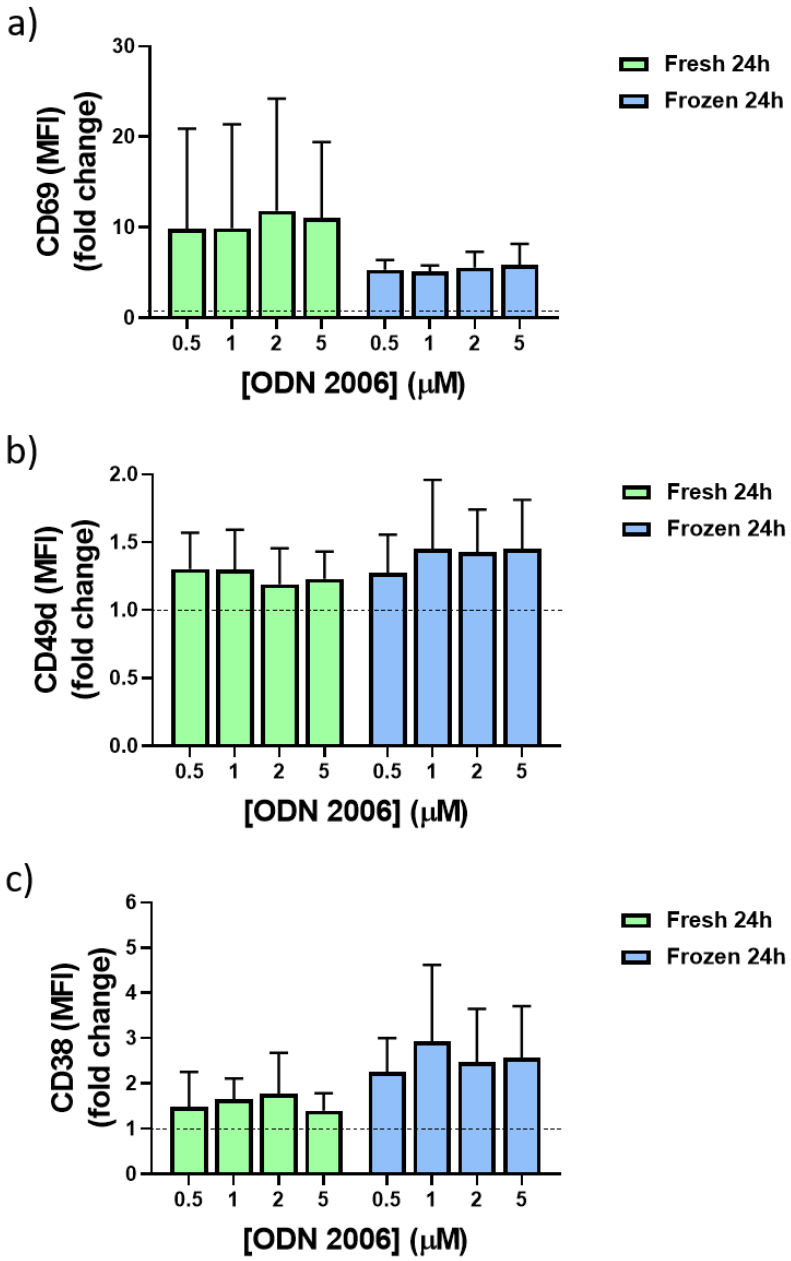

Figure 7.2: ODN 2006 Optimisation: The Effect of ODN 2006 upon the Expression of CD69, CD49d and CD38. Fresh and frozen primary PBMCs were stimulated with 0-5μM ODN 2006 (TLR9 agonist ODN 2006) and incubated for 24h as previously described. Post stimulation, the PBMCs were collected and stained for flow cytometry using an LSR II flow cytometer; viable CLL cells were gated as CD5+/CD19+/FVD- and analysis was performed using FACs Diva software. a) Expression of CD69 in ODN 2006-stimulated CLL cells. b) Expression of CD49d in ODN 2006-stimulated CLL cells. c) Expression of CD38 in ODN 2006-stimulated CLL cells. For each marker, values are given as MFI relative to an unstimulated control (n=5 from 3 individual patients).

7.2: Optimisation of TLR9 Antagonist ODN INH-18

Optimisation experiments for the TLR9 antagonist ODN INH-18 were performed in duplicate using isolated PBMCs from four CLL patients. ODN INH-18 is a competitive inhibitor of the TLR9 agonist ODN 2006 and needed to be introduced into the CLL cells prior to stimulation with ODN 2006. Primary PBMCs were seeded into culture as previously described (see methods section 2.11) and pre-incubated with concentrations of 0-5μM ODN INH-18 for 30 minutes before being stimulated with ODN 2006 for 24h. The PBMCs were then collected and stained for flow cytometry using the LSR II flow cytometer (Antibody Panel A: LSR II, Table 2.1). Live CLL cells were identified as CD5+/CD19+/FVD-.

ODN INH-18 did not affect the viability of ODN 2006-stimulated CLL cells. The unstimulated and ODN 2006-stimulated controls showed a CLL cell % viability (±SD) of 72.6% (±18.4) and 79.8% (±13.6), respectively. In the presence of 0.5μM; 2.0μM and 5μM ODN INH-18, ODN 2006-stimulated CLL cells remained 77.4% (±15.5); 76.8% (±19.6) and 79.4% (±14.03) viable, respectively (n=8 from 4 individual patients) (Figure 7.3a).

In the presence of ODN INH-18, both CD49d and CD69 showed a concentration-dependent reduction of marker expression in ODN 2006-stimulated CLL cells however this was not true of CD38. The MFI (±SD) values at each concentration of ODN INH-18 are shown in Table 7.5 and Figure 7.3b-d. For both CD69 and CD49d, the greatest marker inhibition was achieved at 5μM; 5μM ODN INH-18 was therefore used in subsequent TLR9 inhibition experiments.

Table 7.5: Optimisation of ODN INH-18: CD69, CD49d and CD38

	MFI (Fold Change ± SD)		
[ODN INH-18] (μM)	**CD69**	**CD49d**	**CD38**
0	5.77 (±1.79)	1.35 (±0.26)	1.46 (±0.26)
0.5	3.83 (±1.37)	1.23 (±0.13)	1.39 (±0.31)
2.0	3.31 (± 1.09)	1.16 (±0.16)	1.41 (±0.66)
5.0	2.59 (± 1.15)	1.18 (±0.21)	1.55 (±0.33)

All conditions: n=8 from 4 individual patients.

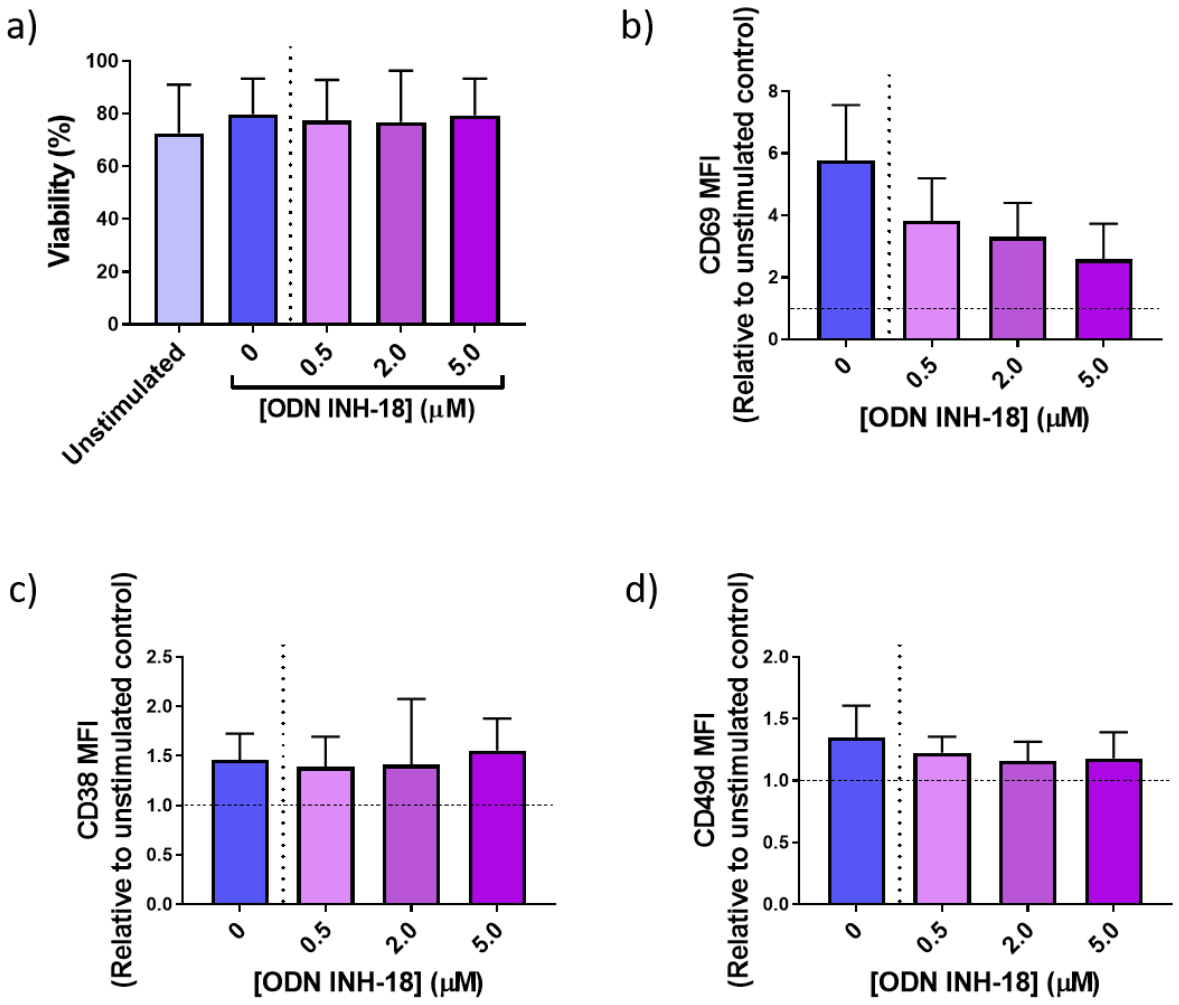

Figure 7.3: ODN INH-18 Optimisation: The Effect of ODN INH-18 Stimulation upon CLL Cell Viability and Expression of CD69, CD49d and CD38 in ODN 2006-Stimulated CLL Cells. Primary PMBCs were pre-incubated with concentrations of 0-5μM ODN INH-18 for 30 minutes prior to a 24h incubation with 1μM ODN 2006 (TLR9 agonist) at 37°C/5% CO_2 (n=8, from 4 individual patients). Post stimulation, PBMCs were collected and stained for flow cytometry using an LSR II flow cytometer. Live CLL cells were gated as CD5+/CD19+/FVD- and data analysis was performed using FACS Diva software. MFI values are shown relative to an ODN 2006-stimulated (uninhibited control) a) ODN INH-18 did not affect the viability of ODN 2006-stimulated CLL cells. b-c) CD69 and CD49d showed concentration-dependent reductions in marker expression in response to ODN INH-18. d) CD38 did not show a concentration-dependent change in marker expression in response to ODN INH-18.

7.3: Optimisation of a Transwell Migration Protocol

CLL cell migration was assessed using a simple transwell migration assay. Briefly, each transwell comprises an apical and basal chamber separated by a porous membrane and a chemotactic gradient is established in the basal chamber to encourage directional migration. Cells are transferred into the apical transwell chamber and incubated for a given number of hours. In this time, migratory cells will pass through the porous membrane and into the basal chamber. These cells are collected from the basal chamber post-incubation and counted (Figure 2.4). A number of factors were considered whilst optimising the experimental conditions for the investigating the effect of ODN 2006-stimulation on CXCL12-driven migration:

- Membrane pore size
- CLL cell identification and quantification post-migration
- Incubation period
- The effect of using fresh (i.e., <24h post-venesection) or frozen (i.e., freeze-thawed from liquid nitrogen) PBMC samples

Each stage of the protocol optimisation is outlined below:

7.3.1: Membrane Pore Size

Transwell migration experiments were performed in 24-well transwell migration plates. Each well comprised an apical (input) and basal (output) chamber, separated by a porous membrane. Cells were transferred into the apical chamber and a chemotactic gradient was established within the basal chamber; cells primed for

migration were able to undergo cytoskeletal changes and manipulate themselves through the pores in the membrane and into the basal chamber.

When designing a transwell migration experiment an appropriate membrane pore size is selected to complement the investigated cell type. The average size of a CLL cell has been calculated at 6.8 microns[168] and an initial a pore size of 3 microns was chosen to facilitate the migration of actively migrating cells only and to avoid the occurrence of chance migration by gravitation pull. Due to a consistently low yield of migrated CLL cells and multiple failed experimental attempts, the pore size was increased to 5 microns.

7.3.2: CLL Cell Identification and Quantification

CLL cells were transferred into the apical transwell migration chambers in a pool of PBMCs. The PBMCs were then left to migrate into the basal transwell chambers, and the mixed pool of migrated cells were collected for quantification; accurate identification of the CLL cell population post-migration was therefore critical for the accuracy of these experiments. PBMCs were stained for the CLL cell identification markers CD3 and CD19 and were counted volumetrically using an Accuri flow cytometer; CLL cells were identified as CD19+/CD3-.

Volumetric quantification: In addition to facilitating the selective counting of a desired cell population, volumetric counting offers a more accurate representation of cell numbers in low density suspensions, compared with other cell counting techniques (e.g., manual [haemocytometer] or automated [Countess II cell counter]). The Accuri flow cytometer counted the number of CLL cells (i.e., CD19+/CD3-

lymphocytes) in a given volume (i.e., 100μl) and this number was used to calculate the total number of harvested CLL cells.

Identification: CLL cells are characteristically CD5+/CD19+ however all experiments performed on the Accuri flow cytometer used CD3 and CD19 in place of the conventional CD5 and CD19; this was due to an earlier identified problem with the accurate identification of post-culture CLL cells using CD5 and CD19 alone when using the LSR II flow cytometer. The expression of CD19 in unstimulated CLL cells was markedly reduced post-culture (relative to baseline i.e., post-thaw levels) and in some cases the CLL population (CD5+/CD19+) was indistinguishable from the T-cell (CD5+/CD19-) population. Figure 7.4 shows LSR II generated FACS plot images of CD5+/CD19 based CLL cell identification. At baseline, CD5+/CD19+ CLL cells form a discrete and easily identified population allowing accurate gating and phenotypic analysis (Figure 7.4a). At 24h post-culture (Figure 7.4b), it is no longer possible to accurately identify the CD5+/CD19+ population. Ideally in this situation, CD3 should be added to the panel to enable the elimination of T-cells from the lymphocyte gate. CD3 is a T-cell marker meaning that T-cells are positive and B-CLL cells are negative. Unfortunately, the addition of extra markers was not possible on the 4-colour Accuri flow cytometer since this would allow space for just one experimental marker on the antibody panel; CD5 was therefore substituted for CD3.

The later arrival of the 21-colour CytoFLEX LX enabled subsequent panels to be designed around a CD5+/CD19+/CD3- gating strategy. Figure 7.4c quantifies the reduction of CD19 MFI from baseline (i.e., immediately after being thawed) to post-

culture; the expression values of CD19 MFI (± SD) were 3252 (±1467) and 2321 (±964.6) respectively (P=0.002, n=31).

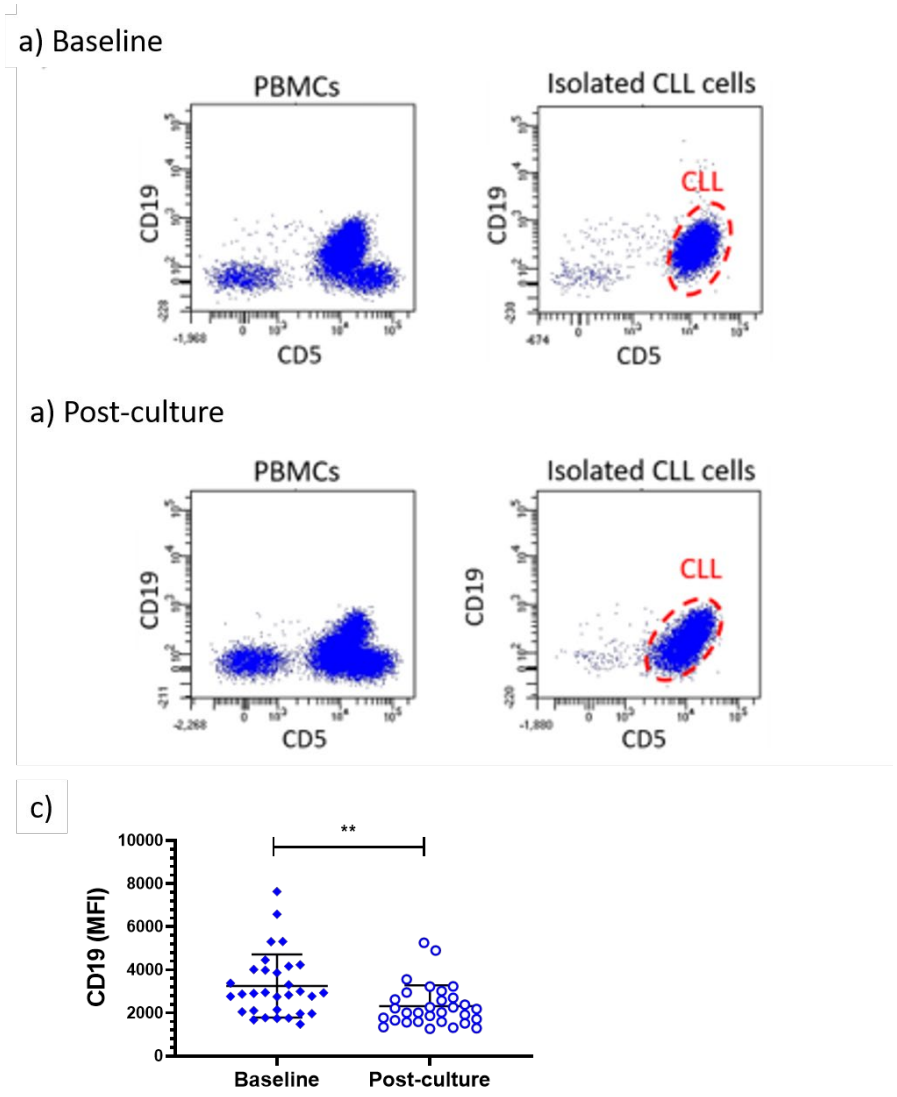

Figure 7.4: CD19 MFI Shows a Significant Reduction 24h Post-Culture. a-b) Primary PBMCs were stained for CD5 and CD19 both pre- (baseline) and post- (24h) culture. FACS plot images are taken from the LSR II flow cytometer during early optimisation of ODN 2006 stimulation protocol and show a representative CLL patient (pt 1118). Images of purified/isolated CLL cell populations are also shown to confirm the location and shape of the CLL population. CLL cells were isolated from the PBMC population prior to culture using the EasySep Human B Cell Enrichment Kit w/o CD43. At baseline, the CLL cell population is easily distinguished from other PBMC populations. At 24h post culture, the CLL cell population has merged with the T cell population. c) CD19 expression data was obtained using the CytoFLEX LX flow cytometer. PBMCs were stained both at baseline and post culture and live CLL cells were identified as CD5+/CD19+/CD3-/FVD-. The cell surface expression (MFI) of CD19 reduces significantly post-culture (P=0.002, n=31). Statistical analyses were performed using GraphPad Prism and the Wilcoxon Matched Pairs test was used as the data were not Gaussian (as determined by the D'Agostino & Pearson normality test).

7.3.3: Transwell Incubation Period

It was necessary to determine the optimal incubation period for PBMCs to migrate towards the CXCL12-gradient. Migration timepoints of 4h and 24h were investigated (n=5) and the results are depicted in Figure 7.5a. Due to patient variation in basal migration, ODN 2006-stimulated CLL cell migration is expressed relative to the unstimulated control (fold change ±SD). At 4h and 24h respectively, CLL cell migration increased by 1.85 (±0.50) and 2.05 (±1.03)-fold. Although the mean migration was higher at 24h, the standard deviation had doubled and so the 4h timepoint was considered optimal. Additionally, since ODN 2006 is known to induce CLL cell proliferation[138,139], a shorter incubation period was more appropriate to ensure any changes in cell numbers collected from the basal transwell chambers were a result of migration and not proliferation.

7.3.4: Fresh vs Frozen PBMC Samples

Each time a patient peripheral blood sample is received, PBMCs are isolated and either used for a current experiment or stored in multiple aliquots in liquid nitrogen. Since it would be resourceful to use frozen patient material for many of the experiments throughout this project, the effect of the freeze-thawing process upon both CLL cell migration (basal/unstimulated) and the capacity to respond to stimulation with ODN 2006 was investigated. Results from patient matched fresh (i.e., from a recent venesection of <24h old) and freeze-thawed PBMC aliquots are shown in Figure 7.5b-c (P=0.813, n=6). The percentage of basal (unstimulated) CLL cell migration (±SD) was higher in fresh samples relative to frozen samples although this did not reach statistical significance (13.3% [±10.1] and 8.9% [± 4.4] respectively,

P= 0.156, n= 6). There was also no significant difference in the ODN 2006-stimualted fold change in migration (±SD) between fresh and frozen CLL cells (i.e., 1.48 [±0.67] and 1.53 [±0.85] respectively, P>0.999, n=6). Frozen samples were therefore deemed suitable for use in future transwell migration experiments. Interestingly, it was noted that two of the six patients appeared not to show an increase in CLL cell migration in either the fresh or frozen samples.

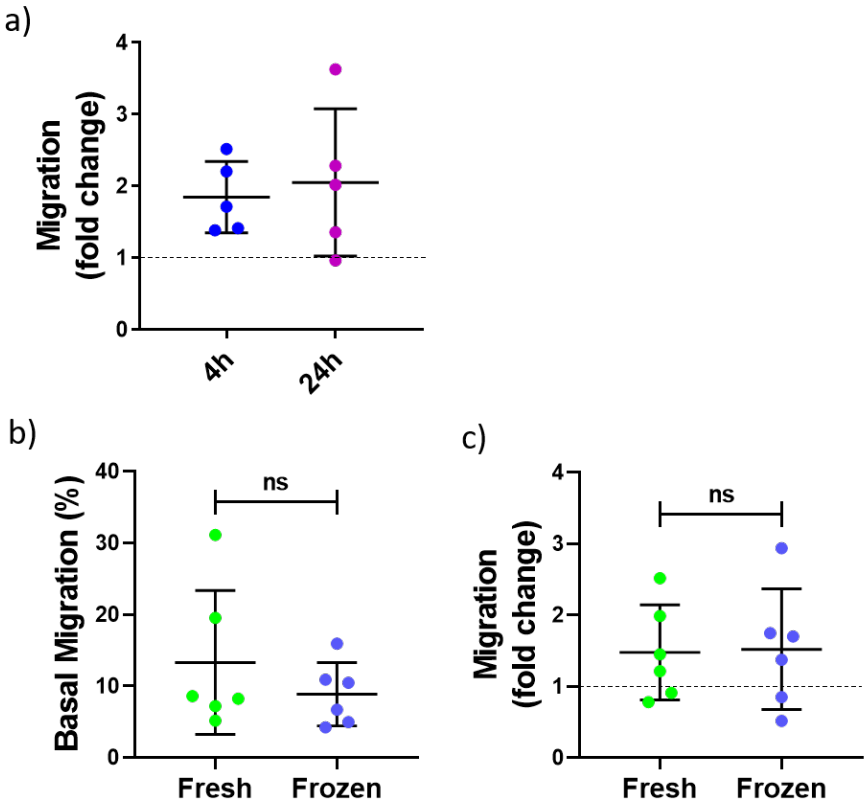

Figure 7.5: Optimisation of the Transwell Migration Protocol: Incubation Period and Sample Type. Primary patient PMBCs were cultured overnight ± 1μM ODN 2006 (TLR9 agonist). PBMCs were either isolated from recently drawn peripheral blood (i.e., fresh – within 24h of venesection) or thawed from liquid nitrogen banked PBMC aliquots. Post stimulation, the PBMCs were transferred into the apical chambers of a 24 well, 3-5μM pore polycarbonate transwell migration plate and a chemotactic gradient of CXCL12 (100ng/ml) in 600ml complete media was established in the basal chambers. Plates were incubated at 37°C/5% $C0_2$ for 4h or 24h. A manual (haemocytometer) or automated (Countess II) cell count was performed prior to transference (i.e., at 0h migration) to obtain the 0h live cell count and migrated CLL cells were counted volumetrically by flow cytometry (Accuri flow cytometer) at 4h or 24h migration. CLL cells were identified as CD19+/CD3- and total migration was calculated as a percentage of the 0h live cell count. a) 4h vs 24h migration: There was no difference between the migratory response of CLL cells at 4h or 24h migration (P=0.813, n=5, Wilcoxon Matched pairs test). b) Fresh vs frozen PBMCs (n=6): There was no significant difference between the basal (unstimulated) migration of CLL cells derived from fresh or frozen PBMC samples (P= 0.156, n=6, Wilcoxon matched pairs test). c) There was no significant difference between the migratory response of fresh or frozen CLL cells (P>0.999, n=6, Wilcoxon matched pairs test). Statistical analysis was performed using GraphPad Prism and the Wilcoxon Matched pairs test was used as the data were not Gaussian (according to the D'Agostino and Pearson test).

7.4: Determining the IGHV-Mutational Status of the CLL Patient Cohort

Table 7.6: The IGHV-Mutational Status and ODN 2006 Responder-Status of a Cohort of 31 CLL Patients Sent for IGHV-Sequencing at The Royal Marsden Hospital

Patient	IGHV Homology (%)	ODN 2006-Responder Status
IGHV-MUTATED		
1. Pt 2	90.97	*Responder*
2. Pt 1104	86.11	*Responder*
3. Pt 1106	72.22	*Responder*
4. Pt 1107	95.49	*Responder*
5. Pt 1108	96.84	*Responder*
6. Pt 1113	86.11	*Non/Reverse-Responder*
7. Pt 1114	95.79	*Responder*
8. Pt 1120	79.93	*Responder*
9. Pt 1124	89.58	*Responder*
10. Pt 1126	94.5	*Responder*
11. Pt 1128	94.39	*Responder*
12. Pt 1129	76.74	*Responder*
13. Pt 1134	92.36	*Responder*
14. Pt 1139	96.9	*Unknown*
15. Pt 1140	95.1	*Unknown*
16. Pt 1141	97.3	*Unknown*

Patient	IGHV Homology (%)	ODN 2006-Responder Status
IGHV-MUTATED		
17. Pt 1143	84	*Responder*
IGHV-UNMUTATED		
1. Pt 1100	100	*Non/Reverse-Responder*
2. Pt 1109	100	*Non/Reverse-Responder*
3. Pt 1110	100	*Non/Reverse-Responder*
4. Pt 1116	100	*Responder*
5. Pt 1118	100	*Non/Reverse-Responder*
6. Pt 1121	100	*Non/Reverse-Responder*
7. Pt 1122	100	*Non/Reverse-Responder*
8. Pt 1123	100	*Responder*
9. Pt 1125	99.31	*Responder*
10. Pt 1127	100	*Responder*
11. Pt 1130	100	*Non/Reverse-Responder*
12. Pt 1132	98.61	*Responder*
13. Pt 1142	100	*Non/Reverse-Responder*
14. Pt 1144	100	*Unknown*

DNA extractions were performed on freeze-thawed patient samples and sent for IGHV-sequencing at The Royal Marsden Hospital, Sutton. The resulting nucleotide sequences were then aligned to the online IMGT reference database.
IGHV-mutated (M-CLL) = <98% sequence homology
IGHV-unmutated (U-CLL) = ≥98% sequence homology
Responder = % CLL cell migration INCREASES (>1.2-fold) post-stimulation with ODN 2006.
Non/Reverse-Responder = % CLL cell migration shows NO CHANGE or DECREASES (≤1.2-fold) post-stimulation with ODN 2006.
Unknown = samples used for phenotyping experiments only – migratory response undetermined

Table 7.7: The ODN 2006 Responder-Status of 7 CLL Patients with Known IGVH-Statuses at the Time of Sample Receipt

Patient	IGHV Mutational Status	ODN 2006-Responder Status
1. LSL 9264	M-CLL	Unknown
2. Pt I-CLL#1	U-CLL	*Non/Reverse-Responder*
3. Pt I-CLL#3	U-CLL	Responder
4. Pt I-CLL#5	U-CLL	Responder
5. Pt I-CLL#6	U-CLL	Responder
6. Pt I-CLL#9	U-CLL	*Non/Reverse-Responder*
7. LSL 9096	U-CLL	Unknown

Responder = % CLL cell migration INCREASES (>1.2-fold) post-stimulation with ODN 2006.
Non/Reverse-Responder = % CLL cell migration shows NO CHANGE or DECREASES (≤1.2-fold) post-stimulation with ODN 2006.
Unknown = viability too poor to analyse